Investigating DNA double-strand break repair in *Dictyostelium discoideum*

A thesis submitted to the Board of the faculty of Biological Sciences, University of Oxford in partial fulfilment of the requirements for the degree of Doctor of Philosophy

Claudia Anne-Marie Couto

Word Count: 44,856

Merton College Trinity term, 2011

Investigating DNA double-strand break repair in *Dictyostelium discoideum*

Claudia Anne-Marie Couto – Merton College

Submitted for the degree of Doctor of Philosophy, Trinity term, 2011

DNA double-strand breaks (DSBs) are toxic lesions that can be repaired by numerous mechanistically distinct pathways. However, regulation of DSB repair pathway utilisation is also essential for maintaining genomic integrity, and eukaryotes have evolved several mechanisms to achieve this. This includes post-translational modifications of DSB repair proteins to modulate their activity at DNA DSB ends. One example of a post-translational modification with a role in DNA repair is Poly-ADP ribosylation (PARylation), which in mammals is mediated by Poly-ADP ribose Polymerase 1 and 2 (PARP1 and 2). The best characterised roles of PARP1 and 2 is in single-strand break repair (SSBR) and base-excision repair (BER). However, their roles in DSB repair remain unclear, and to address this, the eukaryotic model *Dictyostelium discoideum* has been utilised. Several putative repair PARPs are conserved in the *Dictyostelium* genome, and the induction of PARylation following DNA SSBs and base-damage has been observed. Using a genetic approach, multiple *Dictyostelium* PARPs have been implicated in SSBR/BER, as is the case in mammals. PARylation is also induced following DNA DSBs, with the major contributor being Adprt1a. This work has demonstrated the regulatory role of Adprt1a in DSB repair by promoting non-homologous end joining (NHEJ), at the expense of homologous recombination (HR). This may be achieved by the enhanced association of the Ku70/Ku80 heterodimer, the DSB sensor that initiates NHEJ, with chromatin following DNA damage in a PAR-dependent manner. Consistent with this, a PAR binding zinc-finger, the PBZ domain, has been identified in *Dictyostelium* Ku70,

which is involved in the enhanced chromatin-association of Ku post-DSB induction. This work therefore highlights a mechanism by which Adprt1a-induced PARylation post-DSBs promotes NHEJ via Ku recruitment. The enhanced Ku association at damaged chromatin reduces engagement of other DSB repair pathways, placing Adprt1a at the crossroads of DSB repair pathway choice.

Acknowledgements

Many people deserve recognition for their contribution to the production of this thesis. Firstly, I am grateful to my supervisors Nick and Catherine for their advice, patience and encouragement over the course of my DPhil. It is with their help that I have developed as a scientist over the past four years. I would also like to thank members of the Lakin, Pears, Cox and Mahadevan lab, past and present, for lively discussions (scientific or otherwise), use of equipment, and general sustenance. In particular, I would like to mention Rhian and Annette, who were with me from start to finish, and who always offered support and much entertainment through the medium of song and interpretive dance.

I would like to thank Nick Crump, Amanda, Stella, Penny and DW for friendship, and especially their reassurance when I was at the end of my tether. My friends from Oxford and elsewhere have been constant sources of support and fun, especially Gabriela, Yi, Susie, Cherryl, Topaz, Sean and Lawrence – you have all been there for me, in good times and bad, and I am very grateful. I am also indebted to Esther and Noreen, without whom I would never have made the journey to Bristol and Oxford, and to Merton College and the Clarendon fund, for supporting my DPhil research.

I would like express sincere gratitude to my family: my brother, Jonathan, my aunts, Frances, Averil, Mimi, my father, Clement, and my grandmother, Claudia, who offered much needed support from afar. Finally, I am forever indebted to my mother, Teresa, who worked so very hard and sacrificed so much; it is due to her constant support and patience that I am who I am, and where I am, and it is to her that I dedicate my thesis.

Abbreviations

3’ PUA	3’ phospho-α,β unsaturated aldehyde
5’ dRP	5’deoxyribose phosphate
ADPRT	ADP-ribosyl transferase
Agg^-	Aggregation-deficient
Agg^+	Aggregation-proficient
AID	Activation-induced cytidine deaminase
AMD	Automodification domain
APE	AP-endonuclease
APLF	Aprataxin and PNKP-like factor
AP-site	Apurinic/Apyrimidinic site
APTX	Aprataxin
ARH	ADP-ribosylhydrolase
BER	Base excision repair
BIR	Break induced replication
Brca1	Breast cancer 1
Brca2	Breast cancer 2
BRCT	Carboxyl-terminal domain of breast cancer susceptibility protein
BsR	Blasticidin resistance
cAMP	Cyclic adenosine monophosphate
CDK	Cyclin dependent kinase
CO	Crossover
CPD	Cyclobutane pyrimidine dimer
CPT	Camptothecin

CSR	Class switch recombination
CtIP	CtBP interacting protein
DBD	DNA binding domain
DDR	DNA damage response
dHJ	Double Holliday junction
D-loop	Displacement-loop
DNAPKcs	DNA Protein Kinase catalytic subunit
DSB	Double strand break
FA	Fanconi Anaemia
Fen1	Flap Endonuclease 1
GFP	Green fluorescent protein
HR	Homologous recombination
ICL	Intra-strand crosslink
IR	Ionising radiation
Ka	*Klebsiella aerogenes*
LP-repair	Long-patch repair
mAR	Mono-ADP ribose
mART	Mono-ADP ribose transferase
MEF	Mouse embryonic fibroblast
MMS	Methyl methanesulfonate
MRN	Mre11/Rad50/Nbs1
MRX	Mre11/Rad50/Xrs2
NAD^+	Nicotinamide adenine dinucleotide
NCO	Non-crossover
NER	Nucleotide excision repair

NHEJ	Non-homologous end joining
PAR	Poly ADP-ribose
PARG	Poly ADP-ribose Glycohydrolase
PARP	Poly ADP-ribose Polymerase
PBZ	PAR binding zinc finger
PCNA	Proliferating cell nuclear antigen
PCR	Polymerase chain reaction
PNKP	Polynucleotide kinase phosphatase
Polβ/δ/ε	DNA Polymerase β/δ/ε
RAG	Recombination activating gene
RC-BER	Replication-coupled BER
REMI	Restriction enzyme mediated integration
ROS	Reactive Oxygen Species
RPA	Replication Protein A
SAM	S-adenosylmethionine
SCE	Sister chromatid exchange
SDSA	Synthesis dependent strand annealing
SP-repair	Short-patch repair
SSA	Single strand annealing
SSBR	Single strand break repair
TC-BER	Transcription coupled BER
TDP1	Tyrosyl-DNA phosphodiesterase 1
UNG2	Uracil DNA glycosylase 2
UV	Ultraviolet
ZF	Zinc finger

Table of Contents

Abstract……...i

Acknowledgements……...iii

Abbreviations……iv

1: Introduction 6

1.1 Introduction to the DNA damage response.....6

1.2 Sources of DNA damage 7

1.2.1 Endogenous DNA damage.....7

1.2.1.1 DNA hydrolysis 7

1.2.1.2 Endogenously generated DNA damaging agents 8

1.2.1.3 Programmed DNA strand breakage 9

1.2.2 Exogenous DNA damage.....10

1.3 DNA repair.....11

1.3.1 Base Excision Repair (BER).....11

1.3.1.1 Sensing DNA damage: DNA glycosylases.....12

1.3.1.2 Processing of the AP-site to generate a DNA SSB.....13

1.3.2 Single-strand break repair 14

1.3.2.1 DNA SSB detection by PARP1 15

1.3.2.2 DNA end processing.....23

1.3.2.3 DNA gap filling and ligation 24

1.3.3 Double-strand break repair 27

1.3.3.1 Homologous recombination (HR).....27

1.3.3.2 NHEJ.....35

1.3.3.3 Alternative-NHEJ (a-NHEJ) 40

1.3.3.4 Regulation of DSBR 42

1.4 Model organisms to study DNA repair 48

1.4.1 *Dictyostelium discoideum* 49

1.4.2 *Dictyostelium discoideum* as a model organism 50

1.4.3 DNA repair in *Dictyostelium* 52

1.5 Aims 56

2: Materials and Methods 58

2.1 Materials 58

2.2 Methods 65

2.2.1 General cell culture and genetic manipulation 65

2.2.1.1 Cell culture 65

2.2.1.2 Transformation of *Dictyostelium* 65

2.2.1.3 Generation of disruption strains 66

2.2.1.4 Screening of diruptants by PCR 67

2.2.1.5 Cre-loxing 67

2.2.1.6 Fruiting body development and spore hatching 68

2.2.1.7 Liquid nitrogen 68

2.2.2 Molecular biology 69

2.2.2.1 Sequence alignments 69

2.2.2.2 DNA extraction for Southern Blotting 69

2.2.2.3 Southern Blotting 70

2.2.2.4 RNA extraction 71

2.2.2.5 Reverse transcription (RT) and RT-PCR 72

2.2.2.6 DNA manipulations 72

2.2.3 Phenotypic analysis 73
2.2.3.1 Sensitivity assay 73
2.2.3.2 Restriction-Enzyme Mediated Integration (REMI) 74
2.2.3.3 Homologous recombination (HR) assay 74
2.2.3.4 Immunofluorescence analysis and DNA damage-induced staining 75
2.2.3.5 Preparation of samples for Western blotting 76
2.2.3.6 Subcellular fractionation 76
2.2.3.7 Ku80 immunoprecipiation 77
2.2.3.8 Poly-acrylamide gel electrophoresis 78
2.2.3.9 Determination of Poly ADP-ribosylation by Western Blotting 79
2.2.3.10 Determination of γH2AX by Western blotting 79
2.2.3.11 Stripping Western blots 80
2.2.3.12 Statistical Analysis 80

3: Determining the impact of non-homologous end joining on homologous recombination efficiency in G2 of the *Dictyostelium* cell cycle 81

3.1 Introduction 81
3.2 Results 85
3.2.1 Identifying genes to measure gene-targeting efficiency 85
3.2.2 Gene-targeting in Dictyostelium is dependent on components of HR 89
3.2.3 HR is altered in Dictyostelium following disruption of ku80 91
3.3 Discussion 95

4: The role of Poly ADP-ribosylation in DNA single-strand break repair in *Dictyostelium* 105

4.1 Introduction 105

4.2 Results 109

4.2.1. Conservation of the components of single-strand break repair and base excision repair in the Dictyostelium genome 109

4.2.1 Dictyostelium show conservation of PARPs 110

4.2.2. Dictyostelium undergo PARylation in response to DNA single-strand breaks and base damage 115

4.2.3 Generation of putative DNA damage response adprt disruptants 117

4.2.4 PARylation is reduced in the adprt1a$^-$/adprt2$^-$ strain 121

4.2.5 Effects of disrupting adprt genes on sensitivity to MMS and H_2O_2 122

4.2 Discussion 124

5: The role of Poly ADP-ribosylation in *Dictyostelium* DNA double-strand break repair 132

5.1 Introduction 132

5.2 Results 136

5.2.1 *Dictyostelium* undergo PARylation in response to DNA double-strand breaks 136

5.2.2 Genetic dissection of DSB-induced PARylation in response to DNA DSBs 138

5.2.3 The contribution of NHEJ and HR is altered in the *adprt1a*$^-$ strain 139

5.3 Discussion 143

6: The role of the *Dictyostelium* Ku70 PBZ domain in DNA double-strand break repair 151

6.1 Introduction 151

6.2 Results 153

6.2.1 The adprt1a$^-$ strain exhibits defective recruitment of Ku80 to chromatin ... 153

6.2.2 *Dictyostelium* genes contain consensus PAR binding motifs 155

6.2.3 The Ku70 PBZ domain can bind to poly(ADP-ribose) *in vitro* 159

6.2.4 Generation of a *ku70*$^-$ strain 160

6.2.5 Expression of wild-type and mutant Ku70 in the *ku70*$^-$ strain 162

6.2.6 NHEJ and Ku enrichment is defective in the Ku70ΔPBZ strain 163

6.3 Discussion 165

7: General discussion 172

8 : References 179

9: Appendix 203

Appendix A: Primer sequences 203

Appendix B: Publications arising from this work 206

1: Introduction

1.1 Introduction to the DNA damage response

The integrity of our genome is being constantly challenged by a of plethora exogenous and endogenous DNA damaging agents (Lindahl 1993). This is in addition to the spontaneous errors arising from the intrinsic instability of our DNA, and errors that occur during DNA replication through base misincorporation or replication slippage (Lindahl 1993; Jackson and Loeb 2001; Arana and Kunkel 2010). Endogenously generated DNA damage occurs with a much higher frequency than those generated by exogenous agents, and is produced by reactive agents in the cellular environment (Jackson and Loeb 2001). However, exogenous DNA damage created by environmental agents such as ionising radiation (IR), ultraviolet light (UV) and chemical mutagens also generate lesions similar to those created endogenously (De Bont and van Larebeke 2004). The resultant exogenously and endogenously generated DNA damage displays great diversity, and can be represented by small-scale mutations, or large-scale genome alterations, which can both give rise to tumourigenesis. Genome damage can also present a barrier to DNA metabolic processes, and in this case can be cytotoxic, leading to cell death/senescence (Mitchell *et al.* 2003).

The importance of maintaining the fidelity of our genome is explained by the need to faithfully transmit genetic material through cell divisions and successive generations (Ciccia and Elledge 2010). As such, cells have evolved the DNA damage response (DDR) to maintain genomic integrity, which consists of complex networks of proteins that sense and signal the variety of DNA lesions. The DDR culminates in the initiation of DNA repair pathways, often in coincidence with cell cycle delay/arrest and transcriptional alterations. However, if damage is extensive, cells undergo apoptosis or enter senescence (Zhou and Elledge 2000; Khanna and Jackson 2001; Polo and Jackson 2011). The importance of the DDR is highlighted by the disease states arising from its dysfunction. These conditions are characterised by neurological and immunological problems, premature aging and cancer predisposition (Ciccia and Elledge 2010).

1.2 Sources of DNA damage

1.2.1 Endogenous DNA damage

1.2.1.1 DNA hydrolysis

Under physiological conditions, the N-glycosyl bond between the DNA base and sugar-phosphate backbone can undergo spontaneous hydrolysis. This leads to base loss, generating an abasic site known as an apurinic/apyrimidic site (AP-site). AP-sites are more frequently represented by loss of purines and increase the susceptibility of the DNA backbone to chemical cleavage to generate single-strand breaks (SSBs). However, the double-stranded nature of DNA provides a template for nucleotide replacement as part of DNA repair. DNA bases can also undergo hydrolytic

deamination, altering their base pairing properties and leading to base-substitutions following DNA replication. Deamination of 5-methylcytosine to thymine occurs most frequently and can lead to base-substitution on replication. Additionally, cytosine can undergo spontaneous deamination to form uracil (Lindahl 1993).

1.2.1.2 Endogenously generated DNA damaging agents

The major endogenously generated DNA damaging agents are reactive oxygen species (ROS), particularly hydroxyl radicals, generated as by-products of cellular metabolism (Jackson and Loeb 2001; Evans *et al.* 2004). ROS can attack DNA bases leading to nucleotides with altered chemistry and basepairing properties, such as 8-oxo-guanine which mispairs with adenine (Lindahl 1993). ROS can also attack the sugar-phosphate backbone, generating DNA strand breaks (Jackson and Loeb 2001; Khanna and Jackson 2001; Caldecott 2008). The DNA ends generated by strand breakage contain a variety of termini, including 3' phosphate and 3' phosphoglycolate groups which require processing prior to repair (Ward 1988). DNA strand breaks are most frequently represented by SSBs which can block transcription and lead to the stalling or collapse of replication forks (Caldecott 2008). However, the main toxicity of strand breakage is derived from DNA double-strand breaks (DSBs). DSBs arise from the clustered nature of DNA lesions or via replication fork collapse (Willers *et al.* 2004; Jackson and Bartek 2009; Jeggo *et al.* 2011). As a single DSB is sufficient to give rise to cell death, cells have evolved numerous repair pathways to resolve oxidatively generated DNA lesions (Khanna and Jackson 2001).

Other endogenously generated reactive agents include the methylating agent S-adenosylmethionine (SAM). SAM normally regulates gene expression but can also

react with DNA, methylating bases, the most common being 7-methylguanine and 3-methyladenine. Whilst 7-methylguanine is more likely to give rise to AP-sites, the modified base retains its basepairing properties; conversely, 3-methyladenine blocks DNA replication (De Bont and van Larebeke 2004).

1.2.1.3 Programmed DNA strand breakage

The DNA backbone can also be cleaved via programmed mechanisms as an intermediate of different physiological processes. For example, Spo11 functions during eukaryotic meiosis to create DNA DSBs that ensure correct segregation of homologous chromosomes, and to generate allelic and population diversity (Keeney *et al.* 1997). In yeast, meiosis occurs in a/α diploids, which are formed by mating between **a** and α haploids. Haploids of opposite mating type are generated by mating type switching which occurs via DNA DSB induction by an HO endonuclease at the MAT locus (Haber 1998). Higher eukaryotes also induce DNA strand breaks to generate antigen receptor diversity in V(D)J and class-switch recombination (CSR) as part of their adaptive immune system. In V(D)J recombination, DNA DSBs are specifically induced by Recombination Activating Genes 1 and 2 to enhance antigen receptor specificity (McBlane *et al.* 1995; Gellert 2002). Conversely in CSR, strand breaks are generated by Activation Induced Deaminase to direct antigen receptor effector functions (Muramatsu *et al.* 2000). Furthermore, the type I and type II DNA Topoisomerases function in replication, transcription and recombination to modulate DNA topology by incising the DNA backbone on one or both strands (Champoux 2001). In each case, the generation of programmed DNA strand breaks can be highly regulated and directed by DNA sequence specificity and/or controlled expression during the cell cycle or in certain cell types. Furthermore, these programmed lesions

utilise repair pathways and components of repair pathways that also resolve exogenously generated DNA damage.

1.2.2 Exogenous DNA damage

Environmental sources of DNA damage include IR and UV. IR can directly damage DNA via ionisation of the macromolecule, or alternatively, can ionise water molecules to form ROS. ROS can attack DNA bases and the sugar-phosphate backbone as described in section 1.2.1.2. UV also induces large amounts of DNA damage, generating up to 100,000 lesions per cell per day (Jackson and Bartek 2009). Similar to IR, UV can generate ROS, however, the most abundant UV-induced DNA damage is the covalent crosslinking of adjacent pyrimidines, termed cyclobutane pyrimidine dimers (CPD). These lesions present a barrier to replication and transcription, and as such are cytotoxic (Sinha and Hader 2002).

Additional exogenous DNA damaging agents include chemicals that induce a variety of DNA lesions. This includes base alkylating agents such as methyl methanesulfonate (MMS) and temozolomide. Furthermore, alkylating agents such as nitrogen mustard can also form intra- and inter-strand crosslinks (ICLs) which represent cytotoxic lesions due to their ability to block replication and transcription. Some chemical agents such as bleomycin and phleomycin directly attack the sugar-phosphate backbone to generate SSBs and DSBs. Alternatively, chemical agents such as camptothecin (CPT) and etoposide covalently link topoisomerases to DNA which give rise to DNA DSBs when encountered by a replication fork (Froelich-Ammon and Osheroff 1995; Champoux 2001). In many cases chemical DNA damaging agents are exploited as chemotherapeutics to target cancer cells, due to their dysfunctional DDR.

1.3 DNA repair

As mentioned previously, the DDR recognises and responds to DNA damage to prevent tumourigenesis, with one outcome being DNA repair. This DNA repair can occur by several pathways, which have each evolved to recognise and resolve the different types of lesions created by exogenous and endogenous sources outlined in section 1.2. The nature of the DNA helix, with its two complementary strands ensures that one strand is available as a template when the other strand is damaged. However, when damage targets both strands, potentially lethal DNA DSBs can arise. In the following sections, DNA repair pathways will be addressed, focusing on pathways resolving DNA base damage, DNA SSBs and DNA DSBs.

1.3.1 Base Excision Repair (BER)

The BER pathway is an evolutionarily conserved pathway that resolves DNA base damage. These lesions are represented by chemically modified bases generated by oxidative or alkylating agents, or through spontaneous hydrolytic deamination of bases. Furthermore, BER also repairs the AP-sites that arise through hydrolysis of the N-glycosidic bond between DNA bases and the sugar-phosphate backbone. Lesions resolved by BER are non-bulky, induce minimal DNA helix distortion and may retain normal basepairing. This raises an element of complexity in lesion recognition for initiating DNA repair, failure of which can be mutagenic or cytotoxic (Hegde *et al.* 2008). This is due to mutations arising from mispairing of altered bases, replication fork collapse or impeded transcription by RNA polymerase II at DNA SSBs (Kuzminov 2001; Caldecott 2008; Hegde *et al.* 2008). The importance of BER is

evidenced by the neurodegenerative disease states associated with defective BER, such as Ataxia Oculomotor Apraxia 1 (AOA1) and Spinocerebellar Ataxia Axonal Neuropathy 1 (SCAN1) (Caldecott 2008).

This section will focus on the initial stages of BER, represented by DNA damage recognition by DNA glycosylases which remove damaged bases to generate AP sites. These AP sites are substrates for AP-endonucleases (APE), which also process AP sites arising through spontaneous base loss. The APE cleaves the DNA backbone 5' to the abasic site to generate a DNA SSB (Hegde *et al.* 2008), that is subsequently channelled into SSB repair (SSBR) for resolution (SSBR will be discussed in section 1.3.2). BER represents a global repair process, but can also function in the context of replicating and transcribed DNA (RC- and TC-BER), where DNA glycosylases such as Uracil DNA glycosylase 2 (UNG2) may be specifically targeted to repair in these contexts (Otterlei *et al.* 1999; Dou *et al.* 2003; Caldecott 2008).

1.3.1.1 Sensing DNA damage: DNA glycosylases

Recognition of bases with altered chemistry or basepairing properties is achieved by the DNA glycosylase family. These small (30-50kDa), monomeric enzymes dually function to sense DNA lesions and process the damaged base to initiate DNA repair. The relatively limited damage specificity of DNA glycosylases accounts for the different types of enzymes which can be found in prokaryotes and eukaryotes (Table 1.1). Nevertheless, they are sufficiently promiscuous in lesion recognition that mice disrupted in a single DNA glycosylase exhibit mild phenotypes (Robertson *et al.* 2009). For example, a mouse-disruptant of *ung*, which encodes nuclear UNG2, is viable and displays no overt phenotype. This is despite the accumulation of uracil

within the genome due to uracil misincorporation during replication and formation of uracil via cytosine deamination (Lindahl 1993; Nilsen *et al.* 2000; Hegde *et al.* 2008).

DNA glycosylases can be divided into monofunctional or bifunctional enzymes based on their mechanism of lesion processing. Monofunctional DNA glycosylases remove uracil, mispaired bases, or bases damaged by alkyl groups. They cleave the N-glycosidic bond between the base and the DNA backbone, leaving an AP-site (Hegde *et al.* 2008; Hegde *et al.* 2010). Bifunctional DNA glycosylases remove oxidised bases to generate an AP-site, but possess additional lyase activity to cleave the DNA backbone and generate a SSB (See section 1.3.1.2) (Hegde *et al.* 2008; Hegde *et al.* 2010).

1.3.1.2 Processing of the AP-site to generate a DNA SSB

AP-sites generated directly by spontaneous hydrolytic base loss or by monofunctional DNA glycosylases are subsequently processed by the APE to generate DNA SSBs (Hegde *et al.* 2008; Hegde *et al.* 2010). Unlike *E.coli* that encodes two AP endonucleases, Exo III and Endo IV, mammals only possess Exo III orthologues, APE1 and APE2 (Hegde *et al.* 2008). APE1 is the major AP endonuclease against AP-sites, whereas APE2 displays weak AP endonuclease activity (Burkovics *et al.* 2006; Dianov and Parsons 2007). APE1 cleaves the DNA backbone 5' to the AP-site to generate DNA termini with 3' hydroxyl and a 5' deoxyribose phosphate (dRP) ends (Hegde *et al.* 2008).

The bifunctional DNA glycosylases cleave the DNA backbone to generate SSBs subsequent to AP-site generation. These glycosylases can be divided into two

subgroups, Nth and Nei, based on their lyase reaction, which each generate DNA termini with distinct ends that dictate the subsequent stages of repair (Hegde *et al.* 2010). Nth family glycosylases cleave the DNA backbone to generate termini containing 3' phospho-α,β unsaturated aldehyde (3' PUA) and 5' phosphate ends (Aburatani *et al.* 1997; Ikeda *et al.* 1998; Hegde *et al.* 2008). Conversely, the Nei family glycosylases generate DNA with 3' phosphate and 5' phosphate ends (Hegde *et al.* 2008).

SSBs generated by both APE and the bifunctional DNA glycosylases can then be channelled into the SSBR pathway for subsequent lesion resolution.

1.3.2 Single-strand break repair

SSBs are the most commonly arising lesion which, in addition to being generated as BER intermediates are also directly generated by oxidative damage and chemical agents, as previously described (Caldecott 2008). These lesions are repaired by the SSBR pathway (Figure 1.1), the importance of which is reflected in the neurodegenerative conditions associated with its dysfunction (Caldecott 2008). The multistep SSBR pathway is initiated by lesion recognition, which can be mediated by Poly ADP-ribose Polymerase 1 (PARP1). PARP1 then signals the DNA SSBs and recruits downstream proteins, such as the scaffolding protein XRCC1. XRCC1 is conserved only in higher eukaryotes, and coordinates the repair process by interacting with other SSBR components (Caldecott 2003). The final stages of SSBR are DNA end processing to generate 3' hydroxyl and 5' phosphate groups, DNA gap filling by a DNA polymerase and finally, DNA end ligation (Hegde *et al.* 2008). *In situ*

analysis of the accumulation and decay of BER proteins at DNA lesions has indicated the rapid resolution of DNA damage by this pathway (Lan *et al.* 2004).

1.3.2.1 DNA SSB detection by PARP1

As mentioned above, DNA SSB recognition is mediated by PARP1, which is a highly abundant 113kDa nuclear protein. Once activated, PARP1 utilises NAD^+ as a substrate to reversibly modify target nuclear proteins with chains of ADP-ribose known as poly-ADP ribose (PAR). The ADP-ribose units in PAR are linked by glycosidic bonds and the chains demonstrate variable length and branching. The reversibility of the PAR modification is conferred by two genes in mammals, PAR Glycohydrolase (PARG) and the structurally unrelated ARH3. The products of these genes catalyse the hydrolysis of PAR to mono-ADP-ribose molecules and free ADP-ribose (Meyer-Ficca *et al.* 2004; Koh *et al.* 2005; Oka *et al.* 2006).

PARP1 is the founding member of the PARP superfamily that in humans consists of 16 other members that display varying degrees of similarity to PARP1. Significantly, some human PARPs are confirmed or postulated to possess only mono-ADP-ribose (mAR) activity, whilst others display no catalytic activity. Two PARPs, PARP1 and 2, have been demonstrated to play a role in DNA repair, particularly SSBR, where PARP1 function has been the most extensively investigated (D'Amours *et al.* 1999; Ame *et al.* 2004; Otto *et al.* 2005; Hottiger *et al.* 2010; Krishnakumar and Kraus 2010). However, subsequently, PARP activity has also been implicated in modulating chromatin structure, DNA replication, telomere homeostasis, transcription and gene-expression regulation (Hakme *et al.* 2008).

With regards to repair, PARP1 binds SSBs and DSBs *in vitro*, and is rapidly recruited to sites of DNA damage *in vivo* (Gradwohl *et al.* 1990; Ikejima *et al.* 1990; Okano *et al.* 2003; Haince *et al.* 2008; Eustermann *et al.* 2011; Langelier *et al.* 2011). Damage detection leads to PARP1 catalytic activation and the synthesis of PAR chains on target nuclear proteins (Benjamin and Gill 1980; D'Amours *et al.* 1999). *In vitro* and *in vivo* repair assays assessing DNA repair capacity in mammalian cells or their extracts have conveyed defects in SSBR when PARP1 function is inhibited by genetic disruption, dominant-negative inhibition, chemical inhibition or siRNA knockdown. Finally, PARP1 has been shown to interact with components of the BER pathway, and in some cases, to promote their recruitment to DNA damage (D'Amours *et al.* 1999; Caldecott 2008; Hegde *et al.* 2008). The following sections outline the structure of PARP1 and its mechanistic contribution to SSBR.

1.3.2.1.1 The structure of PARP1

Human PARP1 can be divided into three functionally and structurally distinct domains: the N-terminal DNA binding domain (DBD, amino acids 1-374), the central automodification domain (AMD, amino acids 375-525) and the C-terminal catalytic domain (amino acids 526-1014) (Figure 1.2) (Altmeyer *et al.* 2009).

The DBD is the minimal domain that can bind to DNA damage. Two structurally homologous C2HC zinc-fingers (ZF), ZF1 and ZF2, mediate interactions with DNA lesions *in vitro*, including dsDNA containing a nick or 1 nucleotide gap, and dsDNA ends (Gradwohl *et al.* 1990; Ikejima *et al.* 1990; Eustermann *et al.* 2011; Langelier *et al.* 2011). Downstream of ZF2 is a caspase 3 and 7 cleavage site and a nuclear localisation domain (Schreiber *et al.* 1992; Krishnakumar and Kraus 2010). PARP1

cleavage by caspases is an early event in apoptosis and results in the cessation of PAR synthesis and sequestration of DNA damage by the PARP1 DBD, preventing the DNA lesion being accessed by other repair proteins (D'Amours *et al.* 2001). Recently, a third CCCC zinc finger, ZF3, showing no structural resemblance to ZF1 and ZF2 has been identified (Langelier *et al.* 2008; Eustermann *et al.* 2011). *In vitro*, ZF3 is not involved in interacting with DNA but rather transmits the DNA binding signal to the catalytic domain to stimulate PARP1 catalytic activity, in addition to playing a role in chromatin compaction (Langelier *et al.* 2008; Tao *et al.* 2008; Langelier *et al.* 2010; Huambachano *et al.* 2011). Downstream of the DBD is the AMD which is the major target of PARP1 catalytic activity following DNA damage recognition (D'Amours *et al.* 1999). Within the AMD is the BRCT domain that is predominantly present in DNA repair and checkpoint proteins. In PARP1, the BRCT domain may facilitate PARP1 interaction with other proteins, including the SSBR scaffolding protein, XRCC1 (Masson *et al.* 1998; Caldecott 2003).

At the C-terminus of PARP1 is the catalytic domain, composed of the WGR motif and the PARP catalytic domain. The WGR domain which is predominantly composed of Tryptophan (W), Glycine (G) and Arginine (R) residues does not have a defined function. However, it is postulated to function as a nucleic acid binding motif and may also regulate PARP1 catalytic activity post-DNA lesion recognition *in vitro* (Altmeyer *et al.* 2009). Downstream of the WGR motif is the site of enzymatic activity for PAR initiation, elongation and branching, using NAD^+ as a substrate (D'Amours *et al.* 1999). The catalytic domain can be divided into the regulatory N-terminal region between residues 662-784, which may modulate access of NAD^+ into the active site (Trucco *et al.* 1999). The C-terminal region between residues 785-

1014 displays structural homology to the bacterial ADP-ribosylating toxins, and is principally composed of two β-sheets, within which NAD^+ binds (Ruf *et al.* 1996; Ruf *et al.* 1998). Three residues in this C-terminal region, histidine (H863), tyrosine (Y907) and glutamate (E988), form the catalytic triad that make important contacts with NAD^+ (Ruf *et al.* 1996). In particular, E988 enables PAR polymerisation and its mutation converts PARP1 to a mono-ADP ribose-transferase (mART) *in vitro* (Marsischky *et al.* 1995; Rolli *et al.* 1997).

1.3.2.1.2 PARP1 DNA SSB lesion recognition

The purified PARP1 DBD interacts with DNA containing nicks or gaps *in vitro* (Gradwohl *et al.* 1990; Ikejima *et al.* 1990; Eustermann *et al.* 2011). This includes nicked DNA with modified termini resembling structures created as intermediates of the BER pathway (Lavrik *et al.* 2001; Parsons *et al.* 2005; Khodyreva *et al.* 2010; Eustermann *et al.* 2011). *In vivo,* PARP1 accumulates at sites of laser microirradiation induced DNA SSBs in HeLa cells (Mortusewicz *et al.* 2007). More recently, the interaction of purified PARP1 with AP sites has also been demonstrated, although these lesions only minimally activate PARP1 (Khodyreva *et al.* 2010).

1.3.2.1.3 PARP1 activation

Following DNA damage recognition, PARP1 becomes activated and synthesises PAR chains of variable length and branching on target nuclear proteins (Benjamin and Gill 1980; D'Amours *et al.* 1999). PARylation is rapidly observed *in vivo* by immunofluorescence following induction of DNA SSBs or base damage (Ame *et al.* 1999; Okano *et al.* 2003; Mortusewicz *et al.* 2007). PARP1 mediates the major

damage induced PARylation, as indicated by the greatly diminished nuclear PAR synthesis in PARP1$^{-/-}$ mouse embryonic fibroblasts (MEFs) (El-Khamisy *et al.* 2003). Catalytically active PARP1 targets several nuclear proteins, with the main target being itself (Ogata *et al.* 1981; Satoh and Lindahl 1992; D'Amours *et al.* 1999). However, whether this represents automodification by PARP1 or transautomodification by another PARP1 molecule is not clear (Mendoza-Alvarez and Alvarez-Gonzalez 1993). In particular, three glutamate residues (E488, E491 and D387), which are C-terminal to the BRCT domain, were initially identified as automodification targets *in vitro* (Tao *et al.* 2009; Huambachano *et al.* 2011). However, subsequent analysis suggests that lysines (K489, K521 and K524) may actually function as PAR acceptors (Altmeyer *et al.* 2009).

PARP1 also targets histones *in vivo* and *in vitro*, including histone H1 and histone tails of the core histones (Benjamin and Gill 1980; Adamietz and Rudolph 1984; D'Amours *et al.* 1999; Messner *et al.* 2010; Hottiger 2011). The core histones are targeted at lysine residues *in vitro*, as determined by mass spectrometery, providing further weight to the preferential targeting of lysines over glutamate residues by PARP1 (Altmeyer *et al.* 2009; Messner *et al.* 2010). The PARylation of histones facilitates chromatin relaxation *in vitro*, and may increase damage site accessibility to repair proteins (Poirier *et al.* 1982). The PAR post-translational modifications can also recruit other proteins via non-covalent interactions with the PAR chains, mediated by PAR binding domains, of which three have been identified (Pleschke *et al.* 2000; El-Khamisy *et al.* 2003; Okano *et al.* 2003; Karras *et al.* 2005; Ahel *et al.* 2008). This may lead to changes in chromatin architecture, transcriptional alterations and cell cycle effects (El-Khamisy *et al.* 2003; Okano *et al.* 2003; Kanai *et al.* 2007;

Krishnakumar and Kraus 2010). Furthermore, PARP1 automodification leads to its release from DNA due to electrostatic repulsion between the negative charge of DNA and PAR. This has been observed *in vitro* by the loss of DNA binding by automodified PARP1 (Zahradka and Ebisuzaki 1982). The importance of automodification is demonstrated by enhanced retention of catalytically inactive PARP1 at DNA damage sites in MEFs (Mortusewicz *et al.* 2007). Thus, PARP1 automodification triggers its release from DNA in order for downstream stages of repair to occur.

1.3.2.1.4 The role of PARP1 in the early stages of SSBR

Evidence for the role of PARP1 in repair of SSBs arising directly or as intermediates in BER has come from *in vivo* studies in which PARP1 has been knocked-down, depleted or inhibited. Mice containing a disruption at the *parp1* locus, which leads to loss of PARP1 expression, have been developed (Wang *et al.* 1995; de Murcia *et al.* 1997; Masutani *et al.* 1999). These mice display reduced survival against base-damaging and SSB-inducing agents due to enhanced genomic instability as illustrated by increased chromosome breakage and sister-chromatid exchange (SCE) (de Murcia *et al.* 1997; Masutani *et al.* 1999; Menissier de Murcia *et al.* 2003). Cell lines derived from *parp1*$^{-/-}$ mice also have increased sensitivity to alkylating agents and IR (Masutani *et al.* 1999; Trucco *et al.* 1999; El-Khamisy *et al.* 2003). These findings implicate PARP1 in survival post-induction of DNA base damage and strand breakage. Analysis of repair kinetics of PARP1-depleted human and mouse models have demonstrated slower lesion resolution in response to DNA SSBs and base damage (Trucco *et al.* 1998; Fisher *et al.* 2007). However, the fact that repair still

occurs demonstrates that whilst PARP1 contributes to SSBR/BER, its function is not essential.

One mechanism by which PARP1 functions in SSBR is by facilitating the recruitment of the SSBR scaffolding protein XRCC1 to DNA damage sites. This has been supported by the interaction of XRCC1 with the BRCT and DBD domains of PARP1 *in vitro* (Masson *et al.* 1998). This interaction is reliant on the automodification of PARP1 due to the reduced interaction when PARP1 catalytic activity is inhibited (Dantzer *et al.* 2000; Schreiber *et al.* 2002). Immunofluorescence studies have further illustrated the contribution of PARP1 in XRCC1 recruitment to DNA damage sites induced by laser microirradiation, endonucleases and DNA oxidising and alkylating agents (El-Khamisy *et al.* 2003; Okano *et al.* 2003; Fisher *et al.* 2007; Mortusewicz *et al.* 2007). Consistent with the delayed repair of PARP1-depleted mammalian cells, XRCC1 is still recruited to DNA damage sites in *parp1*-deficient cells, albeit with slower kinetics (Lan *et al.* 2004; Mortusewicz *et al.* 2007). Following recruitment to DNA damage sites, XRCC1 interacts with several downstream components of the SSBR pathway to facilitate their recruitment or activate their enzymatic activity (Hegde *et al.* 2008). A further role of PARP1 may also be in protecting BER intermediates from aberrant processing and degradation, and reducing the conversion of DNA SSBs to DSBs on encountering the replication fork (Parsons *et al.* 2005; Woodhouse *et al.* 2008).

1.3.2.1.5 Residual PARylation in *parp1*$^{-/-}$ cells: Evidence for the role of PARP2 in SSBR

Residual PARylation in *parp1*$^{-/-}$ MEFs post-oxidative damage and MMS-treatment, and the catalytic activation of purified PARP2 by DNaseI-treated DNA illustrated the putative function of PARP2 in SSBR (Ame *et al.* 1999). PARP2 is a 62kDa nuclear protein containing an N-terminal DBD, a central domain containing the WGR motif and a C-terminal catalytic domain (Figure 1.3). DNA binding and NLS activity are conferred by the first 69 residues of the DBD, as determined by South-western analysis with DNaseI-digested DNA and GFP localisation studies, respectively (Ame *et al.* 1999). Furthermore, lysine residues in the DBD (K36, K37) are PARylated by PARP2 autoPARylation or PARP1 heteromodification (Schreiber *et al.* 2002; Haenni *et al.* 2008). The PARP2 catalytic domain displays high sequence and structural identity to that of PARP1 (Ame *et al.* 1999; Oliver *et al.* 2004), including the PARP signature motif and the catalytic glutamate (E534) (Ame *et al.* 1999). However, structural deviations of the PARP2 catalytic domain from PARP1 may define distinct PARylation activity and PARylation acceptors (Oliver *et al.* 2004). Consistently, PARP2 does not PARylate core histone tails *in vitro* (Messner *et al.* 2010).

Despite the catalytic activation of PARP2 by SSBs, its role in SSBR is unclear. Whilst lethality and chromosome breaks are enhanced post-irradiation of *parp2*$^{-/-}$ mice (Menissier de Murcia *et al.* 2003), PARP2-depletion in human cells leads to minimal sensitivity and repair defects following oxidative DNA damage (Fisher *et al.* 2007). In addition, XRCC1 is recruited with normal kinetics to sites of laser-microirradation in *parp2*$^{-/-}$ MEFs (Mortusewicz *et al.* 2007). Therefore, PARP2 may play a later role in SSBR, and consistent with this, PARP2 is recruited to DNA

damage more slowly than PARP1 and preferentially recognises DNA flaps, which can appear downstream in SSBR (Schreiber *et al.* 2006; Mortusewicz *et al.* 2007; Haenni *et al.* 2008). Nevertheless, functional redundancy between PARP1 and PARP2 is implied by the embryonic lethality of *parp1*$^{-/-}$/*parp2*$^{-/-}$ double-disruption in mice (Menissier de Murcia *et al.* 2003).

1.3.2.2 DNA end processing

The termini of DNA SSBs produced directly by DNA damaging agents, or during BER by AP endonucleases/bifunctional DNA glycosylases can require processing to create the 3' hydroxyl and 5' phosphate ends necessary for DNA gap filling and ligation. Processing enzymes include APE1, polynucleotide kinase 3' phosphatase (PNKP), tyrosyl-DNA phosphodiesterase 1 (TDP1), DNA Polymerase β (Polβ) and Aprataxin (APTX) (See table 1.2 for a non-exhaustive list) (Caldecott 2008). In this section, APE1, PNKP and Polβ, which together process the majority of DNA termini, will be addressed.

In addition to processing AP-sites generated directly or by monofunctional glycosylases (Dianov and Parsons 2007), APE1 also processes DNA SSB termini. This includes 3' PUA ends created by Nth family bifunctional DNA glycosylases (Wiederhold *et al.* 2004) and 3' phosphoglycolate and 3' phosphoglycoaldehyde ends which are major products of ROS (Parsons *et al.* 2004). In each case, the processing action of APE1 generates 3' hydroxyl groups.

DNA ends containing 3' phosphates, such as those created by Nei family bifunctional DNA glycosylases are poor substrates for APE1 due to its low 3' phosphatase

activity. Instead, these termini are processed by PNKP which possesses 3' phosphatase and 5'kinase activity (Karimi-Busheri *et al.* 1999; Wiederhold *et al.* 2004; Caldecott 2008). PNKP interacts with BER components including XRCC1, and XRCC1 stimulates PNKP enzymatic activity, increases its ability to discriminate between DNA with 5' hydroxyl and 5' phosphate termini and facilitates the release of processed substrates *in vitro* (Whitehouse *et al.* 2001; Mani *et al.* 2007).

Finally, Polβ also confers DNA termini processing activity in addition to its polymerase function in the gap filling step of SSBR. Polβ possesses dRP lyase activity to process 5' dRP formed by the strand-incision action of APE1 at AP-sites (Sobol *et al.* 2000; Hegde *et al.* 2008). Furthermore, its lyase function immediately precedes its polymerase activity without release of the DNA substrate (Prasad *et al.* 2010). Polβ interacts with, and its lyase activity is stimulated by, APE1, providing a sequential mechanism of action in the BER pathway (Bennett *et al.* 1997).

1.3.2.3 DNA gap filling and ligation

Once the 5' phosphate and 3' hydroxyl groups have been restored to DNA ends by the action of processing enzymes, the one nucleotide gap is filled by a DNA polymerase in short patch-repair (SP-repair). If another nucleotide is inserted into the gap, repair proceeds by long-patch repair (LP-repair), where between 2 to 12 bases are inserted (Hegde *et al.* 2008).

1.3.2.3.1 SP-SSBR

The major polymerase in SP-SSBR is Polβ, as determined by *in vitro* repair assays using MEF WCEs with depleted Polβ, which display greatly reduced repair of a uracil base lesion (Braithwaite *et al.* 2005). The recruitment of Polβ to DNA damage sites may be mediated via its interactions with XRCC1, APE1 and PARP1 (Caldecott *et al.* 1996; Kubota *et al.* 1996; Bennett *et al.* 1997; Caldecott 2003; Lan *et al.* 2004; Dantzer *et al.* 2006). The interaction of Polβ with PARP1 *in vitro*, is independent of the PARylation status of PARP1 (Dantzer *et al.* 2000). Once a single nucleotide has been inserted by Polβ, possibly in association with removal of 5' dRP, the resulting oligonucleotide can be ligated by DNA Ligase IIIα, which is found in complex with XRCC1 *in vivo* (Caldecott *et al.* 1994; Wiederhold *et al.* 2004).

1.3.2.3.2 LP-SSBR

When the 5' end of the SSB is refractory to Polβ dRP lyase activity, repair can proceed by LP-repair via the insertion of a patch of nucleotides, and concomitant creation of a flap containing the modified 5' end (Hegde *et al.* 2008). Whilst the repair patch can be up to 12 nucleotides in length, the most common patch is between 2 to 6 bases (Klungland and Lindahl 1997; Pascucci *et al.* 1999). The LP-repair pathway utilises components of the replicative machinery and has been reconstituted *in vitro* with purified PCNA, Fen1, Polδ/Polε, Ligase I and APE1 (Klungland and Lindahl 1997; Pascucci *et al.* 1999). However, DNA Polβ may be the major LP-repair polymerase, as immunodepletion of Polβ in mammalian WCEs leads to defective LP-repair (Klungland and Lindahl 1997; Dianov *et al.* 1999). PCNA is essential in LP-repair (Frosina *et al.* 1996) and may facilitate Fen1 recruitment to

DNA lesions and stimulate its enzymatic activity (Klungland and Lindahl 1997; Pascucci *et al.* 1999). The role of Fen1 is in endonucleolytic cleavage of the oligonucleotide displaced in repair patch synthesis, in addition to a postulated stimulatory function on nucleotide insertion by Polβ in LP-repair (Klungland and Lindahl 1997; Pascucci *et al.* 1999). The final step is ligation of the ends at the DNA nick created by the action of Fen1 (Hegde *et al.* 2008). In LP-repair, Ligase I, which is recruited by PCNA, mediates DNA end ligation activity and limits repair patch length (Pascucci *et al.* 1999; Levin *et al.* 2000).

Studies have illustrated a role for PARP1 in regulating choice between SP- and LP-repair and in promoting LP-repair. Repair of a uracil containing plasmid using MEF WCEs has illustrated reduced BER, particularly, LP-repair in a *parp1*$^{-/-}$ background (Dantzer *et al.* 2000). The stimulatory effect of PARP1 on BER in this case was dependent on NAD^+, implicating PARP1 catalytic activity in this process (Dantzer *et al.* 2000). Consistently, PARP catalytic inhibition reduces PCNA recruitment to DNA SSBs *in vivo* (Lan *et al.* 2004). Whether the contribution of PARP1 catalytic activity reflects its role in recruiting downstream repair components via PAR or the prolonged retention of PARP1 at damage sites in the absence of automodification is not clear. Furthermore, a plasmid repair assay using purified human enzymes has illustrated stimulation of Polβ-mediated strand displacement by PARP1 in association with Fen1 (Prasad *et al.* 2001). The contribution of PARP1 to LP-repair has also been attributed to its transcriptional regulatory role, whereby cellular levels of Ligase I and Fen1 are reduced in *parp1*$^{-/-}$ murine cells (Sanderson and Lindahl 2002).

1.3.3 Double-strand break repair

As mentioned in section 1.2, toxic DNA DSBs can be induced via programmed mechanisms or by DNA damaging agents that lead to DNA strand breakage. With DNA damaging agents, clustered SSBs can form DSBs, but isolated SSBs or base damage can also induce DSBs when encountered by the replication fork. The difficulty posed by DNA DSBs arises from the fact that both strands of the DNA helix are damaged and DNA ends can physically dissociate. This precludes exploitation of the complementary nature of the DNA molecule, as would be the case when DNA damage alters only one strand. Instead, DNA ends need to be rejoined, and cells have evolved numerous mechanistically distinct pathways to resolve DNA DSBs. These DSB repair pathways can be broadly divided into homology directed repair, and non-homologous end joining (NHEJ). Regulation of repair pathway utilisation is critical for maintaining genomic integrity and is determined by the cell type, cell-cycle stage, chromosomal location of the DNA lesion as well as the complexity and extent of damage. Inaccuracies in DSB repair can lead to chromosomal translocations, deletions or amplifications. In multicellular organisms this can cause tumourigenesis via loss of tumour suppressor genes or activation of oncogenes (Khanna and Jackson 2001; Heyer *et al.* 2010).

1.3.3.1 Homologous recombination (HR)

HR is a relatively error-free form of DSB repair, characterised by the use of homologous DNA to serve as a template for repair. In *S. cerevisiae* and mammalian cells, the homologous template preferentially takes the form of sister chromatids (Kadyk and Hartwell 1992; Johnson and Jasin 2000). This is facilitated by regulatory

processes that promote HR in S/G2 phases of the cell-cycle, and by the close association of sister chromatids by cohesion (Heyer *et al.* 2010; Moynahan and Jasin 2010). Diploid cells can also use homologous chromosomes as repair templates, as demonstrated in *S. cerevisiae* (Kadyk and Hartwell 1992), although this can lead to loss of heterozygosity (Moynahan and Jasin 2010).

The defining feature of HR is DNA synapsis, when DNA strand invasion and homology search occurs. On this basis, HR can be divided into three main sections: pre-synapasis, synapsis and post-synapsis (Figure 1.4). In the presynaptic stage of HR, the 5' ending strand of the DNA DSB undergoes processing to generate a 3' ssDNA overhang. In some cases, resection of the DSB ends reveal direct repeats and single-strand annealing (SSA) between these repeats can occur, with the concomitant deletion of the intervening sequence and one of the repeats. However, SSA is not accompanied by DNA synapsis that is characteristic of HR. Conversely, in synapsis, the 3' ssDNA overhang can invade intact duplex DNA to carry out homology search. On locating a suitable template, DNA synthesis occurs, primed by the 3' end of the invading strand of the DSB leading to gene-conversion. The post-synaptic stage of HR can be achieved via several different mechanisms, which broadly gives rise to crossover (CO) or non-crossover (NCO) products. NCO products display gene conversion at the break site, whilst CO products have additional exchange of genetic material flanking the break site. Synthesis dependent strand annealing (SDSA), gives rise to exclusively NCO products via the displacement of the invading strand following DNA synthesis which reanneals with the other end of the DSB. Alternatively, the second resected end of the DSB can also engage with the displaced strand of the template DNA, creating a double Holliday junction (dHJ), which can be

resolved to give CO or NCO products. Whilst resolution by CO is beneficial in the context of meiosis to generate genetic diversity and ensure correct chromosomal segregation, it can also lead loss of heterozygosity, and is thus suppressed in mitotic cells (San Filippo *et al.* 2008; Heyer *et al.* 2010).

HR can also proceed by break induced replication (BIR), where DNA from the strand invasion site to the chromosome end is replicated, leading to extensive LOH downstream of the break site. However, BIR enables repair of broken (one-ended DSB) or stalled replication forks (San Filippo *et al.* 2008).

1.3.3.1.1 Resection of DNA DSB ends

DNA end resection is a key regulatory step in DSB repair that is restricted to S/G2 phases of the cell cycle. The process of resection commits cells to HR and SSA, whilst making DNA ends increasingly refractory to repair by NHEJ. The process of resection is complex, whereby the 5' end of the DNA DSB is nucleolytically processed by several nucleases/helicases to generate a 3' overhang (San Filippo *et al.* 2008). In eukaryotes, DNA end resection is mediated by evolutionarily conserved nucleases/helicases, and is proposed to occur in two stages, namely, initial resection of a few hundred nucleotides, followed by extensive resection (Huertas 2010).

In *S. cerevisiae*, the initiation of end resection is carried out by the MRX/Sae2 complex (Mimitou and Symington 2008; Zhu *et al.* 2008). Disruption of *mre11,* a component of MRX complex, or *sae2* leads to enhanced IR sensitivity and defective resection initiation (Huertas *et al.* 2008; Mimitou and Symington 2008; Zhu *et al.* 2008). However, the nuclease function of MRX/Sae2 is unclear as resection kinetics

in cells only expressing nuclease-dead Mre11 are similar to wild-type (Llorente and Symington 2004), unless DNA ends are occluded, as illustrated by meiotic DSBs, where Spo11 remains bound to DNA ends (Longhese *et al.* 2010). Instead, MRX/Sae2 may primarily bind DNA to prevent interference by NHEJ and to stimulate resection by loading long-range resection components at DNA DSBs (Nicolette *et al.* 2010; Shim *et al.* 2010). In vertebrates, a homologous complex, MRN/CtIP, performs this resection function in association with Brca1 (Sartori *et al.* 2007; Chen *et al.* 2008; Yun and Hiom 2009).

In *S. cerevisiae mre11* and *sae2* mutants, despite the delayed resection initiation, long-range resection occurred with wildtype kinetics, indicating the existence of distinct nucleases in this process (Zhu *et al.* 2008). Consistently, in yeast, long-range resection is carried out by the nuclease Exo1 or the Dna2/Sgs1/Top3/Rmi1 complex, where Dna2 is the nuclease and Sgs1 functions as a helicase (Gravel *et al.* 2008; Mimitou and Symington 2008; Zhu *et al.* 2008). Functional redundancy between Exo1 and the Dna2/Sgs1/Top3/Rmi1 complex is supported by the synergistic reduction of long-range resection in double-mutants at an endonuclease-generated DNA DSB versus the single mutants, which are still competent for resection *in vivo* (Gravel *et al.* 2008; Mimitou and Symington 2008; Zhu *et al.* 2008). In human cells, the *S. cerevisiae* Exo1 and Dna2/Sgs1/Top3/Rmi1 orthologues are EXO1 and DNA2/BLM/TopIIIα/RMI1/RMI2, respectively. EXO1 and BLM may possess some distinct functions in DSB end processing, as ssDNA formation is reduced when each protein is independently depleted (Gravel *et al.* 2008). However, the resection defect following co-depletion of BLM and EXO1 is synergistic, illustrating the functional redundancy between these genes (Gravel *et al.* 2008).

1.3.3.1.2 Synapsis: DNA strand invasion and homology search

Following DNA end resection, the resultant 3' ssDNA overhang is coated in Rad51 monomers to form the Rad51 nucleoprotein filament. This ssDNA-Rad51 nucleoprotein filament can engage in the homologous pairing and strand exchange reactions of synapsis *in vitro* (Benson *et al.* 1994; Baumann *et al.* 1996; Sung 1997a). Formation of the Rad51 filament consists of two stages: Rad51 nucleation on ssDNA followed by Rad51 filament extension (van der Heijden *et al.* 2007; Holthausen *et al.* 2010). However, the 3' DNA overhang is initially coated by RPA, which whilst stimulating recombination by protecting DNA from nucleolytic degradation and removing secondary DNA structure, is also a barrier to Rad51 filament formation (Sung 1997a; Sugiyama *et al.* 1998; San Filippo *et al.* 2008). Recombination mediators overcome the RPA barrier by stimulating Rad51 nucleation (Sung *et al.* 2003; San Filippo *et al.* 2008). The *S. cerevisiae* genome encodes two mediators, Rad52 and the Rad51 homologue complex, Rad55-Rad57 (Heyer *et al.* 2010). Metazoans contain six recombination mediators: Brca2 and five Rad51 homologues, RAD51B-RAD51C, RAD51D-XRCC2 and RAD51C-XRCC3 (Heyer *et al.* 2010).

Although Rad52 is conserved in all domains of life, its importance is only apparent in fungi, where Rad52 is involved in all HR pathways. Consistently, *S. cerevisiae* *ΔRad52* strains are very sensitive to IR, phleomycin and CPT, and display severe HR defects (Gravel *et al.* 2008). In vertebrates Brca2, which is absent from *S. cerevisiae*, is the major mediator (Heyer *et al.* 2010), whilst the importance of Rad52 is only revealed in a Brca2-depleted background (Feng *et al.* 2011). Purified *S. cerevisiae* Rad52 interacts with Rad51, RPA and ssDNA to stimulate Rad51 nucleation on RPA coated ssDNA (Sugiyama and Kowalczykowski 2002). Purified Brca2 may function

similarly to Rad52 by interacting with Rad51 via its BRC repeats and targeting Rad51 nucleation to RPA-bound ssDNA over dsDNA (Jensen *et al.* 2010; Liu *et al.* 2010; Thorslund *et al.* 2010).

Once nucleation has occurred, the Rad51 nucleus expands on ssDNA, forming a nucleoprotein filament, stabilised by Rad55-Rad57. The presynaptic filament searches for homology within duplex DNA, and once located, the Rad51 nucleoprotein filament displaces a strand of the duplex DNA which becomes coated in RPA, and forms a D-loop (San Filippo *et al.* 2008). In humans and *S. cerevisiae*, Rad54 stimulates strand invasion and D-loop formation *in vitro*, in a process dependent on its ATP-dependent dsDNA translocase activity (Petukhova *et al.* 1998; Solinger *et al.* 2001; Alexiadis and Kadonaga 2002; Mazina and Mazin 2004). Subsequent to this, Rad54 may also mediate Rad51 filament disassembly to provide access to downstream enzymes, including DNA polymerases for DNA synthesis (Hilario *et al.* 2009; Li and Heyer 2009). DNA synthesis primed from the 3' end of the invading strand entails the function of Polη, but not Polδ in human cells *in vitro* (McIlwraith *et al.* 2005). More recently, in a reconstituted reaction, *S. cerevisiae* Polη and δ have been implicated in D-loop processive DNA synthesis in a PCNA-dependent manner (Li *et al.* 2009). Following DNA synthesis, HR can proceed via SDSA or dHJ formation, which determines whether DSBs are repaired by CO or NCO mechanisms.

In SDSA, following DNA synthesis across the break site, the invading 3' strand is displaced and base pairs with the 3' overhang of the other half of the DNA DSB, serving as a template for further DNA synthesis (San Filippo *et al.* 2008; Heyer *et al.*

2010). Any additional DNA can be removed as a flap, and the DNA ends ligated together to complete repair. In *S. cerevisiae* NCO products are almost exclusively formed from SDSA, and may represent the major pathway for NCO HR (Mitchel *et al.* 2010). In eukaryotes, a number of helicases are implicated in this process (Heyer *et al.* 2010), and in *S. cerevisiae*, may include the Srs2 helicase given its ability to bind to and unwind D-loop structures *in vitro* (Dupaigne *et al.* 2008). In humans, this function may be mediated by RTEL1, FANCM or BLM (Heyer *et al.* 2010).

1.3.3.1.3 Double Holliday junction (dHJ) formation and resolution

In DSBR, both yeast and human Rad54 catalyse branch migration to form more extensive D-loops, and facilitate bypassing of mismatches, followed by more extensive DNA synthesis (Bugreev *et al.* 2006). The extending strand eventually reanneals with the resected strand of the other half of the DNA DSB. Concomitantly, with further branch migration and DNA synthesis, the displaced strand of the extended D-loop shows homology to non-invading 3' overhang and anneals, to be used as a template for DNA synthesis (second end capture). Following additional DNA synthesis and ligation, a dHJ is formed. *In vitro*, the process of second end capture is attributed to Rad52 and RPA (McIlwraith and West 2008; Nimonkar *et al.* 2009).

The final stage of DSBR, HJ resolution, can proceed by pathways that generate crossover or non-crossover products. Alternatively, the dHJ can undergo dissolution to form exclusively non-crossover products. In humans, HJ dissolution is achieved by the BLM/TopIIIα/RMI1/RMI2 complex (Wu and Hickson 2003). In the absence of

BLM, enhanced sister-chromatid exchange is observed, illustrating the importance of its contribution to genome stability. Conversely, *in vitro,* HJ resolution can be mediated by the human nucleases Gen1 (Ip *et al.* 2008; Rass *et al.* 2010) and Mus81/Eme1 (Taylor and McGowan 2008), which may function in association with the nuclease SLX1-SLX4 (Fekairi *et al.* 2009; Munoz *et al.* 2009; Svendsen *et al.* 2009). A similar arsenal of helicases and nucleases exist in *S. cerevisiae*, namely Sgs1/Top3/Rmi1, Slx1/Slx4, Mus81/Mms4 and Yen1 (Heyer *et al.* 2010). In *S. cerevisiae*, relative to meiotic cells, mitotic cells form a very low number of dHJs (Bzymek *et al.* 2010). Nevertheless, their occurrence illustrates that SDSA is not the sole pathway of HR in mitotic yeast cells.

Human and *S. cerevisiae* Rad52 also engages in the Rad51-independent SSA pathway (Ivanov *et al.* 1996; Stark *et al.* 2004) . *In S. cerevisiae*, this occurs via species specific interactions between Rad52 and RPA, in a process enhanced by Rad59, to promote the annealing of complementary RPA coated ssDNA strands *in vitro* (Ivanov *et al.* 1996; Sugiyama *et al.* 1998; Wu *et al.* 2006). Following homologous pairing between repeats, the 3' non-homologous intervening sequence is removed. This is via the combined action of Slx4/Saw1/Rad1/Rad10, whereby Saw1 directs the Rad1/Rad10 structure specific endonuclease to the flap-structure (Ivanov and Haber 1995; Li *et al.* 2008). Saw1 also interacts with Msh2/Msh3, which also functions in concert with Rad1/Rad10 to remove the 3' flap in SSA (Sugawara *et al.* 1997; Li *et al.* 2008). In vertebrates, the Rad1/Rad10 homologue is ERCC1/XPF.

1.3.3.2 NHEJ

NHEJ is evolutionarily conserved from prokaryotes to eukaryotes and represents a DSB repair subpathway that is mechanistically distinct from HR (Lieber 2010). It is the major DSB repair pathway in mammals, with NHEJ-deficient mutants showing enhanced sensitivity to IR at all stages of the cell cycle (Rothkamm *et al.* 2003; Falck *et al.* 2005; Mao *et al.* 2008; Beucher *et al.* 2009). Conversely, in *S. cerevisiae*, NHEJ-deficient strains have minimal IR sensitivity, except in an HR-deficient background (Boulton and Jackson 1996a; Boulton and Jackson 1996b). In addition, NHEJ is also involved in vertebrate immune system diversity via V(D)J recombination and class-switch recombination (Section 1.2.1.3) (Lieber 2010). NHEJ is characterised by the direct ligation of DNA ends together without the need for a homologous DNA template (Lieber 2010). The repair of endonucleolytically generated DSBs with ligatable and complementary ends can be precise in mammals and *S. cerevisiae* (Clikeman *et al.* 2001; Shrivastav *et al.* 2008). However, mutations can arise from the processing of complex DNA ends to make them ligatable via the insertion or deletion of nucleotides (Lieber 2010), although this pathway is very inefficient in yeast (Clikeman *et al.* 2001). The NHEJ pathway is a multistep pathway comprising of 3 major processes, DNA DSB recognition, DNA end processing and finally, ligation (Lieber 2010), which will be discussed in the sections below (Figure 1.5).

1.3.3.2.1 DNA damage recognition: The DNA-PK holoenzyme

The initial DSB recognition is mediated by the Ku70/Ku80 heterodimer that is conserved throughout eukaryotes and binds DNA ends with high affinity. *In vivo,* Ku rapidly associates with damaged DNA and shows dynamic association with DNA

ends (Mari *et al.* 2006; Uematsu *et al.* 2007). The crystal structure of Ku reveals it to be ring shaped with a broad base that cradles DNA (Walker *et al.* 2001). However, with the exception of some contributions of loops into the major and minor grooves of DNA and minimal contacts with the DNA backbone, Ku does not interact with DNA bases, ensuring its lack of sequence specificity (Walker *et al.* 2001). Subsequent to DNA end binding, Ku likely undergoes structural rearrangements (Rivera-Calzada *et al.* 2007), and in vertebrates, this may facilitate its interaction with the protein kinase, DNAPKcs, to recruit the latter protein to DNA DSBs (Uematsu *et al.* 2007). The C-terminus of Ku80 mediates its interaction with DNAPKcs (Falck *et al.* 2005), and together these proteins form the DNAPK holoenzyme. DNA binding by DNAPKcs activates its kinase activity enabling it to phosphorylate several targets *in vitro,* including Ku, and other downstream components of NHEJ (Dobbs *et al.* 2010). However, the only phosphorylation event shown to be of significance *in vivo* is DNAPKcs autophosphorylation (Dobbs *et al.* 2010). These autophosphorylation events modulate DNAPKcs association with DNA ends and kinase-dead mutants display increased IR sensitivity and repair defects (Kurimasa *et al.* 1999). This is due to enhanced DNAPKcs association at DNA ends that prevent DNA end processing and ligation (Weterings *et al.* 2003; Block *et al.* 2004; Goodarzi *et al.* 2006; Meek *et al.* 2007; Uematsu *et al.* 2007).

Additional functions of DNAPK may be to recruit proteins to the DNA DSB, including NHEJ components downstream in the pathway, such as the Ligase complex (Nick McElhinny *et al.* 2000; Ma *et al.* 2004; Mari *et al.* 2006) and DNA polymerases (Ma *et al.* 2004). In addition, DNA-PKcs may tether DNA ends together, as visualised *in vitro* (Yaneva *et al.* 1997; DeFazio *et al.* 2002; Spagnolo *et al.* 2006). It

should be noted that with the exception of *D. discoideum* (Block and Lees-Miller 2005; Hudson *et al.* 2005) and *A. gambie* (Dore *et al.* 2004), lower eukaryotes do not contain DNAPKcs orthologues. Therefore, in *S. cerevisiae*, DNA end tethering may be mediated by MRX (Chen *et al.* 2001; Hopfner *et al.* 2002) and in vertebrates, MRN may play a similar tethering role in addition to DNAPKcs (Dinkelmann *et al.* 2009; Xie *et al.* 2009).

1.3.3.2.2 DNA end processing

DNA end processing is necessary at complex DNA ends, to create the 3' hydroxyl and 5' phosphate that are necessary for ligation, in a process that can involve the gain or removal of nucleotides. Processing is carried out in an iterative fashion whereby several possible pathways can be undertaken through the action of independently functioning enzymes, to create ligatable DNA ends (Ma *et al.* 2004; Ma *et al.* 2005). The order in which DNA end modification occurs can influence the sequence at the repair junction, and the template independent nature of the processing event can lead to the accumulation of mutations. Several processing enzymes have been implicated in NHEJ, such as Artemis, PolX family polymerases, APTX, APLF, PNKP and MRN. This section will focus on Artemis and APLF, whilst PNKP and APE1 have been discussed previously in SSB repair, and likely confer similar processing roles in DSB repair.

Artemis is a nuclease of the metallo-β-lactamase family that functions in a subset of NHEJ reactions in G0/G1 of the cell cycle and in V(D)J recombination (Moshous *et al.* 2001; Beucher *et al.* 2009). In Artemis deficient cells, repair in G1 is defective for 10-20% of IR induced DSBs (Moshous *et al.* 2001; Riballo *et al.* 2004; Mohapatra *et*

al. 2011). This is relative to cells deficient in components of the ligase complex which are severely defective in DSB repair (Riballo *et al.* 2004; Beucher *et al.* 2009). As such, Artemis is not a core NHEJ component, but rather, functions in a subset of NHEJ events. Artemis displays processive 5'→3' exonuclease activity on ssDNA and on ssDNA overhangs (Ma *et al.* 2002; Ma *et al.* 2005). Artemis also interacts with DNA bound DNAPKcs *in vivo* (Ma *et al.* 2002), and this confers additional endonuclease activity to Artemis to cleave 5' and 3' ssDNA overhangs at the ssDNA/dsDNA junction, and DNA hairpins generated by RAG in V(D)J recombination (Ma *et al.* 2002; Ma *et al.* 2005; Goodarzi *et al.* 2006). The role of Artemis in NHEJ has been attributed to the processing of complex DNA ends (Riballo *et al.* 2004). This is supported by the reversal of the enhanced IR and bleomycin sensitivity in G0/G1 cells by expression of wild-type but not endonuclease-dead Artemis (Mohapatra *et al.* 2011). Furthermore, Artemis can cleave DNA termini containing 3' phosphoglycolate groups (Povirk *et al.* 2007; Yannone *et al.* 2008). In G1, Artemis is involved in the pathways that resolve the slowly repaired fraction of DNA damage. These fractions have also been associated with heterochromatin, implicating Artemis in the NHEJ repair of heterochromatic DSBs in G1 (Goodarzi *et al.* 2008; Beucher *et al.* 2009). In G2, Artemis is also involved in heterochromatic DSB repair via the HR pathway (Beucher *et al.* 2009).

Whilst Artemis is regarded as the major NHEJ nuclease, APLF can also confer this function in a complementary manner to Artemis *in vitro* (Li *et al.* 2011). This may be via a role for APLF in NHEJ repair of incompatible DNA ends to a similar extent as Artemis, and in a manner that cannot be modified by core-NHEJ components *in vitro* (Li *et al.* 2011). The non-compatible NHEJ stimulation by APLF is attributed to its

nuclease activity given the nature of the ligated DNA junctions (Kanno *et al.* 2007; Li *et al.* 2011). *In vitro*, APLF displays 3'→5' exonuclease activity on ssDNA, and ssDNA endonuclease activity on 3' and 5' overhangs (Kanno *et al.* 2007; Li *et al.* 2011), but unlike Artemis, cannot cleave hairpins (Li *et al.* 2011).

1.3.3.2.3 Ligation

The final stage of NHEJ is the ligation of DNA ends together in a process catalysed by Ligase IV/XRCC4 in mammals, and Dnl4/Lig 1 in *S. cerevisiae.* The function of these complexes in NHEJ have been illustrated by *in vivo* plasmid repair assays in *S. cerevisiae* (Teo and Jackson 1997; Wilson *et al.* 1997) and DSB viability and V(D)J recombination assays in mammals (Li *et al.* 1995; Grawunder *et al.* 1997; Grawunder *et al.* 1998). In both cases, disruption of the ligase complex leads to similar defects as when components of Ku are disrupted, implicating it as a core NHEJ component. An additional component of the ligase complex is Nej1 in yeast (Ooi *et al.* 2001; Valencia *et al.* 2001) and XLF in humans (Ahnesorg *et al.* 2006; Buck *et al.* 2006). The role of XLF/Nej1 in ligation may be to facilitate the readenylation of Ligase IV/Dnl4 (Riballo *et al.* 2009), and its contribution to NHEJ is particularly apparent at blunt and non-compatible DNA ends (Gu *et al.* 2007; Tsai *et al.* 2007). The recruitment of XRCC4/Ligase IV/XLF to DNA DSBs is mediated by its interactions with Ku (Nick McElhinny *et al.* 2000; Mari *et al.* 2006), and consistently, the ligase complex is recruited with early kinetics to DNA DSBs in yeast (Zhang *et al.* 2007; Yano *et al.* 2008; Chen and Tomkinson 2011). This interaction with Ku may also serve the further function of stabilising the binding of Ku to DNA ends to promote NHEJ (Zhang *et al.* 2007; Yano *et al.* 2008; Chen and Tomkinson 2011).

1.3.3.3 Alternative-NHEJ (a-NHEJ)

Vertebrate NHEJ-deficient mutants exposed to IR display residual, slow DSB repair that is independent of HR (DiBiase *et al.* 2000; Wang *et al.* 2001; Wang *et al.* 2006; Wu *et al.* 2008). Furthermore, end-joining assays measuring repair of an endonucleolytically generated plasmid/chromosomal DSB further illustrate a slower alternative end-joining in NHEJ-deficient yeast and vertebrate cells (Ma *et al.* 2003; Wang *et al.* 2003; Wang *et al.* 2005; Wang *et al.* 2006; Guirouilh-Barbat *et al.* 2007; Schulte-Uentrop *et al.* 2008; Wu *et al.* 2008; Xie *et al.* 2009; Mansour *et al.* 2010). This led to the identification of alternative-NHEJ (a-NHEJ), also known as backup-NHEJ or microhomology-mediated end joining (MMEJ), as an evolutionarily conserved DSB repair pathway that functions distinctly from NHEJ and HR (Iliakis 2009; Mladenov and Iliakis 2011).

In mammals, PARPs are implicated in a-NHEJ (Audebert *et al.* 2004; Wang *et al.* 2006; Mansour *et al.* 2010), and consistent with this, PARP1 binds dsDNA ends *in vitro* and is activated by DNA DSBs *in vivo* (Audebert *et al.* 2004; Wang *et al.* 2006; Iles *et al.* 2007; Haince *et al.* 2008; Dong *et al.* 2010; Cheng *et al.* 2011; Langelier *et al.* 2011). At DSBs, PARP1 may synapse DNA ends, as has been demonstrated *in vitro* (Audebert *et al.* 2004; Audebert *et al.* 2006; Audebert *et al.* 2008), in a manner that is stimulated by Histone H1 (Rosidi *et al.* 2008). Furthermore, catalytically active PARP1 may recruit downstream components of the repair pathway via the synthesis of PAR. Consistent with this, Mre11 co-immunoprecipitates with PARylated PARP1, and is recruited following PARP1 accumulation at DNA damage (Haince *et al.* 2008). Genetic analysis has implicated CtIP and MRN in mammalian a-NHEJ, possibly to resect DNA ends and reveal microhomology (Dinkelmann *et al.*

2009; Rass *et al.* 2009; Xie *et al.* 2009; Yun and Hiom 2009; Lee-Theilen *et al.* 2011; Zhang and Jasin 2011). However, a consequence of end-resection is increased deletions at a-NHEJ repair junctions, as revealed by repair joint sequencing (Guirouilh-Barbat *et al.* 2007; Schulte-Uentrop *et al.* 2008; Mansour *et al.* 2010). Microhomology may facilitate DNA end synapsis and ligation *in vitro* (Audebert *et al.* 2008), although this is not a prerequisite for a-NHEJ (Audebert *et al.* 2008; Mansour *et al.* 2010). Further processing enzymes which may play a role in a-NHEJ include PNKP in humans, as illustrated *in vitro* (Audebert *et al.* 2006). However, certain complex DNA ends are refractory to a-NHEJ, including terminal abasic sites which are repaired by NHEJ via the dRP lyase activity of Ku (Roberts *et al.* 2010). The final step of mammalian a-NHEJ, DNA end ligation, is mediated by Ligase III/XRCC1, as has been indicated *in vitro* and *in vivo* (Audebert *et al.* 2004; Wang *et al.* 2005; Audebert *et al.* 2006). As in BER, Ligase III/XRCC1 may be recruited to DSBs via its interaction with PARylated PARP1. *In vitro*, a-NHEJ has been reconstituted with PARP1, XRCC1/Ligase III and PNKP, and is capable of ligating various DNA substrates including those with compatible, blunt and non-compatible DNA ends (Audebert *et al.* 2004; Audebert *et al.* 2006; Audebert *et al.* 2008).

Under NHEJ-proficient conditions, Ku negatively regulates a-NHEJ due to its greater affinity for DNA ends versus PARP1 (Wang *et al.* 2006), and the inhibition of end-resection at Ku-bound DNA ends (Liang *et al.* 1998; Lee and Lee 2007). The inhibitory action of Ku is apparent even when downstream components of the NHEJ pathway are absent, likely due to continued Ku binding at DNA ends. This is illustrated by increased plasmid end-joining repair when Ku is depleted in a *ligaseIV*$^{-/-}$ or *dnapkcs*$^{-/-}$ background (Wang *et al.* 2006; Fattah *et al.* 2010). Furthermore, PARP1

and MRN recruitment to chromatin post-DNA DSB induction is enhanced in *ku80*$^{-/-}$ strains, and this is accompanied by increased DNA end-resection (Cheng *et al.* 2011). The benefit of downregulating a-NHEJ when NHEJ is proficient is that a-NHEJ may mediate chromosomal translocations (Simsek and Jasin 2010; Zhang and Jasin 2011). This may account for the exquisite IR sensitivity of mammalian NHEJ-deficient cells, where the multiple DSBs generated may be misjoined by a-NHEJ. Nevertheless, a-NHEJ may be essential in NHEJ deficient cells, particularly in embryonic development as illustrated by the embryonic lethality of *ku80*$^{-/-}$*/parp1*$^{-/-}$ mice (Tong *et al.* 2002; Henrie *et al.* 2003).

1.3.3.4 Regulation of DSBR

DNA DSBs are highly toxic lesions which if unrepaired, can lead to lethality. Eukaryotes have therefore devised numerous DSB repair pathways to resolve this damage, although their misuse can be detrimental. In G0/G1, NHEJ is preferred due to the absence of homologous chromosome templates in haploids, and the risk of loss-of-heterozygosity in diploids. Similarly, HR is preferentially utilised at broken/stalled replication forks, which represent one-sided DSBs that are unsuitable for NHEJ. Misuse of NHEJ in these cases is linked to increased chromosomal translocations/aberrations and lethality, and several regulatory pathways exist to mediate this (Shrivastav *et al.* 2008; Heyer *et al.* 2010).

IR sensitivity profiles of NHEJ- and HR-deficient vertebrate mutants have illustrated the differential contribution of NHEJ and HR during the cell-cycle. Whilst NHEJ is active throughout, it is especially important in G0/G1 when HR cannot occur (Lee *et al.* 1997; Takata *et al.* 1998; Rothkamm *et al.* 2003). Conversely, HR can be utilised

in S/G2, and is particularly important during S-phase, when NHEJ makes little contribution (Lee *et al.* 1997; Takata *et al.* 1998; Rothkamm *et al.* 2003). In M-phase, HR is downregulated, presumably to prevent recombination, which would interfere with chromosome segregation. The question arises as to how HR is upregulated in S/G2 and NHEJ-interference prevented in S-phase. Furthermore, NHEJ and HR compete/collaborate in G2, when both pathways function and active or passive regulatory mechanisms may exist to direct specific repair pathways to resolve DNA lesions.

Competition between NHEJ and HR is implied in vertebrates by the increased HR in NHEJ-deficient mutants (Fukushima *et al.* 2001; Pierce *et al.* 2001; Allen *et al.* 2002). In DT40 cells, this competition has been emphasised by the increased IR-resistance in Ku mutants, implying that NHEJ interferes with HR (Fukushima *et al.* 2001). Consistently, Ku binding to DNA ends makes them refractory to nucleolytic processing in yeast and mammals (Liang and Jasin 1996; Lee *et al.* 1998; Mimitou and Symington 2010), and inhibits DNA binding of other DSB sensors, including PARP1 (Cheng *et al.* 2011). Due to the high DSB-binding affinity of Ku, it is rapidly recruited to DNA DSBs, prior to HR-components (Kim *et al.* 2005). However, processes that downregulate Ku-binding to DNA ends, such as DNA end resection, reduce the likelihood of NHEJ occurring at a particular DSB, in favour of HR (Frank-Vaillant and Marcand 2002; Shibata *et al.* 2011). In line with this, inhibition of DNA-end resection increases NHEJ (Ira *et al.* 2004), whereas mutations that inhibit HR downstream of resection, such as Brca2 deficiency, have less of a positive impact on NHEJ (Stark *et al.* 2004). Thus the balance between NHEJ and HR is likely mediated, in part, by these initial DNA binding/processing events, and represents a

key regulatory position in determining whether DSBs are repaired by NHEJ or HR. Post-translational modifications and transcriptional regulation provides a means of exerting this regulation (Shrivastav *et al.* 2008; Heyer *et al.* 2010).

1.3.3.4.1 Regulation of HR by CDKs

As mentioned previously, HR is restricted to S/G2 phases of the cell cycle, and DNA end-resection is minimal in G1. One mechanism by which this is achieved is via the positive regulation of the resection machinery by CDKs in yeast and mammals, which regulate cell-cycle progression. In *S. cerevisiae*, the positive role of CDK1 in HR has been illustrated by the reduced DNA end-resection in CDK1 inhibited cells (Aylon *et al.* 2004; Ira *et al.* 2004). This was accompanied by reduced HR and increased NHEJ, in line with the competition between the two DSB repair pathways (Ira *et al.* 2004). Subsequently, S267 of Sae2, which initiates resection with MRX, was identified as a CDK1 phosphorylation target (Huertas *et al.* 2008). In *S. cerevisiae*, Sae2 S267A mutants exhibit impaired chromosomal resection similar to *sae2Δ* strains (Huertas *et al.* 2008). The function of Sae2 phosphorylation in Sae2/MRX function is unclear (Longhese *et al.* 2010). However, Sae2/MRX can reduce Ku binding to DNA DSBs, either by initiating minimal resection, or by physically blocking DNA ends from Ku and promoting long-range resection (Mimitou and Symington 2010; Shim *et al.* 2010). During G1, in the absence of Ku, MRX recruitment to DNA DSBs is enhanced and end-resection initiation can occur (Clerici *et al.* 2008). This suggests that CDK phosphorylation of Sae2 may promote its binding to DNA ends in competition with Ku to channel repair into HR. The vertebrate orthologue of Sae2, CtIP, demonstrates evolutionary conservation of Sae2 S267 at T847 (Sartori *et al.* 2007; Yun and Hiom 2009). CtIP T847 is also phosphorylated by CDKs in a cell-

cycle regulated manner during S/G2 and exerts similar effects on vertebrate DNA end resection (Huertas and Jackson 2009; Yun and Hiom 2009). CtIP is also phosphorylated by CDKs at S327 during S-phase (Yu and Chen 2004; Yun and Hiom 2009), which enables its interaction with Brca1 to form the Brca1/MRN/CtIP complex that mediates end resection (Yu and Chen 2004; Chen *et al.* 2008). Mutating S327 to Alanine inhibits formation of this complex and consequently, inhibits CtIP recruitment to DNA damage sites and DNA end resection (Chen *et al.* 2008; Yun and Hiom 2009). In vertebrates, phosphorylation at both these sites is required for efficient DNA end resection and HR (Yun and Hiom 2009).

In *S. cerevisiae*, expression of the phospho-mimicking Sae2 S267E or deletion of *ku70/ku80* is sufficient to overcome inhibition of end-resection initiation in the absence of functional CDK1 (Chen *et al.* 2011). However, long-range end-resection is still defective due to the CDK1-mediated phosphorylation of Dna2 (Chen *et al.* 2011). Dna2 phosphorylation events are required for nuclear localisation of Dna2, although additional CDK1 targets are required for Dna2 DSB localisation to mediate end-resection (Chen *et al.* 2011). Therefore, CDK regulates multiple stages of the DNA resection process to ensure its occurrence during the correct cell cycle stage and promote HR by downregulating Ku association with DNA ends.

In M-phase, CDK activity can also downregulate HR, as evidenced by the negative-regulatory role of Brca2 phosphorylation that has been observed *in vitro* (Esashi *et al*. 2005). Brca2 phosphorylation by CDKs, occur on S3291 at the C-terminal domain of the protein during the G2 to M-phase transition (Esashi *et al.* 2005). This region of Brca2 is implicated in stabilising Rad51 nuclei, and its phosphorylation by CDKs

would prevent it interacting with Rad51 to elicit this stabilisation effect (Esashi *et al.* 2005; Esashi *et al.* 2007). These *in vitro* results are in line with *in vivo* observations whereby in M-phase, whilst CtIP phosphorylation by CDKs stimulates short-range resection and RPA nucleoprotein filament formation, the Rad51 filaments cannot form (Peterson *et al.* 2011). Thus, resection in M-phase precludes DSBs from being repaired by NHEJ, but inhibition of Rad51 filament formation also prevents HR which could interfere with chromosome segregation (Heyer *et al.* 2010; Peterson *et al.* 2011). Whilst a-NHEJ could also mediate repair in these cases (Lee-Theilen *et al.* 2011; Zhang and Jasin 2011), the DSB may also be maintained for repair in a subsequent cell cycle.

1.3.3.4.2 Downregulation of NHEJ during S-phase

In S-phase, NHEJ may be downregulated as determined by sensitivity assay studies illustrating an acute HR-dependence for replication-associated DNA DSBs (Rothkamm *et al.* 2003). The lethality of collapsed or stressed replication forks arising from their encountering SSBs or ICLs is due to the interference of NHEJ at these lesions (Adamo *et al.* 2010; Pace *et al.* 2010; Patel *et al.* 2011). In *brca2*-null cells, PARP inhibition leads to cell lethality, likely due to the accumulation of endogenously generated SSBs/base-damage that cause replication forks to collapse or stall (Bryant *et al.* 2005; Farmer *et al.* 2005). The toxicity of PARP inhibitors in these HR-deficient backgrounds is mainly due to toxic activation of NHEJ at these lesions leading to genomic instability (Patel *et al.* 2011). PARP inhibitor toxicity with respect to endogenous damage is only apparent in HR-deficient backgrounds, illustrating that HR can typically outcompete Ku. The role of PARPs in suppressing the toxic interference of Ku at replication-associated lesions arising from exogenous

damage has been previously illustrated, and functions in parallel with ubiquitylation (Hochegger *et al.* 2006; Saberi *et al.* 2007; Sugimura *et al.* 2008). The molecular basis behind the role of PARylation and ubiquitylation in these observations is unclear, but PARPs/Rad18 may target NHEJ components to downregulate their affinity for DNA damage at this cell-cycle stage.

1.3.3.4.3 Preferential use of HR in G2 at heterochromatin and complex DNA damage

In yeast and DT40 cells, progression through the cell cycle is accompanied by increased and preferential utilisation of HR due to enhanced end-resection capacity (Aylon *et al.* 2004; Sonoda *et al.* 2006). However, in mammals, when both HR and NHEJ can occur, NHEJ remains the predominant pathway. Consistently, in G2 of the cell cycle, NHEJ repairs 85% of IR-induced DSBs with fast kinetics, with HR repairing the remaining 15% of DNA DSBs with slower kinetics. The fraction of DSBs repaired by HR has been illustrated to represent heterochromatin. Thus, despite the high DNA DSB binding affinity of Ku and its rapid recruitment to these lesions, heterochromatin impedes NHEJ progression such that repair then slowly proceeds by HR. This heterochromatic DSB repair pathway employs the endonuclease activity of Artemis and the kinase activity of ATM (Beucher *et al.* 2009). DNA damage complexity has also been illustrated to dictate DSB repair pathway usage, with HR repairing DSBs associated with heightened DNA DSB end complexity (Shibata *et al.* 2011). Consistently, the complex DNA lesions induced by carbon ions are predominantly repaired by HR at all chromatin locations, whilst etoposide-mediated DNA DSBs are predominantly repaired by NHEJ, with HR repairing the heterochromatic fraction (Shibata *et al.* 2011). The scenario arising in mammals

therefore illustrates that NHEJ may primarily attempt DNA DSB repair in G2, and at barriers represented by chromatin and damage complexity, HR is then engaged and resects DNA ends. This DNA end resection precludes usage of NHEJ (Mao *et al.* 2008; Beucher *et al.* 2009; Shibata *et al.* 2011).

1.3.3.4.4 Transcriptional regulation of DSB repair

In some cases, DSB repair pathway capacity is controlled via transcriptional regulation, which has been shown to mediate HR proficiency. With respect to resection, expression of CtIP is controlled over the course of the cell cycle, with levels increasing during S/G2 (Huertas 2010). *S. pombe* Ctp1 exhibits a similar pattern of transcriptional regulation (Limbo *et al.* 2007). Furthermore, expression of HR components Rad51 and Rad52 is also transcriptionally regulated in mammals, independent of DNA DSB induction (Chen *et al.* 1997). With respect to NHEJ, diploid Mat**a**/Matα yeast regulate expression of Nej1, which forms part of the NHEJ Ligase complex. The Mat**a1**/Matα**2** transcriptional repressor, which is only expressed in diploids, downregulates Nej1 expression. This leads to the preferential usage of HR, as homologous chromosomes are present throughout the cell cycle in diploids (Valencia *et al.* 2001).

1.4 Model organisms to study DNA repair

Much of our knowledge of DNA repair has been derived from studies on lower eukaryotes, such as *S. cerevisiae* and *S. pombe*. The strength of these organisms stems from their genetic tractability which allows for generation of disruption strains. In particular, strains disrupted at numerous loci can be made, allowing the genetic

relationship between genes to be determined. Furthermore, several assays have been developed, including those exploiting mating type switching in *S. cerevisiae* and the use of the HO endonuclease. However, despite the strengths of yeast, a limitation is the absence of some repair genes and repair pathways that are present in vertebrates. These include DSB repair genes such as *artemis*, *dnapkcs*, PARPs, members of the Fanconi Anaemia (FA) pathway and components of the SSBR pathways such as XRCC1 and Ligase III. This created the impetus to identify other model organisms displaying repair gene conservation with higher organisms. Whilst *C. elegans* and *D. melanogaster* are useful with regards to conservation of repair genes, their multicellularity can exert some limitations. An alternative unicellular model that has entered the DNA repair arena is the eukaryote, *Dictyostelium discoideum*, which possesses a number of vertebrate repair genes absent in other lower eukaryotes.

1.4.1 *Dictyostelium discoideum*

Dictyostelium discoideum is a member of the eukaryotic *Dictyostelia* (social amoeba) group. These organisms display the unusual ability to exist as a unicellular feeding amoeba and then to aggregate into a multicellular structure upon starvation (Schaap *et al.* 2006). In nature, the soil dwelling *Dictyostelium discoideum* feeds on bacteria and yeast. During this feeding period, cells propagate mitotically and are predominantly in G2, displaying a very short S-phase and M-phase and no obvious G1-phase (Weijer *et al.* 1984; Muramoto and Chubb 2008). *Dictyostelium* monitor the abundance of food relative to cell density, and when food becomes scarce, a developmental cycle is initiated. Development is mediated by the extracellular signalling molecule cyclic AMP (cAMP), which is secreted as a chemoattractant to enable the collective aggregation of cells to form a mound composed of 100,000 cells. This mound can

transition into a slug, and finally a fruiting body, in which 20% of the cells undergo vacuolation to form the stalk, that supports the spore head composed of the remaining 80% of cells in the aggregate. The entire process of development takes approximately 24 hours (Figure 1.6). The spores which are resistant to environmental stress, can remain dormant for long periods of time and undergo germination when conditions are favourable (Schaap 2011). In the laboratory, spore germination can be synchronously induced by heatshock and is completed within 6 to 10 hours (Cotter and Raper 1966; Xu *et al.* 2004; Hudson *et al.* 2005).

1.4.2 *Dictyostelium discoideum* as a model organism

The initiation of *D. discoideum* as a model organism began with the isolation of an NC4-derived strain which could grow in liquid culture (axenic growth) due to mutations that increased macropinocytosis. Ax2 and Ax4 are commonly used axenic strains and their axenic growth is suitable for the culturing of large numbers of cells, facilitating numerous techniques (Watts and Ashworth 1970).

The 34Mbp *Dictyostelium* genome has been fully sequenced and is divided between 6 chromosomes that range in size from 4-9Mbp. Sequence analysis has indicated a 78% A+T bias in the *Dictyostelium* genome, although this can increase to 99% in the abundant, repetitive non-coding sequences (Eichinger *et al.* 2005). Nuclear DNA also contains an extrachromosomal 88kbp palindrome containing rDNA which is present in multiple copies (Ogawa *et al.* 2000; Sucgang *et al.* 2003; Eichinger *et al.* 2005). The *Dictyostelium* genome is predicted to encode 12500 genes (of which 12257 have been curated on dictyBase.org), which rivals that of *Drosophila*, even though its genome is 20% of the size (Eichinger *et al.* 2005). Thus, *Dictyostelium* is regarded as

having a compact genome, with gene numbers showing more similarity to multicellular than unicellular eukaryotes.

The phylogenetic relationship between *Dictyostelium* and other eukaryotes has revealed that *Dictyostelium* split from the branch giving rise to metazoa later than plants but earlier than fungi (Eichinger *et al.* 2005). However, *Dictyostelium* have diverged less than fungi and share protein domains with metazoa that are absent in both fungi and plants (Eichinger *et al.* 2005). Furthermore, the *Dictyostelium* genome encodes more genes related to those whose mutation is known to lead to human disease than yeast, strengthening its use as a model organism in this respect (Eichinger *et al.* 2005). Genes shared between both *Dictyostelium* and metazoa include G-protein coupled receptor (GPCR) groups that were initially thought to be specific to animals. Furthermore, *Dictyostelium* is the only non-metazoan showing conservation of the phosphor-tyrosine binding SH2 domain that is involved in intracellular signalling cascades (Eichinger *et al.* 2005). *Dictyostelium* also demonstrates shared conservation of DNA repair pathways and DNA repair components with vertebrates that are absent in lower eukaryotes, further highlighting them as an excellent model organism for studying this process (Block and Lees-Miller 2005; Hudson *et al.* 2005; Hsu *et al.* 2006). The genome sequence, annotated predicted and identified genes, RNA expression analysis and strain and plasmid resources are available for public access on a database (dictyBase.org).

The further strength of *Dictyostelium* as a model stems from its genetic tractability. Its haploid nature facilitates the disruption of genes which are not essential for growth, by targeted and random means (Kuspa and Loomis 1992; Adachi *et al.* 1994).

Furthermore, multiple targeted gene disruptions can be generated within a single strain via the recycling of selectable markers (Faix *et al.* 2004). Genes can be epitope-tagged and exogenously expressed in their wild-type or mutant form via the use of extrachromosomal shuttle vectors with the capacity to be propagated in both *Dictyostelium* and *E. coli* (Manstein *et al.* 1995).

1.4.3 DNA repair in *Dictyostelium*

Soil-dwelling *Dictyostelium* exhibits unusually high resistance to DNA damaging agents, possibly reflecting the production of mutagenic agents by the microorganisms within its ecosystem. These agents include UV, IR and chemical mutagens such as MMS, the chemotherapeutic agent cisplatin and the naturally occurring chemotherapeutic bleomycin. The basis behind this tolerance is unclear, but may reflect efficient repair pathways, making *Dictyostelium* a model for investigating DNA repair (Hsu *et al.* 2006).

Preliminary assessment of repair in *Dictyostelium* exploited radiation sensitive mutants (*rad* mutants). These mutants were classified into 11 complementation groups and displayed differential sensitivity to γ-radiation, UV, bleomycin and MMS (Welker and Deering 1976; Welker and Deering 1978; Bronner *et al.* 1992; Deering 1994; Deering *et al.* 1996). Some *rad* mutants, such as *radC*, only display sensitivity to UV, illustrating its specific role in the repair of these lesions (Deering 1994). Other mutants are sensitive to a broader range of DNA damaging agents. Parasexual genetics to generate double-mutants illustrated the existence of alternative repair pathways (Welker and Deering 1979). For example, although *radA* and *radB* are epistatic with regards to UV and IR, the *radA/radC* double-mutant has a synergistic

increase in UV sensitivity versus the single mutants, indicating their operation within different pathways (Welker and Deering 1979). Overall, this suggested the presence of alternative, multistep repair pathways to deal with the different forms of damage.

More recent analysis of the *Dictyostelium* genome has revealed conservation of components of several repair pathways. For example, conservation of the components of the nucleotide excision repair (NER) pathway have been illustrated, including the *repB* and *repD*, with homology to the XPD and XPB helicases (Lee *et al.* 1997). Truncated mutants of *repB* show sensitivity to UV, illustrating the contribution of this gene to repair of UV lesions (Lee *et al.* 1998). A homologue of the DNA damage recognition component XPE, *repE*, has also been identified (Alexander *et al.* 1996). Components of the BER pathway such as uracil DNA glycosylase have been purified and partially characterised (Guyer *et al.* 1986). AP endonucleases of the Endo IV and Exo III family have also been identified (Freeland *et al.* 1996; Tsuji *et al.* 2001) and disruptants of the Endo IV orthologue characterised for their sensitivity to DNA damaging agents (Tsuji *et al.* 2001). Components of HR and NHEJ pathways have also been identified in *Dictyostelium* (Block and Lees-Miller 2005; Hasegawa *et al.* 2005; Hudson *et al.* 2005; Hsu *et al.* 2006; Zhang *et al.* 2009). Furthermore, HR is an important pathway in *Dictyostelium*, with disruptions of HR genes, including *rad51*, possibly leading to lethality (Hasegawa *et al.* 2005; Hudson *et al.* 2005). This suggested *rad51*-disruption lethality is similar to the situation in mammals (Tsuzuki *et al.* 1996), indicating a similar contribution of genes to cell survival between *Dictyostelium* and higher eukaryotes.

A key strength of *Dictyostelium* as a model for DNA repair has been the identification of repair genes and repair pathways conserved only in vertebrates, and absent in other lower eukaryotes. For example, *Dictyostelium* encodes orthologues of DNAPKcs and Artemis, which both function in NHEJ, and a Brca2 orthologue has also been identified (Block and Lees-Miller 2005; Hudson *et al.* 2005; Zhang *et al.* 2009; Hsu *et al.* 2011). A minimal FA pathway which contributes to repair of cisplatin-induced intrastrand crosslinks (ICL) operates in *Dictyostelium* (Zhang *et al.* 2009). However, unlike vertebrates, in *Dictyostelium*, the FA pathway contribution to ICL repair is minor. The major ICL repair pathway is mediated via the XPF nuclease, independently of its role in NER and FA (Zhang *et al.* 2009). PARPs which are absent in *S. cerevisiae* and *S. pombe* are also conserved in *Dictyostelium* and similar to higher eukaryotes, respond to oxidative DNA damage (Auer *et al.* 1995; Otto *et al.* 2005; Rajawat *et al.* 2007).

The *Dictyostelium* cell cycle has also been characterised and has been established to consist of a short S and M-phase, and a protracted G2 phase (Weijer *et al.* 1984; Muramoto and Chubb 2008). Both NHEJ and HR repair DNA DSBs in vegetatively growing *Dictyostelium*, although HR is the major pathway, with NHEJ mutants showing minimal sensitivity (Hudson *et al.* 2005; Muramoto and Chubb 2008; Hsu *et al.* 2011). Germinated spores are also in G2 phase of the cell cycle, which should be able to support HR (MacWilliams *et al.* 2006; Muramoto and Chubb 2008), although the contribution of NHEJ in this developmental stage is greater as strains lacking components of NHEJ show sensitivity to bleomycin (Hudson *et al.* 2005). In response to oxidative damage (Garcia *et al.* 2000), and bleomycin (Muramoto and Chubb 2008; Hsu *et al.* 2011) a checkpoint response has also been observed, and

Muramoto *et al* characterised this as a G2/M checkpoint following DSBs (Muramoto and Chubb 2008).

A common theme in *Dictyostelium* for components of the BER and NER pathways is transcriptional upregulation following DNA damage. In response to cisplatin, *repB, repD* and *repE* are transcriptionally upregulated, whilst *repB*, *repD,* the Exo III homologue and *rad51* are upregulated in response to UV (Freeland *et al.* 1996; Yu *et al.* 1998). This transcriptional upregulation may partly account for the high resistance of *Dictyostelium* to UV (Yu *et al.* 1998). The *Dictyostelium* genome also encodes several ABC transporters, which may enable the active exclusion of DNA damaging agents from *Dictyostelium* and may also contribute to the high resistance of chemical DNA damaging agents in this organism (Eichinger *et al.* 2005). Overall, transcriptional upregulation, unusual repair mechanisms and active export of DNA damaging agents may all contribute to the resistance of *Dictyostelium* to DNA damage. Similar methods may be adopted by cancer cells, and so understanding the contribution of these mechanisms in *Dictyostelium,* may have applications to understanding the basis of chemotherapy resistance in humans. For example with regards to cisplatin, random mutagenesis of the *Dictyostelium* genome has been used to identify genes involved in resistance (Li *et al.* 2000). Microarray analysis has further illustrated the transcriptional changes accompanying cisplatin treatment (Van Driessche *et al.* 2007) and may provide insight into mechanisms of resistance and heightened sensitivity to the chemotherapeutic agents.

1.5 Aims

Whilst insight has been gained into the mechanisms of different DSB repair pathways, the factors governing their regulation remain unclear. This is particularly apparent in G2 phase of the cell cycle when both pathways can occur. It is now becoming clear that the preferential binding/retention of repair factors to DNA lesions does not occur by a simply passive process to give rise to particular repair pathways. Instead, active processes also regulate the balance of repair pathway utilisation, including post-translational modifications. One such avenue of interest is the role of PARylation in DSB repair regulation, which is particularly apparent with regards to downregulation of NHEJ during S-phase at replication forks. However, the role that PARylation may be playing in DSB repair pathway choice at other stages of the cell-cycle, particularly in G2 are unclear. In addition, the point within repair pathways at which commitment occurs is also unclear. These are therefore the primary aims of this thesis, and *Dictyostelium discoideum* will be utilised as a model organism to investigate this DSB repair pathway regulation. Its application is particularly useful due to its high degree of repair pathway and repair component conservation, including of PARPs.

In this thesis, an assay to measure HR will be developed to enable the effects of NHEJ disruption on HR levels to be elucidated. Furthermore, the conservation of PARPs and PARylation in the SSBR/BER response will be characterised in *Dictyostelium*. This will be undertaken not only elucidate some of the uncertainty surrounding PARP function in this respect, but will also strengthen the application of *Dictyostelium* to address more novel questions surrounding PARP function, including in DSB repair. Finally, the contribution of PARylation in DSB repair will be addressed using genetic disruption of the putative repair PARP genes identified through bioinformatic

analysis. The DSB repair assays will be applied in the various PARP disruptants, including the HR assay developed in the primary chapter as well as looking at chromatin enrichment of the NHEJ gatekeeper, Ku80. This will enable any alterations in repair pathway levels to be determined in a comparative context. If PARylation is playing a role in mediating DSB repair pathway regulation in vegetative *Dictyostelium*, which are in G2, alterations in repair pathway utilisation versus parental controls would be expected. Given the established role of Ku80 as a gatekeeper in favour of NHEJ whilst downregulating the ability of HR to occur, alterations in Ku80 chromatin enrichment may provide insight into the molecular basis behind the observations made.

2: Materials and Methods

2.1 Materials

Unless otherwise stated, solutions were sterilised by autoclaving (125ºC, 15min) or filtration (0.2µm filter, Nalgene) and stored at room temperature.

Chemiluminescent detection reagents

Solution A: 10mM Tris [pH 8.5]

0.386mM P-coumaric acid

2.5mM Luminol

Solution B: 10mM Tris [pH 8.5]

0.19% H_2O_2

Solutions were not sterilised, and stored in the dark at 4ºC

Church Buffer

0.5M $NaHPO_4$ [pH 7.2]

1% (w/v) bovine serum albumin fraction V

1mM EDTA [pH 8]

7% (w/v) sodium dodecyl sulphate

Filter sterilised

DNA loading Dye

0.25% bromophenol blue

40% sucrose

H50 Buffer

50mM KCl

20mM Hepes

10mM NaCl

5mM $NaHCO_3$

1mM $NaH_2PO_4.H_2O$

1mM $MgSO_4.7H_2O$

[pH 7.0]

Filter sterilised and stored at -20ºC for no more than 4 weeks

HL-5

53mM maltose

1.4% bacteriological peptone

0.7% yeast extract

4mM Na_2HPO_4

3.5mM KH_2PO_4

340µm dihydrostreptomycin sulphate

74µm vitamin B12 (cyanocobalamin)

82µm biotin

532µm Riboflavin

[pH6.5]

Autoclaved

KK2

19mM KH_2PO_4

3.6mM K_2HPO_4

Autoclaved

SSC (20X)

3M NaCl

300mM sodium citrate tribasic ($C_6H_5Na_3O_7.2H_2O$)

Autoclaved

LB agar

1% bactotryptone

0.5% yeast extract

85mM NaCl

1.5% agar

Autoclaved

LB Broth

1% bactotryptone

0.5% yeast extract

85mM NaCl

Autoclaved

LPB agar

2.92mM Lactose

0.1% bactopeptone

19mM $Na_2HPO_4.2H_2O$

30mM KH_2PO_4

2% agar

10µg/ml Blasticidin S (Axxora, added after autoclaving)

Autoclaved

Lower Pad Solution (LPS)

40mM KH_2PO_4

20mM KCl

[pH 7.2]

Filter sterilised

Nuclear Extraction Buffer

10mM PIPES (pH 6.8)

300mM Sucrose

3mM $MgCl_2$

20mM NaCl

0.5% Triton X-100

Stored at 4ºC and used within a 24 hour period

Nuclear Lysis Buffer

50mM Hepes

150mM NaCl

1mM EDTA

1μM microcystin

1mM NaF

2mM sodium orthovanadate

Protease inhibitor cocktail (Roche) (2 mini tablets per 10mls)

[pH 7.5]

Solution was not sterilised

Phosphate buffered saline (PBS)

One PBS tablet dissolved in 200ml deionised water yields:

10mM Phosphate buffer

2.7mM KCl

137mM NaCl

[pH 7.4]

Autoclaved

SDS PAGE Running Buffer

25mM Tris

192mM Glycine

[pH 8.3]

0.1% SDS

SM agar

1% peptone

56mM glucose

0.1% yeast extract

16mM KH_2PO_4

5.5mM $K_2HPO_4.3H_2O$

4mM $MgSO_4$

1.7% agar

Autoclaved

2x sodium dodecyl sulphate gel (SDS) loading buffer

50mM Tris [pH 6.8]

20% Glycerol

4% SDS

0.2% bromophenol blue

100mM Dithiothreitol

Stored at -20ºC

SDS-Page Transfer Buffer

50mM Tris

384mM Glycine

[pH 8.3]

0.1% SDS

20% Methanol

20x SSC

3M NaCl

150mM Sodium Citrate

[pH 7.0]

TAE (50X)

2M Tris Base

50mM EDTA

5.71% 1M glacial acetic acid

[pH 8.2]

Tris-Buffered Saline (TBS)

2.48mM Tris

137mM NaCl

[pH 7.4]

Autoclaved

2.2 Methods

2.2.1 General cell culture and genetic manipulation

2.2.1.1 Cell culture

Dictyostelium (Ax2 and disruption strains) were grown axenically in HL5 medium at 22ºC, and maintained in a dark incubator. For growth in suspension, cells were cultured in volumes that were a fifth of the flask capacity, and shaken at 220 rpm. Cells were maintained at densities between $5x10^4$ cells/ml and $5x10^6$ cells/ml, and utilised for experiments in the exponential phase of growth (1-$5x10^6$ cells/ml). Cell density was determined with a haemocytometer using a Leica DMLS microscope. Alternatively, where indicated, cells were grown in 90mm dishes, or 6-, 24-, or 96-well plates as monolayers, and subcultured when cells became confluent. Antibiotic selection to select for successful transformants and integrants in culture was carried out using 10µg/ml blasticidin (Axxora), 10µg/ml G418 (Sigma), or 40µg/ml hygromcyin (Sigma).

For bacterial-associated growth, *Dictyostelium* was grown on SM-agar containing a lawn of *Klebsiella aerogenes* (*Ka*).

2.2.1.2 Transformation of *Dictyostelium*

Exponentially growing *Dictyostelium* were washed twice in ice-cold H50 buffer (1500g, 3 mins) and resuspended in H50 to $5x10^7$ cells/ml. A tenth of the cells ($5x10^6$ cells) was mixed with 3-8µg plasmid DNA (in the case of pDXA vector DNA, an equal amount of pREP helper plasmid was included) and incubated on ice for 5 mins

in a 0.1cm gap electroporation cuvette (Biorad). Cells were electroporated using a Gene Pulser Xcell (Biorad) by applying two consecutive pulses (0.65kV, 25μF capacitance), separated by a 5 second interval. After recovery on ice for 5 mins, cells were plated in HL5 in a 90mm dish for extrachromosomal transformations or in 96 well-plates for transfections. After 24 hours, the appropriate antibiotic was added to the following final concentrations: 10μg/ml blasticidin-S (Axxora), 10-15μg/ml G418 (Sigma), or 35-40μg/ml hygromycin (Sigma). Plates were incubated at 22ºC in the dark.

2.2.1.3 Generation of disruption strains

Using standard cloning techniques, fragments of DNA flanking the region of interest being targeted for disruption were cloned on either side of the blasticidin-resistance (*BsR*) cassette in pLPBLP. A large quantity of the plasmid was made by maxipreparation (Qiagen) according to the manufacturer's instructions, and digested using restriction enzymes that would liberate a fragment of DNA containing the homologous arms and the *BsR* cassette. Prior to transformation, the digested DNA was purified by phenol/chloroform extraction using a 1:1 ratio of phenol/chloroform to DNA, and centrifuged at 20,000g for 5 mins. The upper aqueous layer was transferred to a fresh tube containing an equal volume of chloroform, and subjected to the same treatment. The DNA in the upper aqueous layer was precipitated with 2 volumes of 100% ethanol and 100mM sodium acetate, and incubated at -80°C for 30mins. DNA was pelleted by centrifugation at 20,000g for 5 mins, and the DNA pellet was washed with 70% ethanol before being air-dried, resuspended in a minimal volume of dH_2O, and the DNA concentration quantified on a spectrophotometer (GeneQuant *Pro*).

Transfection of *Dictyostelium* was carried out as above, and cells were plated in 96 well-plates at different densities to acquire a transformation efficiency of one transformant per well. After 24 hours, 10µg/ml of blasticidin was added and selection was carried out for 12-14 days before screening surviving colonies in pools of 12 by PCR to identify disruptants. Individual colonies within positive pools were screened, and the identified disruptant was spread onto *Ka*. After 3-5 days, clones from the *Ka* plate were picked, rescreened for the disruption, and frozen down to make permanent stocks. The screening procedure is described below.

2.2.1.4 Screening of diruptants by PCR

Genomic DNA was isolated from blasticidin-resistant colonies using the Wizard Genomic DNA Purification Kit (Promega) according to the manufacturer's instructions. The genomic DNA (100ng) was subject to PCR using *Taq* DNA polymerase (Sigma), according to the manufacturer's instructions. Primers were synthesised by Genosys (Sigma), and are listed in Appendix A.

2.2.1.5 Cre-loxing

The *BsR* cassette was removed from disruptants as described previously (Faix *et al.* 2004). Briefly, strains were transformed with the PDXA-NLS-Cre plasmid and serial diluted into 96-well plates to ensure only single clones per well. The next day, 20µg/ml G418 was added and the plate incubated for 5-7 days at 22°C. Following this, the G418 was removed and replaced with media containing no selection. Surviving colonies were replica plated into media containing 10µg/ml blasticidin,

20µg/ml G418 or no selection. Colonies which showed growth only in the absence of selection were plated onto *Ka*, and clones were selected and screened by PCR to confirm loss of the blasticidin-resistance cassette. Successful clones were scaled up and permanent stocks made.

2.2.1.6 Fruiting body development and spore hatching

Exponentially growing *Dictyostelium* were washed three times in KK2 and resuspended in KK2 to give a final cell density of $1x10^8$cells/ml. Washed cells were incubated on filter paper at a final density of $3.5x10^6$ cells/cm^2 at 22°C in the dark. After 24 hours, fruiting bodies had developed, and were maintained in the dark at 22°C for a further 48 hours to allow spores to mature. Following maturation, fruiting bodies were transferred from the filter into KK2 containing 0.1% NP-40 and passed through a 19.5 gauge needle to disrupt the fruiting body and liberate spores. Spores were harvested by centrifugation at 1500g for 3 mins and washed twice in KK2, 0.1% NP-40 and once in KK2 before being resuspended to $2x10^7$cells/ml in KK2 and divided into 1-2 ml aliquots. Germination was induced by heat-shock at 45°C for 30 mins, and the cells were immediately diluted to $1x10^6$cells/ml in room-temperature HL5 and incubated for 10 hours at 22°C.

2.2.1.7 Liquid nitrogen

To make permanent *Dictyostelium* liquid nitrogen stocks, exponentially growing *Dictyostelium* were pelleted and resuspended to a final cell density of $5x10^7$cells/ml in a 1:1 mixture of HL5 and Fetal calf serum containing 5% DMSO. The cells were divided into 1ml aliquots, and gradually cooled by incubating vials on ice for 5 mins,

at -21ºC for 1 hour and finally storing at -80ºC at least 24 hours before being transferred to liquid nitrogen. Alternatively, cell pellets were resuspended in Horse serum (Oxoid) containing 5% DMSO and stored in bull semen straws, plugged with plasticine. Straws were incubated at 4ºC for 1 hour, -21ºC for 1 hour, -80ºC for 1 hour before being transferred to liquid nitrogen for long-term storage.

Cell lines were recovered from liquid nitrogen stocks every 4 weeks by rapidly thawing the frozen cells on SM-agar plates containing a lawn of *Ka*. After 4-5 days *Dictyostelium* was recovered from the SM-agar plate and transferred to shaking suspension to initiate axenic cultures to be used for experiments.

2.2.2 Molecular biology

2.2.2.1 Sequence alignments

Dictyostelium sequences were acquired from Dictybase (www.dictybase.org). Sequences for other organisms were obtained from NCBI (www.ncbi.nlm.nih.gov). Sequence alignments were performed using the MultAlin Interface (http://multalin.toulouse.inra.fr/multalin/multalin.html) (Corpet 1988). Protein domains were identified using IntroPro Scan.

2.2.2.2 DNA extraction for Southern Blotting

Between 2-4x10^8 cells were collected by centrifugation and washed twice in 0.2% NaCl. The resulting cell pellet was resuspended in nuclear lysis buffer (NLB, 10mM MgOAc, 10mM NaCl, 30mM Hepes [pH 7.5], 10% sucrose, 2% NP-40) to a final density of 1x10^8 cells/ml, and incubated on ice for 10 mins before being pelleted

(9000g, 10 mins, 4°C). The pellet was resuspended in a volume of HMK solution (50mM Hepes [pH 7.5], 40mM MgOAc, 20mM KCl) that was double that of the NLB volume used, and NaCl and SDS were added to a final concentration of 200mM and 1%, respectively, to lyse the nuclei. DNA was purified by phenol/chloroform extraction and ethanol precipitation, as described previously, with the slight modification of repeating the phenol/chloroform extraction until the upper aqueous layer was clear. The final DNA pellet was resuspended in a minimal volume of dH_2O and the DNA concentration was quantified using a GeneQuant *Pro*.

2.2.2.3 Southern Blotting

Genomic DNA (25µg) purified as described above, was digested overnight with 250 units of the relevant restriction enzymes. The next morning, another 25 units restriction enzyme was added to ensure complete digestion. The digested DNA was ethanol precipitated, resuspended in a volume of dH_2O small enough to load into the well of a 0.7% TAE-agarose/ethidium bromide gel, and separated by electrophoresis at 50 volts. The agarose gel was washed in 0.2N HCl for 10 mins, rinsed in dH_2O, and gently agitated in a solution of 0.5N NaOH, 1.5M NaCl for 45 mins to fragment the DNA. Following this, the gel was rinsed in dH_2O and neutralised by two washes in 1M Tris (pH 7.4), 1.5M NaCl, for 45 mins and then 15 mins, respectively. The genomic DNA was transferred overnight onto a nylon Hybond-N^+ membrane (Amersham) by capillary action using 10x SSC, following which, the membrane was washed in 2x SSC and the DNA covalently cross-linked to the membrane by UV irradiation using a UV Stratalinker (Stratagene).

The probe to be used in Southern hybridisation was synthesised by PCR and radioactively labelled with [α^{32}P]-dCTP using the Rediprime II Random Prime Labelling System (GE Healthcare), according to the manufacturer's instructions. Unincorporated [α^{32}P]-dCTP nucleotides were removed using SigmaSpin Post-reaction Clean up columns (Sigma), according to the manufacturer's instructions.

Prior to incubation with the radioactively labelled probe, the membrane was rinsed in 2x SSC and prehybridised by rotation in Church buffer for 1 hour at 65ºC. The labelled probe, which was first denatured by incubation at 100ºC for 10 mins was then added directly to the prehybridisation solution and incubated with the membrane at 65ºC overnight. Following hybridisation, the membrane was washed twice in 2x SSC, 0.1% SDS and then twice in 0.2x SSC, 0.1% SDS, for 10 mins per wash at 65ºC, before being exposed to autoradiographic film (Hyperfilm, GE Healthcare).

To strip the blot, the membrane was immersed in boiling 0.1% SDS, and allowed to cool before repeating the washing procedure another two times and reprobed as described above.

2.2.2.4 RNA extraction

To isolate RNA from *Dictyostelium*, 1x10^7 cells, isolated from an exponential culture was pelleted and the pellet resuspended in 1ml of TRI reagent (Sigma). Repeated pipetting to resuspend the sample ensured cell lysis, following which, cells were incubated at room temperature for 5 mins before adding 0.2ml of chloroform. The sample was mixed vigorously for 15 seconds, incubated for 2-15 mins at room temperature, and centrifuged at 12,000g for 15 mins. The upper aqueous phase was

isolated, transferred to a fresh tube containing 0.5ml isopropanol and mixed before incubating the sample at 4ºC for 5-10 mins. The sample was then centrifuged at 12,000g for 20 mins and the resulting RNA pellet was washed with 70% ethanol and centrifuged again at 7,500g for 5 mins at 4ºC. The RNA pellet was air dried and resuspended in dH_2O.

2.2.2.5 Reverse transcription (RT) and RT-PCR

RNA isolated using the procedure described above was quantified GeneQuant *Pro* and 5µg of RNA subject to reverse transcription using Superscript II Reverse Transcriptase (Invitrogen) and Oligo(dT) and random hexamer primers, according to the manufacturer's instructions. The final product was diluted to a final volume of 100µl and 1-2µl were used for PCR analysis.

2.2.2.6 DNA manipulations

Genomic and plasmid DNA was subject to restriction enzyme digest, PCR, ligation, phenol-chloroform extraction, ethanol and isopropanol precipitation and TAE gel electrophoresis according to standard protocols. Plasmid DNA was transformed into *E.coli* (DH5-α, Invitrogen) and a large quantity of plasmid made by minipreparation or maxipreparation (Qiagen). Gel extraction and PCR purifications (Qiagen) were carried out according to the manufacturer's instructions. DNA sequencing was carried out by the Genesevice sequencing facility (Oxford), using primers available at Geneservice or synthesised by Genosys (Sigma).

2.2.3 Phenotypic analysis

2.2.3.1 Sensitivity assay

Exponentially growing *Dictyostelium* were seeded at a density of $1x10^6$ cells/ml and divided into 1-2ml aliquots. Phleomycin (Sigma) (in water), methyl methanesulfonate (MMS, Sigma) or hydrogen peroxide (H_2O_2, Sigma) were added at various concentrations and cells were incubated at 22ºC whilst being shaken at 100rpm. After 1 hour, cells were diluted to $1x10^4$ cells/ml in KK2 and 25µl of this was mixed with 350µl *Ka* and plated onto a 140mm Petri dishes containing SM-agar. Two SM-agar plates were used per treatment. Petri dishes were incubated in the dark at 22ºC, and survival was assessed by counting the number of colonies visible 3, 4 and 5 days after plating.

To perform sensitivity assays in hatched spores, spores were hatched as described in Section 2.2.1.6 and diluted to $1x10^6$cells/ml in a 1:5 ratio of HL5:KK2 containing phleomycin. Cells were incubated in shaking suspension (100rpm) for 18 hours at 22°C before being plated as described above and colonies counted after 3, 4 and 5 days.

The H_2O_2 concentration was checked prior to use in sensitivity assays by measuring the A_{240} of the 30% stock solution at a 1:800 dilution. The concentration was determined from the H_2O_2 extinction coefficient of $43.4A_{240}M^{-1}cm^{-1}$ (Garcia *et al.* 2000).

2.2.3.2 Restriction-Enzyme Mediated Integration (REMI)

REMI was performed as described previously (Kuspa and Loomis 1992). Exponentially growing *Dictyostelium* were prepared for transformation as in section 2.2.1.2 and resuspended to a final density of $5.6x10^6$cells/ml. Prior to electroporation, 2µg *Bam*HI-linearised pLPBLP which had been treated with calf-intestinal phosphatase and cleaned-up for transformation was mixed with cells, with or without 20units of *Bam*HI. After electroporation, and following 5 mins recovery on ice, $4x10^6$ cells were resuspended in HL5 to a density of $5x10^6$ cells/ml and incubated for 15 hours at 22ºC without shaking. Cells were pelleted and mixed with 1500µl *E.coli B/r*, which had been previously washed twice in KK2, and this was divided equally over three 140mm plates containing LPB agar. Plates were incubated at 22ºC, and colonies were counted on days 3, 4 and 5 after plating. REMI was assessed by measuring the fold induction of colony number in the presence of *Bam*HI.

2.2.3.3 Homologous recombination (HR) assay

The *cdk8*-knockout plasmid (Lin *et al.* 2004; Greene *et al.* 2011), prepared by maxipreparation, was digested with restriction enzyme in order to liberate a fragment of DNA containing regions homologous to the *cdk8* gene flanking the *BsR* cassette. DNA was purified by phenol/chloroform extraction and ethanol precipitation before resuspending the DNA in a small volume of dH_2O. The concentration of DNA was quantified and 7µg transformed into cells as previously described. Following a 5 mins recovery period on ice, the cells were transferred to HL5, serial-diluted and plated into 96-well plates. After 24 hours, 10µg/ml blasticidin was added and the plates incubated in the dark at 22ºC for 14 days. Following selection, clonal

suspensions of successful transformants were spotted onto SM-agar containing a lawn of *Ka*. After 5-6 days, plaques were large enough for phenotypic analysis. Genomic DNA was extracted from representative plaques as described in section 2.2.1.4 and subject to PCR analysis.

2.2.3.4 Immunofluorescence analysis and DNA damage-induced staining

Cells were diluted to a density of $1x10^6$cells/ml and allowed to adhere to a coverslip for 1 hour. Coverslips were gently washed with HL5 before being incubated in media containing either PARP inhibitors at the relevant concentration (see individual figures for details), 100µg/ml phleomycin, 0.5mM H_2O_2 or 5mM MMS. At time points following addition of the DNA damaging agent, coverslips were incubated for 5 mins in nuclear extraction buffer before being washed in TBS, and the nuclei fixed by incubating with 70% ethanol for a further 5 mins. Coverslips were finally rinsed in 100% methanol and washed twice with TBS.

Coverslips were processed for immunofluroescence by blocking for 1 hour, at room temperature in 10% serum (diluted in TBS) from the animal in which the secondary antibody was raised in. Coverslips were then incubated with the relevant primary antibody at the appropriate concentration either for 1 hour at room temperature, or overnight at 4ºC (see Table 2.1). The coverslips were rinsed thrice in TBS to remove the primary antibody and incubated with the relevant fluorescently-labelled secondary antibody at a dilution of 1:80, for 1 hour at room temperature in the dark before washing them thrice more in TBS.

Antibody	Manufacturer	Dilution and incubation conditions
α-Poly(ADP-ribose) Rabbit polyclonal	Trevigen	1:300 (1 hour, room temperature)
α-$\gamma_{(Ser139)}$H2AX Rabbit polyclonal	Abcam	1:500 (1 hour, room temperature)

Table 2.1: Antibodies used for immunofluorescence analysis.

Coverslips were mounted onto glass slides with Vector Shield Mounting Media containing 4'-6'-diamino-2-phenylindole (DAPI) (Vector Laboratories) and visualised with a Zeiss Axioscope 2 microscope at 100X magnification. Images were captured on an Olympus 1X71 microscope at a magnification of 100X using a Hamamatsu C10600-10B-H camera and HCI image software before being processed in Photoshop.

2.2.3.5 Preparation of samples for Western blotting

Following treatment of cells in shaking suspension, $5x10^6$cells were removed and spun down at 1500g for 3 mins. The pellet was resuspended in 1X SDS gel loading buffer to give a final cell density of $5x10^7$cells/ml, and boiled for 5 mins.

2.2.3.6 Subcellular fractionation

Subcellular fractionation experiments were performed as described previously (Drouet *et al.* 2005). Briefly, exponentially growing cells were seeded at $5x10^6$ cells/ml and exposed to phleomycin or mock-treated. At indicated time points, cells were washed in KK2 buffer and resuspended in nuclear lysis buffer, supplemented

with 0.1% Triton X-100 to a final density of $3x10^7$ cells/ml. Cells were incubated for 15 mins at 4ºC and then centrifuged at 14,000g for 3 mins, giving rise to a pellet, and supernatant fraction S1. The pellet was resuspended in nuclear lysis buffer + 0.1% Triton X-100 for a further 15 mins at 4ºC and centrifuged at 14,000g for 3 mins. The supernatant was pooled with the S1 fraction, and the pellet resuspended in nuclear lysis buffer + 200µg/ml RNaseA (Sigma) and incubated with rotation at room temperature for 30 mins, and repelleted as before to give fraction P2, which is the insoluble nuclear pellet, including chromatin. The P2 pellet was resuspended in 1x SDS loading buffer containing 100mM DTT. Fractions were analysed by Western blotting using the indicated antibodies.

2.2.3.7 Ku80 immunoprecipiation

Exponentially growing cells were washed twice in KK2 and resuspended to a final density of $1x10^7$ cells/ml in lysis buffer (50mM Tris [pH 8.0], 200mM NaCl, 1% Triton X-100, 1mM DTT, 1mM EDTA, 50u/ml benzonase (Novagen), 10mM sodium butyrate, 1mM NaF, 20mM β-glycerophosphate, 1mM sodium orthovanadate, 1µM microcystin, protease inhibitor cocktail (Roche)), and incubated with rotation for 30 mins at 4ºC. Cell lysates were centrifuged (14,000g, 10 mins) and the supernatant isolated and incubated with Ku80 serum for 30 mins at 4ºC, followed by an incubation with protein G sepharose beads for 45 mins at 4ºC, with rotation. The beads were pelleted (600g, 2 mins) and washed three times with lysis buffer before resuspending the beads in 1x SDS loading buffer containing 100mM DTT. Samples were analysed by Western blot.

2.2.3.8 Poly-acrylamide gel electrophoresis

Between $5x10^5$ to $1x10^6$ cells were loaded into the wells of a sodium dodecyl sulphate polyacrylamide gel (SDS-PAGE) and run at 150 volts alongside a prestained protein ladder (Pageruler plus, Fermentas). Samples were then transferred onto a nitrocellulose (Protran, SLS, 0.2µm pore size) membrane at 250mA for 2 hours, followed by blocking of the membrane in 1X TBS, 0.2% Tween-20, 5% non-fat dried milk (blocking solution) for 1 hour at room temperature or overnight at 4ºC. The membrane was incubated with primary antibody in blocking buffer at the relevant antibody dilution for 1 hour at room temperature, or 4ºC overnight (see Table 2.2), followed by three 10 mins washes in 1x TBS, 0.2% Tween-20.

Antibody	**Manufacturer**	**Dilution and incubation conditions**
α-Ku80 (serum, goat)	Diagnostics Scotland	1:2000, 1 hour
α-Myc (monoclonal, mouse)	Santa Cruz	1:1250, 1 hour
α-Actin (polyclonal, goat)	Santa Cruz	1:250, 1 hour

Table 2.2: Antibodies used for Western blot analysis on nitrocellulose

Horseradish peroxidase-conjugated (HRP) secondary antibody was added at a 1:4000 dilution in blocking buffer for 1 hour, and the membrane was washed again as described above. The protein of interest was detected using autoradiography film (Hyperfilm, GE Healthcare) following incubation of the membrane for 1 mins in equal volumes of solution A and B of enhanced chemiluminescent reagent.

2.2.3.9 Determination of Poly ADP-ribosylation by Western Blotting

Western blot samples were prepared as in section 2.2.3.5 and $1x10^6$ cells were run on an SDS-PAGE gel as previously described in 2.2.3.8. Samples were transferred onto a polyvinylidine fluoride (PVDF) (Immobilon, 0.45μm pore size) membrane for 2 hours at 250mA according to the manufacturer's instructions (Immobilon). Briefly, after running the samples on the SDS-PAGE, the gel was soaked in the Immobilon recommended transfer buffer (1x SDS running buffer, 10% methanol) for 15 mins. During this time, the PVDF membrane was prepared for transfer by soaking it in 100% methanol for 15 seconds, water for 2 mins and finally transfer buffer for 5 mins. After transfer, the membrane was soaked in 100% methanol for 10 seconds and allowed to dry for 45 mins. The membrane was blocked in 1x PBS, 5% non-fat dried milk for 1 hour at room temperature, and incubated in a 1:1000 dilution of the α-Poly(ADP-ribose) antibody (Polyclonal, Trevigen) in 1x PBS, 5% non-fat dried milk, 0.05% Tween-20 (antibody solution) at 4ºC overnight. Following this, the membrane was washed thrice in 1xPBS containing 0.05% Tween-20, for 10 mins per wash and incubated in a 1:4000 dilution of HRP-conjugated α-rabbit secondary antibody in the antibody solution followed by membrane washing as described above. Visualisation of the bands of interest was by ECL and autoradiographic film as previously described.

2.2.3.10 Determination of γH2AX by Western blotting

Western blot samples were prepared as before and $1x10^6$ cells were run on an SDS-PAGE gel. Samples were transferred onto a PVDF membrane which had been previously soaked in methanol for 10 seconds and then transfer buffer for 2 mins. Following transfer, the membrane was blocked in 1x TBS, 0.1% Tween-20, 5% non-

fat dried milk for 1 hour at room temperature, and incubated overnight at 4ºC in the blocking solution containing a 1:500 dilution of the α-γH2AX (Abcam). The membrane was then rinsed once in dH_2O and incubated for 1 hour at room temperature with an HRP-conjugated α-rabbit secondary antibody at a 1:4000 dilution in the blocking solution. The membrane was washed three times in 1x TBS, 0.1% Tween-20, with 10 mins per wash and visualised on autoradiographic film following incubation in ECL as before.

2.2.3.11 Stripping Western blots

In order to reprobe Western blot membranes with a different primary antibody, it is first necessary to strip existing antibodies from the membrane. This was achieved by incubating the membrane at 50ºC in 100mM 2-mercaptoethanol, 2% SDS, 62.5mM Tris [pH 6.7] for 30 mins, followed by washing the membrane twice in 1x PBS for 10 mins per wash. The membrane was then processed for the second round of antibody incubations following incubation in the appropriate blocking solution for 1 hour at room temperature.

2.2.3.12 Statistical Analysis

The statistical significance of data was determined using the unpaired, two-tailed Student's *t*-test using a significance threshold of 0.05, where $p < 0.05$ was considered statistically significant.

3: Determining the impact of non-homologous end joining on homologous recombination efficiency in G2 of the *Dictyostelium* cell cycle

3.1 Introduction

Genomic instability and tumourigenesis can arise when DNA DSB repair pathways are aberrantly utilised (Hiom 2010). For example, misuse of NHEJ at replication forks can lead to chromosomal abnormalities and reduced cell viability (Adamo *et al.* 2010; Bunting *et al.* 2010; Pace *et al.* 2010; Patel *et al.* 2011). Similarly, whilst HR is predominantly error-free, its misuse can result in loss-of-heterozygosity, chromosomal aberrations and increased cancer predisposition (Shrivastav *et al.* 2008). Correct usage of DSB repair pathways is therefore vital, and the molecular basis behind the regulation of pathway 'choice' remains unclear.

Whilst NHEJ can occur throughout the cell-cycle (Takata *et al.* 1998; Rothkamm *et al.* 2003), the capacity of cells to carry out HR is restricted to S and G2 (Takata *et al.* 1998; Rothkamm *et al.* 2003). The HR cell-cycle restriction is attributed to the role of CDKs in promoting DNA end-resection as an initiating step in the formation of the recombinogenic Rad51 nucleoprotein filament (Aylon *et al.* 2004; Ira *et al.* 2004; Jazayeri *et al.* 2006; Huertas *et al.* 2008; Huertas and Jackson 2009; Yun and Hiom 2009; Chen *et al.* 2011). However, Ku also has a high DNA DSB binding affinity and

its presence at DNA ends is postulated to reduce nucleolytic processing (Lee *et al.* 1998; Liang *et al.* 1998; Shim *et al.* 2010). Conversely, resected DNA ends are poor substrates for Ku binding, and therefore, nucleolytic processing precludes DSB repair by NHEJ (Frank-Vaillant and Marcand 2002).

In G2, both HR and NHEJ can occur, and it is posited that these pathways compete, with HR upregulation when NHEJ is defective; this is particularly striking following Ku disruption (Fukushima *et al.* 2001; Pierce *et al.* 2001; Allen *et al.* 2002). Similarly, inhibiting DSB end-resection upregulates NHEJ, whilst inhibition of HR downstream of resection has less of a stimulatory effect on NHEJ (Ira *et al.* 2004; Stark *et al.* 2004). Thus, DNA end-binding by Ku or DNA end-resection may represent the switch towards NHEJ or HR, respectively (Fukushima *et al.* 2001; Pierce *et al.* 2001; Allen *et al.* 2002; Clerici *et al.* 2008; Mimitou and Symington 2010; Shibata *et al.* 2011). Recently, NHEJ has been proposed as the initial and predominant DSB repair pathway in mammalian cells, whilst HR slowly repairs DNA damage associated with heightened complexity or in heterochromatin (Beucher *et al.* 2009; Shibata *et al.* 2011). Furthermore, cells may attempt NHEJ, failing which, HR will be utilised (Shibata *et al.* 2011). Thus, whilst insights into repair pathway regulation are advancing, much remains to be determined regarding the molecular basis of pathway choice. In this respect, DSB repair assays have enabled alterations in repair levels in different genetic backgrounds to be determined. This has provided insights into stages at which cells commit to a particular DSB repair pathway, as well as factors that influence repair pathway utilisation.

Several *in vivo* assays have been developed to measure HR in different organisms. Assays specifically measuring a particular DSB repair pathway provide distinct advantages over those monitoring overall repair capacity, such as γH2AX decay, as a means of directly determining how repair pathway contributions vary. The most widely used mammalian HR assay utilises a genome-integrated construct, containing a direct repeat of truncated, non-functional GFP or neomycin phosphotransferase (*neo*), one of which encodes a site for the I-SceI endonuclease (Pierce *et al.* 1999). On DSB induction by I-SceI, recombination between these repeats creates a functional *gfp* or *neo* gene, giving rise to a fluorescence/antibiotic-resistance based readout of HR (Johnson *et al.* 1999; Pierce *et al.* 1999). Similarly, in yeast, the HO-endonuclease can be transiently expressed to induce a single DSB at the endogenous MAT locus and the repair outcome monitored by mating type switching (Haber 1998).

Another assay that has been extensively employed for measuring HR is gene-targeting, which monitors integration of exogenous DNA into the homologous region of the genome. In vertebrate and invertebrate organisms, the mechanism and genetic requirements of targeted-integration have been extensively studied. The process is dependent on Rad51 (Yanez and Porter 1999; Dominguez-Bendala *et al.* 2003; Ninomiya *et al.* 2004; Schaefer *et al.* 2010) and/or Rad52 (Schiestl *et al.* 1994; Rijkers *et al.* 1998; Yamaguchi-Iwai *et al.* 1998; Kooistra *et al.* 2004; Ninomiya *et al.* 2004), although the absolute requirement for these genes varies between species. Similar to the I-SceI and HO endonuclease assay, gene-targeting measures HR in the context of chromatin, and thus represents a more physiologically relevant system in which to study repair, versus earlier extrachromosomal recombination assays (Liang

and Jasin 1995). Furthermore, the gene-targeting assay has the benefit of enabling HR assessment at several different genetic loci, to address the contribution of loci specific effects. This is particularly relevant in the context of chromatin during G2, with NHEJ repairing euchromatic DSBs, whilst HR repairs DSBs in heterochromatin (Beucher *et al.* 2009). Thus, targeting genes in heterochromatin versus euchromatin in different genetic backgrounds may enable the genetic basis behind this preferential usage to be unravelled.

In *Dictyostelium*, various repair assays have been developed to assess DSB repair capacity. This includes sensitivity assays which enable cell viability in different genetic backgrounds to be measured following DSB induction (Hudson *et al.* 2005), and analysis of γH2AX decay as a readout of DSB repair kinetics (Hsu *et al.* 2011). However, the potential for repair pathways to compensate for each other raises the necessity of developing assays to more directly measure the relative contributions of each DSB repair pathway. An assay measure to NHEJ has already been developed in *Dictyostelium*, termed Restriction-Enzyme Mediated Integration (REMI), which measures integration of a *Bam*HI-linearised plasmid into *Bam*HI-generated DSBs in the genome (Kuspa and Loomis 1992; Adachi *et al.* 1994; Hsu *et al.* 2011). The dependence of REMI on NHEJ in *Dictyostelium* has been illustrated via the significantly reduced REMI efficiency in NHEJ-disrupted *ku80*$^{-}$ and *dnapkcs*$^{-}$ strains (see section 1.3.3.2) relative to Ax2 (Hsu *et al.* 2011). Vegetative *ku80*$^{-}$ and *dnapkcs*$^{-}$ strains show no enhanced DNA DSB sensitivity (Hudson *et al.* 2005), whilst the *exo1*$^{-}$ strain, which is deficient in an enzyme implicated in HR (see section 1.3.3.1) is extremely sensitive to DNA DSBs (Hsu *et al.* 2011). This implies that HR, not NHEJ is required for viability in vegetative *Dictyostelium* following DNA DSBs.

Nevertheless, recent analysis of these NHEJ mutants has illustrated the occurrence and contribution of NHEJ to repair of genomic DSBs (Muramoto and Chubb 2008; Hsu *et al.* 2011).

An assay to directly measure HR in *Dictyostelium* has not been developed, preventing parallel assessment of HR and NHEJ efficiency in DNA repair mutants. This has impeded understanding of the lack of DSB sensitivity in NHEJ mutants, which may suggest compensatory upregulation of HR. Development of an HR assay in *Dictyostelium* would facilitate its application to investigate factors regulating DSB repair pathway choice in G2 of the cell-cycle, when both HR and NHEJ can occur. Furthermore, the position at which cells commit to repair pathway, and preclude usage of another DSB repair pathway would be addressed. The aims of this chapter were therefore to develop and verify a gene-targeting assay to measure HR in *Dictyostelium* NHEJ-mutants and determine how altered DSB repair pathway contributions impact on the overall repair proficiency.

3.2 Results

3.2.1 Identifying genes to measure gene-targeting efficiency

Gene-targeting to measure HR has been used in many different organisms, and I wished to establish a similar system in *Dictyostelium*. To ensure the practical application of this assay, a binary readout of gene-targeting is required. One possibility was to target genes that would give rise to a developmental phenotype in *Dictyostelium*. In particular, genes involved in cAMP relay and chemotaxis, which

facilitate aggregation, were primarily assessed (Meima and Schaap 1999; Schaap 2011). The phenotypic readout of disrupting aggregation genes by gene-targeting would be an inability of cells to undergo starvation-induced aggregation (agg^-) and form fruiting bodies. Agg^- cells would thus serve as an easy and convenient measure of gene-targeting versus cells that form fruiting bodies (agg^+), which would represent random-integration events. Thus, the genes *cdk8* (Takeda *et al.* 2002), *erkB* (Segall *et al.* 1995) and *rasC* (Lim *et al.* 2001), which are all involved in aggregation, were assessed for their suitability as disruption targets. This would be based on the clarity of the aggregation defect their disruption would give rise to.

Initially, *erkB* was assessed as a gene candidate due to the defective cAMP relay response necessary for aggregation when disrupted (Segall *et al.* 1995; Maeda *et al.* 1996). Recapitulation of this observation in Ax2 involved modification of an *erkB*-disruption construct (Segall *et al.* 1995) to replace the *pyr5-6* selectable marker with the Blasticidin S resistance cassette from pLPBLP (Faix *et al.* 2004). The *erkB*-disruption construct targets the 3'UTR of *erkB*, giving rise to an agg^- phenotype due to the loss of termination signals and the nuclear accumulation of the transcript (Segall *et al.* 1995).

Ax2 was transfected with the *Cla*I-linearised *erkB*-BSR plasmid, and successful integrants selected with blasticidin. To distinguish random integration from targeted integration events, blasticidin-resistant colonies were assessed for their aggregation phenotype. This was determined by plating blasticidin-resistant *Dictyostelium* onto a *Klebsiela aerogenes* (*Ka*) lawn and assessing the ability of colonies to form fruiting bodies (Figure 3.1). Whilst 5% of colonies had an agg^- phenotype, 27% were

observed to have an intermediate phenotype, often arising from apparent agg$^-$colonies (Figure 3.2). Intermediate colonies may arise due to the ability of neighbouring agg$^+$ colonies to secrete developmental rescuing factors capable of rescuing the *erkB*$^-$ developmental defect (Kuwayama *et al.* 2000; Maeda and Kuwayama 2000; Tsujioka *et al.* 2004). Alternatively, a low level of ErkB expression from the disrupted gene may enable phenotypic rescue (Segall *et al.* 1995). To formally assess this possibility, the aggregation phenotype of each blasticidin-resistant colony was determined in isolation of any other colony. Of the 213 colonies assessed, 19% were agg$^-$, and 0.47% had an intermediate phenotype. This supported the possibility that agg$^+$ colonies were leading to phenotypic rescue of neighbouring agg$^-$ colonies. Thus, despite the binary phenotype and high targeting efficiency of the *erkB* gene, the technical complications led to its rejection as a potential gene target in the assay.

Disruption plasmids to assess *rasC* and *cdk8* were constructed previously by Lim *et al* (Lim *et al.* 2001) and Greene *et al* (Lin *et al.* 2004; Greene *et al.* 2011), respectively. The *cdk8*- and *rasC*-disruption constructs disrupt the gene coding regions with blasticidin at positions +524 and +291, respectively, relative to the transcription start site, leading to elimination of gene expression. The small GTPase, RasC, is involved in cAMP relay and chemotaxis through its roles in activating ACA (Adenylate cyclase A) and protein kinase B, respectively (Lim *et al.* 2001). Similarly, *Dictyostelium* Cdk8 is indirectly involved in cAMP relay as part of the RNA polymerase II holoenzyme, playing a regulatory role in starvation-induced transcription of the early developmental genes *aca* (Takeda *et al.* 2002; Lin *et al.* 2004) and *carA* (Lin *et al.* 2004). In both cases, disruption of these genes prevents processes required for aggregation, giving rise to an agg$^-$ phenotype.

Following liberation of the disruption cassette of *rasC* and *cdk8*, with *Pvu*II and *Kpn*I/*Not*I digestion, respectively, DNA was transfected into Ax2 and gene-targeting efficiency assessed. Phenotypic assessment of colonies for both genes revealed a binary agg^+ or agg^- phenotype (Figure 3.3). Furthermore, agg^- colonies were assessed 48 hours after initial characterisation, and showed no sign of reversion. Representative agg^+ and agg^- colonies were assessed by PCR to determine whether the aggregation-phenotype was corroborated on the genotype level in addition to a control PCR to assess genomic DNA quality (Figure 3.4). For *cdk8*, the 14 agg^- colonies assessed produced a PCR product of the expected size for targeted integration, whilst none of the 14 agg^+ colonies produced a product (Figure 3.4A). For *rasC*, the number of colonies assessed by PCR was limited by the low transfection efficiency. None of the 10 agg^+ colonies assessed gave rise to a PCR product, whilst the 3 agg^- colonies generated were all targeted integrants (Figure 3.4B). Thus, for both *cdk8* and *rasC*, the aggregation capacity of colonies can be regarded as a readout in the gene-targeting assay, with targeted versus random integration events giving rise to distinct agg^+ or agg^- phenotypes, respectively.

Gene-targeting efficiency was measured as the proportion of agg^- colonies over the total number of colonies assessed. In Ax2, gene-targeting efficiency at the *cdk8* and *rasC* locus was 2.03% and 1.1%, respectively (Table 3.1). Slow vegetative growth following disruption of *cdk8* has been described (Takeda *et al.* 2002). To discount the possibility of assay bias towards earlier-arising random-integration events, blasticidin-resistant colonies appearing either 10- or 14-days after transfection were

phenotypically assessed. No difference in gene-targeting efficiency was observed between early and late arising colonies. Thus, both *rasC* and *cdk8* represent suitable targets in the gene-targeting assay to compare gene-targeting efficiency in different genetic backgrounds. However, given the higher transfection and targeting efficiency at the *cdk*8 locus, *cdk8* was deemed a more suitable gene target and focused on for assay verification.

3.2.2 Gene-targeting in *Dictyostelium* is dependent on components of HR

The mechanism of gene-targeting has been investigated in several eukaryotic organisms, and is proposed to occur by HR, although the specific genetic requirements vary between species. In *Dictyostelium*, the mechanism of gene-targeting remains unclear. I thus wanted to assess the genetic requirements of this process, and determine whether HR components are required for targeted-integration of exogenous linear DNA. Similar to mice (Lim and Hasty 1996; Tsuzuki *et al.* 1996) and DT40 cells (Sonoda *et al.* 1998), *rad51* disruption in *Dictyostelium* is lethal (Hasegawa *et al.* 2005). This complicates determination of the role of HR in *Dictyostelium* gene-targeting. Nevertheless, a disruptant at the *exo1*$^{-}$ locus has been generated (Hsu *et al*. 2011), which encodes a nuclease required for DNA end resection to promote HR (Fiorentini *et al.* 1997; Qiu *et al.* 1999). In other organisms, Exo1 functions redundantly with Dna2 to generate extensive ssDNA that forms the Rad51 nucleoprotein filament required for synapsis (Gravel *et al.* 2008; Mimitou and Symington 2008; Zhu *et al.* 2008). Unlike *Dictyostelium* strains disrupted in NHEJ components (Hudson *et al.* 2005; Hsu *et al.* 2011), *exo1*$^{-}$ cells show increased DNA

DSB sensitivity relative to Ax2 in the vegetative stage (Figure 3.5A) (Hsu *et al.* 2011). This highlights the differential contribution of NHEJ and HR in vegetative *Dictyostelium* survival to DSBs. To assess the reliance of gene-targeting on HR in *Dictyostelium*, the *exo1*$^{-}$ strain (Hsu *et al.* 2011) was assessed in the gene-targeting assay.

Due to the limited availability of selectable markers in *Dictyostelium*, a technique has been developed, termed cre-loxing, to remove the blasticidin-resistance cassette incorporated during gene disruption to enable its reuse in subsequent processes (Faix *et al.* 2004). In this process, transiently expressed cre-recombinase excises the blasticidin-resistance cassette whilst maintaining the gene disruption (Faix *et al.* 2004). The blasticidin-resistance cassette can thus be recycled for generation of multiple disruptions, and for use in assays, including the *cdk8* gene-targeting assay. However, the nature of *exo1*$^{-}$ strain generation prevented removal of the blasticidin-resistance cassette, and hygromycin was therefore selected as an alternative selectable marker (Egelhoff *et al.* 1989). The blasticidin-resistance cassette of the *cdk8*-knockout construct was replaced with the hygromycin-resistance cassette from pHygTm-plus (M. Fukusawa, Figure 3.5B). The resultant *cdk8*(Hyg)-disruption construct, was assessed for gene-targeting as before.

Consistent with the role of Exo1 in HR, no agg^{-} colonies were observed relative to Ax2, which had a targeted integration efficiency of 5.5% (Figure 3.5C). One interpretation of this is that the *cdk8*$^{-}$/*exo1*$^{-}$ disruption is lethal. To discount this possibility, the *cdk8*$^{-}$ strain (Greene *et al.* 2011) was transfected with the *exo1*$^{-}$ disruption cassette (Hsu *et al.* 2011), and targeted integration assessed by PCR of

pools of blasticidin-resistant colonies (Figure 3.5D). The presence of a PCR product in 3 independent pools revealed targeted integration of the *exo1*$^{-}$ cassette, and illustrates that disruption of *cdk8* in the *exo1*$^{-}$ strain is not lethal. Thus, targeted integration in vegetative *Dictyostelium* is dependent on components of the HR pathway. The gene-targeting assay was therefore used to assess the balance between the two predominant DSB repair pathways, HR and NHEJ, in vegetative *Dictyostelium* disrupted in NHEJ components.

3.2.3 HR is altered in *Dictyostelium* following disruption of ku80

Similar to yeast, mammals and avian cells, both NHEJ and HR can occur in G2 *Dictyostelium* (Weijer *et al.* 1984; Muramoto and Chubb 2008; Hsu *et al.* 2011), although, there is greater dependence on HR for tolerance to DSBs at this stage of the cell cycle (Hsu *et al.* 2011). In yeast and vertebrates, the competition between NHEJ and HR to maintain genomic integrity has been postulated. This is due to the increased HR as determined by I-Sce/HO endonuclease assays when NHEJ components, such as Ku or DNAPKcs, are disrupted (Clikeman *et al.* 2001; Fukushima *et al.* 2001; Pierce *et al.* 2001; Allen *et al.* 2002). Similarly, gene-targeting efficiency also increases when certain NHEJ components are disrupted (Kooistra *et al.* 2004; Ninomiya *et al.* 2004; Ishibashi *et al.* 2006; Iiizumi *et al.* 2008). However, the molecular basis behind the upregulated HR is unclear. For example, whether increased HR with NHEJ-deficiency represents the general loss of NHEJ or a regulatory function of a specific NHEJ component needs to be addressed. In line with this, Ku-disruption particularly upregulates HR (Pierce *et al.* 2001; Zhang *et al.*

2007), which is attributed to its end protection function inhibiting DNA end-resection (Liang and Jasin 1996; Lee *et al.* 1998; Mimitou and Symington 2010).

As both HR and NHEJ occur in vegetative *Dictyostelium*, the possible competition between these pathways was assessed, in addition to which NHEJ components may exert a regulatory role over repair pathway choice. To achieve this, the different DSB repair assays available were applied to assess DSB repair phenotypes in strains disrupted in *ku80* and the putative Artemis orthologue, *dclre1*. In humans, the Artemis nuclease functions downstream of Ku in a subset of NHEJ reactions and IR repair (Ma *et al.* 2002; Riballo *et al.* 2004; Goodarzi *et al.* 2006; Beucher *et al.* 2009). This would enable for determination of whether the HR/NHEJ competition observations reflect the gate-keeper function of Ku, or a general loss of NHEJ.

Before embarking on any investigation of DSB repair regulation in the different NHEJ strains, it was necessary to determine the DSB repair role, if any, of *dclre1*$^-$ cells. Towards this, the DSB sensitivity of the *dclre1*$^-$ strain was assessed by exposing cells to the DSB-inducing agent bleomycin (Figure 3.6A). The *dclre1*$^-$ strain showed no differential bleomycin sensitivity relative to Ax2, possibly suggesting a lack Dclre1 function in tolerance to DNA DSBs. Disruption of *ku80* in *Dictyostelium* also does not give rise to enhanced bleomycin sensitivity in vegetative cells (Hudson *et al.* 2005). Therefore, based on the similar sensitivity profiles of *dclre1*$^-$ and *ku80*$^-$ strains, an alternative interpretation is that Dclre1 is functioning in NHEJ. To formally assess this, exponentially growing *dclre1*$^-$ cells were subjected to the REMI assay alongside Ax2 and *ku80*$^-$, as described in the materials and methods to measure NHEJ (Figure 3.6B). Both the *ku80*$^-$ and *dclre1*$^-$ strains had been

previously generated in the laboratory and subjected to cre-loxing, enabling their direct application in REMI (Hsu *et al.* 2011). REMI was significantly reduced in the *ku80*$^{-}$ and *dclre1*$^{-}$ strains, relative to Ax2. This supports the function of Dclre1 in the *Dictyostelium* NHEJ pathway.

Having determined and confirmed the NHEJ function of Dclre1 and Ku80, respectively, I wanted to determine whether defects in NHEJ in *Dictyostelium* give rise to enhanced HR. To achieve this, the gene-targeting assay was applied to the *ku80*$^{-}$ and *dclre1*$^{-}$ strains and gene-targeting efficiency measured (Figure 3.6C). Both Ax2 and the *dclre1*$^{-}$ strain showed a similar gene-targeting efficiency. However, gene-targeting efficiency in the *ku80*$^{-}$ strain was 6-fold higher than Ax2 or *dclre1*$^{-}$. Thus, in *Dictyostelium,* HR may be upregulated in the *ku80*$^{-}$ strain, suggesting a situation similar to human, yeast and fungi (Kooistra *et al.* 2004; Ninomiya *et al.* 2004; Ishibashi *et al.* 2006; Iiizumi *et al.* 2008), and a specific regulatory function of Ku.

The HR assay observations give rise to an interesting situation where although NHEJ is significantly reduced following disruption of both *ku80* and *dclre1*, only the *ku80*$^{-}$ disruption is accompanied by increased HR. DSB sensitivity assay analysis suggests no long-term consequences of the disruption of these NHEJ components with regards to damage, suggesting that *dclre1*$^{-}$ cells retain DNA DSBs repair capacity. To assess the situation in more detail, the kinetics of DSB resolution were determined by measuring γH2AX decay, as used in other systems (Figure 3.7A) (Riballo *et al.* 2004; Shibata *et al.* 2011). Whilst γH2AX does not strictly reflect DNA damage, its abundance is correlated with DSB levels, and its decay is linked to DSB resolution

(Lobrich *et al.* 2010). Exponentially growing Ax2, *ku80*$^{-}$ and *dclre1*$^{-}$ cells were transiently exposed to bleomycin and γH2AX decay post-exposure was determined by immunofluorescence (Figure 3.7B). Both Ax2 and the *ku80*$^{-}$ strain showed similar kinetics of γH2AX decay, with the rate being slightly enhanced in *ku80*$^{-}$ cells. On the other hand, γH2AX decay was slower in the *dclre1*$^{-}$ strain relative to Ax2, reflecting a slight defect in DSB repair in this case. The delay in γH2AX decay in the *dclre1*$^{-}$ strain likely reflects an NHEJ defect that is not compensated for by increased HR as is the case with the *ku80*$^{-}$ strain. Nevertheless, at later time points, levels of γH2AX are comparable to those of Ax2 and *ku80*$^{-}$. This indicates eventual damage resolution, which is further supported by the sensitivity assay data. To address whether the difference in γH2AX decay between *ku80*$^{-}$ and *dclre1*$^{-}$ strains is specific to the putative gate-keeper function of Ku80, γH2AX decay was assessed in a *ku80*$^{-}$/*dclre1*$^{-}$ double-disruptant (Figure 3.7C). The rationale behind this experiment is that if Ku is playing a dominant gate-keeper function, then the additional disruption of *ku80* in the *dclre1*$^{-}$ strain would give rise to a double-disruptant exhibiting phenotypes similar to the *ku80*$^{-}$ single-disruptant. Consistent with this hypothesis, whilst the *dclre1*$^{-}$ strain again displayed slower γH2AX decay relative to Ax2, γH2AX decay in the double-disruptant was similar, and indeed slightly faster than Ax2 and the *ku80*-disruptants. Thus, the additional disruption of *ku80* reverses the delayed DSB repair kinetics in the *dclre1*$^{-}$ strain. In conclusion, this data highlights Ku as a potential regulator of DSB repair pathway choice in *Dictyostelium*.

3.3 Discussion

In G2, cells are proficient in both HR and NHEJ, and this has given rise to a passive competition model. According to this model, components of the two pathways compete for DNA end binding and processing, and in doing so, preclude DNA ends from the alternative repair pathway. In support of this, *ku*-null strains show increased DNA end-resection (Lee *et al.* 1998; Liang *et al.* 1998), whilst resected DNA ends display reduced Ku binding (Frank-Vaillant and Marcand 2002). However, it is now becoming clear that in addition to the passive competition between pathways, active regulation also plays a role. For example, the initiating step of HR, DNA end resection, is regulated, at least in part, by CDKs which phosphorylate Sae2/CtIP, Dna2 and other targets (Aylon *et al.* 2004; Ira *et al.* 2004; Jazayeri *et al.* 2006; Huertas *et al.* 2008; Huertas and Jackson 2009; Chen *et al.* 2011). Therefore, in G1 of the cell cycle, resection machinery cannot be activated by CDKs, precluding long-range resection necessary for HR (Aylon *et al.* 2004; Ira *et al.* 2004; Jazayeri *et al.* 2006; Huertas *et al.* 2008; Huertas and Jackson 2009; Chen *et al.* 2011). This minimises the potential of HR being engaged in the absence of sister-chromatids. Furthermore, in G2, DNA damage and chromatin complexity may also influence choice, with HR repairing the fraction of DSBs associated with greater complexity (Barlow *et al.* 2008; Beucher *et al.* 2009; Shibata *et al.* 2011). Thus, DNA repair pathway choice may not be a simple passive competition model, but may display a degree of active regulation. However, the mechanisms governing regulation remain

to be determined, including the point at which cells commit to a particular repair pathway.

Given the evidence of DSB repair pathway choice and regulation in other organisms, I wished to establish whether a similar situation existed in *Dictyostelium*. This would enable the subsequent use of *Dictyostelium* as a model for investigating mechanisms of regulation. To date, such investigations have been hindered by the absence of an assay to measure HR directly. In *Dictyostelium*, DSB repair capacity can be assessed via sensitivity assays and γH2AX decay. However, neither of these experimental procedures allow for contribution of different DSB repair pathways to be assessed. Methods for specifically assessing HR include measuring DNA end-resection at DSBs either directly or via the accumulation of ssDNA binding proteins such as RPA and Rad51 (Clerici *et al.* 2008; Shibata *et al.* 2011). Whilst this assessment indicates HR initiation, it may not reflect HR proficiency. Gene-targeting assays, which are dependent on HR components in other organisms, particularly Rad51 and Rad52, can also be used to measure HR efficiency, with the advantage of measuring completed HR events (Schiestl *et al.* 1994; Rijkers *et al.* 1998; Yamaguchi-Iwai *et al.* 1998; Yanez and Porter 1999; Dominguez-Bendala *et al.* 2003; Kooistra *et al.* 2004; Ninomiya *et al.* 2004; Schaefer *et al.* 2010). A further benefit of developing a gene-targeting assay in *Dictyostelium* is that existing disruption strains can be investigated in the assay, and the potential exists for investigating targeting-efficiency at multiple, independent loci to eliminate loci-specific effects.

The HR assay designed exploited the developmental aspect of the *Dictyostelium* lifecycle by targeting *cdk8*, *rasC* and *erkB*, which are genes involved in the

aggregation step of development. Disruption of aggregation by targeting genes involved in cAMP relay and/or chemotaxis gives rise to *Dictyostelium* colonies that are unable to form fruiting bodies on starvation. This provides a binary, high-throughput read-out of targeted integration. Developmental genes are also less likely to play a role in vegetative survival or repair proficiency, which would otherwise influence the interpretation of HR efficiency results. Whilst *erkB* was discarded as a target in the HR assay due to the intermediate phenotype of targeted integrants, *cdk8* and *rasC* had much more binary phenotypes, which were corroborated on the genotype level. However, the transfection efficiency with the *rasC*-construct was very low. Thus, *cdk8* was selected as the preliminary gene-target in the assay, with the potential of enabling increases in gene-targeting to be observed in different genetic backgrounds. However, several alternative candidate genetic loci exist for use in the HR assay that give rise to an agg^- phenotype. These genes can be found on dictyBase, and include *acaA*, which is involved in the cAMP relay response (Meima and Schaap 1999; Schaap 2011).

Although we and others have attempted to generate HR-deficient mutants in *Dictyostelium*, this has proved difficult (Hasegawa *et al.* 2005), emphasising the importance of HR in these organisms. However, an $exo1^-$ strain has been generated in *Dictyostelium*, which shows enhanced DNA DSB sensitivity in vegetative cells, relative to Ax2 and NHEJ mutants. To verify the gene-targeting assay, gene-targeting at the $cdk8^-$ locus was assessed in the $exo1^-$ strain, and consistent with its putative role in HR, no gene-targeting was observed at this locus, supporting the reliance of gene-targeting on HR machinery. The reliance of gene-targeting on other HR components

has also been demonstrated by Zhang *et al*, whereby an *xpf*-disrupted strain had severely compromised gene-targeting at two independent loci (Zhang *et al.* 2009).

The exquisite DSB sensitivity of the *exo1*$^{-}$ strain in vegetative *Dictyostelium* contrasts with the lack of IR or phleomycin sensitivity in the equivalent *S. cerevisiae* mutant strain, likely due to redundancy between Exo1 and Dna2 (Gravel *et al.* 2008; Mimitou and Symington 2008; Zhu *et al.* 2008). A putative *Dictyostelium* Dna2 orthologue has not been identified, although the genome encodes the Mre11-nuclease, which in other organisms initiates DNA end-resection by generating short stretches of ssDNA (Hsu *et al.* 2006; Mimitou and Symington 2008; Zhu *et al.* 2008). Whilst the *Dictyostelium exo1*$^{-}$ strain is very sensitive to DNA DSBs, its lack of lethality may reflect the residual presence of Mre11 (Hsu *et al.* 2006). Therefore, Mre11 may confer sufficient functionality to enable *Dictyostelium* cells to undergo limited resection, allowing for the survival of *exo1*$^{-}$ cells. In *S. cerevisiae*, the limited resection mediated by MRX/Sae2 is sufficient to enable gene-conversion, although the number of events is reduced relative to wildtype cells (Zhu *et al.* 2008). Therefore, limited resection may also enable *Dictyostelium* to partake in some HR or alternative DSB repair pathways, although not enough to undergo gene-targeting.

It has been suggested the Ku and the Mre11 complex independently bind DNA ends in yeast (Wu *et al.* 2008). The Mre11-complex can reduce Ku binding to DNA DSBs, either via its DNA resection activity, or by the physical presence of Mre11 at DNA ends (Llorente and Symington 2004; Wu *et al.* 2008; Mimitou and Symington 2010; Shim *et al.* 2010). The greatly increased IR sensitivity of yeast *mre11*-null mutants is thought to arise specifically via the inhibitory action of Ku on long-range resection,

and can be reversed by the additional deletion of Ku (Mimitou and Symington 2010; Shim *et al.* 2010; Chen *et al.* 2011).

The function of the Mre11-complex has remained elusive in *Dictyostelium* due to an inability to generate an *mre11*$^{-}$mutant, likely due to the lethality of this strain, although an *mre11*$^{-}$ strain has been generated in a *ku80*$^{-}$ background (J. Hudson, unpublished). Thus additional *ku80* disruption may suppress *mre11*$^{-}$ lethality, possibly by suppressing the inhibitory effect of Ku on DNA end-resection, in agreement with the situation in other organisms. The severity of the *mre11*-disruption in *Dictyostelium* relative to yeast may be due to the nature of endogenous damage being encountered, which is a particularly good substrate for Ku in the absence of Mre11. Furthermore, *in vitro*, the Mre11-complex has a stimulatory role on resection by Exo1, when Exo1 levels are limiting (Nicolette *et al.* 2010). Thus, the absence of the Mre11-complex in *Dictyostelium* may severely limit the resection proficiency of Exo1, compounded by the absence of a Dna2 orthologue and the inhibitory binding of Ku to DNA ends. Overall, the essential function of Mre11 in *Dictyostelium* is clearly indicated by these observations and may account for the lack of lethality of the *exo1*$^{-}$ strain. It would be interesting to determine whether conditional expression of nuclease-dead Mre11 could suppress the *mre11*$^{-}$ strain lethality. This would allow the contribution of the nuclease function of Mre11 to be determined. Furthermore, it would lend support to the hypothesis that the inhibitory activity of Ku at DNA ends gives rise to *mre11*$^{-}$ strain lethality. In yeast, nuclease-dead MRX can complement the IR sensitivity of *mre11*$^{-}$ strains, likely by precluding Ku binding to DNA ends, and recruiting and stimulating long-range resection components (Barlow *et al.* 2008; Mimitou and Symington 2010).

The lack of DSB sensitivity of NHEJ mutants in G2 *Dictyostelium* relative to Ax2 implied that NHEJ does not contribute to tolerance to DSBs at this cell-cycle phase. However, the REMI data with *ku80*$^{-}$ and *dclre1*$^{-}$ mutants (Hsu *et al.* 2011), and work by Muramoto *et al* (Muramoto and Chubb 2008) illustrated the occurrence and importance of NHEJ at this developmental stage. Furthermore, the delay in γH2AX decay post-bleomycin treatment in the *dclre1*$^{-}$ strain indicated the contribution of NHEJ to DSB repair, at least for a subset of DNA damage. This is consistent with the situation in other organisms, describing the contribution of both NHEJ and HR in G2 of the cell cycle (Takata *et al.* 1998; Rothkamm *et al.* 2003; Beucher *et al.* 2009). Although, unlike human cells where NHEJ functions as the major DSB repair in G2 (Beucher *et al.* 2009; Shibata *et al.* 2011), HR is the major DSB repair pathway in *Dictyostelium*. This may be due to the complexity of DNA damage, or the nature of the *Dictyostelium* chromatin. Nevertheless, given the occurrence of HR and NHEJ in *Dictyostelium*, its potential as a model to investigate DSB repair pathway choice regulation was highlighted.

The application of the HR assay to measure changes in gene-targeting levels in different genetic backgrounds allowed us to make headway in the balance and regulation between NHEJ and HR. Although both *ku80*$^{-}$ and *dclre1*$^{-}$ mutant strains showed reduced REMI, increased gene-targeting was only seen in the *ku80*$^{-}$ strain, highlighting the potential regulatory function of Ku. Disruption of Ku has been shown to lead to enhanced HR and gene-targeting in other organisms. This identified Ku as a DNA DSB repair regulator by inhibiting DNA end resection, preventing the initiation of HR. The fact that *dclre1*$^{-}$ cells do not show enhanced gene-targeting

indicates that in *Dictyostelium* this regulatory effect is limited to Ku. Other early components in the NHEJ pathway may also exert a regulatory role, including DNAPKcs, as has been illustrated in mammalian cells (Pierce *et al.* 2001; Allen *et al.* 2002; Shibata *et al.* 2011), although this remains to be determined in *Dictyostelium*. The role of downstream NHEJ components in regulation should also not be ignored, with increased HR being observed in the absence of XRCC4 in mammals (Pierce *et al.* 2001) and Dnl4 or Lif1 in yeast (Zhang *et al.* 2007).

The major regulatory gate-keeper potential of Ku is supported by its primary binding to DNA DSBs in humans, upstream of HR components *in vivo* (Kim *et al.* 2005; Shibata *et al.* 2011). However, Ku association with DNA DSBs is dynamic (Mari *et al.* 2006; Uematsu *et al.* 2007). Thus, factors which can modulate Ku DNA end binding affinity or stability could also modulate repair pathway choice, by increasing or reducing the accessibility of DNA ends to nucleases. In line with this, the NHEJ Ligase IV-complex has been illustrated to enhance the stability of Ku binding to DNA ends (Zhang *et al.* 2007; Chen and Tomkinson 2011; Yano *et al.* 2011), with a concomitant reduction in DNA end resection (Zhang *et al.* 2007), directing repair towards NHEJ. Post-translational modifications of Ku may also modulate its affinity for DNA ends. For example, Ku is known to be a target of PARylation which may serve to alter its activity in NHEJ to promote HR (Li *et al.* 2004; Hochegger *et al.* 2006; Saberi *et al.* 2007).

The γH2AX decay profiles of *ku80*$^{-}$ and *dclre1*$^{-}$ strains provide further insight into *Dictyostelium* DSB repair mechanisms. The enhanced γH2AX decay kinetics of *ku80*$^{-}$ strains relative to Ax2 suggests enhanced DNA DSB repair efficiency in the

absence of the Ku heterodimer. A similarly enhanced repair efficiency is observed in DT40 cells, where *ku*-disruptants have increased IR-resistance (Fukushima *et al.* 2001). This suggests that Ku may interfere with some HR events in *Dictyostelium*, possibly by interfering with DNA end-resection. Dclre1 is also a component of NHEJ as illustrated by significantly defective REMI. However, unlike *ku80*$^{-}$ strains, its disruption delays γH2AX decay relative to Ax2, suggesting that at least a fraction of DNA DSBs are repaired by NHEJ. Whether this NHEJ-usage occurs via passive engagement of DSBs by NHEJ or represents a specific subset of damage with respect to damage or chromatin complexity is unclear. The eventual reduction in γH2AX to background levels in *dclre1*$^{-}$ cells and the lack of a DSB sensitivity phenotype suggests engagement of alternative DSB repair pathways. This data also highlights that if NHEJ pathway commitment occurs, it is downstream of Dclre1. Consistently in human cells, NHEJ may be initially attempted (Kim *et al.* 2005; Shibata *et al.* 2011), and failure of which leads to the engagement of HR as illustrated by increased DNA end-resection (Shibata *et al.* 2011). This is in contrast to initiation of HR by end-resection, which precludes NHEJ (Frank-Vaillant and Marcand 2002; Shibata *et al.* 2011). The delayed γH2AX decay kinetics of *dclre1*$^{-}$ cells likely illustrates the interference by Ku at DNA DSBs which cannot be repaired by NHEJ due to the absence of Dclre1. This is supported by reversal of the γH2AX decay phenotype in *dclre1*$^{-}$ cells, by the additional deletion of *ku80*. Thus, the failed attempt to undergo NHEJ and futile cycles of Ku engagement at DNA DSBs may limit DNA end resection, and explain the lack of increased gene-targeting efficiency in the *dclre1*$^{-}$ strain. However, further experimentation is required to assess the relationship between these observations as the gene-targeting assay measures HR at a single-locus. In comparison, γH2AX decay assesses repair at multiple loci, a subset of which may

have a different requirement for specific HR pathways. Whilst Ku can modulate DSB repair efficiency, HR is still the major repair pathway in vegetative *Dictyostelium* for DSB tolerance. Thus, additional factors may operate at this developmental stage to modulate Ku binding to DNA ends, whilst NHEJ may also be engaged to resolve a subset of damage. Germinating spores which are also in G2 (MacWilliams *et al.* 2006; Muramoto and Chubb 2008), display enhanced DSB-sensitivity in NHEJ-deficient strains relative to parental Ax2, suggesting increased NHEJ reliance at this developmental stage. However, whether this reflects altered DSB repair pathway input, with reduced HR contribution, or an increased reliance on both pathways remains to be determined, and the molecular basis behind observations dissected.

Overall, an interesting mechanism of DSB repair regulation is being revealed in the G2 cell cycle stage of *Dictyostelium*. Whilst HR may be the major repair pathway in this organism, NHEJ can occur at a subset of DNA ends, precluding their repair by HR (Figure 3.8). This channelling activity is mediated early on in the NHEJ pathway via Ku. Ku may be regulated by post-translational modifications, or via affinity for DNA with differently damaged ends or in different chromatin environments. For a subset of DNA damage, NHEJ is clearly the primary repair pathway employed. However, in instances where NHEJ is initiated but cannot be completed, alternative repair pathways are then utilised. In the case of the *ku80*$^{-}$strain, NHEJ cannot be initiated and thus DNA ends are available for DNA-end resection, and the initiation of HR, leading to enhanced gene-targeting. However, in the *dclre1*$^{-}$ strain, Ku binding to DNA ends may lead to unsuccessful NHEJ attempts, followed by the engagement of other DSB repair pathways not measured by the gene-targeting assay. This

accounts for the lack of DSB sensitivity in NHEJ mutants, and the delay in γH2AX decay in the *dclre1*$^{-}$ strain.

In conclusion, a gene-targeting assay showing dependence on HR components has been developed in *Dictyostelium*, raising the possibility of using this as a readout of HR. The possibility of targeting other genetic loci, to overcome loci-specific effects is also possible, and will be used in the future to verify these findings. The opportunity to look at how repair pathway levels change in different genetic backgrounds will shed further light on the regulation of repair pathway choice in *Dictyostelium*. Furthermore, the regulatory role of genes that are absent in other genetically tractable organisms such as yeast can be investigated, as has been done with Dclre1, including Poly(ADP-ribose) Polymerases (PARPs).

4: The role of Poly ADP-ribosylation in DNA single-strand break repair in *Dictyostelium*

4.1 Introduction

PARylation is one of the earliest responses to DNA damage (Okano *et al.* 2003). It is characterised by the post-translational modification of nuclear proteins with chains of ADP-ribose, which are derived from NAD^+ (D'Amours *et al.* 1999). The ADP-ribose units in PAR are covalently linked by glycosidic bonds and can be over 200 units *in vitro*, with branching arising every 20-50 units (D'Amours *et al.* 1999). However, ADP-ribosylation can also be represented by shorter oligomers and by mAR (D'Amours *et al.* 1999). The significance of this PAR heterogeneity is not clear but may play a role in mediating specific recognition events to direct the diverse functions of PARPs in regulating gene-expression and modulating chromatin structure and DNA repair (Fahrer *et al.* 2007; Hakme *et al.* 2008).

In mammals, ADP-ribosylation is mediated by ADP-ribosyltransferases (ARTs), of which there are 17 encoded by the human genome (Otto *et al.* 2005). However, only a proportion of human ARTs have been characterised (Ame *et al.* 2004). The catalytic capacity of uncharacterised ARTs can be predicted from catalytic domain sequence analysis (Ame *et al.* 2004). This has suggested that some ARTs are catalytically inactive, or exhibit mAR activity (Ame *et al.* 2004). Conversely, the

ARTs PARP1 and 2 have PAR capacity and have been implicated in SSBR (Trucco *et al.* 1998; Schreiber *et al.* 2002; Menissier de Murcia *et al.* 2003). PARP1 and 2 disruptions lead to SSB and base-damaging agent sensitivity in vertebrate cells (Masutani *et al.* 1999; El-Khamisy *et al.* 2003; Menissier de Murcia *et al.* 2003; Hochegger *et al.* 2006), and radiation and alkylating agent sensitivity in whole animal models (de Murcia *et al.* 1997; Masutani *et al.* 1999; Menissier de Murcia *et al.* 2003). Due to greatly diminished PARylation in *parp1*$^{-/-}$ cells, PARP1 is regarded as the major responder to DNA damage (El-Khamisy *et al.* 2003; Fisher *et al.* 2007), with PARP2 showing a fraction of the activity of PARP1 *in vivo* (Ame *et al.* 1999; Fisher *et al.* 2007) and *in vitro* (Schreiber *et al.* 2002). However, redundancy between these proteins may exist (Schreiber *et al.* 2002; Menissier de Murcia *et al.* 2003), and embryonic lethality is observed in double-disruptants (Menissier de Murcia *et al.* 2003).

PARP1 damage recognition is mediated by two N-terminal zinc fingers (Gradwohl *et al.* 1990; Ikejima *et al.* 1990). The mechanism of damage recognition by PARP2 is less clear, but it contains an N-terminal NLS and a DNA binding domain (Ame *et al.* 1999) with similarity to the nucleic acid binding SAP domain (Aravind and Koonin 2000). PARP1 recognises SSBs, whilst PARP2 recognises gaps and flap structures, which are intermediates that can arise later in BER/SSBR (Schreiber *et al.* 2006). Consistently, *in vivo*, PARP1 is primarily recruited, followed by PARP2 recruitment (Mortusewicz *et al.* 2007). Following damage recognition, PARP1 and PARP2 become activated and catalyse PARylation of nuclear proteins. PARylation targets of PARP1 include histones (Ogata *et al.* 1981; Adamietz and Rudolph 1984; Huletsky *et al.* 1989; D'Amours *et al.* 1999), with the major target of PARP1 activity being itself

(Ogata *et al.* 1981). PARylation of histones may facilitate chromatin relaxation and damage site access (Poirier *et al.* 1982), whilst autoPARylated PARP1 may recruit XRCC1 (Schreiber *et al.* 2002; El-Khamisy *et al.* 2003; Okano *et al.* 2003). XRCC1 is a scaffolding protein that coordinates the SSBR/BER process via interactions with downstream components of the repair pathway (Caldecott 2003). The role of PARP1 in recruiting XRCC1 may therefore explain the genetic instability and the defective BER/SSBR phenotypes observed with PARP1 disruption or inhibition. However, more recent reports suggest that despite a positive role of PARP1 in SSBR, it may play no role or an inhibitory role in BER (Vodenicharov *et al.* 2000; Allinson *et al.* 2003; Strom *et al.* 2011). Thus the molecular basis of PARP1 function in SSBR and BER requires further characterisation.

The absence of ARTs in genetically tractable model organisms has somewhat hindered investigation of ART function. Neither the *S. cerevisiae* nor *S. pombe* genome encode any ARTs (Scovassi *et al.* 1986; Hottiger *et al.* 2010), and *D. melanogaster* and *C. elegans*, contain only 2 or 3 ARTs, respectively (Hottiger *et al.* 2010). This is in contrast to the 17 ARTs encoded by the human genome (Otto *et al.* 2005). A limitation of *D. melanogaster* is that it contains a single repair PARP orthologue (Uchida *et al.* 1993), precluding investigation of the overlapping functions of repair PARPs, as is the case in mammals (Menissier de Murcia *et al.* 2003). In organisms with a single PARP1-like orthologue, such as *D. melanogaster* (Miwa *et al.* 1999; Tulin *et al.* 2002) and *A. nidulans* (Semighini *et al*. 2006), its gene disruption is lethal. This hinders investigation of the isolated function of these PARPs. However, DT40 cells disrupted at the PARP1 locus are viable, providing some insight into PARP1 function (Hochegger *et al.* 2006).

In silico analysis of the *Dictyostelium discoideum* genome has indicated conservation of at least nine putative ARTs (Otto *et al.* 2005), including those showing similarity to human PARP1 (Citarelli *et al.* 2010). A purified *Dictyostelium* ART demonstrated a PARylation *in vitro* in response to nicked DNA (Kofler *et al.* 1993). PARylation also occurs *in vivo* in *Dictyostelium* following DNA damage (Rickwood and Osman 1979; Rajawat *et al.* 2007), which can be inhibited by commercially available PARP inhibitors (Rajawat *et al.* 2007). This preliminary ART analysis makes *Dictyostelium* a strong candidate to investigate the biological functions of these enzymes. This is especially true with regards to clarifying the currently ambiguous role of ARTs in the repair response. The conservation of multiple *Dictyostelium* ARTs, and in particular several putative PARP1-orthologues (Otto *et al.* 2005; Citarelli *et al.* 2010) would allow for redundant and non-redundant ART functions in the repair response to be elucidated. This coupled with the high degree of repair pathway and repair component conservation in *Dictyostelium* make it likely that observations could be extrapolated to higher eukaryotes.

To exploit *Dictyostelium* as a model to more fully assess ART function in repair, I wanted to initially assess whether, if similar to humans, ARTs function in *Dictyostelium* SSBR/BER. Towards this, my aims were to more completely characterise the conservation of ARTs and SSBR/BER components in the *Dictyostelium* genome. In addition I wanted to determine whether a PARylation response is induced in *Dictyostelium* following base damage and SSBs. This would be followed by a genetic approach to dissect the contribution of putative repair ARTs to PARylation and survival following DNA base damage and SSB induction. Overall,

the work in this chapter has enabled us to more fully determine the conservation of ART function in *Dictyostelium* relative to mammals, paving the way for more novel investigations into the molecular basis behind ART functions in SSBR/BER.

4.2 Results

4.2.1. Conservation of the components of single-strand break repair and base excision repair in the *Dictyostelium* genome

The best established role of PARP1 and PARP2 is in SSBR/BER. Thus, before embarking on an extensive study of the PARylation response in *Dictyostelium*, the level of core BER component conservation was determined. This conservation seemed highly likely given the conservation of ARTs (Otto *et al.* 2005) and the induction of a PARylation response in *Dictyostelium* following administration of DNA SSBs (Rajawat *et al.* 2007). Consistent with the high degree of evolutionary conservation of the BER pathway (Robertson *et al.* 2009), all major components of the BER/SSBR pathway could be identified in *Dictyostelium* by searching its genome and predicted genes on dictyBase.org (Table 4.1). This included the previously described type III (Freeland *et al.* 1996) and type IV (Tsuji *et al.* 2001) APE orthologues, DDB_G0277701 and DDB_G0279923, respectively. The type IV APE is present in bacteria, fungi, *C. elegans* and archaea, but is absent in humans or other higher eukaryotes (Johnson *et al.* 1998). Of particular interest was the conservation of an *xrcc1* orthologue, DDB_G0275653 in *Dictyostelium*, which has not been

identified in lower-eukaryotes (Caldecott 2008). A constitutive partner of XRCC1 is Ligase III (Caldecott *et al.* 1994), and consistent with this, the absence of an XRCC1 orthologue in *S. cerevisiae* coincides with the absence of a Ligase III orthologue. Conversely, a Ligase III orthologue, DDB_G0283857, has been identified in *Dictyostelium*. In mammals, XRCC1 recruitment to DNA damaged by oxidating or methylating agents may be facilitated by PARylated PARP1 (Masson *et al.* 1998; El-Khamisy *et al.* 2003; Okano *et al.* 2003; Mortusewicz *et al.* 2007). Given the conservation of damage-induced PARylation and XRCC1 in *Dictyostelium*, it is interesting to speculate that a similar mechanism of XRCC1 recruitment to DNA damage may exist in this organism to facilitate SSBR/BER.

4.2.1 *Dictyostelium* show conservation of PARPs

Having identified core components of the BER/SSBR pathway in the *Dictyostelium* genome, the extent of ART conservation in this organism was addressed. ARTs are widely conserved amongst a range of organisms, but the presence of PARPs has been linked to multicellularity (Semighini *et al.* 2006). The mammalian genome encodes 17 ARTs, including several PARPs (Otto *et al.* 2005). PARP orthologues and PARP activity have also been identified in *Dictyostelium* (Rickwood and Osman 1979; Kofler *et al.* 1993; Otto *et al.* 2005; Rajawat *et al.* 2007), consistent with its ability to become multicellular. However, PARPs have not been identified in the unicellular *S. cerevisiae* (Scovassi *et al.* 1986) or *S. pombe* (Hottiger *et al.* 2010).

To more fully assess ART conservation in *Dictyostelium*, a BLASTp search was performed against the entire *Dictyostelium* genome on dictyBase.org, searching for genes with homology to the human PARP1 catalytic domain (amino acids 663-1014 as defined by Altmeyer *et al*. 2009) (Table 4.2). This identified 8 genes, and increasing the e-value threshold revealed a further 2 genes. Several predicted *Dictyostelium* genes have been annotated, and putative functions assigned based on domain conservation and similarity to human genes (Chisholm *et al.* 2006). Searching dictyBase.org for genes with characterised or putative NAD^+ ADP-ribosyltransferase activity identified an additional 4 genes, as well as 9 of the genes located in the BLASTp search, except DDB_G0276785. Comparison with results from a recently published analysis of the *Dictyostelium* genome (Citarelli *et al.* 2010) also highlighted an additional gene, DDB_G0278045. Thus, the *Dictyostelium* genome contains 15 genes with similarity to human PARP1, or with putative ADP-ribosyltransferase activity.

The transient nature of the PAR modification is conferred by enzymes that have the capacity to degrade PAR. In mammals, PAR Glycohydrolase (PARG) is an enzyme that catalyses the hydrolysis of PAR to ADP-ribose molecules and free ADP-ribose (Meyer-Ficca *et al.* 2004). In addition, another enzyme with PAR glycohydrolase activity was identified in mammals, ADP-ribose-(arginine) protein hydrolase 3 (ARH3) (Oka *et al.* 2006). ARH3 is in a family that contains 2 other members, ARH1 and the poorly characterised ARH2 (Oka *et al.* 2006). However, only ARH3 confers PAR activity, whilst ARH1 is a mono-ADP-ribose arginine-hydrolase (Oka *et al.* 2006). Through searching dictyBase.org, a putative ARH1 orthologue, DDB_G0289675, was identified in *Dictyostelium,* whilst an orthologue of ARH3 was

not found. Nevertheless, *Dictyostelium* does encode a predicted orthologue of PAR glycohydrolase (PARG), DDB_G0277943. Therefore, the *Dictyostelium* genome encodes enzymes that may confer PAR synthesis and hydrolysis activity.

Putative protein domains within genes have been bioinformatically characterised on dictyBase.org via Interpro. Interpro merges information to create a database against which other proteins can be compared to enable domain identification (Hunter *et al.* 2009). This facility was used to identify protein domains in the bioinformatically identified *Dictyostelium* ARTs (Figure 4.1). The diversity of human ART function likely stems from the association of its catalytic domain with many different protein domains (Otto *et al.* 2005; Krishnakumar and Kraus 2010). These protein domains may determine, amongst other things, cellular localisation or protein partners of ARTs (Otto *et al.* 2005; Krishnakumar and Kraus 2010). The same may be true in *Dictyostelium,* given the diversity of protein domains associated with the NAD^+ ADP-ribosyltransferase domain. In some cases, the identified *Dictyostelium* ARTs displayed only catalytic domain conservation, indicating that they may also contain as yet uncharacterised protein domains.

Dictyostelium ARTs display conservation of protein domains found in human ARTs. It is therefore interesting to consider the possibility of assigning *Dictyostelium* ARTs to human counterparts. This would be based not only on conservation of individual domains, but also their association with other domains. In line with this, the degree of identity and similarity between *Dictyostelium* PARPs and full-length hPARP1 was determined. A BLASTp search with full-length hPARP1 was performed against predicted *Dictyostelium* proteins and identified several genes (Table 4.3A). With the

exception of DDB_G0271766, the remaining ART genes that were not highlighted from this BLAST search were those that had no identifiable protein domains, other than the PARP catalytic domain. Genes sharing high identity to full-length hPARP1 were *adprt1a*, *adprt1b*, *adprt2* and *adprt4*, whereas the remaining genes showed % identity of <10%.

Interestingly, Citarelli *et al* (Citarelli *et al.* 2010) organised *adprt1a*, *adprt1b* and *adprt2* into the same clade as hPARP1 and hPARP3, both of which have been implicated in the DNA damage response (Trucco *et al.* 1998; Rouleau *et al.* 2007; Citarelli *et al.* 2010; Rulten *et al.* 2011). Consistently, these genes all have DNA interacting domains in the form of the unique 28-30 amino acid CCHC ZF motif, as found in human PARP1 (D'Amours *et al.* 1999) and/or the WGR domain (Citarelli *et al.* 2010). No nucleic acid interacting domain was identified in *adprt4*. Unlike the two tandem ZFs in hPARP1, *adprt1a* and *adprt1b* contain only a single ZF. Nevertheless, the presence of nucleic acid binding domains may implicate these *Dictyostelium* ARTs in the DNA damage response. Further analysis of *adprt1a, adprt1b* and *adprt2* indicated that both *adprt1a* and *adprt1b* have a very similar domain organisation to PARP1, although *adprt1b* lacks a BRCT domain. Furthermore, *adprt1a* and *adprt1b* contain a third zinc-finger, ZF3, in the pADR1 domain, which is a domain of unknown function (Staub *et al.* 2004). ZNF3 has only been identified in hPARP1 and is involved in catalytic activation and homodimerisation (Langelier *et al.* 2008). This supports the hypothesis that these *Dictyostelium* ARTs may contain DNA damage-induced catalytic activity.

To assess the likelihood of the putative DNA damage response ARTs, *adprt1a, adprt1b* and *adprt2*, functioning as ARTs, the degree of catalytic domain conservation to hPARP1 was determined. A high sequence identity and similarity between *adprt1a*, *adprt1b* and *adprt2* and the hPARP1 catalytic domain (amino acids 663-1014) was calculated by BLASTp (Table 4.3 B). However, with regards to PARP function, of particular interest is the highly conserved 50 amino acid NAD^+ binding core (amino acids 859-908) (Ruf *et al.* 1996), and the H_{862}-Y_{907}-E_{988} catalytic triad. This catalytic triad forms key NAD^+ interactions, and the glutamate residue confers ADP-ribose elongation, and therefore, PARP activity (Marsischky *et al.* 1995). In humans, the catalytic triad is between amino acids 862 to 988, and via BLASTp analysis was demonstrated to share high amino acid sequence identity and similarity with *Dictyostelium adprt1a*, *adprt1b* and *adprt2* (Table 4.3C).

Further analysis of these three *Dictyostelium* ARTs, to determine conservation of the H-Y-E residues of the catalytic triad was performed using ClustalW (Chenna *et al.* 2003) (Figure 4.2). Based on the alignments, *adprt1a* shows conservation of the HYE catalytic triad. For *adprt1b*, the H and Y residues align with those of hPARP1, whilst the residue in alignment with the E of hPARP1 is a glutamine. However, there is a glutamate residue two amino acids upstream that may form the catalytic glutamate. Citarelli *et al* performed an alignment of *adprt2*, and demonstrated conservation of the catalytic triad (Citarelli *et al.* 2010). Overall, *adprt1a, adprt1b* and *adprt2* contain putative DNA binding domains and display a high degree of sequence conservation to hPARP1. This includes conservation of the catalytic glutamate, indicating that these ARTs may possess PAR function. Thus, contribution of *adprt1a, adprt1b* and *adprt2*

in DNA BER/SSBR repair, which is the most well established role of PARPs, was determined.

4.2.2. *Dictyostelium* undergo PARylation in response to DNA single-strand breaks and base damage

Having confirmed the conservation of ARTs in *Dictyostelium*, any putative PARP activity was characterised in this organism. In mammalian cells, nuclear PARylation is rapidly and transiently induced following exposure of cells to DNA SSB and base-damaging agents, such as H_2O_2 (Bradley and Kohn 1979) and MMS (Beranek 1990). To initially investigate PARylation in *Dictyostelium,* cells were treated with MMS. MMS preferentially methylates adenine and guanine bases, and is repaired by an XRCC1-dependent BER pathway in mammalian cells (Lundin *et al.* 2005). Immunofluorescence post-MMS treatment using an anti-PAR antibody demonstrated nuclear staining appearing as early as 10 mins following 5mM MMS treatment (Figure 4.3A). Staining increased proportionally with the MMS dose and treatment time (Figure 4.3B and C), and went from focal to pan-nuclear (data not shown).

Clustered DNA SSBs arising either directly or indirectly, can give rise to DNA DSBs (Bradley and Kohn 1979). To ensure that PAR staining post-MMS was not a result of DSBs, the DSB marker, γH2AX, was assessed at the maximal MMS dose and time (Rogakou *et al.* 1998) (Figure 4.3D). Following MMS treatment, γH2AX levels were not significantly greater than untreated cells, but were significantly less than the phleomycin-treated controls ($p<0.05$). Thus, MMS-induced PARylation in

Dictyostelium is likely arising from base-damage or indirect SSBs, and not DNA DSBs.

I wanted to determine whether commercially available PARP inhibitors were able to inhibit the MMS-induced nuclear PARylation in *Dictyostelium* to assess whether the damage-induced PAR staining was being mediated by PARPs. In these experiments, first and second generation competitive PARP inhibitors benzamide or 8-Hydroxy-2-methyl-4(3H)-quinazolinone (NU1025) were used (Griffin *et al.* 1998; Cepeda *et al.* 2006). Benzamide has been previously used in *Dictyostelium* to inhibit PARylation (Rajawat *et al.* 2007), whilst NU1025 was used as a higher potency alternative. Given that PARP inhibitors exert their function by binding into the highly conserved NAD^+ binding domain, they can be regarded as having a broad specificity. However, determination of PARP inhibitor specificity has indicated preferential targeting of human PARP1, 2 and 3, with the greatest specificity for PARP1 and PARP2 (Hoffmann and Meneghini 1979; Farmer *et al.* 2005; Loseva *et al.* 2010; Rouleau *et al.* 2010).

To determine the role of PARPs in damage-induced PAR staining, Ax2 cells were pre-treated with benzamide or NU1025, and MMS-induced PARylation determined by immunofluorescence (Figure 4.4A). PARylation post-MMS was reduced for both benzamide and NU1025. Under the conditions utilised in these experiments, benzamide gave rise to complete inhibition (Figure 4.4B), whilst NU1025 reduced PARylation by 50% (Figure 4.4C). This difference may reflect insufficient NU1025 being administered, or its instability. However, an alternative explanation may be that the broader specificity PARP inhibitor, benzamide, is more effective at targeting the

Dictyostelium PARPs that mediate the PARylation in response to MMS induced damage than NU1025.

MMS predominantly gives rise to base-damage, therefore, to assess whether DNA PARylation is also induced by DNA SSBs in *Dictyostelium*, cells were treated with H_2O_2 (Hoffmann and Meneghini 1979; Mello Filho and Meneghini 1984). Treatment of Ax2 with H_2O_2 once again gave rise to nuclear PARylation in Ax2 (Figure 4.5A), which could be inhibited by Benzamide (Figure 4.5B) and reduced following NU1025 treatment (Figure 4.5C). This is consistent with published data illustrating that hydroxylamine-induced oxidative damage gives rise to PARylation that can be inhibited by benzamide (Rajawat *et al.* 2007). Thus, PARylation can be induced by DNA base-damage and SSBs in a manner that can be reduced by PARP inhibitors, supporting the role of PARPs in this response.

4.2.3 Generation of putative DNA damage response *adprt* disruptants

The reduction of PARylation in *Dictyostelium* post-MMS and -H_2O_2 treatment by benzamide and NU1025 indicated the role of PARPs in this response. I therefore wanted to dissect this observation and to address the specific *Dictyostelium* ARTs contributing to the DNA damage response. Currently available PARP inhibitors have a broad PARP specificity, as illustrated by their inhibition of hPARP1, hPARP2 and hPARP3 (Farmer *et al.* 2005; Loseva *et al.* 2010). Therefore, a genetic approach was adopted to dissect the contribution of specific *Dictyostelium* ARTs to DNA damage-induced PARylation.

PARP1 is regarded as the main responder to DNA SSBs and base damage. Thus, due to hPARP1 sequence similarity, the presence of putative nucleic acid binding domains and the conservation of the HYE catalytic triad, genetic disruptions of *adprt1a*, *adprt1b* and *adprt2* were primarily considered. The *adprt1b*-disrupted strain, generated in an Ax4 background, was a gift from Ted Cox (Sawai *et al.* 2007). For *adprt1a* and *adprt2*, disruption-constructs, targeting the C-terminal catalytic domain containing portion of the gene were generated (Figure 4.6). These constructs contain arms homologous to regions of the Ax2 genome, which were amplified by PCR from Ax2 genomic DNA, and cloned into pLPBLP on either side of a *BsR* cassette. In the case of *adprt1a*, the homologous arms were positioned upstream (+1070 to +1907bp) and downstream (+3643 to +4325bp) of the catalytic domain (+2420 to +3404bp). For *adprt2*, the upstream (+543 to +1500bp) and downstream (+2482 to +3236bp) arms once again flanked the catalytic domain (+1559 to +2262bp). Targeted integration would replace the entire catalytic domain with the *BsR* cassette in *adprt1a* and *adprt2*, giving rise to *adprt* genes incapable of catalytic activity. Thus, the catalytic contribution of the different *adprt* genes following treatment with DNA damaging agents could be determined. This would be followed by further phenotypic assessment with regards to SSBR/BER.

For *adprt1a*, the disruption construct was digested with the relevant restriction enzymes to liberate the disruption cassette (Figure 4.6A). The excised disruption cassette was transfected into Ax2 as outlined in the Materials and Methods, and integrants selected with blasticidin. Blasticidin-positive colonies were screened by PCR to distinguish targeted from random integration events. The screening PCR gave rise to a 2kbp product which would only appear for targeted integration events (data

not shown). Alongside, a control PCR to confirm genomic DNA quality was performed which gave rise to a 1.7kbp product in all cases (data not shown). Single targeted-disruptants were isolated, and then screened as before to ensure a clonal population. Isolated clones were further verified by Southern blotting using a probe against the downstream homologous arm (Figure 4.7A) or the *BsR* cassette (data not shown), to confirm the nature of the integration and ensure a single integration event, respectively. Ax2 was similarly analysed as a control, and in all cases, the correct band sizes were observed. Thus, based on PCR and Southern blotting verification, two clones of the *adprt1a*$^{-}$ strain were taken forward for phenotypic analysis. Generation and verification of the *adprt2*$^{-}$ strain was carried out similarly. Integrants were screened by PCR (Figure 4.7B) and successful integrants gave rise to a 1.6 or 1.9kbp product for the 5' and 3' screen, respectively. A control PCR was once again run alongside the screens to confirm that the genomic DNA was a suitable template for PCR, and gave rise to a 1.3kbp band for both the 5' and 3' control in all cases. Confirmation of a single disruption-cassette integration event at the target locus was achieved by Southern blotting using a probe against *BsR* following digestion of the genomic DNA with *Pvu*II (Figure 4.7B). As expected, no band was observed for Ax2, but a 2.4kbp band was observed for the *adprt2*$^{-}$. As was the case for the *adprt1a*$^{-}$ strain, two independent *adprt2*$^{-}$ clones were generated.

In mammals, functional redundancy may exist between PARP1 and 2 in response to DNA SSBs and base-damage and the mouse *parp1*$^{-/-}$/*parp2*$^{-/-}$ double-disruptant is embryonic lethal (Menissier de Murcia *et al.* 2003). To address the possibility of functional redundancy between *Dictyostelium* ARTs, attempts were made to generate a double-disruptant of the hPARP1 and hPARP2 orthologues. It has been previously

stated that PARPs of lower eukaryotes cannot be assigned to a specific vertebrate counterpart based on domain and sequence similarity alone (Hottiger *et al.* 2010). Preliminary analysis of domain structure that I have carried out supports this, with only subtle differences being observed between *adprt1a, adprt1b* and *adprt2* genes. In particular, *adprt1a* and *adprt1b* differ only by the presence of a BRCT domain in *adprt1a*, and both show a high degree of domain structure similarity to human PARP1. Conversely, on dictyBase.org, *adprt2* has been identified as an orthologue of hPARP2. Therefore, to create a putative *parp1/parp2* disruption in *Dictyostelium*, generation of *adprt1a*$^{-}$*/adprt2*$^{-}$ and *adprt1b*$^{-}$*/adprt2*$^{-}$ strains were attempted.

To generate the *adprt1a*$^{-}$*/adprt2*$^{-}$ double disruptant, the *adprt2* locus was disrupted in the *adprt1a*$^{-}$ strain. However, prior to this, the blasticidin-resistance cassette was removed from the *adprt1a*$^{-}$ strain to render it blasticidin-sensitive. The cre-loxed *apdrt1a*$^{-}$ strain was then transfected with the *adprt2*-disruption cassette (Figure 4.6B), and successful integrants selected with blasticidin. Integrants were screened by PCR and Southern blot as performed for the *adprt2*$^{-}$ strain. Two clones were acquired, although screening results for only a single clone have been shown (Figure 4.7B). To generate an *adprt1b*$^{-}$*/adprt2*$^{-}$ strain, an *adprt1b*-disruption construct was transfected into a blasticidin sensitive *adprt2*$^{-}$ strain. However, despite several attempts, this double-disruptant could not be generated, perhaps suggesting its lethality, although further work would be required to verify this (data not shown).

4.2.4 PARylation is reduced in the *adprt1a⁻/adprt2⁻* strain

Having verified the *adprt1a⁻*, *adprt2⁻* and *adprt1a⁻/adprt2⁻* strains, phenotypic analysis was performed in these strains and the *adprt1b⁻* strain. In mammalian cells, disruption of PARP1 leads to reduced PARylation as evidenced by immunofluorescence and radioactive activity blots (Wang *et al.* 1995; de Murcia *et al.* 1997). Therefore, as an initial characterisation of *adprt* disruptants, PARylation following treatment of cells with MMS was determined by immunofluorescence (Figure 4.8). To assess PARylation in the *adprt1b⁻* strain, Ax4 was used as the parental control, and no significant difference in PARylation was observed in the mutant strain (Figure 4.8A). For the *adprt1a⁻*, *adprt2⁻* and *adprt1a⁻/adprt2⁻* strain, Ax2 was used as the parental control (Figure 4.8B). Once again, no significant difference in PARylation was observed in the *adprt1a⁻* strain, and PARylation appeared to be significantly increased ($p<0.05$) in the *adprt2⁻* strain, relative to Ax2. The *adprt1a⁻/adprt2⁻* strain showed significantly reduced ($p<0.05$) PARylation following MMS treatment. This latter observation is reminiscent of the situation in mammals, where PARP functional redundancy exists in SSBR/BER (Ame *et al.* 1999; Menissier de Murcia *et al.* 2003).

The significantly reduced PARylation in the *adprt1a⁻/adprt2⁻* strain is interesting given that the single mutants do not show reduced MMS-induced PARylation. In mammalian cells, the ability of PARP2 to contribute to the PARylation response after H_2O_2 or MMS induced DNA damage is only apparent at high doses (Ame *et al.* 1999). Thus, one possibility is that the treatment conditions being used in these experiments are excessive enough for other PARPs to be activated and compensate in

the PARylation response. From Figure 4.3, one can see that the induction of PARylation at lower MMS doses is minimal. However, there is a more robust induction of PARylation at early timepoints following administration of 5mM MMS. I therefore measured PARylation over time following 5mM MMS in the *adprt* single-mutants to determine whether delays in the induction of PARylation could be observed (Figure 4.9). As with PARylation at the 30 mins, there was no apparent difference in PARylation at 10 and 20 mins in *adprt1a*$^-$ and *adprt1b*$^-$, relative to the parental controls at the equivalent timepoint. However, in the case of *adprt2*$^-$, whilst PARylation was significantly greater ($p<0.05$) than Ax2 at 20 mins, there was no significant PARylation difference at 10 mins. These experiments were carried out in two *adprt* clones for each strain, and gave rise to similar observations (Figure 4.9). Thus, despite the significantly reduced PARylation in the *adprt1a*$^-$*/adprt2*$^-$ double-disruptant, no loss of PARylation following MMS treatment is apparent in the single-disruptant strains. To determine whether similar observations could be made following oxidative damage as determined after DNA base damage with MMS, experiments were repeated with H_2O_2, and gave rise to similar results (data not shown).

4.2.5 Effects of disrupting *adprt* genes on sensitivity to MMS and H_2O_2

In mammalian cells, the reduced PARylation associated with *parp1*-disruption is accompanied by increased SSB and base-damaging agent sensitivity (Trucco *et al.* 1998; Masutani *et al.* 1999; El-Khamisy *et al.* 2003). To determine whether a similar correlation exists in *Dictyostelium* in response to base-damage and DNA SSBs, sensitivity assays were performed with MMS and H_2O_2. Of interest was whether the

significantly reduced PARylation post-H_2O_2 and -MMS in the *adprt1a*$^-$*/adprt2*$^-$ double-disruptant would be accompanied by enhanced sensitivity to these agents relative to Ax2. Furthermore, viability assays would be more sensitive in determining long-term consequences of even slightly reduced PARylation in the single disruptants, which may not be detectable by immunofluorescence. This is especially with regards to the *adprt1a*$^-$ and *adprt2*$^-$ single-disruptant strains given the reduced PARylation in the double disruptant.

Exponentially growing cells were treated with increasing doses of MMS to induce DNA damage, and % survival relative to the untreated control determined for each strain (Figure 4.10 A and B). Whilst the *adprt1a*$^-$ strain showed no enhanced MMS sensitivity relative to Ax2, the *adprt1a*$^-$*/adprt2*$^-$ double-disruptant was sensitive, consistent with PARylation data. Surprisingly, the *adprt2*$^-$ and *adprt1b*$^-$ strains were also sensitive to MMS versus their parental controls, although this was subtle, but nevertheless reproducible in different clones (Figure 4.10 C and D). This subtle sensitivity in *adprt1b*$^-$ and *adprt2*$^-$ cells was also observed following oxidative damage by H_2O_2 which gives rise to SSBs and base lesions (Figure 4.11 A and B). It should be noted that the increased sensitivity in the *adprt2*$^-$ and *adprt1b*$^-$ strains is not due to the induction of DNA DSBs in response to the higher concentrations of either MMS or H_2O_2, because the sensitivity of these strains to phleomycin was not reduced relative to the parental controls (Figure 4.11 C and D). Overall, the enhanced sensitivity of *adprt1b*$^-$ relative to Ax4 was unexpected given the lack of reduced damage-induced PARylation. Similarly, whilst *adprt2*$^-$ showed increased PARylation after DNA damage, it also exhibited greater sensitivity. The subtle sensitivity of the *adprt2*$^-$ and *adprt1b*$^-$ single disruptants to MMS and H_2O_2, led us to speculate that

these were players in the SSB/BER. The *adprt1a*$^{-}$*/adprt2*$^{-}$ double-disruptant on the other hand which showed abrogated PARylation had the greatest sensitivity to MMS. This observation is interesting and implies that in the absence of Adprt2, Adprt1a may exert a function in SSBR/BER that cannot be compensated by Adprt1b. It will be interesting to determine whether the additional disruption of *adprt1a* in the *adprt1b*$^{-}$ strain gives rise to similar observations. The implications of these results will be addressed in the discussion.

4.2 Discussion

In this chapter, bioinformatics analysis of the *Dictyostelium* genome was performed to identify ART orthologues and components of the BER/SSBR pathway. Furthermore, functional analysis of putative DNA repair PARPs was initiated to determine whether, if similar to mammals, PARylation plays a role in *Dictyostelium* SSBR, and to clarify the role of PARylation in BER.

Much experimental work has been undertaken to characterise the biological roles of PARylation, predominantly focusing on higher eukaryotes, which show a broad conservation of PARPs (Scovassi *et al.* 1986). However, the inability to identify PARPs in the commonly used model organisms *S. cerevisiae* and *S. pombe* (Otto *et al.* 2005) has hindered investigation of PARP function somewhat. More recently, bioinformatics analysis of ARTs has incorporated lower eukaryotes. This has led to the identification of putative PARPs amongst members of the amoeba and fungal family (Otto *et al.* 2005; Semighini *et al.* 2006; Citarelli *et al.* 2010; Hottiger *et al.*

2010). Bioinformatics analysis of ART conservation in the *Dictyostelium* genome revealed conservation of 15 putative ARTs, including putative PARP1 orthologues; 6 more PARPs than identified by Otto *et al* (Otto *et al.* 2005). The catalytic domains highlighted in these searches were found in association with a variety of protein domains. This suggested that *Dictyostelium* ARTs may function in a diverse range of cellular processes. This is a situation similar to humans, where a proportion of the 17 identified ARTs have been designated to different functions and cellular localisations (Ame *et al.* 2004). Interestingly, for five of the identified *Dictyostelium* ARTs, DDB_G0288069, DDB_G0287911, DDB_G0276785, DDB_G0278045 and DDB_G0271966, the only recognisable domain is a catalytic domain. However, it is likely that the remaining amino acids within these genes encode currently uncharacterised domains, and may suggest novel functions for ARTs. A further limitation of this bioinformatics analysis is the inability to assume ART function, or more specifically, PARP function. Conservation of the HYE catalytic triad is associated with the capacity of ARTs to synthesise PAR (Marsischky *et al.* 1995). However, this is not always the case, and hPARP3 which shows HYE conservation, possesses mono- or oligo-ADP-ribosylation activity *in vitro* (Hottiger *et al.* 2010; Loseva *et al.* 2010; Rulten *et al.* 2011). Thus, *in vitro* functional characterisation of *Dictyostelium* ARTs will be required to determine ART capacity.

The *Dictyostelium* genome also demonstrates conservation of core SSBR/BER components. This is not surprising as the BER/SSBR is highly conserved in prokaryotes and eukaryotes (Robertson *et al.* 2009), including *S. cerevisiae.* However, what was surprising was the conservation orthologues of *ligase III* and *xrcc1*, which are both absent from other lower eukaryotes. In mammals,

autoPARylated hPARP1 may aid in recruitment of XRCC1 *in vivo* (Schreiber *et al.* 2002; El-Khamisy *et al.* 2003; Okano *et al.* 2003) and Ligase III *in vitro* (Leppard *et al.* 2003). It is therefore interesting to speculate about the presence of *parp1*, *xrcc1* and *ligase III* orthologues in *Dictyostelium*. This suggests a possible joint evolutionary conservation of these genes and may support the functional relationship of these genes in the SSBR response as indicated in mammalian systems.

Analysis of *Dictyostelium* ARTs revealed some with a high degree of amino acid sequence conservation to full-length hPARP1. Significantly, *adprt1a, adprt1b* and *adprt2* genes, which were identified as having the highest degree of sequence conservation to the full-length and catalytic domain of hPARP1, also contained putative DNA binding domains in the form of Zn fingers or WGR motifs. The WGR motif has been recently highlighted as an RNA binding module (Huambachano *et al.* 2011) and as playing an important role in catalytic domain activation post-DNA binding (Altmeyer *et al.* 2009). In hPARP1, the two tandem Zn fingers jointly contribute to DNA binding and catalytic activation (Gradwohl *et al.* 1990; Ikejima *et al.* 1990). The most N-terminal ZF is important for DNA damage binding-induced catalytic activation, whilst the second ZF mediates the major DNA interactions (Ikejima *et al.* 1990; Eustermann *et al.* 2011). In PARP1, a third ZF has been identified, ZF3, which also transmits the damaged-DNA binding event to the catalytic domain (Langelier *et al.* 2008). The single DNA binding-like Zn finger in *adprt1a* and *adprt1b* is interesting, and future analysis will need to determine whether it confers DNA binding affinity. Nevertheless, genetic analysis has implicated *adprt1a* and *adprt1b* in responding to DNA damage, and thus, the mechanism of their damage-induced activation remains to be determined. However, the conservation of

the ZF3 domain in these two *Dictyostelium* ARTs suggests a mechanism by which DNA binding events may be transmitted to the catalytic domain.

Both *adprt1a* and *adprt2* demonstrate conservation of the HYE catalytic triad (Citarelli *et al.* 2010). Whilst this was not observed for *adprt1b*, a glutamate residue two positions upstream in the alignment may serve this putative catalytic function. *In vitro* analysis of these PARPs, as has been undertaken with their human counterparts (Loseva *et al.* 2010) will be required to confirm my hypotheses of the catalytic capacity of these gene products. In summary, *adprt1a, adprt1b* and *adprt2* demonstrate high similarity to hPARP1. This in combination with the presence of putative DNA binding domains and the HYE catalytic triad support the possible functioning of these genes as DNA damage response PARPs.

The identification of 15 putative ARTs in *Dictyostelium* raises the question of why this organism shows such extensive conservation of this family of genes, including several putative hPARP1 orthologues. This is especially apparent when considering that *A. nidulans*, *N. crassa*, and the higher eukaryotes *C. elegans* and *D. melanogaster* encode far fewer PARPs (Hottiger *et al.* 2010). Furthermore, the genomes of *D. melanogaster, G. gallus*, *A. nidulans* and *N.crassa* only encode a single PARP1 orthologue (Uchida *et al.* 1993; Hochegger *et al.* 2006; Semighini *et al.* 2006; Kothe *et al.* 2010). In *D. melanogaster* and *A. nidulans*, disruption of this gene is lethal (Miwa *et al.* 1999; Tulin *et al.* 2002; Semighini *et al.* 2006). Nevertheless, the multiple putative DNA damage response PARPs in *Dictyostelium* could account for the high degree of resistance to DNA damaging agents observed (Deering 1988; Yu *et al.* 1998). This also leads to a situation similar to humans, offering a genetically

tractable model in which to determine the functions and functional overlaps between PARPs, as observed between mammalian PARP1 and PARP2.

To characterise the functions of PARPs, catalytic domain disruptions of *adprt1a* and *adprt2* were generated. The significance of catalytic domain disruptants is that they cannot be catalytically activated, even if they bind to DNA damage. This is an important consideration given that the lack of automodification capacity may lead to the persistence of PARPs at DNA damage sites (Mortusewicz *et al.* 2007), and the concomitant preclusion of these DNA ends from other repair factors. This needs to be taken into account when analysing the results, although published data in mammals suggests good agreement between results generated from catalytically inactive mutants (via over-expression the DNA binding domain in isolation, giving rise to a dominant negative effect) and mutants in which PARP1 is not being expressed (Beneke *et al.* 2000)

Mutants were treated with MMS, which generates base-damage, or H_2O_2 which generates base damage and SSBs. *Dictyostelium* are predominantly in G2 of the cell cycle (Weijer *et al.* 1984; Muramoto and Chubb 2008). It therefore seems unlikely that MMS and H_2O_2 treatment would give rise to replication associated DSBs in the time-frame of the experiment. Clustered damage can also directly generate DNA DSBs, however, γH2AX immunofluorescence post-damage illustrated this was not the case. Analysis of PARylation post-damage in the single-mutants revealed no apparent loss of PARylation, not even when PARylation was monitored at earlier timepoints. However, *adprt2*$^-$ had significantly increased PARylation, indicating possible aberrant PARylation by a compensating PARP. One implication from these experiments was

redundancy between DNA damage responsive PARPs, as is the case with hPARP1 and 2 (Ame *et al.* 1999). To address this, double-disruptants of the putative hPARP1 orthologues *adprt1a*$^{-}$ and *adprt1b*$^{-}$ with the putative hPARP2 orthologue, *adprt2*$^{-}$, was considered. Redundancy between *adprt1a* and *adprt2* was supported by the significantly reduced PARylation in the double-disruptant. However, an *adprt1b*$^{-}$*/adprt2*$^{-}$ double-disruptant could not be generated, preventing assessment of redundancy in this case. This may imply lethality of the *adprt1b*$^{-}$*/adprt2*$^{-}$ double-disruptant, although this remains to be formally assessed, and may suggest a situation reminiscent of the early embryonic lethality between hPARP1 and 2 (Menissier de Murcia *et al.* 2003).

In mammals, *parp1*-disruption is associated with a more severe repair phenotype than *parp2*-disruption, and this correlates with the loss of PARylation in these strains (Fisher *et al.* 2007). However, a correlation between loss of PARylation and MMS and H_2O_2 sensitivity was not apparent in the single *adprt* disruptants. The sensitivity assay data of the single *adprt* disruptants illustrated mild sensitivity in the *adprt1b*$^{-}$ and *adprt2*$^{-}$ strains, and no sensitivity in the *adprt1a*$^{-}$ strain. This led to the initial model that Adprt1b and Adprt2 may function redundantly in the SSBR/BER response, with some distinct roles in the tolerance to this damage as well. However, the enhanced sensitivity of the *adprt1a*$^{-}$*/adprt2*$^{-}$ double-disruptant, relative to either of the single disruptant strains also implicates Adprt1a as functioning in this repair pathway. However, the contribution of Adprt1a may only become important or apparent in the absence of either Adprt1b or Adprt2. The inability of Adprt1b to compensate in the *adprt1a*$^{-}$*/adprt2*$^{-}$ double mutant suggests that the combined activity of Adprt1b and Adprt2 may be important in the SSBR/BER pathway, and that Adprt1a can

compensate for the absence of Adprt2. Whether Adprt1a can also compensate in the absence of Adprt1b remains to be determined and will require generation of the *adprt1a⁻/adprt1b⁻* double-disruptant; future work will address this possibility. Overall, a situation is arising in *Dictyostelium* similar to that observed in mammals, with functional redundancy between several PARPs, all of which contribute to different extents in the cellular response to MMS. Furthermore, the sensitivity of the mutants to MMS and H_2O_2 suggest that *Dictyostelium* PARPs may contribute to both SSBR and BER *in vivo* in this organism. The mechanistic aspect of this contribution remains to be determined, including the hypothesised conservation of PAR-mediated XRCC1 recruitment to DNA damage sites.

Finally, it is important to note that whilst a PARylation defect was not seen with immunofluorescence analysis, it is important to make the distinction between my quantitative analysis, and a more qualitative analysis. It has been shown for example, that PARP1 and PARP2 have different targets with regards to histones (Messner *et al.* 2010), and it seems likely that additional differences in targets may exist. This is further supported by the structure of murine PARP1 and PARP2 catalytic domains, showing differences in the vicinity of the acceptor site, which may direct substrate specificity (Oliver *et al.* 2004). In my experiments, targets of the *adprt* gene products have not been assessed, and it is possible that these may vary considerably between different PARPs, to direct the cellular response to DNA damage. PARylation is already known to be an extremely heterogeneous modification, the significance of which is not clear. Therefore, whilst quantitatively PAR is unchanged, a more qualitative assessment is lacking with regards to the nature of the PAR chain, and the

targets of PARylation. Future work will address these issues as a step towards more fully characterising the role PARylation in SSBR and BER.

5: The role of Poly ADP-ribosylation in *Dictyostelium* DNA double-strand break repair

5.1 Introduction

The role of PARP1, PARP2 and PARylation in SSBR/BER is well established in mammals. However, the putative role of PARPs in other repair pathways, particularly in DSB repair, is less clear. The role of PARPs in the DSB repair response was initially suggested by *in vitro* analysis showing PARylation in response to dsDNA (Benjamin and Gill 1980). Further *in vitro* characterisation has implicated PARP1 as the major responder to dsDNA, with PARP2 also showing some stimulation (Altmeyer *et al.* 2009; Jorgensen *et al.* 2009). *In vitro* analysis suggests that recognition of dsDNA by PARP1 is allocated to the N-terminal zinc-finger of this protein (Ikejima *et al.* 1990). PARylation post-DSB induction has also been observed in mammalian cells (Dong *et al.* 2010), and their treatment with PARP inhibitors leads to enhanced DSB sensitivity post-IR and calicheamicin-γ1 (Boulton *et al.* 1999; Audebert *et al.* 2004). However, PARP inhibitors in addition to targeting PARP1 can also abrogate PARP2 and PARP3 activity, albeit with lower affinity (Farmer *et al.* 2005; Loseva *et al.* 2010). Thus, whilst inhibitor studies indicate a role for PARPs in DSB repair, they offer little in the way of enabling the nature of the contribution to be elucidated.

The characterisation of PARP isoforms in DSB repair has focused mainly on PARP1, suggesting varied roles in the damage response, with putative functions in both end-joining and HR pathways. A role for PARP1 in NHEJ has been suggested *in vitro* and *in vivo* via interactions with and heteromodification of Ku (Galande and Kohwi-Shigematsu 1999; Li *et al.* 2004), and DNA-PKcs (Ruscetti *et al.* 1998; Ariumi *et al.* 1999). Furthermore, DNAPKcs and Ku70 also contain PAR-binding domains, providing additional mechanisms by which PAR can govern their functions and localisation (Pleschke *et al.* 2000). However, more recently PARP1 has been suggested to play no role in classical NHEJ, as implied by the unaltered chromosomal end-joining efficiency in ES cells, regardless of their *parp1* status (Yang *et al.* 2004). Instead, PARP1 may function in a-NHEJ as a synapsis factor *in vitro*, with additional roles in recruiting downstream components of the pathway (Audebert *et al.* 2004; Audebert *et al.* 2006; Wang *et al.* 2006; Audebert *et al.* 2008; Haince *et al.* 2008). A-NHEJ occurs in the absence of functional NHEJ, and is more error prone (Boulton *et al.* 1999; Audebert *et al.* 2004; Wang *et al.* 2006; Mansour *et al.* 2010). The role of PARP1 in this alternative end-joining pathway may account for the embryonic lethality of the *parp1*$^{-/-}$*/ku80*$^{-/-}$ double-null mice (Tong *et al.* 2002; Henrie *et al.* 2003), where both end-joining pathways are eliminated.

The role of PARP1 in HR is also unclear. For example, in *parp1*$^{-/-}$ DT40 cells HR-mediated repair of a single endonucleolytically-generated DSB is reduced (Hochegger *et al.* 2006). However, HR measured by a similar assay in *parp1*$^{-/-}$ mammalian cells is unchanged (Yang *et al.* 2004). The difference in these findings brings into question the possibility of functional redundancy between PARPs due to the absence of a PARP2 orthologue in DT40 cells (Hochegger *et al.* 2006). Recently, PARP1 has been

implicated as a regulator of DSB repair, promoting HR at stalled replication forks and inhibiting toxic interference by NHEJ (Hochegger *et al.* 2006; Saberi *et al.* 2007; Sugimura *et al.* 2008). In line with this, PARylation of Ku *in vitro* by PARP1 reduces its affinity for DNA ends (Li *et al.* 2004). PARP1 may also function at replication forks to promote HR, independent of its postulated role in suppressing NHEJ (Bryant *et al.* 2009). PARP2 was additionally implicated in this process in the study by Bryant *et al* (Bryant *et al.* 2009), illustrating that the contribution of PARPs in DSB repair is not limited to PARP1. Further support for the contribution of multiple PARP isoforms to the DNA damage response is the interaction of PARP3 with NHEJ components DNAPkcs, Ku70, Ku80 and Ligase IV (Rouleau *et al.* 2007).

The above reports reveal a complicated and sometimes conflicting picture of the role of PARylation and PARPs in DNA DSB repair, particularly with regards PARP1. PARP1 is efficiently activated by and localises to DSBs *in vivo*, although no role for PARP1 in the major DSB repair pathways, NHEJ or HR, has been revealed in mammals. Nevertheless, PARP1 PARylates and interacts with NHEJ components. This is despite its characterised role in a-NHEJ, which is only functional in DSB repair in the absence of NHEJ. Furthermore, PARP1 may directly and indirectly contribute to replication fork repair by HR, as a recruitment factor and a negative regulator of NHEJ. Thus, the mechanism by which PARP1 exerts its putative diverse functions in DSB repair remains unclear. Furthermore, with other PARP isoforms being implicated in DSB repair, the possibility of functional redundancy and cooperativity in these repair pathways also arises.

In the previous chapter I established conservation of ARTs, ART function and the PARylation response in *Dictyostelium* SSB/BER. Given the emerging evidence that several mammalian PARPs may be implicated in the DSB repair response, the utility of *Dictyostelium*, which also shows conservation of several putative DNA damage response PARPs is highlighted. Moreover, *Dictyostelium* demonstrates conservation of DSB repair pathways and components of NHEJ, a-NHEJ and HR that were previously believed to be conserved only in higher eukaryotes, and in some cases vertebrates. This includes DNAPKcs, Artemis, Brca2 and XRCC1/Ligase III in *Dictyostelium*, further strengthening its application as a model organism in the DNA damage response (Block and Lees-Miller 2005; Hudson *et al.* 2005; Hsu *et al.* 2006; Caldecott 2008; Zhang *et al.* 2009; Hsu *et al.* 2011).

Two *Dictyostelium* ARTs, Adprt1b and Adprt2 were implicated in tolerance to SSBs and base damage, with a possible contribution from Adprt1a in the absence of Adprt2. In this chapter the contribution of the putative *Dictyostelium* repair ARTs in DSB repair was characterised. Towards this I wanted to determine whether DNA DSBs induce PARylation in *Dictyostelium* and to use a genetic approach to characterise the specific ARTs mediating this response. Finally, I wanted to determine whether phenotypic consequences arise from the genetic disruption of DSB-activated ARTs.

5.2 Results

5.2.1 *Dictyostelium* undergo PARylation in response to DNA double-strand breaks

Having established conservation of PARylation in SSBR/BER, I wanted to use *Dictyostelium* to address the role of PARylation following DNA DSBs. Towards this end, exponentially growing cells were treated with the radiomimetic drugs bleomycin and phleomycin, which are commonly used inducers of DNA DSBs. These DNA damaging agents create SSBs and DSBs by a free-radical mediated mechanism that may rely in part, on their ability to intercalate into DNA (Sleigh 1976; Povirk *et al.* 1979; Wu *et al.* 2002). The cytotoxicity of phleomycin and bleomycin arise from their DSB-inducing ability, and phleomycin may give rise to a greater number of DNA breaks, accounting for its greater cytotoxicity (Koy *et al.* 1995). To monitor bleomycin- and phleomycin-induced PARylation, Western blotting (Figure 5.1A) and immunofluorescence (Figure 5.1B) using an antibody against PAR were employed.

Whole-cell extracts from Ax2 were analysed by Western blot post-bleomycin treatment (Figure 5.1A). Consistent with bleomycin generating DNA DSBs, γH2AX was induced in a time-dependent manner, appearing after approximately 20mins. Proteins were also PARylated in a time-dependent manner, with a signal becoming visible at 10 mins and diminishing after 40 mins. This indicated the transient nature of PARylation in *Dictyostelium*. Damage-induced PARylation was represented by an approximately 100kDa band, and diffuse bands between 100 to 250kDa, and another above 250kDa. In mammals, the major catalytic activity of PARP1 is represented by

automodification (Ogata *et al.* 1981; Satoh and Lindahl 1992). The broad 100kDa band may therefore correspond to heterogeneous modification of Adprt1a, which has this predicted molecular weight, although this requires experimental verification.

Nuclear PARylation following treatment of cells with phleomycin was also assessed by immunofluorescence using an antibody against PAR (Figure 5.1B and C). Phleomycin-induced PAR staining increased in a dose-dependent manner, with staining predominantly focal at low concentrations, and pan-nuclear at higher concentrations. One may speculate that the PARylation foci correspond to sites of DNA damage. The transition in the PARylation staining pattern from focal to pan-nuclear may therefore reflect increasing DNA damage levels giving rise to overlapping PARylation at higher doses. Furthermore, a nuclear PARylation signal was visible after 20 mins, and in the time frame of the experiment, this signal did not diminish (Figure 5.1D). As with Western blot analysis, DNA DSB-induction was determined by nuclear γH2AX staining (Figure 5.1D), and appeared with similar kinetics to that of PARylation. Cells were treated with H_2O_2 as a control, and conditions that induced robust PARylation, similar to that seen at 60 mins phleomycin treatment, led to minimal γH2AX staining, implying a lack of DSBs in this case. Thus, in *Dictyostelium*, in addition to DNA SSBs and base damage, PARylation can also be induced by DNA DSBs.

To confirm that PARPs were mediating damage-induced PARylation, competitive PARP inhibitors were utilised. Exponentially growing Ax2 were pre-treated with NU1025 (Figure 5.2A, left panel), benzamide (Figure 5.2A, right panel), or their respective carriers, and PARylation determined by microscopy. Both inhibitors

reduced the DNA DSB-induced nuclear PARylation signal. Quantification of inhibition by NU1025 indicated substantially reduced PARylation levels, indicating that this damage-induced staining is mediated by PARPs (Figure 5.2B).

5.2.2 Genetic dissection of DSB-induced PARylation in response to DNA DSBs

Having determined the conservation of ART-mediated DSB-induced PARylation in *Dictyostelium*, the next aim was to determine the specific PARPs mediating this response. The broad PARP specificity of NU1025 and Benzamide would hinder identification of the specific *Dictyostelium* ARTs activated by DNA DSBs. Furthermore, the lower efficacy of PARP inhibitors when cells are present at high densities, or when longer treatment times are required would limit their experimental application (Satoh *et al.* 1994). Thus, a genetic approach was applied to dissect the PARylation response and determine those ARTs contributing post-DSB induction.

To initiate investigations, the level of DSB-induced PARylation was measured in the putative *Dictyostelium* repair ARTs, *adprt1a*$^-$, *adprt1b*$^-$, *adprt2*$^-$ and *adprt1a*$^-$/*adprt2*$^-$ strains. Exponentially growing cells were treated with phleomycin and PARylation assessed by immunofluorescence (Figure 5.3A, B, C). PARylation was unchanged in *adprt1b*$^-$ relative to Ax4 (Figure 5.3A), but was reduced in *adprt1a*$^-$, *adprt2*$^-$ and *adprt1a*$^-$/*adprt2*$^-$ relative to Ax2 (Figure 5.3B). In the *adprt1a*$^-$ and *adprt1a*$^-$/*adprt2*$^-$ strains, the PARylation reduction was significant ($p<0.05$), but the additionally reduced PARylation in the double-disruptant was only slightly more than the *adprt1a*$^-$ single disruptant (Figure 5.3B). Another independent *adprt1a*$^-$ clone also had significantly reduced PARylation post-phleomycin treatment ($p<0.05$), illustrating

that observations in this strain were not clone specific (Figure 5.3C). Therefore, based on this data, Adprt1a is the major mediator of PARylation post-DNA DSB induction, with Adprt2 making minimal contributions to the PARylation response.

In mammalian cells, the reduced PARylation of *parp1*$^{-/-}$ vertebrate cells is linked to increased sensitivity to DNA SSB and base damaging agents. A similar correlation between the PARylation defect and DNA DSB sensitivity may also exist in *Dictyostelium*. Consistent with this, in the previous chapter, neither the *adprt2*$^{-}$ nor *adprt1b*$^{-}$ strains with slightly reduced and unchanged PARylation, had increased phleomycin sensitivity relative to their parental controls. To test whether the reduced PARylation in the two *adprt1a*$^{-}$ clones was accompanied by increased DSB-sensitivity, cells were treated with phleomycin, and survival determined (Figure 5.3D). However, neither of the *adprt1a*$^{-}$ clones tested displayed enhanced sensitivity to phleomycin relative to Ax2.

5.2.3 The contribution of NHEJ and HR is altered in the *adprt1a*$^{-}$ strain

Sensitivity assays indicate the overall capacity of cells to survive DNA DSBs but the contributions of HR and NHEJ to survival cannot be inferred from this data. Consistent with this, whilst NHEJ occurs in vegetative *Dictyostelium* and contributes to DSB repair (Muramoto and Chubb 2008; Hsu *et al.* 2011), NHEJ-mutants have unaltered DNA DSB sensitivity (Hudson *et al.* 2005). This is likely due to the predominance of HR at this developmental stage or the substitution by other DSB repair pathways (Hsu *et al.* 2011). Therefore, to determine whether the significantly

reduced DSB-induced PARylation in the *adprt1a*$^-$ strain gave rise to phenotypic consequences in DSB repair, HR and NHEJ were analysed.

HR was initially measured using the *cdk8* gene-targeting assay in exponentially growing Ax2 and the *adprt1a*$^-$ strain (Figure 5.4A). Gene-targeting efficiency at the *cdk8* locus was enhanced in *adprt1a*$^-$ cells relative to Ax2, indicating increased HR proficiency in the *adprt1a*$^-$ strain. An interpretation of the increased gene-targeting in the *adprt1a*$^-$ strain is activation of HR in these cells, leading to greater DNA DSB repair capacity in association with NHEJ. However, DNA DSBs are likely to be rapidly engaged in a DSB repair pathway to minimise the risk of mutagenesis. Therefore, an alternative explanation is that in the *adprt1a*$^-$ strain, increased HR is accompanied by downregulation of NHEJ. This would arise due to competition between NHEJ and HR in G2 of the cell-cycle, as evidenced by genetic studies demonstrating increased HR when NHEJ components are disrupted in eukaryotes (Clikeman *et al.* 2001; Fukushima *et al.* 2001; Pierce *et al.* 2001; Allen *et al.* 2002; Zhang *et al.* 2007). To determine whether the increased HR in the *adprt1a*$^-$ strain in *Dictyostelium* was accompanied by a concomitant decrease in NHEJ, REMI was performed as described in Materials and Methods. Exponentially growing Ax2 and *adprt1a*$^-$ cells representing the two *adprt1a*$^-$ clones were transfected with *Bam*HI-linearised pLPBLP, in either the presence or absence of *Bam*HI, and REMI induction relative to Ax2 determined (Figure 5.4B). REMI was significantly reduced in both *adprt1a*$^-$ clones, to a similar degree as in the *ku80*$^-$ strain, relative to Ax2. This indicates that upregulation of HR is accompanied by a reduction in NHEJ in the *adprt1a*$^-$ strain, supporting the competition between these two pathways.

The fact that reduced NHEJ in the *adprt1a*$^-$ strains is accompanied by increased HR suggests that interference of NHEJ on HR repair is reduced in the absence of Adprt1a. However, whether this reflects a direct role of Adprt1a in promoting NHEJ, or alternatively, whether Adprt1a directly downregulates HR is unclear. To address this, the phleomycin sensitivity of germinating spores from an *adprt1a*$^-$ mutant was assessed. Unlike vegetative cells, germinating spores disrupted in NHEJ components are highly sensitive to DNA DSBs, suggesting a reliance on NHEJ at this developmental stage (Hudson *et al.* 2005). Therefore, if Adprt1a is playing a role in promoting NHEJ, one would expect to see enhanced phleomycin sensitivity relative to Ax2 in *adprt1a*$^-$ strains. Fruiting bodies were made for Ax2 and *adprt1a*$^-$ and *ku80*$^-$ strains, which all showed similar developmental time-frames, with fruiting bodies forming after 24 hours in the strains. When fruiting bodies were mature, spores were harvested and germinated into increasing phleomycin concentrations and sensitivity determined (Hudson *et al.* 2005) (Figure 5.4C). Relative to Ax2, the *adprt1a*$^-$ strain showed enhanced phleomycin sensitivity that was comparable to the *ku80*$^-$ strain, indicating the role of Adprt1a in the NHEJ pathway. The similar spore phleomycin sensitivity profile and REMI defect between the *adprt1a*$^-$ and *ku80*$^-$ strains illustrates that Adprt1a plays a similarly important role in NHEJ as Ku. It should be noted that the other *adprt1a*$^-$ strain utilised in Figure 5.3D (clone z) was also tested in the spore phleomycin sensitivity assay and demonstrated a similarly enhanced phleomycin sensitivity as *adprt1a*$^-$.w relative to Ax2 (data not shown).

The disruption of *adprt2*$^-$ also modestly reduces DSB-induced PARylation, and its disruption in the *adprt1a*$^-$ background further enhances the significant PARylation defect of the *adprt1a*$^-$ strain. Having demonstrated the role of Adprt1a in NHEJ, the

role of Adprt2, in the context of its minimal PARylation contribution post-phleomycin, was also determined. This was achieved by REMI in order to measure NHEJ in the context of the single-disruptant and also in the *adprt1a*$^{-}$ background. The rationale behind doing the REMI in the *adprt1a*$^{-}$/*adprt2*$^{-}$ double-disruptant in addition to the single mutant was to determine the possibility of functional redundancy or cooperativity between Adprt1a and Adprt2. Exponentially growing Ax2, *ku80*$^{-}$ and *adprt*-mutant strains were subjected to REMI (Figure 5.4D). Whereas REMI induction was marginally reduced in the *adprt2*$^{-}$ strain, it was significantly reduced ($p<0.05$) in the *adprt1a*$^{-}$ and *ku80*$^{-}$ strain, as demonstrated previously. Furthermore, REMI was also significantly reduced in the *adprt1a*$^{-}$/*adprt2*$^{-}$ double-disruptant, although whether this was to a similar degree or greater than the *adprt1a*$^{-}$ strain could not be determined due to already low REMI in the single-mutant. Based on my results, it appears that Adprt2 may play a minor role in DSB repair in *Dictyostelium*, but its contribution is minimal relative to that of Adprt1a, which is the major contributor.

In mammalian cells, PARP1 has been implicated in an erroneous backup end-joining pathway, termed a-NHEJ, which is observed in *ku80*$^{-}$ strains (Boulton *et al.* 1999; Audebert *et al.* 2004; Wang *et al.* 2006; Mansour *et al.* 2010). However, the reduced REMI in the *adprt1a*$^{-}$ strain implicates Adprt1a in the classical NHEJ pathway. The dependence of REMI induction on classical Ku-mediated NHEJ is illustrated by the significantly reduced REMI levels in the *ku80*$^{-}$ strain (Kuspa and Loomis 1992; Hsu *et al.* 2011), indicating that REMI is dependent on Ku80 in *Dictyostelium*. Furthermore in contrast to a-NHEJ where repair is accompanied by deletions at repair junctions, REMI occurs at *Bam*HI sites, the integrity of which is maintained.

Overall, these results highlight a role for Adprt1a in NHEJ, likely via its DSB-induced PARylation activity. It is tempting to speculate that the PARylation function of Adprt1a is playing a role early in the NHEJ pathway due to the increased HR and reduced NHEJ in the *adprt1a*$^-$ strain. This is similarly observed in the *ku80*$^-$ but not *dclre1*$^-$ strain. Thus, Adprt1a may function in NHEJ as a DSB repair gate-keeper like Ku, although whether is upstream or downstream of Ku remains unclear.

5.3 Discussion

In the previous chapter I addressed the conservation of ARTs and determined whether, if similar to vertebrates, these genes played a role in SSBR/BER. Towards this, conservation of several ARTs was demonstrated, and *Dictyostelium* Adprt1b and Adprt2 were implicated in SSBR/BER. Having established a degree of conservation of PARPs with their vertebrate counterparts, I wanted to exploit *Dictyostelium* to address more novel questions surrounding PARP function. One such avenue of research is the role of PARPs in DSB repair which remains unclear.

To initiate this study, I determined whether *Dictyostelium* induces PARylation following DNA DSBs by bleomycin and phleomycin. As has been done in higher eukaryotes, Western blot and immunofluorescence analysis was utilised to measure PARylation, alongside γH2AX to confirm DNA DSB induction. In both cases, the kinetics of PARylation and H2AX phosphorylation were similar. H2AX phosphorylation is an early response to DNA DSBs, and thus, γH2AX is regarded as

an early DNA DSB marker in eukaryotes (Riballo *et al.* 2004; Lobrich *et al.* 2010). My observations now further implicate *Dictyostelium* PARPs as early DNA damage responders, with PARylation being an additional early marker of DNA DSBs, with a possible independent role in dictating the repair response. Immunofluorescence analysis demonstrates nuclear damage-induced PARylation, with likely coincidence between the location of PARylation and DNA damage sites. The coincidence of location is implied by the transition of PARylation staining from focal to pan-nuclear with increasing phleomycin concentrations. This transition likely results from the increased DNA damage load and proximity of damage sites with greater phleomycin concentrations, leading to eventual overlapping of PARylation. Determining the colocalisation between PARylation and γH2AX foci would enable confirmation of the hypothesis in *Dictyostelium*, although Haince *et al* (Haince *et al.* 2008) demonstrated this colocalisation in human cells. Western blot analysis illustrated protein PARylation to occur soon after DNA damage, although their identities remain unknown. Following DNA damage, a predominant activity of PARP1 is autoPARylation (Ogata *et al.* 1981; Satoh and Lindahl 1992). Therefore, one possibility is that the PARylated band at approximately 100kDa may correspond to Adprt1a, although this remains to be verified. Additional potential PARylation targets include histones and repair factors such as Ku (D'Amours *et al.* 1999; Li *et al.* 2004). It is likely that characterisation of the PARylated proteins following DNA DSB-induction in *Dictyostelium* would facilitate the molecular dissection of observations made in the repair response.

Reduction in PARylation by the commercial PARP inhibitors NU1025 and Benzamide support the damage-induced post-translational modification being

mediated by PARPs. In addition, it indicates that the *Dictyostelium* PARPs in question are sufficiently conserved in the NAD^+ binding site to be capable of interacting with the inhibitor. This immediately allowed the search to be narrowed to those PARPs showing a high degree of conversation in the NAD^+ binding domain. Given that the arsenal of PARP mutants includes those genes with a high degree of conservation to PARP1 in the catalytic domain, I initially explored their contribution to the DNA DSB PARylation response. Interestingly, with the exception of the *adprt1b*$^-$ strain, the other single-mutants investigated demonstrated reduced PARylation following DNA DSBs, relative to their parental controls. The *adprt1a*$^-$ strain showed significantly reduced PARylation, implicating Adprt1a as the major responder to DNA DSBs, with Adprt2 making a minor contribution. The possibility of Adprt1a and Adprt2 both contributing to PARylation post-DNA DSBs, is further illustrated by abrogated PARylation in the *adprt1a*$^-$/*adprt2*$^-$ double-disruptant. The reduced PARylation in response to DNA DSBs in the *adprt1a*$^-$ strain is in comparison to the lack of a measurable PARylation defect post-SSB/base damage in any of the *adprt*-mutants. This, in combination with γH2AX induction, lends further support to the conclusion that the damage giving rise to PARylation in this case, is distinct from that induced by H_2O_2 and MMS, and likely represents DNA DSBs. These observations lend support to the hypothesis that different PARPs may respond to different forms of DNA damage, with Adprt1a as the major responder to DNA DSBs.

Analysis of the domain structure of Adprt1a and Adprt2 reveal them to have quite dissimilar domain organisation upstream of the C-terminal catalytic and regulatory domains. Adprt1a is characterised by a zinc-finger similar to that of PARP1, which may facilitate damage recognition, a ZnF3, BRCT and WGR domain. Conversely,

Adprt2 contains a WGR domain which may serve the function of damage recognition (Citarelli *et al.* 2010), as well as a BRCT domain. Adprt1b on the other hand has a similar domain conservation to Adprt1a, and therefore, sequence variations, or its lack of a BRCT domain may prevent it from recognising the same damage as Adprt1a. Identifying these differences may enable a greater understanding of how specific PARPs respond to DNA damage in a manner which can be extended to higher eukaryotes. Nevertheless, these different PARPs may consequently direct the repair response by PARylating distinct targets or synthesising specific types of PAR chains. For example, whilst PARP1 synthesises chains of PAR (Loseva *et al.* 2010), PARP3 predominantly synthesises PAR chains containing up to 15 units (Loseva *et al.* 2010; Rulten *et al.* 2011). Furthermore, whilst PARP1 can PARylate core histones, PARP2 cannot (Messner *et al.* 2010). These qualitative differences may dictate the downstream repair response, possibly via differences in the repair proteins recruited.

In mammals, the PARylation defect of *parp1*$^{-/-}$ strains correlates with the SSBR/BER defect as determined by delayed repair kinetics and enhanced sensitivity. To determine the phenotypic consequences of the significantly reduced PARylation in the *adprt1a*$^{-}$ strain, sensitivity assays were performed post-DSB induction by phleomycin. Whereas vegetative mutants did not exhibit reduced survival following phleomycin treatment, survival was reduced in germinating spores following *adprt1a*-disruption. A key difference in DSB repair between these developmental stages is the predominance of NHEJ in contributing to cell survival. In vegetative *Dictyostelium*, whilst NHEJ can contribute to DSB tolerance, HR is the predominant pathway (Hudson *et al.* 2005; Muramoto and Chubb 2008; Hsu *et al.* 2011). In contrast, NHEJ is the predominant pathway for DSB survival in germinating spores (Hudson *et al.*

2005), and the sensitivity of the *adprt1a*$^{-}$ strain at this developmental stage implicated this gene in NHEJ. Consistent with the role of Adprt1a in NHEJ, REMI was reduced in the vegetative *adprt1a*$^{-}$ mutant strain relative to Ax2. The role of Adprt1a in NHEJ is in contrast to the proposed role of PARP1 in the a-NHEJ pathway in mammalian cells. A-NHEJ functions in competition with NHEJ. However, due to the lower DNA binding affinity of PARP1 versus Ku, PARP1 can only engage in repair in the absence of the core NHEJ components (Boulton *et al.* 1999; Audebert *et al.* 2004; Wang *et al.* 2006; Mansour *et al.* 2010). The REMI assay employed here is likely to be a specific measure of c-NHEJ, given that REMI is significantly defective in *ku80*$^{-}$. The fact that *adprt1a*$^{-}$ cells, which express Ku, have the same REMI defect as *ku80*$^{-}$ cells implies its role in c-NHEJ. Overall, it seems unlikely that *Dictyostelium* Adprt1a is functioning as a PARP1 homologue, but rather is playing a direct role in promoting c-NHEJ.

In vegetative cells, the reduced REMI in *adprt1a*$^{-}$ cells is accompanied by a concomitant increase in HR, as assessed by gene-targeting at the *cdk8* locus. This implicates Adprt1a as a regulator of DSB repair pathway choice by enhancing NHEJ. This data therefore also illustrates competition between DSB repair pathways at this developmental stage, as was highlighted in a previous chapter, in agreement with observations in other eukaryotes. However, the mechanistic basis behind the regulatory role of Adprt1a is not clear. The *adprt1a*$^{-}$ and *ku80*$^{-}$ strains exhibit strikingly similar phenotypes, particularly with regards to the up-regulated *cdk8* gene-targeting efficiency. This contrasts with the unaltered gene-targeting efficiency in the *dclre1*$^{-}$ strain, and places Adprt1a early on in the NHEJ pathway as a repair gatekeeper, possibly at the DSB recognition stage. However, whether Adprt1a

functions upstream of Ku, to enhance its association with DNA damage, or downstream of Ku, enhancing its stability at DNA DSBs, similarly to Nej1/Lif1/Dnl4 in yeast (Zhang *et al.* 2007; Chen and Tomkinson 2011), is not clear.

Although HR is the predominant repair pathway in vegetative *Dictyostelium*, NHEJ contributes to DSB repair at this developmental stage. This is illustrated by the delayed resumption of cell growth post-DSB induction in NHEJ-deficient mutants, which may illustrate the contribution of NHEJ at a fraction of DSBs (Muramoto and Chubb 2008; Hsu *et al.* 2011). Therefore, Adprt1a may be involved in promoting NHEJ, particularly at this fraction of damage, with a consequent competition with HR at other DSBs. The importance of Adprt1a in NHEJ is illustrated by the similarity of the REMI defect in *adprt1a*$^-$ and *ku80*$^-$ strains. It should be noted, however, that although Adprt1a is a key component in the NHEJ pathway, I cannot exclude the function of Adprt2, which while not playing a major role appears to make some contribution to PARylation and REMI in addition to Adprt1a. The significance of this contribution and how it may differ from that of Adprt1a is unclear, but cannot be discounted.

In conclusion, I have shown that Adprt1a is the major responder to DNA DSBs, not SSBs or base damage. This provides the first indication of the function of a third PARP in the DNA damage response, and illustrates the possible division of function of PARP isoforms in the repair. Furthermore, the role of Adprt1a appears to be in promoting NHEJ, at the expense of HR, suggesting a putative regulatory function of this repair protein. In particular, Adprt1a may regulate the initiation of NHEJ, possibly by promoting Ku binding to DSBs, or stabilising the association of Ku at

DNA damage. The data therefore provides further illumination with regards to the mechanisms by which repair pathway choice may be regulated, pointing to repair pathway initiation as a major regulatory point. The functioning of Adprt1a in NHEJ contrasts with the role of PARP1 in a-NHEJ, and as a negative regulator of NHEJ at replication forks. More recently, Rulten *et al* (Rulten *et al.* 2011), also suggested the role of a third PARP, PARP3 in DSB repair. In human cells, PARP3 has been implicated in NHEJ by promoting the retention of Ligase IV/XRCC4 at DSBs and its absence leads to delayed γH2AX decay kinetics (Rulten *et al.* 2011). Therefore, Adprt1a in *Dictyostelium* may be functioning as a PARP3 orthologue. In contrast to human cells, however, where a single PARP mediates NHEJ, in *Dictyostelium*, another PARP, Adprt2 also minimally contributes to DSB-induced PARylation and possibly NHEJ. This may reflect differences in the contribution of NHEJ in vegetative *Dictyostelium* versus human cells, with NHEJ being a major pathway in DSB tolerance at all cell cycle stages in the latter organism. Therefore, the role of PARP3 in humans may be to promote NHEJ at all DSBs, with HR repairing the fraction of damage that NHEJ cannot. In contrast, in *Dictyostelium*, Adprt1a and Adprt2 may recognise a specific fraction/fractions of damage to preferentially promote NHEJ at these sites. It is therefore possible that Adprt1a recognises the major fraction of damage, whilst Adprt2 may recognise a smaller subfraction. Consistent with this possibility, the putative nucleic acid binding motifs of Adprt1a and Adprt2 differ in *Dictyostelium*.

Overall, the work in this chapter further highlights the evolutionary similarity between *Dictyostelium* and human DSB repair mechanisms. Future work will address the molecular basis behind these observations. This includes targets of Adprt1a catalytic

activity and the mechanism by which the promotion of NHEJ is achieved; the latter point will be discussed in the next chapter.

6: The role of the *Dictyostelium* Ku70 PBZ domain in DNA double-strand break repair

6.1 Introduction

PARylation plays a role in several cellular processes, including transcription, chromatin structure and DNA repair. One way in which this post-translational modification can mediate its function is via direct modification of target proteins. This is illustrated by PARP1 automodification which reduces its affinity for DNA ends, leading to its release, and the access of the DNA lesion to downstream repair proteins (Mortusewicz *et al.* 2007). Furthermore, *in vitro* data has suggested that Ku80 is a target for PARylation, the effect of which is to reduce its affinity for DNA (Li *et al.* 2004). Another mechanism by which PARylation can exert effects, however, is via non-covalent interactions, whereby PAR chains synthesised in response to DNA damage can be recognised by PAR binding motifs present in proteins. So far, three PAR binding domains have been identified which show predominance amongst DNA repair and checkpoint proteins. These domains include the 8 amino acid hydrophobic/basic amino acid motif, the macro-domain and the PAR binding zinc finger domain (Pleschke *et al.* 2000; Karras *et al.* 2005; Ahel *et al.* 2008; Gagne *et al.* 2008). Already the significance of these PAR binding domains in the repair response is implied.

With regards to SSBR/BER, the basic/hydrophobic PAR binding motif in the BRCT domain of XRCC1 facilitates its efficient recruitment to DNA damage sites (Pleschke *et al.* 2000; El-Khamisy *et al.* 2003; Okano *et al.* 2003). Furthermore, the functions of ALC1 and macroH2A.1 in repair are mediated in part by their macro-domains (Ahel *et al.* 2009; Timinszky *et al.* 2009). Like XRCC1, the macrodomain of ALC1 facilitates its rapid recruitment to DNA damage sites where it can undertake nucleosome repositioning activities to promote cell survival following DNA damage induction (Ahel *et al.* 2009). Finally, APLF and CHFR (Checkpoint protein with FHA and Ring domain) both contain PBZ domains that are essential for their function in the DDR (Ahel *et al.* 2008; Rulten *et al.* 2011). Thus, PAR-binding domains in repair proteins likely contribute to their function, and such conservation can be utilised to facilitate the molecular characterisation of any observations made. However, the nature of PAR recognition is only now being elucidated and the mechanism by which heterogeneity in PAR chains can be determined is still unclear (Karras *et al.* 2005; Timinszky *et al.* 2009; Eustermann *et al.* 2010; Li *et al.* 2010). For example, it has been shown that despite containing the same hydrophobic/basic amino acid PAR binding motif, p53 and the NER protein, XPA, each display affinity for PAR chains of different lengths (Fahrer *et al.* 2007). Residues surrounding the PAR binding site may contribute to this differential affinity.

In the previous chapter, a role for PARylation in *Dictyostelium* DNA DSB repair was established. This response was shown to be mediated via Adprt1a, which was catalytically activated by DNA DSBs to synthesise PAR and promote NHEJ. This observation is inline with that of Rulten *et al* (Rulten *et al.* 2011), and highlighted Adprt1a as a putative PARP3 orthologue. However, the molecular basis behind this

observation, including the mechanism by which Adprt1a induced PARylation promoted NHEJ, remains unclear. However, given the role of PAR binding domains in protein function, I wished to address its possible contribution to the DNA DSB repair response. Towards this end, I demonstrated the conservation of a PBZ PAR binding domain in *Dictyostelium* Ku70. This PBZ domain facilitates Ku70 recruitment to chromatin after DNA damage, and clarifies the mechanism by which Adprt1a can regulate DNA DSB repair pathway choice by promoting NHEJ.

6.2 Results

6.2.1 The *adprt1a*$^-$ strain exhibits defective recruitment of Ku80 to chromatin

In the previous chapter, the contribution of Adprt1a to NHEJ was illustrated by the REMI defect and heightened phleomycin sensitivity of germinating *adprt1a*$^-$ spores. Furthermore, the reduced NHEJ was accompanied by an increase in HR efficiency as determined by the gene-targeting assay. The DSB repair phenotypes accompanying *adprt1a*-deficiency are reminiscent of those in the *ku80*$^-$ strain, which relative to Ax2 also show reduced NHEJ and enhanced HR in vegetative cells and DSB sensitivity in germinating spores. The increase in gene-targeting efficiency in the *adprt1a*$^-$ and *ku80*$^-$ strains is particularly striking as this was not observed for the putative NHEJ component, Dclre1, which may function downstream in the NHEJ pathway. These observations led to the suggestion that Adprt1a is playing a role in NHEJ at a similar position to the Ku heterodimer. However, whether this was upstream or downstream of Ku to facilitate its recruitment or stability at DNA DSBs, or at a subsequent stage of the NHEJ pathway was not clear. To address the possibility that Adprt1a is

exerting its function via Ku80 recruitment/retention, the chromatin enrichment of Ku80 post-phleomycin treatment was determined in Ax2 and the *adprt1a*$^-$ strain.

In human cells, sub-cellular fractionation has been applied to look at enrichment of NHEJ proteins in a detergent-resistant nuclear fraction, presumed to contain chromatin, after DNA damage (Drouet *et al.* 2005) (Figure 6.1A). Validation of chromatin-enrichment in the detergent-resistant fraction following sub-cellular fractionation has been demonstrated in *Dictyostelium* (performed by S. Lempidaki, data not shown). Briefly, DNase I treatment of the detergent-soluble fraction post-phleomycin treatment reverses Ku80 enrichment in this fraction and leads to its transfer to the soluble fraction, in line with DNA solubilisation by its DNase I digestion. The sub-cellular fractionation technique was subsequently applied to measure Ku80 chromatin enrichment in Ax2 and the *adprt1a*$^-$ strain post-phleomycin treatment (Figure 6.1B). Exponentially growing cells were treated with phleomycin and at time-points following DNA damage, sub-cellular fractionation was performed as outlined in the Materials and methods. The extent of endogenous Ku80 recruitment to chromatin following DNA damage was determined by Western blot. In Ax2, the mobilisation of Ku80 to the detergent resistant fraction was observed following phleomycin treatment, and seen to increase over time. In contrast, although Ku80 recruitment in *adprt1a*$^-$ cells was observed, it was reduced at every time point analysed relative to Ax2. The lower Ku80 chromatin enrichment was determined not to be a consequence of reduced endogenous Ku80 in the *adprt1a*$^-$ strain versus Ax2 as determined by Western blotting Ku80 in whole-cell extracts (Figure 6.1C). Thus, in *adprt1a*$^-$ cells, Ku80 recruitment is reduced rather than completely defective. Quantification of Ku80 enrichment in the *adprt1a*$^-$ strain supported the preliminary

findings that Ku80 recruitment is defective, and indicates the reproducibility of the results (Figure 6.1D).

Given the subtle reduction in PARylation and REMI in the *adprt2*$^{-}$ strain, the possibility of reduced to Ku80 chromatin enrichment post-damage was explored (Figure 6.1E). In line with my predictions, the *adprt2*$^{-}$ strain did indeed have reduced Ku80 chromatin recruitment post-phleomycin treatment relative to Ax2. However, this defect was to a lesser degree than in *adprt1a*$^{-}$ cells. In the *adprt1a*$^{-}$/*adprt2*$^{-}$ strain the double disruption had an additive effect on the reduction in Ku80 recruitment. Thus it appears that the PARylation defect in the different *adprt1*-disruption strain correlates to a proportional reduction in Ku80 chromatin recruitment post-damage. In line with this, Adprt1a plays the major role in this response, as a significant REMI defect was only observed when this gene was disrupted. Thus, unlike in SSBR/BER in *Dictyostelium*, where Adprt1b and Adprt2 may be primarily functioning, Adprt1a is playing the key role in DNA DSB repair by NHEJ, with Adprt2 playing a minor role in this response. The degree of the delay in Ku80 chromatin recruitment post-DNA DSBs in Adprt1a and Adprt2 correlates with the extent of their reduction in REMI as determined in the previous chapter, and may account for the NHEJ defect observed, particularly in *adprt1a*$^{-}$ cells.

6.2.2 *Dictyostelium* genes contain consensus PAR binding motifs

Although my data implicates Adprt1a in promoting NHEJ via Ku80 recruitment/retention to chromatin post-DNA damage, the molecular mechanism by

which this is achieved remains unclear. To determine the contribution of covalent interaction with PAR via PAR binding domains to this observation, the conservation of the 8 amino acid hydrophobic/basic motif (Pleschke *et al.* 2000; Gagne *et al.* 2008), the macro-domain (Karras *et al.* 2005) and the 25 amino acid PAR-binding zinc finger (PBZ) (Ahel *et al.* 2008) was assessed. In the human proteome, these three domains differ in their apparent abundance, with the 8 amino acid motif being found in the largest number of proteins, followed by the macro-domain and then the PBZ domain (Gagne *et al.* 2008). However, a consistent observation is the predominance of PAR binding domains amongst DNA repair and checkpoint proteins, highlighting the potential contribution of the non-covalent PAR interaction to the maintenance of genome stability. To explore the possibility of a PAR-binding motif mediating my observations, I searched the *Dictyostelium* genome for genes containing any of the three PAR-binding consensus motifs. Of interest to us were genes that may play a role in DNA repair, and in particular, NHEJ.

I first searched the *Dictyostelium* protein database for proteins containing the 8 amino acid PAR binding motif. Pleschke *et al* originally described this motif as a cluster of basic residues followed by a combination of hydrophobic and basic amino acids, with the hydrophobic residues making more important contributions to PAR binding (Pleschke *et al.* 2000; Gagne *et al.* 2003). Subsequently, Gagne *et al* refined this consensus through a more extensive peptide analysis, and narrowed it down to the basic/hydrophobic cluster: [H/K/R]-X-X-[A/I/Q/V/Y]-[K/R]-[K/R]-[A/I/L/V]-[F/I/L/P/V], where one of the amino acids in square brackets would be found at that position (Gagne *et al.* 2008). This sequence was used in the PattInProt search engine (http://npsa-pbil.ibcp.fr) (Combet *et al.* 2000) to search the Swiss-Prot database,

giving rise to 94 hits for *Dictyostelium discoideum*, including AP endonuclease (DDB_G0277701), DNA ligase I (DDB_G0274493), Histone H1 (DDB_G0285319) and Ku80 (DDB_G0286303). In Ku80, this PAR binding domain, between residues 128 to 135, maps to the vWA domain, which is important for Ku80 interaction with other proteins (Walker *et al.* 2001).

I then went on to determine the extent of conservation the macro-domain in the *Dictyostelium* proteome. In humans, only 10 proteins containing the macro-domain motif have been identified (Kleine and Luscher 2009). This motif displays a high degree of sequence variation, although the adenine and ribose binding pockets show conservation of hydrophobic residues (Karras *et al.* 2005). An additional two residues capable of hydrogen-bonding to ADP-ribose are also conserved (Karras *et al.* 2005). Several of these macrodomain containing proteins can interact with PAR and play roles in the DNA damage response. In particular, the macrodomain-containing chromatin-remodelling enzyme, ALC1, interacts with players in the NHEJ pathway, although the significance of this is unknown (Ahel *et al.* 2009). Furthermore, macroH2A.1 histone is also involved in chromatin rearrangement, although its role in NHEJ appears to be inhibitory (Timinszky *et al.* 2009). I searched the annotated *Dictyostelium* proteome via dictyBase.org for putative macro-domain containing proteins. My search yielded 2 genes with known roles in DNA metabolism and repair, namely, Ligase III (DDB_G0283857) and APTX (DDB_G0293866). Ligase III is implicated in SSBR/BER (Caldecott 2008), and APTX is implicated in resolving abortive DNA ligation intermediates in SSB and DSB repair (Ahel *et al.* 2006). APTX can interact with XRCC4, implicating it in the ligation step of NHEJ (Clements *et al.* 2004; Ahel *et al.* 2006). However, none of the macrodomain

containing proteins identified are involved in the early stages of NHEJ response, which is the position at which Adprt1a was hypothesised to exert its effects.

As a final step in the search of PAR binding motifs in *Dictyostelium*, I considered those genes that show conservation of the recently characterised PBZ domain (Ahel *et al.* 2008). The PBZ domain is encoded by a 24 residue C2H2 zinc-finger ([K/R]xxCx[F/Y]GxxCxbbxxxxHxxx[F/Y]xH; where b denotes a basic amino-acid), and is present in those organisms showing conservation of PARPs (Ahel *et al.* 2008), unlike the macro-domain which is found in other domains of life (Karras *et al.* 2005). The PBZ domain is found in three vertebrate proteins, APLF, SNM1 and CHFR, which have all been implicated in DNA repair or the checkpoint response (Ahel *et al.* 2008). However, there is a greater predominance of this motif in *Dictyostelium*, being present in seven genes including a putative APTX orthologue (DDB_G0293866); putative PARP orthologue (DDB_G0284015); putative Chk2 orthologue (DDB_G0280321); putative Rad17 orthologue (DDB_G0292504); a uracil DNA glycosylase (DDB_G0291872); CHFR (DDB_G0279263) and Ku70 (DDB_G0286069) (Ahel *et al.* 2008). Of particular interest was the PBZ domain at the C-terminus of Ku70 (Figure 6.2). This motif shows a good degree of similarity to the PBZ domain of its human counterparts, with absolute conservation of the residues that coordinate zinc ions, necessary for stabilising the structure of the zinc-finger (Eustermann *et al.* 2010). Furthermore, starred residues are shown to play key roles in PAR binding of one of the APLF zinc-fingers, and those residues highlighted by a red star play essential roles in this interaction (Eustermann *et al.* 2010). The presence of these residues in *Dictyostelium* Ku70, suggest that a similar PAR binding ability may be conferred by this motif.

6.2.3 The Ku70 PBZ domain can bind to poly(ADP-ribose) *in vitro*

The nature of the DSB repair defect in *adprt1a*$^{-}$ cells suggests that Adprt1a is playing a role early in the NHEJ pathway. Therefore, Ku70 and Ku80, which were found to contain a C-terminal PBZ domain and a 20 amino-acid PAR binding motif, respectively, through *in silico* analysis were investigated first. The nature of the PAR binding motif in Ku80 is such that it could represent a nucleic acid binding domain (Kleine and Luscher 2009), rather than a bona fide PAR binding domain. Conversely, Ku70 shows a high degree of sequence conservation to the consensus PBZ motif, and is likely to function in PAR binding. The terminal location of the PBZ domain would allow for the generation of mutant versions of the gene, with unlikely affects on protein structure, or non-PAR related function. This may not be the case for Ku80 with its PAR motif in the centrally located vWA domain. Thus the PBZ domain of Ku70 was considered in the first instance.

Before embarking on experiments to determine the function of the PBZ domain in Ku70, the ability of this domain to bind PAR was first assessed. In order to do this, either the C-terminal 74 residues of Ku70, or the same fragment lacking the 25 amino-acid PBZ domain, were cloned into the pGex6P-1 vector using the restriction enzymes *Bam*HI and *Not*I. This gave rise to a GST-tagged fusion protein, which when expressed in the *E.coli* strain BL21, could be purified via the GST-tag. Between 2.5 to 0.625pmol of purified protein was slot-blotted onto a nitrocellulose membrane, and the membrane incubated with PAR before the PAR was visualised

using an anti-PAR antibody (Figure 6.3). In accordance with the Ku70 PBZ domain functioning as a PAR binding motif, PAR binding was observed for the wild-type fragment of Ku70, but not when the PBZ domain was deleted. Whether this interaction occurs *in vivo* has not been assessed, but it seems plausible that this motif may confer PAR binding to *Dictyostelium* Ku70.

6.2.4 Generation of a *ku70*$^-$ strain

To assess the contribution of the PBZ domain to Ku70 function, a *ku70*$^-$ strain was generated in which wild-type Ku70, or Ku70 in which the PBZ domain had been deleted would be exogenously expressed. To generate a *ku70*$^-$ strain, a *ku70*-knockout construct was generated in pLPBLP where arms homologous to the upstream (nucleotides -880 to +27) and downstream (nucleotides +2357 to +2786) regions of Ku70 (+1 to +2813) flanked the *BsR* cassette (Figure 6.4A and B). A targeted disruption event using the *ku70*-disruption construct would replace much of the gene coding region with the *BsR* cassette, including those domains involved in protein and DNA interactions. The disruption construct was liberated using *Kpn*I and *Bam*HI, and transfected into Ax2 prior to selection of successfully integrated cells with blasticidin. To identify integrants disrupted at the *ku70* locus, cells were screened by PCR on the 5' and 3' side, and gave products of 1.4 and 1.5kbp, respectively (Figure 6.4C). A control PCR was run alongside the screening PCRs and gave rise to the expected 450bp band. To further verify the three putative *ku70*$^-$ clones, reverse transcriptase PCR (RT-PCR) was performed, to determine whether the disruption would interfere with the expression of Ku70. RNA was prepared from Ax2 and the putative *ku70*$^-$ strains, and converted to cDNA as outlined in materials and methods prior to analysis

by PCR. The primers utilised for this analysis were at positions +332bp and +1707bp, which flanks an intron (+373bp to +454bp) (Figure 6.4A). A lack of expression from the *ku70* gene was indicated by the lack of a PCR product from *ku70*$^-$ cDNA only, whilst Ax2 gave rise to a RT-PCR product (Figure 6.4D). The integrity of the cDNA preparation is indicated by the control PCR run alongside the *ku70* screen, using primers against the ERK gene. It is important to note that in order to see contaminating genomic DNA, primers for both genes were designed to flank an intron. However, PCR attempts with these primer pairs using genomic DNA were unsuccessful. Furthermore, in line with the PCR products for the ERK PCRs representing successful reverse transcription events, no PCR products were acquired in the absence of the reverse transcriptase enzyme. Therefore, it appears that the *ku70*$^-$ strains represent knockouts, rather than disruptants due to the absence of any expression from this gene.

As a final verification, Southern blotting was carried out on *Eco*RI or *Hind*III digested genomic DNA and analysed with a probe against the 3'arm to determine the nature of the integration (Figure 6.4E), or the *BsR* cassette to ensure a single integration event (data not shown). As expected for Ax2 and the *ku70*$^-$ strain, genomic DNA digestion with *Eco*RI gave rise to the predicted 6kb and 7.4kb bands, while *Hind*III digestion gave rise to 11.7kb and 5.4kb bands, respectively. For one of the clones, the wrong band sizes were generated in the Southern blot, possibly representing a duplicate integration event given the presence of two bands using the *BsR* probe (data not shown). This clone was discarded and *ku70*$^-$ strain clone 1 was utilised for future experiments.

6.2.5 Expression of wild-type and mutant Ku70 in the *ku70*$^-$ strain

Following generation of the *ku70*$^-$ cells and removal of the *BsR* cassette by the cre-recombinase, Ku70 was exogenously expressed in these strains. Full-length Ku70 was amplified from Ax2 genomic DNA, in which the N-terminal primer contained a *Kpn*I site and a MYC-tag, whilst the C-terminal primer contained an *Xba*I site (Figure 6.5A). The PCR product was sequenced to ensure no mutations were present and cloned into pDXA-3C (Manstein *et al.* 1995). To generate the PBZ-deletion strain (ΔPBZ), the pDXA-MYC-Ku70 plasmid was digested with *Bse*RI, which is a site internal to the *ku70* gene, and the terminal *Xba*I site. This liberated the C-terminal portion of the *ku70* gene which was replaced with a PCR product generated using a primer at the *ku70 Bse*RI site and a 3' primer directed at a site 25 amino-acids upstream of the stop codon (Figure 6.5B). This primer contained both a stop codon and an *Xba*I site, and led to the exclusion of the PBZ domain from the PCR product. After sequencing revealed no mutations, this fragment was cloned into the *Bse*RI/*Xba*I site of pDXA-MYC-Ku70, to generate pDXA-MYC-Ku70ΔPBZ.

The empty pDXA vector or constructed plasmids were transformed into the *ku70*$^-$ strain, and successfully transformed cells were selected with G418. Pools of G418 resistant cells were analysed for exogenous expression of MYC-Ku70 or MYC-Ku70ΔPBZ by Western blot of whole-cell extracts using an antibody against MYC (Figure 6.6A). Both proteins appeared to be expressed to similar levels and furthermore, in the absence of Ku70, Ku80 expression is consistently reduced. This is in agreement with the functioning of Ku70 and Ku80 as a heterodimer and the instability of each subunit in isolation (Singleton *et al.* 1997). To further verify the

functionality of the exogenously expressed Ku70, its ability to interact with Ku80 was assessed. This interaction seems likely, given the rescue of Ku80 expression when either wild-type or the ΔPBZ Ku70 is exogenously expressed. Exponentially growing cells of the different strains were lysed and Ku80 immunoprecipitated as outlined in materials and methods, before probing for wild-type or ΔPBZ Ku70 via the MYC-tag (Figure 6.6B). Both the wild-type and mutant Ku70 interacted with Ku80, indicating that the exogenously expressed proteins are capable of heterodimerising with endogenous Ku80. Furthermore, the notion that the PBZ domain is not involved in Ku heterodimerisation is supported, and in each case, the level of heterodimer was the same. The equal expression and dimerisation between wild-type and ΔPBZ Ku70 enables us to determine the functional contribution of the Ku70 PBZ domain to DSB repair, independent of Ku levels.

6.2.6 NHEJ and Ku enrichment is defective in the Ku70ΔPBZ strain

Having confirmed the expression of Ku70 from the pDXA-3C vector and its heterodimerisation with Ku80, I went on to assess levels of NHEJ and Ku chromatin retention following DNA damage. This would allow us to determine whether the phenotypes observed in the *adprt1a*$^{-}$ strain are being mediated by the PBZ domain, strengthening the hypothesis that PARylation by Adprt1a, rather than Adprt1a itself, is playing a role in promoting NHEJ. As a first step towards doing this, enrichment of Ku80 in chromatin post-phleomycin treatment was determined. Exponentially growing MYC-Ku70 and MYC-Ku70ΔPBZ cells were treated with phleomycin. At time-points following DNA damage, sub-cellular fractionation was performed and samples were analysed by Western blot using an antibody against Ku80 (Figure

6.7A). Ku80 was enriched in the chromatin fraction of MYC-Ku70 in a time-dependent manner, but this was reduced in the MYC-Ku70ΔPBZ. This phenotype mirrors that seen in the *adprt1a*$^{-}$ strain, and suggests a role for the PBZ domain in facilitating recruitment or retention of Ku to chromatin. The reduction of Ku enrichment for MYC-Ku70ΔPBZ was observed consistently, and quantification of Ku80 levels at a single-time point revealed this reduction to be to approximately 50% of the level of the MYC-Ku70 strain (Figure 6.7B).

I then went on to determine whether the defect in Ku DNA association was sufficient to give rise to a NHEJ defect. In the case of the *adprt1a*$^{-}$, but not the *adprt2*$^{-}$ strain, the extent of the delay in Ku enrichment was correlated with a rise to a REMI-defect. Given that the Ku DNA association defect in the MYC-Ku70ΔPBZ relative to MYC-Ku70 is similar to that of the *adprt1a*$^{-}$ strain relative to Ax2, it seems possible that this may be the case. REMI was performed as previously described on cells grown without antibiotic for 24 hours (Figure 6.7C). In the *ku70*$^{-}$ strain, no REMI induction was observed, as would be expected, given the dependence of REMI on components of the Ku heterodimer (Hsu *et al.* 2011). This defect could be rescued by expression of MYC-Ku70, but to a lesser extent by MYC-Ku70ΔPBZ. It is important to note that ectopic protein levels of MYC-Ku70 and MYC-Ku70ΔPBZ were unchanged in this period of no antibiotic selection (data not shown). Thus, the PBZ domain appears to play a pivotal role in the recruitment of Ku to chromatin following DNA damage, and this defect in the ΔPBZ strain translates into an NHEJ defect. Overall, it appears that the DSB induced PARylation by Adprt1a is exerting its effects in NHEJ by promoting the recruitment/retention of Ku to chromatin via the Ku70 PBZ domain.

6.3 Discussion

In the previous chapter, the role of PARylation in DNA DSB repair and particularly NHEJ was indicated, with Adprt1a acting as the primary mediator of the DSB-induced PARylation response. The concomitant increase in HR that accompanied the reduced NHEJ in *adprt1a*$^-$ strains highlighted the putative role of this gene early on in the NHEJ pathway. This suggested a possible gatekeeper function for Adprt1a, similar to that which has been assigned to the Ku heterodimer. This chapter therefore aimed to characterise the molecular basis behind the role of Adprt1a in NHEJ.

To initiate this study, the position of Adprt1a as an early component of the NHEJ pathway was verified. The fact that NHEJ and HR phenotypes in the *adprt1a*$^-$ strain were reminiscent of *ku80*$^-$ cells led to the hypothesis that Adprt1a may function to recruit or stabilise Ku binding at DNA DSBs. To address this possibility, enrichment of Ku80 in chromatin post-phleomycin treatment was assessed in *adprt1a*$^-$ cells and illustrated to be reduced relative to Ax2. Surprisingly, Ku80 recruitment was reduced in the *adprt2*$^-$ strain as well, albeit less severely. This suggests a correlation between the reduction in PARylation and Ku-chromatin association post-DNA DSBs, and highlights Adprt1a as the major contributor in this response.

Whether the action of Adprt1a in DNA DSB repair is dependent on its PARylation function is unclear. However, given the direct correlation between the extent of the *adprt1a*$^-$ strain PARylation defect and the reduction in Ku80 chromatin enrichment,

this would appear to be the case. This may indicate a situation reminiscent of the catalytic function of PARP1 in XRCC1 recruitment (El-Khamisy *et al.* 2003; Okano *et al.* 2003; Mortusewicz *et al.* 2007), whereby PARylation by Adprt1a may assist in the recruitment of Ku80 following DNA damage. Nevertheless, this is something that remains to be formally assessed. A possible means of determining the contribution of Adprt1a catalytic activity to this response may be to determine whether Ku chromatin recruitment is altered following DNA damage when cells are pre-treated with competitive PARP inhibitors. These inhibitors target PARP catalytic activity without preventing DNA binding (Mortusewicz *et al.* 2007). Thus, a situation is provided where the possible direct function of Adprt1a in NHEJ can be dissected, in addition to the effects it may exert via its catalytic activity. A caveat of this experiment would be the broad specificity of PARP inhibitors, which have been shown to be capable of targeting *Dictyostelium* ARTs functioning in both SSBR/BER and DSB repair. However, the genetic approach has illustrated the major function of Adprt1a in the DSB repair response, making non-specific ART targeting less of an issue. Whilst the data may suggest a role for damage-induced Adprt1a catalytic activity, the putative acceptors of Adprt1a mediated PARylation cannot be determine. However, possible targets may include Adprt1a itself, as well as histones, given their identification as major acceptors of PAR in humans. Furthermore, histone H1 has been previously implicated in the repair response, and in particular, in NHEJ (Rosidi *et al.* 2008; Rulten *et al.* 2011).

One mechanism by which PARPs exert their function is via the direct modification of proteins, which can alter their structure/function. This direct modification has been observed *in vitro* with Ku; although in this case, the modification is inhibitory to Ku

interaction with DNA (Li *et al.* 2004). An alternative mechanism of action is through non-covalent interactions which have already been shown to positively influence repair (El-Khamisy *et al.* 2003; Okano *et al.* 2003; Ahel *et al.* 2008; Ahel *et al.* 2009; Rulten *et al.* 2011). Towards this end, I searched the *Dictyostelium* genome for the presence of the three PAR binding domains, focusing in particular on genes playing a role in the repair response. *Dictyostelium* showed conservation of all three PAR binding motifs in a range of proteins. Of particular significance however, was the presence of a PBZ domain and the basic/hydrophobic amino acid PAR binding domain in Ku70 and Ku80, respectively. Interest in this conservation stemmed from the fact that it would provide a relationship between Adprt1a damage-induced catalytic activity, and Ku recruitment. This would lead to a situation reminiscent of that seen with XRCC1 and DNA ligase IV/XRCC4 recruitment to damage sites (El-Khamisy *et al.* 2003; Okano *et al.* 2003; Mortusewicz *et al.* 2007; Rulten *et al.* 2011). The basic/hydrophobic amino-acid PAR binding motif whilst being implicated in PAR binding has properties that could lead to its assignment as a nucleic acid binding motif, with no specific preference for PAR. The possible diversity in binding specificity is highlighted by its abundance in the human genome, with over 800 genes identified to contain this domain (Gagne *et al.* 2008). However, only a fraction of these genes may possess PAR binding activity. Conversely, the PBZ domain is much less abundant, and likely represents a specific PAR binding motif. It was therefore selected for initial characterisation in Ku70. The conservation of the PBZ motif in *Dictyostelium* has already been described by Ahel *et al* (Ahel *et al*. 2008), and is a highly prominent domain in the *Dictyostelium* genome, relative to vertebrates. The significance of the relative abundance of the PBZ domain in *Dictyostelium*,

particularly in repair/checkpoint proteins, is unclear, but suggests the importance of the PAR modification in the repair/checkpoint response.

Based on the analysis of protein PARylation following DNA DSBs in the previous chapter, and the major role of Adprt1a in the DSB response, it seems likely that Adprt1a may have multiple protein targets following DNA DSB induction. Deletion of the PBZ domain from Ku70 eliminated its PAR-binding capacity, and allowed for observations to be limited to the role of PARylation in the NHEJ pathway. In support of the Adprt1a-induced PARylation post-DNA DSBs being exerted via the Ku70 PBZ domain, many of the NHEJ observations made in the *adprt1a*$^{-}$ strain were mirrored in the Ku70ΔPBZ expressing strain. In particular, this function is mediated via promoting the association of Ku to damaged DNA. However, whether this is achieved via enhanced Ku recruitment or retention at DNA damage sites is not clear from out data. *In vivo*, Ku association at DNA ends is dynamic and transient post-DNA damage in human cells (Mari *et al.* 2006; Uematsu *et al.* 2007). Therefore, the overall outcome of Adprt1a action on Ku may be to shift the Ku DNA-binding equilibrium in favour of its association with DNA. The result of this would be a reduced likelihood of DNA ends being exposed for nucleolytic degradation that favours repair by HR or a-NHEJ pathways. In *Dictyostelium* Ku70, the PBZ domain is located at the extreme C-terminus of the *ku70* gene, following a putative SAP-domain encoding region that may interact with nucleic acids (Aravind and Koonin 2000; Block and Lees-Miller 2005). In humans, the C-terminal portion of Ku70 encodes the SAP domain which is joined to the Ku70 core via a flexible linker. On DNA binding, the SAP domain is postulated to undergo structural rearrangements that may stablise Ku binding to DNA ends (Rivera-Calzada *et al.* 2007; Lehman *et al.*

2008). Thus, the PBZ domain at the extreme C-terminus of *Dictyostelium* Ku70 may further stabilise this interaction with DNA.

In the previous chapter, it was speculated that *Dictyostelium* Adprt1a may be functioning as a putative PARP3 homologue, given their roles in NHEJ, distinct from the other identified DDR PARPs. Unlike Adprt1a, PARP3 does not appear to encode a known DNA interacting motif, other than the putative nucleic acid binding WGR motif. However, the ability of PARP3 to be activated *in vitro* by DNA DSBs, independent of other factors suggests that it can recognise this form of DNA damage (Rulten *et al.* 2011). In human cells, PARylation by PARP3 has been found to promote NHEJ through the recruitment of APLF via its PBZ domains, which in turn facilitates recruitment/retention of Ligase IV/XRCC4 (Rulten *et al.* 2011). In other eukaryotes, the recruitment of the NHEJ Ligase complex to DNA stabilises Ku binding at DNA ends to promote NHEJ (Zhang *et al.* 2007; Yano and Chen 2008; Chen and Tomkinson 2011; Yano *et al.* 2011). It is therefore possible that at least part of the mechanism by which APLF promotes NHEJ is via Ku stabilisation and that in *Dictyostelium* this is being achieved directly via the Ku70 PBZ domain. In support of the Ku-stabilisation function of APLF, *aplf*$^{-/-}$ mouse cells display greater a-NHEJ which is associated with greater DNA degradation (Rulten *et al.* 2011).

In mammalian cells, APLF is implicated in SSBR and DSB repair, via interactions with XRCC1, XRCC4 and Ku80 (Iles *et al.* 2007; Rulten *et al.* 2011). *Dictyostelium* lacks an APLF orthologue. The abundance of PBZ domains in this organism, including in Ku70, may therefore arise from the need to divide the PAR-recognition function of APLF over many different repair genes to mediate its diverse functions.

However, human Ku70 also contains a basic/hydrophobic PAR binding domain at its N-terminus (Pleschke *et al.* 2000), which confers PAR binding ability to Ku70 *in vitro* and *in vivo* (Pleschke *et al.* 2000; Ahel *et al.* 2009). Furthermore, in response to DNA damage, Ku70 interacts with ALC1 in a PAR-dependent manner (Ahel *et al.* 2009). Thus, in humans, NHEJ may also be modulated via the direct regulation of Ku association to DNA, in addition to its stabilisation as mediated by APLF. Overall, the data suggests a possible evolutionary conservation between DSB-induced PARylation and promotion of NHEJ either directly or indirectly.

With regards to DSB repair, and particularly NHEJ, APLF has been shown to interact with PARylated histone H1 to promote the recruitment/retention of XRCC4/Ligase IV (Rulten *et al.* 2011). This promotional, but non-essential role of APLF in NHEJ is reflected in the delayed kinetics of γH2AX decay when APLF is absent or its PBZ domains are mutated (Rulten *et al.* 2011). A similar situation is likely to be true in *Dictyostelium*, whereby the recruitment of the Ku heterodimer to DNA damage is stimulated by recognition of Adprt1a mediated PARylation, but not essential. Thus in the *adprt1a*$^{-}$ and Ku70ΔPBZ-expressing cells, Ku-chromatin recruitment is reduced rather than completely defective, but may nevertheless account for reduced REMI in both cases. This data further points to the gatekeeper function of Adprt1a, whereby the reduced Ku recruitment to DNA ends, leaves ends accessible for processing by DNA end-resection enzyme (Lee *et al.* 1998; Liang *et al.* 1998). DNA end processing is inhibitory to NHEJ, which may result in the channelling of repair into other pathways such as HR and a-NHEJ. Vegetative *Dictyostelium* are in G2 when both HR and NHEJ occur as determined by the HR assay and REMI. Furthermore, Ku chromatin enrichment data post-phleomycin indicates that NHEJ is indeed playing a

role in resolving at least a subset of DNA DSBs at this developmental stage, in line with those observations of Muramoto *et al* (Muramoto and Chubb 2008). This may be in competition with HR, although the enrichment of HR components using this technique remains to be performed. Overall, the potential of Adprt1a as a regulator of DNA DSB repair in G2 *Dictyostelium* is highlighted by the data, with Adprt1a promoting NHEJ. It is important to note that Adprt1a may recognise specific DNA lesions, perhaps those displaying enhanced damage complexity, and serve to promote NHEJ at these sites (Shibata *et al.* 2011).

In conclusion, I have shown that the DSB induced PARylation in *Dictyostelium* following DNA DSBs is predominantly mediated by Adprt1a. Adprt1a may also function as a gatekeeper between NHEJ and HR by promoting NHEJ. This NHEJ promotion is via the recruitment or retention of the Ku heterodimer to chromatin post-DNA damage via the Ku70 PBZ domain. Future work will address the targets of Adprt1a catalytic activity, and the additional roles it may be playing in the response to DNA DSBs.

7: General discussion

HR and NHEJ are the predominant DSB repair pathways in eukaryotes. In G2 of the cell-cycle these pathways exist in parallel and can compete for repair of DNA lesions. This competition has been illustrated by repair assays illustrating the upregulation of HR when NHEJ is downregulated, and vice versa when HR is disrupted. However, given the predominant usage of repair pathways in different organisms, such as NHEJ in mammals and HR in yeast during G2, active regulation must also participate. A key position at which regulation can be exerted is in the initiation of repair pathways. In line with this, Ku exhibits high binding affinity for DNA and its presence at DNA DSBs is inhibitory to DNA end resection (Ira *et al.* 2004). The MRX/Sae2 complex in yeast and its orthologous complexes in other organisms are proposed overcome the inhibitory action of Ku in favour of HR (Mimitou and Symington 2008; Mimitou and Symington 2010; Nicolette *et al.* 2010; Shim *et al.* 2010). HR is restricted in G1 and its usage is upregulated in G2 and G2/S of the cell cycle (Aylon *et al.* 2004; Ira *et al.* 2004; Jazayeri *et al.* 2006). This activity profile correlates with that of CDKs, which phosphorylates Sae2/CtIP and enhances end resection (Sartori *et al.* 2007; Huertas *et al.* 2008; Huertas and Jackson 2009). Similarly, post-translational modifications that modulate Ku DNA affinity would also mediate the balance between DSB repair pathway utilisation in G2. Finally, the position at which repair pathway commitment occurs is unclear, and there have been suggestions that NHEJ can be initiated, followed by HR engagement, whilst initiation of HR precludes utilisation of NHEJ (Frank-Vaillant and Marcand 2002; Shibata *et al.* 2011). Several aspects of DSB repair pathway regulation thus remain to be elucidated.

This thesis aimed to clarify aspects of DSB repair pathway regulation, particularly with regards to the role of the damage-induced post-translational modification, Poly-ADP ribosylation. Towards this, *Dictyostelium discoideum* was used as a model organism. The strength of *Dictyostelium* is the high degree of conservation of repair pathways and repair components with vertebrates (Block and Lees-Miller 2005; Hudson *et al.* 2005; Hsu *et al.* 2006). Therefore, observations made in this system, are applicable to higher eukaryotes. Furthermore, with regards to regulation, *Dictyostelium* is in G2 of the cell-cycle, and is proficient in NHEJ and HR. NHEJ contributes to damage resolution as illustrated by delayed resumption of cell division following DNA DSBs (Muramoto and Chubb 2008). However, HR is likely the predominant pathway in vegetative cells for DNA DSB tolerance as illustrated by the DSB sensitivity of the *exo1*$^{-}$ strain compared to the lack of sensitivity of NHEJ mutants (Hudson *et al.* 2005; Hsu *et al.* 2011). The NHEJ DSB sensitivity is reversed in germinating spores and provides an optimal situation to verify results and determine factors that are altered and may account for the shift in NHEJ contribution (Hudson *et al.* 2005). This includes post-translational modifications that are specific to a particular developmental stage and alterations in chromatin structure.

To initiate investigations into DSB repair regulation in *Dictyostelium*, the possibility of repair pathway competition was investigated. Whilst sensitivity assays provide insight into overall repair capacity, they do not indicate the contribution of each repair pathway to this survival. Towards this, a gene-targeting assay measuring HR efficiency was developed in *Dictyostelium* and enabled assessment of HR in parallel with NHEJ by REMI. In line with the competition between DSB repair pathways, upregulated HR efficiency was illustrated in the *ku80*$^{-}$ strain, but not when the

Artemis orthologue, *dclre1* was disrupted. This differential effect on HR efficiency further highlighted the gate-keeper function of Ku, independent of its role in NHEJ. A similar proposition of Ku as a DSB repair regulatory gatekeeper has been made in eukaryotes, where Ku disruption in particular, and less so for downstream NHEJ components, leads to HR upregulation (Pierce *et al.* 2001; Allen *et al.* 2002; Zhang *et al.* 2007). Furthermore, the data illustrates the inhibitory action of Ku on HR, whereby even in the absence of a functional NHEJ pathway, such as in the *dclre1*$^{-}$ strain, Ku continued to engage some DNA ends. This prevented their channelling into HR at the *cdk8* locus and suggested that, at least for some genomic regions, Ku is primarily and possibly preferentially engaged at DSBs, preventing HR initiation. In other eukaryotes, Ku is proposed to initially bind and occlude DNA ends (Frank-Vaillant and Marcand 2002; Kim *et al.* 2005; Shibata *et al.* 2011). However, Ku dynamically associates with DSBs and exposed DNA ends can be nucleolytically processed and engaged in HR (Lee *et al.* 1997; Liang *et al.* 1998; Mari *et al.* 2006; Uematsu *et al.* 2007). The question arises as to the molecular basis behind preferential and sometimes futile engagement of NHEJ at certain DSBs. Furthermore, given that HR is the major pathway in DSB tolerance in *Dictyostelium*, regulatory processes must modulate Ku engagement at DNA ends to downregulate its inhibitory action and enable HR to predominate.

The impetus to determine the contribution of PARylation in DSB repair regulation was due, in part, to the increasing evidence of the negative regulatory role exerted by PARPs on NHEJ (Hochegger *et al.* 2006; Saberi *et al.* 2007). Whilst this data was in the context of replication forks, it was tempting to speculate that a similar regulatory mechanism may exist at other stages of the cell cycle. The predominance of

Dictyostelium in G2 enabled the specific role of PARylation at this cell cycle stage to be determined, with minimal interference by replication. The study was initiated by the identification of PARP1 orthologues in *Dictyostelium* via bioinformatics analysis. This led to the identification of 15 putative *Dictyostelium* ARTs, with unknown PARylation capacity, although three ARTs were identified as putative components of the DDR: *adprt1a, adprt1b* and *adprt2*. Consistent with the conservation of PARP function in DNA repair, Adprt1b and Adprt2 were implicated in SSBR/BER. The enhanced BER and SSB sensitivity clarified some of the uncertainty surrounding PARP contribution to the BER in mammals (Strom *et al.* 2011), and the mechanism of their contribution now needs to be elucidated. Interestingly, some insight into the mechanism by which Adprt1b and Adprt2 may function in SSBR/BER was gained from the *adprt1a*$^{-}$*/adprt2*$^{-}$ double-disruptant, which was more sensitive to the base-damaging agent MMS than the single-disruptants. The inability of Adprt1b to mediate tolerance to MMS-induced damage in this case suggested that Adprt1b cannot function in isolation to contribute to repair. Instead, Adprt1b and Adprt2 may function together as a complex, or in the same pathway in response to MMS, in a manner that can be compensated by Adprt1a in the single-disruptants. PARP1 and PARP2 can interact *in vitro* (Schreiber *et al.* 2002), and the kinetics of PARP2 recruitment at DNA damage sites is downstream of PARP1 (Mortusewicz *et al.* 2007). Thus a similar model for SSBR/BER may apply to hPARP1 and hPARP2, and Adprt1a and Adprt1b may be orthologues of these proteins in *Dictyostelium*.

Until this point, PARP1 and PARP2 were the only characterised DDR PARPs in mammals (Ame *et al.* 2004). Therefore, the identification of a third DDR PARP in *Dictyostelium*, Adprt1a, in the DNA DSB repair response was surprising.

Furthermore, it suggested specific and distinct damage recognition roles of the different *Dictyostelium* DDR PARPs, although the qualitative significance of this could not be established from this data. For example, whether variation of targets or PAR chain length/branching is mediated by the different Adprt proteins could not be determined, but would provide a mechanism by which the DDR could be regulated. In line with these observations, different PARPs possess different PAR capacity, as evidenced by the limited PAR sythesis by PARP3 to oligomers of ADP-ribose (Loseva *et al.* 2010; Rulten *et al.* 2011). Furthermore, proteins with PAR binding capacity demonstrate differential PAR binding affinity as a function of PAR chain length (Fahrer *et al.* 2007). This work suggested the existence of further human DDR PARPs and consistently, PARP3 was subsequently identified by Rulten *et al* in the DSB repair response (Rulten *et al.* 2011).

A mechanism by which PARP1 may negatively-regulate NHEJ is via Ku PARylation which reduces its DNA affinity *in vitro* and may account for the *in vivo* observations (Li *et al.* 2004; Hochegger *et al.* 2006; Saberi *et al.* 2007). Furthermore, PARP1 is implicated in a-NHEJ that functions in competition with Ku (Audebert *et al.* 2004; Cheng *et al.* 2011), and would likely be outcompeted by Ku, due to the lower DNA binding affinity of PARP1 (Wang *et al.* 2006). Thus, the finding that Adprt1a positively regulates NHEJ via promoting Ku recruitment/retention to chromatin post-damage was surprising. This was particularly in the context of the predominant role of HR in *Dictyostelium*, and the inhibitory competition by Ku on HR. Nevertheless, the engagement of NHEJ in vegetative *Dictyostelium* DSB repair was again illustrated, and the gate-keeper function of Ku in regulating DSB repair pathway choice in favour of NHEJ was supported. This work also extended a regulatory DSB

repair gate-keeper function to Adprt1a. In line with this, disruption of *adprt1a* led to enhanced HR, and illustrated the regulation of repair pathway utilisation by modulating Ku DNA end association.

To characterise the molecular basis of the positive role of Adprt1a on NHEJ via Ku chromatin association the contribution of the Ku70 PBZ domain was considered and was illustrated to facilitate Ku recruitment to DNA post-DSBs. This implicated PARylation, likely by Adprt1a, in promoting Ku chromatin association, to promote NHEJ. Furthermore, this data enhanced the hypothesis that modulation of Ku DNA end-binding affinity can direct repair pathway utilisation. Consistent with my findings, PARP3 was also implicated in promoting NHEJ, but in this case, functioned via the recruitment of APLF, which in turn recruited the Ligase IV complex to DNA DSBs (Rulten *et al.* 2011). Whilst it is tempting to speculate that this may simply promote NHEJ by enhancing the efficiency of DNA DSB ligation, the ligase complex has also been implicated in stabilising Ku DNA end association. Thus, this raises an interesting possibility that Adprt1a and its putative human orthologue, PARP3, mediate similar functions, although the mechanistic details vary.

In humans, NHEJ is the predominant pathway with HR repairing the fraction of damage associated with enhanced chromatin and damage complexity (Shibata *et al.* 2011). Thus the promotion of NHEJ by PARP3 to reduce interference by more inhibitory pathways such as a-NHEJ has a clear advantage (Rulten *et al.* 2011). The mechanistic basis behind the predominant usage of HR in vegetative *Dictyostelium* is unclear, and the significance of Adprt1a in promoting NHEJ at this developmental stage is hard to comprehend. This is in comparison to the illustrated importance of

Adprt1a and NHEJ contribution to DSB survival in germinating spores. In vegetative *Dictyostelium*, Adprt1a may therefore function to promote NHEJ at subset of DNA damage that cannot be repaired by HR, with the negative effect of promoting inhibitory NHEJ at other DNA DSBs. However, this may not be the case at all DSBs, implicating additional regulatory factors in downregulating NHEJ or upregulating HR at a fraction of DNA damage.

In conclusion, the exertion of DSB repair pathway regulation via the Ku heterodimer has been illustrated. Furthermore, the modulation of Ku DNA association as a means of modulating repair pathway utilisation has also been demonstrated via the effect of PARylation. With regards to PARylation, I have shown the conservation of DNA DSB, SSB and base-damage induced PARylation, in addition to the contribution of PARP1 and PARP2 orthologues to BER and SSBR. Significantly, however, I have also identified a third DNA repair PARP, Adprt1a, with a positive role on NHEJ. The combination of mammalian and *Dictyostelium* studies therefore suggests that PARylation may exert both a positive and negative regulatory role on NHEJ. The mechanism by which these differential effects are achieved needs to be elucidated. This includes targets of PARylation and the mechanism by which PARylation by different PARPs can differentially dictate specific repair pathways.

8 : References

Aburatani, H., *et al.* (1997). "Cloning and characterization of mammalian 8-hydroxyguanine-specific DNA glycosylase/apurinic, apyrimidinic lyase, a functional mutM homologue." Cancer Research **57**(11): 2151-2156.

Adachi, H., *et al.* (1994). "Isolation of *Dictyostelium discoideum* cytokinesis mutants by restriction enzyme-mediated integration of the blasticidin S resistance marker." Biochemical and Biophysical Research Communications **205**(3): 1808-1814.

Adamietz, P. and A. Rudolph (1984). "ADP-ribosylation of nuclear proteins in vivo. Identification of histone H2B as a major acceptor for mono- and poly(ADP-ribose) in dimethyl sulfate-treated hepatoma AH 7974 cells." The Journal of Biological Chemistry **259**(11): 6841-6846.

Adamo, A., *et al.* (2010). "Preventing nonhomologous end joining suppresses DNA repair defects of Fanconi anemia." Molecular Cell **39**(1): 25-35.

Ahel, D., *et al.* (2009). "Poly(ADP-ribose)-dependent regulation of DNA repair by the chromatin remodeling enzyme ALC1." Science **325**(5945): 1240-1243.

Ahel, I., *et al.* (2008). "Poly(ADP-ribose)-binding zinc finger motifs in DNA repair/checkpoint proteins." Nature **451**(7174): 81-85.

Ahel, I., *et al.* (2006). "The neurodegenerative disease protein aprataxin resolves abortive DNA ligation intermediates." Nature **443**(7112): 713-716.

Ahnesorg, P., *et al.* (2006). "XLF interacts with the XRCC4-DNA ligase IV complex to promote DNA nonhomologous end-joining." Cell **124**(2): 301-313.

Alexander, H., *et al.* (1996). "repE--the *Dictyostelium* homolog of the human Xeroderma Pigmentosum group E gene is developmentally regulated and contains a leucine zipper motif." Nucleic Acids Research **24**(12): 2295-2301.

Alexiadis, V. and J. T. Kadonaga (2002). "Strand pairing by Rad54 and Rad51 is enhanced by chromatin." Genes & Development **16**(21): 2767-2771.

Allen, C., *et al.* (2002). "DNA-dependent protein kinase suppresses double-strand break-induced and spontaneous homologous recombination." Proceedings of the National Academy of Sciences of the United States of America **99**(6): 3758-3763.

Allinson, S. L., *et al.* (2003). "Poly(ADP-ribose) polymerase in base excision repair: always engaged, but not essential for DNA damage processing." Acta Biochimica Polonica **50**(1): 169-179.

Altmeyer, M., *et al.* (2009). "Molecular mechanism of poly(ADP-ribosyl)ation by PARP1 and identification of lysine residues as ADP-ribose acceptor sites." Nucleic Acids Research **37**(11): 3723-3738.

Ame, J. C., *et al.* (1999). "PARP-2, A novel mammalian DNA damage-dependent poly(ADP-ribose) polymerase." The Journal of Biological Chemistry **274**(25): 17860-17868.

Ame, J. C., *et al.* (2004). "The PARP superfamily." Bioessays **26**(8): 882-893.

Arana, M. E. and T. A. Kunkel (2010). "Mutator phenotypes due to DNA replication infidelity." Seminars in Cancer Biology **20**(5): 304-311.

Aravind, L. and E. V. Koonin (2000). "SAP - a putative DNA-binding motif involved in chromosomal organization." Trends in Biochemical Sciences **25**(3): 112-114.

Ariumi, Y., *et al.* (1999). "Suppression of the poly(ADP-ribose) polymerase activity by DNA-dependent protein kinase in vitro." Oncogene **18**(32): 4616-4625.

Audebert, M., *et al.* (2004). "Involvement of poly(ADP-ribose) polymerase-1 and XRCC1/DNA ligase III in an alternative route for DNA double-strand breaks rejoining." The Journal of Biological Chemistry **279**(53): 55117-55126.

Audebert, M., *et al.* (2008). "Effect of double-strand break DNA sequence on the PARP-1 NHEJ pathway." Biochemical and Biophysical Research Communications **369**(3): 982-988.

Audebert, M., *et al.* (2006). "Involvement of polynucleotide kinase in a poly(ADP-ribose) polymerase-1-dependent DNA double-strand breaks rejoining pathway." Journal of Molecular Biology **356**(2): 257-265.

Auer, B., *et al.* (1995). "On the biological role of the nuclear polymerizing NAD+: protein(ADP-ribosyl) transferase (ADPRT): ADPRT from Dictyostelium discoideum and inactivation of the ADPRT gene in the mouse." Biochimie **77**(6): 444-449.

Aylon, Y., *et al.* (2004). "The CDK regulates repair of double-strand breaks by homologous recombination during the cell cycle." The EMBO Journal **23**(24): 4868-4875.

Barlow, J. H., *et al.* (2008). "Differential regulation of the cellular response to DNA double-strand breaks in G1." Molecular Cell **30**(1): 73-85.

Baumann, P., *et al.* (1996). "Human Rad51 protein promotes ATP-dependent homologous pairing and strand transfer reactions *in vitro*." Cell **87**(4): 757-766.

Beneke, R., *et al.* (2000). "DNA excision repair and DNA damage-induced apoptosis are linked to Poly(ADP-ribosyl)ation but have different requirements for p53." Molecular and Cellular Biology **20**(18): 6695-6703.

Benjamin, R. C. and D. M. Gill (1980). "Poly(ADP-ribose) synthesis in vitro programmed by damaged DNA. A comparison of DNA molecules containing different types of strand breaks." The Journal of Biological Chemistry **255**(21): 10502-10508.

Bennett, R. A., *et al.* (1997). "Interaction of human apurinic endonuclease and DNA polymerase beta in the base excision repair pathway." Proceedings of the National Academy of Sciences of the United States of America **94**(14): 7166-7169.

Benson, F. E., *et al.* (1994). "Purification and characterization of the human Rad51 protein, an analogue of E. coli RecA." The EMBO Journal **13**(23): 5764-5771.

Beranek, D. T. (1990). "Distribution of methyl and ethyl adducts following alkylation with monofunctional alkylating agents." Mutation Research **231**(1): 11-30.

Beucher, A., *et al.* (2009). "ATM and Artemis promote homologous recombination of radiation-induced DNA double-strand breaks in G2." The EMBO Journal **28**(21): 3413-3427.

Block, W. D. and S. P. Lees-Miller (2005). "Putative homologues of the DNA-dependent protein kinase catalytic subunit (DNA-PKcs) and other components of the non-homologous end joining machinery in *Dictyostelium discoideum*." DNA Repair (Amst) **4**(10): 1061-1065.

Block, W. D., *et al.* (2004). "Autophosphorylation-dependent remodeling of the DNA-dependent protein kinase catalytic subunit regulates ligation of DNA ends." Nucleic Acids Research **32**(14): 4351-4357.

Boulton, S., *et al.* (1999). "Interactive effects of inhibitors of poly(ADP-ribose) polymerase and DNA-dependent protein kinase on cellular responses to DNA damage." Carcinogenesis **20**(2): 199-203.

Boulton, S. J. and S. P. Jackson (1996a). "*Saccharomyces cerevisiae* Ku70 potentiates illegitimate DNA double-strand break repair and serves as a barrier to error-prone DNA repair pathways." The EMBO Journal **15**(18): 5093-5103.

Boulton, S. J. and S. P. Jackson (1996b). "Identification of a *Saccharomyces cerevisiae* Ku80 homologue: roles in DNA double strand break rejoining and in telomeric maintenance." Nucleic Acids Research **24**(23): 4639-4648.

Bradley, M. O. and K. W. Kohn (1979). "X-ray induced DNA double strand break production and repair in mammalian cells as measured by neutral filter elution." Nucleic Acids Research **7**(3): 793-804.

Braithwaite, E. K.*, et al.* (2005). "DNA polymerase lambda mediates a back-up base excision repair activity in extracts of mouse embryonic fibroblasts." The Journal of Biological Chemistry **280**(18): 18469-18475.

Bronner, C. E.*, et al.* (1992). "Mutations affecting sensitivity of the cellular slime mold *Dictyostelium discoideum* to DNA-damaging agents." Mutation Research **274**(3): 187-200.

Bryant, H. E.*, et al.* (2009). "PARP is activated at stalled forks to mediate Mre11-dependent replication restart and recombination." The EMBO Journal **28**(17): 2601-2615.

Bryant, H. E.*, et al.* (2005). "Specific killing of BRCA2-deficient tumours with inhibitors of poly(ADP-ribose) polymerase." Nature **434**(7035): 913-917.

Buck, D.*, et al.* (2006). "Cernunnos, a novel nonhomologous end-joining factor, is mutated in human immunodeficiency with microcephaly." Cell **124**(2): 287-299.

Bugreev, D. V.*, et al.* (2006). "Rad54 protein promotes branch migration of Holliday junctions." Nature **442**(7102): 590-593.

Bunting, S. F.*, et al.* (2010). "53BP1 inhibits homologous recombination in Brca1-deficient cells by blocking resection of DNA breaks." Cell **141**(2): 243-254.

Burkovics, P.*, et al.* (2006). "Human Ape2 protein has a 3'-5' exonuclease activity that acts preferentially on mismatched base pairs." Nucleic Acids Research **34**(9): 2508-2515.

Bzymek, M.*, et al.* (2010). "Double Holliday junctions are intermediates of DNA break repair." Nature **464**(7290): 937-941.

Caldecott, K. W. (2003). "XRCC1 and DNA strand break repair." DNA Repair (Amst) **2**(9): 955-969.

Caldecott, K. W. (2008). "Single-strand break repair and genetic disease." Nature Reviews Genetics **9**(8): 619-631.

Caldecott, K. W.*, et al.* (1996). "XRCC1 polypeptide interacts with DNA polymerase beta and possibly poly (ADP-ribose) polymerase, and DNA ligase III is a novel molecular 'nick-sensor' in vitro." Nucleic Acids Research **24**(22): 4387-4394.

Caldecott, K. W.*, et al.* (1994). "An interaction between the mammalian DNA repair protein XRCC1 and DNA ligase III." Molecular and Cellular Biology **14**(1): 68-76.

Cepeda, V.*, et al.* (2006). "Poly(ADP-ribose) polymerase-1 (PARP-1) inhibitors in cancer chemotherapy." Recent Patents on Anti-cancer Drug Discovery **1**(1): 39-53.

Champoux, J. J. (2001). "DNA topoisomerases: structure, function, and mechanism." Annual Review of Biochemistry **70**: 369-413.

Chen, F., *et al.* (1997). "Cell cycle-dependent protein expression of mammalian homologs of yeast DNA double-strand break repair genes Rad51 and Rad52." Mutation Research **384**(3): 205-211.
Chen, L., *et al.* (2008). "Cell cycle-dependent complex formation of BRCA1.CtIP.MRN is important for DNA double-strand break repair." The Journal of Biological Chemistry **283**(12): 7713-7720.
Chen, L., *et al.* (2001). "Promotion of Dnl4-catalyzed DNA end-joining by the Rad50/Mre11/Xrs2 and Hdf1/Hdf2 complexes." Molecular Cell **8**(5): 1105-1115.
Chen, X., *et al.* (2011). "Cell cycle regulation of DNA double-strand break end resection by Cdk1-dependent Dna2 phosphorylation." Nature Structural & Molecular Biology **18**(9): 1015-1019.
Chen, X. and A. E. Tomkinson (2011). "Yeast Nej1 is a key participant in the initial end binding and final ligation steps of nonhomologous end joining." The Journal of Biological Chemistry **286**(6): 4931-4940.
Cheng, Q., *et al.* (2011). "Ku counteracts mobilization of PARP1 and MRN in chromatin damaged with DNA double-strand breaks." Nucleic Acids Research.
Chenna, R., *et al.* (2003). "Multiple sequence alignment with the Clustal series of programs." Nucleic Acids Research **31**(13): 3497-3500.
Chisholm, R. L., *et al.* (2006). "dictyBase, the model organism database for Dictyostelium discoideum." Nucleic Acids Research **34**(Database issue): D423-427.
Ciccia, A. and S. J. Elledge (2010). "The DNA damage response: making it safe to play with knives." Molecular Cell **40**(2): 179-204.
Citarelli, M., *et al.* (2010). "Evolutionary history of the poly(ADP-ribose) polymerase gene family in eukaryotes." BMC Evolutionary Biology **10**: 308.
Clements, P. M., *et al.* (2004). "The ataxia-oculomotor apraxia 1 gene product has a role distinct from ATM and interacts with the DNA strand break repair proteins XRCC1 and XRCC4." DNA Repair **3**(11): 1493-1502.
Clerici, M., *et al.* (2008). "The Yku70-Yku80 complex contributes to regulate double-strand break processing and checkpoint activation during the cell cycle." EMBO Reports **9**(8): 810-818.
Clikeman, J. A., *et al.* (2001). "Homologous recombinational repair of double-strand breaks in yeast is enhanced by MAT heterozygosity through yKU-dependent and -independent mechanisms." Genetics **157**(2): 579-589.
Combet, C., *et al.* (2000). "NPS@: network protein sequence analysis." Trends in Biochemical Sciences **25**(3): 147-150.
Corpet, F. (1988). "Multiple sequence alignment with hierarchical clustering." Nucleic Acids Research **16**(22): 10881-10890.
Cotter, D. A. and K. B. Raper (1966). "Spore germination in *Dictyostelium discoideum*." Proceedings of the National Academy of Sciences of the United States of America **56**(3): 880-887.
D'Amours, D., *et al.* (1999). "Poly(ADP-ribosyl)ation reactions in the regulation of nuclear functions." The Biochemical Journal **342 (Pt 2)**: 249-268.
D'Amours, D., *et al.* (2001). "Gain-of-function of poly(ADP-ribose) polymerase-1 upon cleavage by apoptotic proteases: implications for apoptosis." Journal of Cell Science **114**(Pt 20): 3771-3778.
Dantzer, F., *et al.* (2006). "Poly(ADP-ribose) polymerase-1 activation during DNA damage and repair." Methods in Enzymology **409**: 493-510.

Dantzer, F., *et al.* (2000). "Base excision repair is impaired in mammalian cells lacking Poly(ADP-ribose) polymerase-1." Biochemistry **39**(25): 7559-7569.
De Bont, R. and N. van Larebeke (2004). "Endogenous DNA damage in humans: a review of quantitative data." Mutagenesis **19**(3): 169-185.
de Murcia, J. M., *et al.* (1997). "Requirement of poly(ADP-ribose) polymerase in recovery from DNA damage in mice and in cells." Proceedings of the National Academy of Sciences of the United States of America **94**(14): 7303-7307.
Deering, R. A. (1988). "DNA repair in *Dictyostelium*." Developmental Genetics **9**(4-5): 483-493.
Deering, R. A. (1994). "*Dictyostelium discoideum*, a lower eukaryote model for the study of DNA repair: implications for the role of DNA-damaging chemicals in the evolution of repair proficient cells." Advances in space research : the official journal of the Committee on Space Research **14**(10): 389-393.
Deering, R. A., *et al.* (1996). "Some repair-deficient mutants of *Dictyostelium discoideum* display enhanced susceptibilities to bleomycin." Antimicrobial Agents and Chemotherapy **40**(2): 464-467.
DeFazio, L. G., *et al.* (2002). "Synapsis of DNA ends by DNA-dependent protein kinase." The EMBO Journal **21**(12): 3192-3200.
Dianov, G. L. and J. L. Parsons (2007). "Co-ordination of DNA single strand break repair." DNA Repair (Amst) **6**(4): 454-460.
Dianov, G. L., *et al.* (1999). "Role of DNA polymerase beta in the excision step of long patch mammalian base excision repair." The Journal of Biological Chemistry **274**(20): 13741-13743.
DiBiase, S. J., *et al.* (2000). "DNA-dependent protein kinase stimulates an independently active, nonhomologous, end-joining apparatus." Cancer Research **60**(5): 1245-1253.
Dinkelmann, M., *et al.* (2009). "Multiple functions of MRN in end-joining pathways during isotype class switching." Nature Structural & Molecular Biology **16**(8): 808-813.
Dobbs, T. A., *et al.* (2010). "A structural model for regulation of NHEJ by DNA-PKcs autophosphorylation." DNA Repair (Amst) **9**(12): 1307-1314.
Dominguez-Bendala, J., *et al.* (2003). "Elevated expression of exogenous Rad51 leads to identical increases in gene-targeting frequency in murine embryonic stem (ES) cells with both functional and dysfunctional p53 genes." Experimental Cell Research **286**(2): 298-307.
Dong, F., *et al.* (2010). "Activation of PARP-1 in response to bleomycin depends on the Ku antigen and protein phosphatase 5." Oncogene **29**(14): 2093-2103.
Dore, A. S., *et al.* (2004). "Identification of DNA-PK in the arthropods. Evidence for the ancient ancestry of vertebrate non-homologous end-joining." DNA Repair **3**(1): 33-41.
Dou, H., *et al.* (2003). "Repair of oxidized bases in DNA bubble structures by human DNA glycosylases NEIL1 and NEIL2." The Journal of Biological Chemistry **278**(50): 49679-49684.
Drouet, J., *et al.* (2005). "DNA-dependent protein kinase and XRCC4-DNA ligase IV mobilization in the cell in response to DNA double strand breaks." The Journal of Biological Chemistry **280**(8): 7060-7069.
Dupaigne, P., *et al.* (2008). "The Srs2 helicase activity is stimulated by Rad51 filaments on dsDNA: implications for crossover incidence during mitotic recombination." Molecular Cell **29**(2): 243-254.

Egelhoff, T. T., *et al.* (1989). "Hygromycin resistance as a selectable marker in *Dictyostelium discoideum*." Molecular and Cellular Biology **9**(5): 1965-1968.
Eichinger, L., *et al.* (2005). "The genome of the social amoeba *Dictyostelium discoideum*." Nature **435**(7038): 43-57.
El-Khamisy, S. F., *et al.* (2003). "A requirement for PARP-1 for the assembly or stability of XRCC1 nuclear foci at sites of oxidative DNA damage." Nucleic Acids Research **31**(19): 5526-5533.
Esashi, F., *et al.* (2005). "CDK-dependent phosphorylation of BRCA2 as a regulatory mechanism for recombinational repair." Nature **434**(7033): 598-604.
Esashi, F., *et al.* (2007). "Stabilization of RAD51 nucleoprotein filaments by the C-terminal region of BRCA2." Nature Structural & Molecular Biology **14**(6): 468-474.
Eustermann, S., *et al.* (2010). "Solution structures of the two PBZ domains from human APLF and their interaction with poly(ADP-ribose)." Nature Structural & Molecular Biology **17**(2): 241-243.
Eustermann, S., *et al.* (2011). "The DNA-binding domain of human PARP-1 interacts with DNA single-strand breaks as a monomer through its second zinc finger." Journal of Molecular Biology **407**(1): 149-170.
Evans, M. D., *et al.* (2004). "Oxidative DNA damage and disease: induction, repair and significance." Mutation Research **567**(1): 1-61.
Fahrer, J., *et al.* (2007). "Quantitative analysis of the binding affinity of poly(ADP-ribose) to specific binding proteins as a function of chain length." Nucleic Acids Research **35**(21): e143.
Faix, J., *et al.* (2004). "A rapid and efficient method to generate multiple gene disruptions in *Dictyostelium discoideum* using a single selectable marker and the Cre-loxP system." Nucleic Acids Research **32**(19): e143.
Falck, J., *et al.* (2005). "Conserved modes of recruitment of ATM, ATR and DNA-PKcs to sites of DNA damage." Nature **434**(7033): 605-611.
Farmer, H., *et al.* (2005). "Targeting the DNA repair defect in BRCA mutant cells as a therapeutic strategy." Nature **434**(7035): 917-921.
Fattah, F., *et al.* (2010). "Ku regulates the non-homologous end joining pathway choice of DNA double-strand break repair in human somatic cells." PLoS Genetics **6**(2): e1000855.
Fekairi, S., *et al.* (2009). "Human SLX4 is a Holliday junction resolvase subunit that binds multiple DNA repair/recombination endonucleases." Cell **138**(1): 78-89.
Feng, Z., *et al.* (2011). "Rad52 inactivation is synthetically lethal with BRCA2 deficiency." Proceedings of the National Academy of Sciences of the United States of America **108**(2): 686-691.
Fiorentini, P., *et al.* (1997). "Exonuclease I of *Saccharomyces cerevisiae* functions in mitotic recombination in vivo and in vitro." Molecular and Cellular Biology **17**(5): 2764-2773.
Fisher, A. E., *et al.* (2007). "Poly(ADP-ribose) polymerase 1 accelerates single-strand break repair in concert with poly(ADP-ribose) glycohydrolase." Molecular and Cellular Biology **27**(15): 5597-5605.
Frank-Vaillant, M. and S. Marcand (2002). "Transient stability of DNA ends allows nonhomologous end joining to precede homologous recombination." Molecular Cell **10**(5): 1189-1199.
Freeland, T. M., *et al.* (1996). "Apurinic/apyrimidinic (AP) endonuclease from *Dictyostelium discoideum*: cloning, nucleotide sequence and induction by

sublethal levels of DNA damaging agents." Nucleic Acids Research **24**(10): 1950-1953.

Froelich-Ammon, S. J. and N. Osheroff (1995). "Topoisomerase poisons: harnessing the dark side of enzyme mechanism." The Journal of Biological Chemistry **270**(37): 21429-21432.

Frosina, G.*, et al.* (1996). "Two pathways for base excision repair in mammalian cells." The Journal of Biological Chemistry **271**(16): 9573-9578.

Fukushima, T.*, et al.* (2001). "Genetic analysis of the DNA-dependent protein kinase reveals an inhibitory role of Ku in late S-G2 phase DNA double-strand break repair." The Journal of Biological Chemistry **276**(48): 44413-44418.

Gagne, J. P.*, et al.* (2003). "A proteomic approach to the identification of heterogeneous nuclear ribonucleoproteins as a new family of poly(ADP-ribose)-binding proteins." The Biochemical Journal **371**(Pt 2): 331-340.

Gagne, J. P.*, et al.* (2008). "Proteome-wide identification of poly(ADP-ribose) binding proteins and poly(ADP-ribose)-associated protein complexes." Nucleic Acids Research **36**(22): 6959-6976.

Galande, S. and T. Kohwi-Shigematsu (1999). "Poly(ADP-ribose) polymerase and Ku autoantigen form a complex and synergistically bind to matrix attachment sequences." The Journal of Biological Chemistry **274**(29): 20521-20528.

Garcia, M. X.*, et al.* (2000). "Differential developmental expression and cell type specificity of *Dictyostelium* catalases and their response to oxidative stress and UV-light." Biochimica et biophysica acta **1492**(2-3): 295-310.

Gellert, M. (2002). "V(D)J recombination: RAG proteins, repair factors, and regulation." Annual Review of Biochemistry **71**: 101-132.

Goodarzi, A. A.*, et al.* (2008). "ATM signaling facilitates repair of DNA double-strand breaks associated with heterochromatin." Molecular Cell **31**(2): 167-177.

Goodarzi, A. A.*, et al.* (2006). "DNA-PK autophosphorylation facilitates Artemis endonuclease activity." The EMBO Journal **25**(16): 3880-3889.

Gradwohl, G.*, et al.* (1990). "The second zinc-finger domain of poly(ADP-ribose) polymerase determines specificity for single-stranded breaks in DNA." Proceedings of the National Academy of Sciences of the United States of America **87**(8): 2990-2994.

Gravel, S.*, et al.* (2008). "DNA helicases Sgs1 and BLM promote DNA double-strand break resection." Genes & Development **22**(20): 2767-2772.

Grawunder, U.*, et al.* (1997). "Activity of DNA ligase IV stimulated by complex formation with XRCC4 protein in mammalian cells." Nature **388**(6641): 492-495.

Grawunder, U.*, et al.* (1998). "DNA ligase IV is essential for V(D)J recombination and DNA double-strand break repair in human precursor lymphocytes." Molecular Cell **2**(4): 477-484.

Greene, D. M.*, et al.* (2011). "Targets downstream of Cdk8 in *Dictyostelium development*." BMC Developmental Biology **11**(1): 2.

Griffin, R. J.*, et al.* (1998). "Resistance-modifying agents. 5. Synthesis and biological properties of quinazolinone inhibitors of the DNA repair enzyme poly(ADP-ribose) polymerase (PARP)." Journal of Medicinal Chemistry **41**(26): 5247-5256.

Gu, J.*, et al.* (2007). "Single-stranded DNA ligation and XLF-stimulated incompatible DNA end ligation by the XRCC4-DNA ligase IV complex: influence of terminal DNA sequence." Nucleic Acids Research **35**(17): 5755-5762.

Guirouilh-Barbat, J., *et al.* (2007). "Defects in XRCC4 and KU80 differentially affect the joining of distal nonhomologous ends." Proceedings of the National Academy of Sciences of the United States of America **104**(52): 20902-20907.
Guyer, R. B., *et al.* (1986). "Uracil-DNA glycosylase activity from *Dictyostelium discoideum*." Biochimica et biophysica acta **868**(4): 262-264.
Haber, J. E. (1998). "Mating-type gene switching in *Saccharomyces cerevisiae*." Annual Review of Genetics **32**: 561-599.
Haenni, S. S., *et al.* (2008). "Identification of lysines 36 and 37 of PARP-2 as targets for acetylation and auto-ADP-ribosylation." The International Journal of Biochemistry & Cell Biology **40**(10): 2274-2283.
Haince, J. F., *et al.* (2008). "PARP1-dependent kinetics of recruitment of MRE11 and NBS1 proteins to multiple DNA damage sites." The Journal of Biological Chemistry **283**(2): 1197-1208.
Hakme, A., *et al.* (2008). "The expanding field of poly(ADP-ribosyl)ation reactions. 'Protein Modifications: Beyond the Usual Suspects' Review Series." EMBO Reports **9**(11): 1094-1100.
Hasegawa, Y., *et al.* (2005). "Analysis of Rad51 in the Social Amoeba *Dictyostelium Discoideum*: Sequence, Induction and Disruption." Microbes and Environments **20**(3): 186-189.
Hegde, M. L., *et al.* (2008). "Early steps in the DNA base excision/single-strand interruption repair pathway in mammalian cells." Cell Research **18**(1): 27-47.
Hegde, M. L., *et al.* (2010). "Functions of disordered regions in mammalian early base excision repair proteins." Cellular and Molecular Life Sciences **67**(21): 3573-3587.
Hegde, M. L., *et al.* (2008). "Physical and functional interaction between human oxidized base-specific DNA glycosylase NEIL1 and flap endonuclease 1." The Journal of Biological Chemistry **283**(40): 27028-27037.
Henrie, M. S., *et al.* (2003). "Lethality in PARP-1/Ku80 double mutant mice reveals physiological synergy during early embryogenesis." DNA Repair **2**(2): 151-158.
Heyer, W. D., *et al.* (2010). "Regulation of homologous recombination in eukaryotes." Annual Review of Genetics **44**: 113-139.
Hilario, J., *et al.* (2009). "Direct imaging of human Rad51 nucleoprotein dynamics on individual DNA molecules." Proceedings of the National Academy of Sciences of the United States of America **106**(2): 361-368.
Hiom, K. (2010). "Coping with DNA double strand breaks." DNA Repair (Amst) **9**(12): 1256-1263.
Hochegger, H., *et al.* (2006). "Parp-1 protects homologous recombination from interference by Ku and Ligase IV in vertebrate cells." The EMBO Journal **25**(6): 1305-1314.
Hoffmann, M. E. and R. Meneghini (1979). "Action of hydrogen peroxide on human fibroblast in culture." Photochemistry and Photobiology **30**(1): 151-155.
Holthausen, J. T., *et al.* (2010). "Regulation of DNA strand exchange in homologous recombination." DNA Repair (Amst) **9**(12): 1264-1272.
Hopfner, K. P., *et al.* (2002). "The Rad50 zinc-hook is a structure joining Mre11 complexes in DNA recombination and repair." Nature **418**(6897): 562-566.
Hottiger, M. O. (2011). "ADP-ribosylation of histones by ARTD1: an additional module of the histone code?" FEBS letters **585**(11): 1595-1599.
Hottiger, M. O., *et al.* (2010). "Toward a unified nomenclature for mammalian ADP-ribosyltransferases." Trends in Biochemical Sciences **35**(4): 208-219.

Hsu, D. W., *et al.* (2006). "DNA damage signaling and repair in *Dictyostelium discoideum*." Cell Cycle **5**(7): 702-708.
Hsu, D. W., *et al.* (2011). "DNA double-strand break repair pathway choice in *Dictyostelium*." Journal of Cell Science **124**(Pt 10): 1655-1663.
Huambachano, O., *et al.* (2011). "Double-stranded DNA binding domain of poly(ADP-ribose) polymerase-1 and molecular insight into the regulation of its activity." The Journal of Biological Chemistry **286**(9): 7149-7160.
Hudson, J. J., *et al.* (2005). "DNA-PKcs-dependent signaling of DNA damage in *Dictyostelium discoideum*." Current Biology **15**(20): 1880-1885.
Huertas, P. (2010). "DNA resection in eukaryotes: deciding how to fix the break." Nature Structural & Molecular Biology **17**(1): 11-16.
Huertas, P., *et al.* (2008). "CDK targets Sae2 to control DNA-end resection and homologous recombination." Nature **455**(7213): 689-692.
Huertas, P. and S. P. Jackson (2009). "Human CtIP mediates cell cycle control of DNA end resection and double strand break repair." The Journal of Biological Chemistry **284**(14): 9558-9565.
Huletsky, A., *et al.* (1989). "The effect of poly(ADP-ribosyl)ation on native and H1-depleted chromatin. A role of poly(ADP-ribosyl)ation on core nucleosome structure." The Journal of Biological Chemistry **264**(15): 8878-8886.
Hunter, S., *et al.* (2009). "InterPro: the integrative protein signature database." Nucleic Acids Research **37**(Database issue): D211-215.
Iiizumi, S., *et al.* (2008). "Impact of non-homologous end-joining deficiency on random and targeted DNA integration: implications for gene targeting." Nucleic Acids Research **36**(19): 6333-6342.
Ikeda, S., *et al.* (1998). "Purification and characterization of human NTH1, a homolog of Escherichia coli endonuclease III. Direct identification of Lys-212 as the active nucleophilic residue." The Journal of Biological Chemistry **273**(34): 21585-21593.
Ikejima, M., *et al.* (1990). "The zinc fingers of human poly(ADP-ribose) polymerase are differentially required for the recognition of DNA breaks and nicks and the consequent enzyme activation. Other structures recognize intact DNA." The Journal of Biological Chemistry **265**(35): 21907-21913.
Iles, N., *et al.* (2007). "APLF (C2orf13) is a novel human protein involved in the cellular response to chromosomal DNA strand breaks." Molecular and Cellular Biology **27**(10): 3793-3803.
Iliakis, G. (2009). "Backup pathways of NHEJ in cells of higher eukaryotes: cell cycle dependence." Radiotherapy and oncology : journal of the European Society for Therapeutic Radiology and Oncology **92**(3): 310-315.
Ip, S. C., *et al.* (2008). "Identification of Holliday junction resolvases from humans and yeast." Nature **456**(7220): 357-361.
Ira, G., *et al.* (2004). "DNA end resection, homologous recombination and DNA damage checkpoint activation require CDK1." Nature **431**(7011): 1011-1017.
Ishibashi, K., *et al.* (2006). "Nonhomologous chromosomal integration of foreign DNA is completely dependent on MUS-53 (human Lig4 homolog) in *Neurospora*." Proceedings of the National Academy of Sciences of the United States of America **103**(40): 14871-14876.
Ivanov, E. L. and J. E. Haber (1995). "RAD1 and RAD10, but not other excision repair genes, are required for double-strand break-induced recombination in *Saccharomyces cerevisiae*." Molecular and Cellular Biology **15**(4): 2245-2251.

Ivanov, E. L., *et al.* (1996). "Genetic requirements for the single-strand annealing pathway of double-strand break repair in *Saccharomyces cerevisiae*." Genetics **142**(3): 693-704.

Jackson, A. L. and L. A. Loeb (2001). "The contribution of endogenous sources of DNA damage to the multiple mutations in cancer." Mutation Research **477**(1-2): 7-21.

Jackson, S. P. and J. Bartek (2009). "The DNA-damage response in human biology and disease." Nature **461**(7267): 1071-1078.

Jazayeri, A., *et al.* (2006). "ATM- and cell cycle-dependent regulation of ATR in response to DNA double-strand breaks." Nature Cell Biology **8**(1): 37-45.

Jeggo, P. A., *et al.* (2011). "The role of homologous recombination in radiation-induced double-strand break repair." Radiotherapy and oncology : journal of the European Society for Therapeutic Radiology and Oncology.

Jensen, R. B., *et al.* (2010). "Purified human BRCA2 stimulates RAD51-mediated recombination." Nature **467**(7316): 678-683.

Johnson, R. D. and M. Jasin (2000). "Sister chromatid gene conversion is a prominent double-strand break repair pathway in mammalian cells." The EMBO Journal **19**(13): 3398-3407.

Johnson, R. D., *et al.* (1999). "Mammalian XRCC2 promotes the repair of DNA double-strand breaks by homologous recombination." Nature **401**(6751): 397-399.

Johnson, R. E., *et al.* (1998). "Identification of APN2, the *Saccharomyces cerevisiae* homolog of the major human AP endonuclease HAP1, and its role in the repair of abasic sites." Genes & Development **12**(19): 3137-3143.

Jorgensen, T. J., *et al.* (2009). "Binding kinetics and activity of human poly(ADP-ribose) polymerase-1 on oligo-deoxyribonucleotide substrates." Journal of Molecular Recognition.

Kadyk, L. C. and L. H. Hartwell (1992). "Sister chromatids are preferred over homologs as substrates for recombinational repair in *Saccharomyces cerevisiae*." Genetics **132**(2): 387-402.

Kanai, M., *et al.* (2007). "Inhibition of Crm1-p53 interaction and nuclear export of p53 by poly(ADP-ribosyl)ation." Nature Cell Biology **9**(10): 1175-1183.

Kanno, S., *et al.* (2007). "A novel human AP endonuclease with conserved zinc-finger-like motifs involved in DNA strand break responses." The EMBO Journal **26**(8): 2094-2103.

Karimi-Busheri, F., *et al.* (1999). "Molecular characterization of a human DNA kinase." The Journal of Biological Chemistry **274**(34): 24187-24194.

Karras, G. I., *et al.* (2005). "The macro domain is an ADP-ribose binding module." The EMBO Journal **24**(11): 1911-1920.

Keeney, S., *et al.* (1997). "Meiosis-specific DNA double-strand breaks are catalyzed by Spo11, a member of a widely conserved protein family." Cell **88**(3): 375-384.

Khanna, K. K. and S. P. Jackson (2001). "DNA double-strand breaks: signaling, repair and the cancer connection." Nature Genetics **27**(3): 247-254.

Khodyreva, S. N., *et al.* (2010). "Apurinic/apyrimidinic (AP) site recognition by the 5'-dRP/AP lyase in poly(ADP-ribose) polymerase-1 (PARP-1)." Proceedings of the National Academy of Sciences of the United States of America **107**(51): 22090-22095.

Kim, J. S., *et al.* (2005). "Independent and sequential recruitment of NHEJ and HR factors to DNA damage sites in mammalian cells." The Journal of Cell Biology **170**(3): 341-347.

Kleine, H. and B. Luscher (2009). "Learning how to read ADP-ribosylation." Cell **139**(1): 17-19.

Klungland, A. and T. Lindahl (1997). "Second pathway for completion of human DNA base excision-repair: reconstitution with purified proteins and requirement for DNase IV (FEN1)." The EMBO Journal **16**(11): 3341-3348.

Kofler, B., *et al.* (1993). "Purification and characterization of NAD+:ADP-ribosyltransferase (polymerizing) from *Dictyostelium discoideum*." The Biochemical Journal **293 (Pt 1)**: 275-281.

Koh, D. W., *et al.* (2005). "The road to survival goes through PARG." Cell cycle **4**(3): 397-399.

Kooistra, R., *et al.* (2004). "Efficient gene targeting in *Kluyveromyces lactis*." Yeast **21**(9): 781-792.

Kothe, G. O., *et al.* (2010). "PARP is involved in replicative aging in *Neurospora crassa*." Fungal Genetics and Biology **47**(4): 297-309.

Koy, J. F., *et al.* (1995). "Genetic changes and bioassays in bleomycin- and phleomycin-treated cells, and their relationship to chromosomal breaks." Mutation Research **336**(1): 19-27.

Krishnakumar, R. and W. L. Kraus (2010). "The PARP side of the nucleus: molecular actions, physiological outcomes, and clinical targets." Molecular Cell **39**(1): 8-24.

Kubota, Y., *et al.* (1996). "Reconstitution of DNA base excision-repair with purified human proteins: interaction between DNA polymerase beta and the XRCC1 protein." The EMBO Journal **15**(23): 6662-6670.

Kurimasa, A., *et al.* (1999). "Requirement for the kinase activity of human DNA-dependent protein kinase catalytic subunit in DNA strand break rejoining." Molecular and Cellular Biology **19**(5): 3877-3884.

Kuspa, A. and W. F. Loomis (1992). "Tagging developmental genes in *Dictyostelium* by restriction enzyme-mediated integration of plasmid DNA." Proceedings of the National Academy of Sciences of the United States of America **89**(18): 8803-8807.

Kuwayama, H., *et al.* (2000). "A novel role of differentiation-inducing factor-1 in *Dictyostelium* development, assessed by the restoration of a developmental defect in a mutant lacking mitogen-activated protein kinase ERK2." Development Growth & Differentiation **42**(5): 531-538.

Kuzminov, A. (2001). "Single-strand interruptions in replicating chromosomes cause double-strand breaks." Proceedings of the National Academy of Sciences of the United States of America **98**(15): 8241-8246.

Lan, L., *et al.* (2004). "In situ analysis of repair processes for oxidative DNA damage in mammalian cells." Proceedings of the National Academy of Sciences of the United States of America **101**(38): 13738-13743.

Langelier, M. F., *et al.* (2011). "Crystal structures of poly(ADP-ribose) polymerase-1 (PARP-1) zinc fingers bound to DNA: structural and functional insights into DNA-dependent PARP-1 activity." The Journal of Biological Chemistry.

Langelier, M. F., *et al.* (2010). "The Zn3 domain of human poly(ADP-ribose) polymerase-1 (PARP-1) functions in both DNA-dependent poly(ADP-ribose) synthesis activity and chromatin compaction." The Journal of Biological Chemistry **285**(24): 18877-18887.

Langelier, M. F., *et al.* (2008). "A third zinc-binding domain of human poly(ADP-ribose) polymerase-1 coordinates DNA-dependent enzyme activation." The Journal of Biological Chemistry **283**(7): 4105-4114.

Lavrik, O. I., *et al.* (2001). "Photoaffinity labeling of mouse fibroblast enzymes by a base excision repair intermediate. Evidence for the role of poly(ADP-ribose) polymerase-1 in DNA repair." The Journal of Biological Chemistry **276**(27): 25541-25548.

Lee-Theilen, M., *et al.* (2011). "CtIP promotes microhomology-mediated alternative end joining during class-switch recombination." Nature Structural & Molecular Biology **18**(1): 75-79.

Lee, K. and S. E. Lee (2007). "*Saccharomyces cerevisiae* Sae2- and Tel1-dependent single-strand DNA formation at DNA break promotes microhomology-mediated end joining." Genetics **176**(4): 2003-2014.

Lee, S. E., *et al.* (1997). "Evidence for DNA-PK-dependent and -independent DNA double-strand break repair pathways in mammalian cells as a function of the cell cycle." Molecular and Cellular Biology **17**(3): 1425-1433.

Lee, S. E., *et al.* (1998). "*Saccharomyces* Ku70, mre11/rad50 and RPA proteins regulate adaptation to G2/M arrest after DNA damage." Cell **94**(3): 399-409.

Lee, S. K., *et al.* (1998). "A mutation in *repB*, the *dictyostelium homolog* of the human Xeroderma Pigmentosum B gene, has increased sensitivity to UV-light but normal morphogenesis." Biochimica et biophysica acta **1399**(2-3): 161-172.

Lee, S. K., *et al.* (1997). "Differential developmental expression of the *rep B* and *rep D* Xeroderma Pigmentosum related DNA helicase genes from *Dictyostelium discoideum*." Nucleic Acids Research **25**(12): 2365-2374.

Lehman, J. A., *et al.* (2008). "DNA-dependent conformational changes in the Ku heterodimer." Biochemistry **47**(15): 4359-4368.

Leppard, J. B., *et al.* (2003). "Physical and functional interaction between DNA ligase IIIalpha and poly(ADP-Ribose) polymerase 1 in DNA single-strand break repair." Molecular and Cellular Biology **23**(16): 5919-5927.

Levin, D. S., *et al.* (2000). "Interaction between PCNA and DNA ligase I is critical for joining of Okazaki fragments and long-patch base-excision repair." Current Biology **10**(15): 919-922.

Li, B., *et al.* (2004). "Identification and biochemical characterization of a Werner's syndrome protein complex with Ku70/80 and poly(ADP-ribose) polymerase-1." The Journal of Biological Chemistry **279**(14): 13659-13667.

Li, F., *et al.* (2008). "Microarray-based genetic screen defines SAW1, a gene required for Rad1/Rad10-dependent processing of recombination intermediates." Molecular Cell **30**(3): 325-335.

Li, G., *et al.* (2000). "Molecular basis for resistance to the anticancer drug cisplatin in *Dictyostelium*." Microbiology **146 (Pt 9)**: 2219-2227.

Li, G. Y., *et al.* (2010). "Structure and identification of ADP-ribose recognition motifs of APLF and role in the DNA damage response." Proceedings of the National Academy of Sciences of the United States of America **107**(20): 9129-9134.

Li, S., *et al.* (2011). "PALF Acts as both a single-stranded DNA endonuclease and a single-stranded DNA 3'-exonuclease and can participate in DNA end joining in a biochemical system." The Journal of Biological Chemistry.

Li, X. and W. D. Heyer (2009). "RAD54 controls access to the invading 3'-OH end after RAD51-mediated DNA strand invasion in homologous recombination in *Saccharomyces cerevisiae*." Nucleic Acids Research **37**(2): 638-646.

Li, X., *et al.* (2009). "PCNA is required for initiation of recombination-associated DNA synthesis by DNA polymerase delta." Molecular Cell **36**(4): 704-713.
Li, Z., *et al.* (1995). "The XRCC4 gene encodes a novel protein involved in DNA double-strand break repair and V(D)J recombination." Cell **83**(7): 1079-1089.
Liang, F., *et al.* (1998). "Homology-directed repair is a major double-strand break repair pathway in mammalian cells." Proceedings of the National Academy of Sciences of the United States of America **95**(9): 5172-5177.
Liang, F. and M. Jasin (1995). "Studies on the influence of cytosine methylation on DNA recombination and end-joining in mammalian cells." The Journal of Biological Chemistry **270**(40): 23838-23844.
Liang, F. and M. Jasin (1996). "Ku80-deficient cells exhibit excess degradation of extrachromosomal DNA." The Journal of Biological Chemistry **271**(24): 14405-14411.
Lieber, M. R. (2010). "The mechanism of double-strand DNA break repair by the nonhomologous DNA end-joining pathway." Annual Review of Biochemistry **79**: 181-211.
Lim, C. J., *et al.* (2001). "RasC is required for optimal activation of adenylyl cyclase and Akt/PKB during aggregation." The EMBO Journal **20**(16): 4490-4499.
Lim, D. S. and P. Hasty (1996). "A mutation in mouse *rad51* results in an early embryonic lethal that is suppressed by a mutation in *p53*." Molecular and Cellular Biology **16**(12): 7133-7143.
Limbo, O., *et al.* (2007). "Ctp1 is a cell-cycle-regulated protein that functions with Mre11 complex to control double-strand break repair by homologous recombination." Molecular Cell **28**(1): 134-146.
Lin, H. H., *et al.* (2004). "A homologue of Cdk8 is required for spore cell differentiation in *Dictyostelium*." Developmental Biology **271**(1): 49-58.
Lindahl, T. (1993). "Instability and decay of the primary structure of DNA." Nature **362**(6422): 709-715.
Liu, J., *et al.* (2010). "Human BRCA2 protein promotes RAD51 filament formation on RPA-covered single-stranded DNA." Nature Structural & Molecular Biology **17**(10): 1260-1262.
Llorente, B. and L. S. Symington (2004). "The Mre11 nuclease is not required for 5' to 3' resection at multiple HO-induced double-strand breaks." Molecular and Cellular Biology **24**(21): 9682-9694.
Lobrich, M., *et al.* (2010). "gammaH2AX foci analysis for monitoring DNA double-strand break repair: strengths, limitations and optimization." Cell cycle **9**(4): 662-669.
Longhese, M. P., *et al.* (2010). "Mechanisms and regulation of DNA end resection." The EMBO Journal **29**(17): 2864-2874.
Loseva, O., *et al.* (2010). "PARP-3 is a mono-ADP-ribosylase that activates PARP-1 in the absence of DNA." The Journal of Biological Chemistry **285**(11): 8054-8060.
Lundin, C., *et al.* (2005). "Methyl methanesulfonate (MMS) produces heat-labile DNA damage but no detectable in vivo DNA double-strand breaks." Nucleic Acids Research **33**(12): 3799-3811.
Ma, J. L., *et al.* (2003). "Yeast Mre11 and Rad1 proteins define a Ku-independent mechanism to repair double-strand breaks lacking overlapping end sequences." Molecular and Cellular Biology **23**(23): 8820-8828.

Ma, Y., *et al.* (2005). "Repair of double-strand DNA breaks by the human nonhomologous DNA end joining pathway: the iterative processing model." Cell cycle **4**(9): 1193-1200.
Ma, Y., *et al.* (2004). "A biochemically defined system for mammalian nonhomologous DNA end joining." Molecular Cell **16**(5): 701-713.
Ma, Y., *et al.* (2002). "Hairpin opening and overhang processing by an Artemis/DNA-dependent protein kinase complex in nonhomologous end joining and V(D)J recombination." Cell **108**(6): 781-794.
Ma, Y., *et al.* (2005). "The Artemis:DNA-PKcs endonuclease cleaves DNA loops, flaps, and gaps." DNA repair **4**(7): 845-851.
MacWilliams, H., *et al.* (2006). "A retinoblastoma ortholog controls stalk/spore preference in *Dictyostelium*." Development **133**(7): 1287-1297.
Maeda, M., *et al.* (1996). "Seven helix chemoattractant receptors transiently stimulate mitogen-activated protein kinase in *Dictyostelium*. Role of heterotrimeric G proteins." The Journal of Biological Chemistry **271**(7): 3351-3354.
Maeda, M. and H. Kuwayama (2000). "A diffusible factor involved in MAP-kinase ERK2-regulated development of *Dictyostelium*." Development Growth & Differentiation **42**(3): 275-284.
Mani, R. S., *et al.* (2007). "XRCC1 stimulates polynucleotide kinase by enhancing its damage discrimination and displacement from DNA repair intermediates." The Journal of Biological Chemistry **282**(38): 28004-28013.
Mansour, W. Y., *et al.* (2010). "The alternative end-joining pathway for repair of DNA double-strand breaks requires PARP1 but is not dependent upon microhomologies." Nucleic Acids Research **38**(18): 6065-6077.
Manstein, D. J., *et al.* (1995). "Cloning vectors for the production of proteins in *Dictyostelium discoideum*." Gene **162**(1): 129-134.
Mao, Z., *et al.* (2008). "Comparison of nonhomologous end joining and homologous recombination in human cells." DNA Repair **7**(10): 1765-1771.
Mao, Z., *et al.* (2008). "DNA repair by nonhomologous end joining and homologous recombination during cell cycle in human cells." Cell cycle **7**(18): 2902-2906.
Mari, P. O., *et al.* (2006). "Dynamic assembly of end-joining complexes requires interaction between Ku70/80 and XRCC4." Proceedings of the National Academy of Sciences of the United States of America **103**(49): 18597-18602.
Marsischky, G. T., *et al.* (1995). "Role of glutamic acid 988 of human poly-ADP-ribose polymerase in polymer formation. Evidence for active site similarities to the ADP-ribosylating toxins." The Journal of Biological Chemistry **270**(7): 3247-3254.
Masson, M., *et al.* (1998). "XRCC1 is specifically associated with poly(ADP-ribose) polymerase and negatively regulates its activity following DNA damage." Molecular and Cellular Biology **18**(6): 3563-3571.
Masutani, M., *et al.* (1999). "Function of poly(ADP-ribose) polymerase in response to DNA damage: gene-disruption study in mice." Molecular and Cellular Biochemistry **193**(1-2): 149-152.
Mazina, O. M. and A. V. Mazin (2004). "Human Rad54 protein stimulates DNA strand exchange activity of hRad51 protein in the presence of Ca2+." The Journal of Biological Chemistry **279**(50): 52042-52051.
McBlane, J. F., *et al.* (1995). "Cleavage at a V(D)J recombination signal requires only RAG1 and RAG2 proteins and occurs in two steps." Cell **83**(3): 387-395.

McIlwraith, M. J., *et al.* (2005). "Human DNA polymerase eta promotes DNA synthesis from strand invasion intermediates of homologous recombination." Molecular Cell **20**(5): 783-792.

McIlwraith, M. J. and S. C. West (2008). "DNA repair synthesis facilitates RAD52-mediated second-end capture during DSB repair." Molecular Cell **29**(4): 510-516.

Meek, K., *et al.* (2007). "trans Autophosphorylation at DNA-dependent protein kinase's two major autophosphorylation site clusters facilitates end processing but not end joining." Molecular and Cellular Biology **27**(10): 3881-3890.

Meima, M. and P. Schaap (1999). "*Dictyostelium development* - socializing through cAMP." Seminars in Cell & Developmental Biology **10**(6): 567-576.

Mello Filho, A. C. and R. Meneghini (1984). "*In vivo* formation of single-strand breaks in DNA by hydrogen peroxide is mediated by the Haber-Weiss reaction." Biochimica et biophysica acta **781**(1-2): 56-63.

Mendoza-Alvarez, H. and R. Alvarez-Gonzalez (1993). "Poly(ADP-ribose) polymerase is a catalytic dimer and the automodification reaction is intermolecular." The Journal of Biological Chemistry **268**(30): 22575-22580.

Menissier de Murcia, J., *et al.* (2003). "Functional interaction between PARP-1 and PARP-2 in chromosome stability and embryonic development in mouse." The EMBO Journal **22**(9): 2255-2263.

Messner, S., *et al.* (2010). "PARP1 ADP-ribosylates lysine residues of the core histone tails." Nucleic Acids Research **38**(19): 6350-6362.

Meyer-Ficca, M. L., *et al.* (2004). "Human poly(ADP-ribose) glycohydrolase is expressed in alternative splice variants yielding isoforms that localize to different cell compartments." Experimental Cell Research **297**(2): 521-532.

Mimitou, E. P. and L. S. Symington (2008). "Sae2, Exo1 and Sgs1 collaborate in DNA double-strand break processing." Nature **455**(7214): 770-774.

Mimitou, E. P. and L. S. Symington (2010). "Ku prevents Exo1 and Sgs1-dependent resection of DNA ends in the absence of a functional MRX complex or Sae2." The EMBO Journal **29**(19): 3358-3369.

Mitchel, K., *et al.* (2010). "Molecular structures of crossover and noncrossover intermediates during gap repair in yeast: implications for recombination." Molecular Cell **38**(2): 211-222.

Mitchell, J. R., *et al.* (2003). "Divide and conquer: nucleotide excision repair battles cancer and ageing." Current Opinion in Cell Biology **15**(2): 232-240.

Miwa, M., *et al.* (1999). "Functional analysis of poly(ADP-ribose) polymerase in *Drosophila melanogaster*." Molecular and Cellular Biochemistry **193**(1-2): 103-107.

Mladenov, E. and G. Iliakis (2011). "Induction and repair of DNA double strand breaks: the increasing spectrum of non-homologous end joining pathways." Mutation Research **711**(1-2): 61-72.

Mohapatra, S., *et al.* (2011). "Restoration of G1 chemo/radioresistance and double-strand-break repair proficiency by wild-type but not endonuclease-deficient Artemis." Nucleic Acids Research **39**(15): 6500-6510.

Mortusewicz, O., *et al.* (2007). "Feedback-regulated poly(ADP-ribosyl)ation by PARP-1 is required for rapid response to DNA damage in living cells." Nucleic Acids Research **35**(22): 7665-7675.

Moshous, D., *et al.* (2001). "Artemis, a novel DNA double-strand break repair/V(D)J recombination protein, is mutated in human severe combined immune deficiency." Cell **105**(2): 177-186.

Moynahan, M. E. and M. Jasin (2010). "Mitotic homologous recombination maintains genomic stability and suppresses tumorigenesis." Nature Reviews Molecular Cell Biology **11**(3): 196-207.

Munoz, I. M.*, et al.* (2009). "Coordination of structure-specific nucleases by human SLX4/BTBD12 is required for DNA repair." Molecular Cell **35**(1): 116-127.

Muramatsu, M.*, et al.* (2000). "Class switch recombination and hypermutation require activation-induced cytidine deaminase (AID), a potential RNA editing enzyme." Cell **102**(5): 553-563.

Muramoto, T. and J. R. Chubb (2008). "Live imaging of the *Dictyostelium* cell cycle reveals widespread S phase during development, a G2 bias in spore differentiation and a premitotic checkpoint." Development **135**(9): 1647-1657.

Nick McElhinny, S. A.*, et al.* (2000). "Ku recruits the XRCC4-ligase IV complex to DNA ends." Molecular and Cellular Biology **20**(9): 2996-3003.

Nicolette, M. L.*, et al.* (2010). "Mre11-Rad50-Xrs2 and Sae2 promote 5' strand resection of DNA double-strand breaks." Nature Structural & Molecular Biology **17**(12): 1478-1485.

Nilsen, H.*, et al.* (2000). "Uracil-DNA glycosylase (UNG)-deficient mice reveal a primary role of the enzyme during DNA replication." Molecular Cell **5**(6): 1059-1065.

Nimonkar, A. V.*, et al.* (2009). "Rad52 promotes second-end DNA capture in double-stranded break repair to form complement-stabilized joint molecules." Proceedings of the National Academy of Sciences of the United States of America **106**(9): 3077-3082.

Ninomiya, Y.*, et al.* (2004). "Highly efficient gene replacements in *Neurospora* strains deficient for nonhomologous end-joining." Proceedings of the National Academy of Sciences of the United States of America **101**(33): 12248-12253.

Ogata, N.*, et al.* (1981). "Poly(ADP-ribose) synthetase, a main acceptor of poly(ADP-ribose) in isolated nuclei." The Journal of Biological Chemistry **256**(9): 4135-4137.

Ogawa, S.*, et al.* (2000). "The mitochondrial DNA of *Dictyostelium discoideum*: complete sequence, gene content and genome organization." Molecular & General Genetics **263**(3): 514-519.

Oka, S.*, et al.* (2006). "Identification and characterization of a mammalian 39-kDa poly(ADP-ribose) glycohydrolase." The Journal of Biological Chemistry **281**(2): 705-713.

Okano, S.*, et al.* (2003). "Spatial and temporal cellular responses to single-strand breaks in human cells." Molecular and Cellular Biology **23**(11): 3974-3981.

Oliver, A. W.*, et al.* (2004). "Crystal structure of the catalytic fragment of murine poly(ADP-ribose) polymerase-2." Nucleic Acids Research **32**(2): 456-464.

Ooi, S. L.*, et al.* (2001). "A DNA microarray-based genetic screen for nonhomologous end-joining mutants in *Saccharomyces cerevisiae*." Science **294**(5551): 2552-2556.

Otterlei, M.*, et al.* (1999). "Post-replicative base excision repair in replication foci." The EMBO Journal **18**(13): 3834-3844.

Otto, H.*, et al.* (2005). "In silico characterization of the family of PARP-like poly(ADP-ribosyl)transferases (pARTs)." BMC Genomics **6**: 139.

Pace, P.*, et al.* (2010). "Ku70 corrupts DNA Repair in the Absence of the Fanconi Anemia Pathway." Science.

Parsons, J. L., *et al.* (2005). "Poly(ADP-ribose) polymerase-1 protects excessive DNA strand breaks from deterioration during repair in human cell extracts." The FEBS Journal **272**(8): 2012-2021.

Parsons, J. L., *et al.* (2004). "APE1 is the major 3'-phosphoglycolate activity in human cell extracts." Nucleic Acids Research **32**(12): 3531-3536.

Pascucci, B., *et al.* (1999). "Long patch base excision repair with purified human proteins. DNA ligase I as patch size mediator for DNA polymerases delta and epsilon." The Journal of Biological Chemistry **274**(47): 33696-33702.

Patel, A. G., *et al.* (2011). "Nonhomologous end joining drives poly(ADP-ribose) polymerase (PARP) inhibitor lethality in homologous recombination-deficient cells." Proceedings of the National Academy of Sciences of the United States of America **108**(8): 3406-3411.

Peterson, S. E., *et al.* (2011). "Cdk1 uncouples CtIP-dependent resection and Rad51 filament formation during M-phase double-strand break repair." The Journal of Cell Biology **194**(5): 705-720.

Petukhova, G., *et al.* (1998). "Catalysis of homologous DNA pairing by yeast Rad51 and Rad54 proteins." Nature **393**(6680): 91-94.

Pierce, A. J., *et al.* (2001). "Ku DNA end-binding protein modulates homologous repair of double-strand breaks in mammalian cells." Genes & Development **15**(24): 3237-3242.

Pierce, A. J., *et al.* (1999). "XRCC3 promotes homology-directed repair of DNA damage in mammalian cells." Genes & Development **13**(20): 2633-2638.

Pleschke, J. M., *et al.* (2000). "Poly(ADP-ribose) binds to specific domains in DNA damage checkpoint proteins." The Journal of Biological Chemistry **275**(52): 40974-40980.

Poirier, G. G., *et al.* (1982). "Poly(ADP-ribosyl)ation of polynucleosomes causes relaxation of chromatin structure." Proceedings of the National Academy of Sciences of the United States of America **79**(11): 3423-3427.

Polo, S. E. and S. P. Jackson (2011). "Dynamics of DNA damage response proteins at DNA breaks: a focus on protein modifications." Genes & Development **25**(5): 409-433.

Povirk, L. F., *et al.* (1979). "Binding of bleomycin to DNA: intercalation of the bithiazole rings." Biochemistry **18**(1): 96-101.

Povirk, L. F., *et al.* (2007). "Processing of 3'-phosphoglycolate-terminated DNA double strand breaks by Artemis nuclease." The Journal of Biological Chemistry **282**(6): 3547-3558.

Prasad, R., *et al.* (2001). "DNA polymerase beta -mediated long patch base excision repair. Poly(ADP-ribose)polymerase-1 stimulates strand displacement DNA synthesis." The Journal of Biological Chemistry **276**(35): 32411-32414.

Prasad, R., *et al.* (2010). "Substrate channeling in mammalian base excision repair pathways: passing the baton." The Journal of Biological Chemistry **285**(52): 40479-40488.

Qiu, J., *et al.* (1999). "Human exonuclease 1 functionally complements its yeast homologues in DNA recombination, RNA primer removal, and mutation avoidance." The Journal of Biological Chemistry **274**(25): 17893-17900.

Rajawat, J., *et al.* (2007). "Effect of oxidative stress and involvement of poly(ADP-ribose) polymerase (PARP) in *Dictyostelium discoideum* development." The FEBS Journal **274**(21): 5611-5618.

Rass, E., *et al.* (2009). "Role of Mre11 in chromosomal nonhomologous end joining in mammalian cells." Nature Structural & Molecular Biology **16**(8): 819-824.

Rass, U., *et al.* (2010). "Mechanism of Holliday junction resolution by the human GEN1 protein." Genes & Development **24**(14): 1559-1569.
Riballo, E., *et al.* (2004). "A pathway of double-strand break rejoining dependent upon ATM, Artemis, and proteins locating to gamma-H2AX foci." Molecular Cell **16**(5): 715-724.
Riballo, E., *et al.* (2009). "XLF-Cernunnos promotes DNA ligase IV-XRCC4 re-adenylation following ligation." Nucleic Acids Research **37**(2): 482-492.
Rickwood, D. and M. S. Osman (1979). "Characterisation of poly(ADP-Rib) polymerase activity in nuclei from the slime mould *Dictyostelium discoideum*." Molecular and Cellular Biochemistry **27**(2): 79-84.
Rijkers, T., *et al.* (1998). "Targeted inactivation of mouse RAD52 reduces homologous recombination but not resistance to ionizing radiation." Molecular and Cellular Biology **18**(11): 6423-6429.
Rivera-Calzada, A., *et al.* (2007). "Structural model of full-length human Ku70-Ku80 heterodimer and its recognition of DNA and DNA-PKcs." EMBO Reports **8**(1): 56-62.
Roberts, S. A., *et al.* (2010). "Ku is a 5'-dRP/AP lyase that excises nucleotide damage near broken ends." Nature **464**(7292): 1214-1217.
Robertson, A. B., *et al.* (2009). "DNA repair in mammalian cells: Base excision repair: the long and short of it." Cellular and Molecular Life Sciences **66**(6): 981-993.
Rogakou, E. P., *et al.* (1998). "DNA double-stranded breaks induce histone H2AX phosphorylation on serine 139." The Journal of Biological Chemistry **273**(10): 5858-5868.
Rolli, V., *et al.* (1997). "Random mutagenesis of the poly(ADP-ribose) polymerase catalytic domain reveals amino acids involved in polymer branching." Biochemistry **36**(40): 12147-12154.
Rosidi, B., *et al.* (2008). "Histone H1 functions as a stimulatory factor in backup pathways of NHEJ." Nucleic Acids Research **36**(5): 1610-1623.
Rothkamm, K., *et al.* (2003). "Pathways of DNA double-strand break repair during the mammalian cell cycle." Molecular and Cellular Biology **23**(16): 5706-5715.
Rouleau, M., *et al.* (2007). "PARP-3 associates with polycomb group bodies and with components of the DNA damage repair machinery." Journal of Cellular Biochemistry **100**(2): 385-401.
Rouleau, M., *et al.* (2010). "PARP inhibition: PARP1 and beyond." Nature Reviews Cancer **10**(4): 293-301.
Ruf, A., *et al.* (1996). "Structure of the catalytic fragment of poly(AD-ribose) polymerase from chicken." Proceedings of the National Academy of Sciences of the United States of America **93**(15): 7481-7485.
Ruf, A., *et al.* (1998). "The mechanism of the elongation and branching reaction of poly(ADP-ribose) polymerase as derived from crystal structures and mutagenesis." Journal of Molecular Biology **278**(1): 57-65.
Rulten, S. L., *et al.* (2011). "PARP-3 and APLF Function Together to Accelerate Nonhomologous End-Joining." Molecular Cell **41**(1): 33-45.
Ruscetti, T., *et al.* (1998). "Stimulation of the DNA-dependent protein kinase by poly(ADP-ribose) polymerase." The Journal of Biological Chemistry **273**(23): 14461-14467.
Saberi, A., *et al.* (2007). "RAD18 and poly(ADP-ribose) polymerase independently suppress the access of nonhomologous end joining to double-strand breaks and

facilitate homologous recombination-mediated repair." Molecular and Cellular Biology **27**(7): 2562-2571.
San Filippo, J.*, et al.* (2008). "Mechanism of eukaryotic homologous recombination." Annual Review of Biochemistry **77**: 229-257.
Sanderson, R. J. and T. Lindahl (2002). "Down-regulation of DNA repair synthesis at DNA single-strand interruptions in poly(ADP-ribose) polymerase-1 deficient murine cell extracts." DNA Repair **1**(7): 547-558.
Sartori, A. A.*, et al.* (2007). "Human CtIP promotes DNA end resection." Nature **450**(7169): 509-514.
Satoh, M. S. and T. Lindahl (1992). "Role of poly(ADP-ribose) formation in DNA repair." Nature **356**(6367): 356-358.
Satoh, M. S.*, et al.* (1994). "Dual function for poly(ADP-ribose) synthesis in response to DNA strand breakage." Biochemistry **33**(23): 7099-7106.
Sawai, S.*, et al.* (2007). "High-throughput analysis of spatio-temporal dynamics in *Dictyostelium*." Genome Biology **8**(7): R144.
Schaap, P. (2011). "Evolutionary crossroads in developmental biology: *Dictyostelium discoideum*." Development **138**(3): 387-396.
Schaap, P.*, et al.* (2006). "Molecular phylogeny and evolution of morphology in the social amoebas." Science **314**(5799): 661-663.
Schaefer, D. G.*, et al.* (2010). "RAD51 loss of function abolishes gene targeting and de-represses illegitimate integration in the moss *Physcomitrella patens*." DNA Repair (Amst) **9**(5): 526-533.
Schiestl, R. H.*, et al.* (1994). "Effect of mutations in genes affecting homologous recombination on restriction enzyme-mediated and illegitimate recombination in *Saccharomyces cerevisiae*." Molecular and Cellular Biology **14**(7): 4493-4500.
Schreiber, V.*, et al.* (2002). "Poly(ADP-ribose) polymerase-2 (PARP-2) is required for efficient base excision DNA repair in association with PARP-1 and XRCC1." The Journal of Biological Chemistry **277**(25): 23028-23036.
Schreiber, V.*, et al.* (2006). "Poly(ADP-ribose): novel functions for an old molecule." Nature Reviews Molecular Cell Biology **7**(7): 517-528.
Schreiber, V.*, et al.* (1992). "The human poly(ADP-ribose) polymerase nuclear localization signal is a bipartite element functionally separate from DNA binding and catalytic activity." The EMBO Journal **11**(9): 3263-3269.
Schulte-Uentrop, L.*, et al.* (2008). "Distinct roles of XRCC4 and Ku80 in non-homologous end-joining of endonuclease- and ionizing radiation-induced DNA double-strand breaks." Nucleic Acids Research **36**(8): 2561-2569.
Scovassi, A. I.*, et al.* (1986). "Structural analysis of poly(ADP-ribose)polymerase in higher and lower eukaryotes." European journal of biochemistry / FEBS **159**(1): 77-84.
Segall, J. E.*, et al.* (1995). "A Map Kinase Necessary for Receptor-Mediated Activation of Adenylyl-Cyclase in *Dictyostelium*." Journal of Cell Biology **128**(3): 405-413.
Semighini, C. P.*, et al.* (2006). "Functional characterization of the putative *Aspergillus nidulans* poly(ADP-ribose) polymerase homolog PrpA." Genetics **173**(1): 87-98.
Shibata, A.*, et al.* (2011). "Factors determining DNA double-strand break repair pathway choice in G2 phase." The EMBO Journal **30**(6): 1079-1092.

Shim, E. Y., *et al.* (2010). "*Saccharomyces cerevisiae* Mre11/Rad50/Xrs2 and Ku proteins regulate association of Exo1 and Dna2 with DNA breaks." The EMBO Journal **29**(19): 3370-3380.

Shrivastav, M., *et al.* (2008). "Regulation of DNA double-strand break repair pathway choice." Cell Research **18**(1): 134-147.

Simsek, D. and M. Jasin (2010). "Alternative end-joining is suppressed by the canonical NHEJ component Xrcc4-ligase IV during chromosomal translocation formation." Nature Structural & Molecular Biology **17**(4): 410-416.

Singleton, B. K., *et al.* (1997). "Molecular and biochemical characterization of *xrs* mutants defective in Ku80." Molecular and Cellular Biology **17**(3): 1264-1273.

Sinha, R. P. and D. P. Hader (2002). "UV-induced DNA damage and repair: a review." Photochemical & photobiological sciences : Official journal of the European Photochemistry Association and the European Society for Photobiology **1**(4): 225-236.

Sleigh, M. J. (1976). "The mechanism of DNA breakage by phleomycin in vitro." Nucleic Acids Research **3**(4): 891-901.

Sobol, R. W., *et al.* (2000). "The lyase activity of the DNA repair protein beta-polymerase protects from DNA-damage-induced cytotoxicity." Nature **405**(6788): 807-810.

Solinger, J. A., *et al.* (2001). "Rad54 protein stimulates heteroduplex DNA formation in the synaptic phase of DNA strand exchange via specific interactions with the presynaptic Rad51 nucleoprotein filament." Journal of Molecular Biology **307**(5): 1207-1221.

Sonoda, E., *et al.* (2006). "Differential usage of non-homologous end-joining and homologous recombination in double strand break repair." DNA Repair **5**(9-10): 1021-1029.

Sonoda, E., *et al.* (1998). "Rad51-deficient vertebrate cells accumulate chromosomal breaks prior to cell death." The EMBO Journal **17**(2): 598-608.

Spagnolo, L., *et al.* (2006). "Three-dimensional structure of the human DNA-PKcs/Ku70/Ku80 complex assembled on DNA and its implications for DNA DSB repair." Molecular Cell **22**(4): 511-519.

Stark, J. M., *et al.* (2004). "Genetic steps of mammalian homologous repair with distinct mutagenic consequences." Molecular and Cellular biology **24**(21): 9305-9316.

Staub, E., *et al.* (2004). "Insights into the evolution of the nucleolus by an analysis of its protein domain repertoire." BioEssays : news and reviews in molecular, cellular and developmental biology **26**(5): 567-581.

Strom, C. E., *et al.* (2011). "Poly (ADP-ribose) polymerase (PARP) is not involved in base excision repair but PARP inhibition traps a single-strand intermediate." Nucleic Acids Research **39**(8): 3166-3175.

Sucgang, R., *et al.* (2003). "Sequence and structure of the extrachromosomal palindrome encoding the ribosomal RNA genes in Dictyostelium." Nucleic Acids Research **31**(9): 2361-2368.

Sugawara, N., *et al.* (1997). "Role of *Saccharomyces cerevisiae* Msh2 and Msh3 repair proteins in double-strand break-induced recombination." Proceedings of the National Academy of Sciences of the United States of America **94**(17): 9214-9219.

Sugimura, K., *et al.* (2008). "PARP-1 ensures regulation of replication fork progression by homologous recombination on damaged DNA." The Journal of Cell Biology **183**(7): 1203-1212.

Sugiyama, T. and S. C. Kowalczykowski (2002). "Rad52 protein associates with replication protein A (RPA)-single-stranded DNA to accelerate Rad51-mediated displacement of RPA and presynaptic complex formation." The Journal of Biological Chemistry **277**(35): 31663-31672.

Sugiyama, T., *et al.* (1998). "DNA annealing by RAD52 protein is stimulated by specific interaction with the complex of replication protein A and single-stranded DNA." Proceedings of the National Academy of Sciences of the United States of America **95**(11): 6049-6054.

Sung, P. (1997a). "Yeast Rad55 and Rad57 proteins form a heterodimer that functions with replication protein A to promote DNA strand exchange by Rad51 recombinase." Genes & Development **11**(9): 1111-1121.

Sung, P., *et al.* (2003). "Rad51 recombinase and recombination mediators." The Journal of Biological Chemistry **278**(44): 42729-42732.

Svendsen, J. M., *et al.* (2009). "Mammalian BTBD12/SLX4 assembles a Holliday junction resolvase and is required for DNA repair." Cell **138**(1): 63-77.

Takata, M., *et al.* (1998). "Homologous recombination and non-homologous end-joining pathways of DNA double-strand break repair have overlapping roles in the maintenance of chromosomal integrity in vertebrate cells." The EMBO Journal **17**(18): 5497-5508.

Takeda, K., *et al.* (2002). "A novel *Dictyostelium* Cdk8 is required for aggregation, but is dispensable for growth." Development Growth & Differentiation **44**(3): 213-223.

Tao, Z., *et al.* (2008). "Domain C of human poly(ADP-ribose) polymerase-1 is important for enzyme activity and contains a novel zinc-ribbon motif." Biochemistry **47**(21): 5804-5813.

Tao, Z., *et al.* (2009). "Identification of the ADP-ribosylation sites in the PARP-1 automodification domain: analysis and implications." Journal of the American Chemical Society **131**(40): 14258-14260.

Taylor, E. R. and C. H. McGowan (2008). "Cleavage mechanism of human Mus81-Eme1 acting on Holliday-junction structures." Proceedings of the National Academy of Sciences of the United States of America **105**(10): 3757-3762.

Teo, S. H. and S. P. Jackson (1997). "Identification of *Saccharomyces cerevisiae* DNA ligase IV: involvement in DNA double-strand break repair." The EMBO journal **16**(15): 4788-4795.

Thorslund, T., *et al.* (2010). "The breast cancer tumor suppressor BRCA2 promotes the specific targeting of RAD51 to single-stranded DNA." Nature Structural & Molecular Biology **17**(10): 1263-1265.

Timinszky, G., *et al.* (2009). "A macrodomain-containing histone rearranges chromatin upon sensing PARP1 activation." Nature Structural & Molecular Biology **16**(9): 923-929.

Tong, W. M., *et al.* (2002). "Synergistic role of Ku80 and poly(ADP-ribose) polymerase in suppressing chromosomal aberrations and liver cancer formation." Cancer Research **62**(23): 6990-6996.

Trucco, C., *et al.* (1998). "DNA repair defect in poly(ADP-ribose) polymerase-deficient cell lines." Nucleic Acids Research **26**(11): 2644-2649.

Trucco, C., *et al.* (1999). "A dual approach in the study of poly (ADP-ribose) polymerase: in vitro random mutagenesis and generation of deficient mice." Molecular and Cellular Biochemistry **193**(1-2): 53-60.

Tsai, C. J., *et al.* (2007). "Cernunnos/XLF promotes the ligation of mismatched and noncohesive DNA ends." Proceedings of the National Academy of Sciences of the United States of America **104**(19): 7851-7856.

Tsuji, A., *et al.* (2001). "Endonuclease IV homolog from *Dictyostelium discoideum*: sequencing and functional expression in AP endonuclease-deficient *Escherichia coli*." Mutation Research **486**(1): 53-57.

Tsujioka, M., *et al.* (2004). "Novel development rescuing factors (DRFs) secreted by the developing *Dictyostelium* cells, that are involved in the restoration of a mutant lacking MAP-kinase ERK2." Zoological Science **21**(8): 829-834.

Tsuzuki, T., *et al.* (1996). "Targeted disruption of the *rad51* gene leads to lethality in embryonic mice." Proceedings of the National Academy of Sciences of the United States of America **93**(13): 6236-6240.

Tulin, A., *et al.* (2002). "The *Drosophila* heterochromatic gene encoding poly(ADP-ribose) polymerase (PARP) is required to modulate chromatin structure during development." Genes & Development **16**(16): 2108-2119.

Uchida, K., *et al.* (1993). "Cloning of cDNA encoding *Drosophila* poly(ADP-ribose) polymerase: leucine zipper in the auto-modification domain." Proceedings of the National Academy of Sciences of the United States of America **90**(8): 3481-3485.

Uematsu, N., *et al.* (2007). "Autophosphorylation of DNA-PKCS regulates its dynamics at DNA double-strand breaks." The Journal of Cell Biology **177**(2): 219-229.

Valencia, M., *et al.* (2001). "NEJ1 controls non-homologous end joining in *Saccharomyces cerevisiae*." Nature **414**(6864): 666-669.

van der Heijden, T., *et al.* (2007). "Real-time assembly and disassembly of human RAD51 filaments on individual DNA molecules." Nucleic Acids Research **35**(17): 5646-5657.

Van Driessche, N., *et al.* (2007). "Global transcriptional responses to cisplatin in *Dictyostelium discoideum* identify potential drug targets." Proceedings of the National Academy of Sciences of the United States of America **104**(39): 15406-15411.

Vodenicharov, M. D., *et al.* (2000). "Base excision repair is efficient in cells lacking poly(ADP-ribose) polymerase 1." Nucleic Acids Research **28**(20): 3887-3896.

Walker, J. R., *et al.* (2001). "Structure of the Ku heterodimer bound to DNA and its implications for double-strand break repair." Nature **412**(6847): 607-614.

Wang, H., *et al.* (2003). "Biochemical evidence for Ku-independent backup pathways of NHEJ." Nucleic Acids Research **31**(18): 5377-5388.

Wang, H., *et al.* (2005). "DNA ligase III as a candidate component of backup pathways of nonhomologous end joining." Cancer Research **65**(10): 4020-4030.

Wang, H., *et al.* (2001). "Efficient rejoining of radiation-induced DNA double-strand breaks in vertebrate cells deficient in genes of the RAD52 epistasis group." Oncogene **20**(18): 2212-2224.

Wang, M., *et al.* (2006). "PARP-1 and Ku compete for repair of DNA double strand breaks by distinct NHEJ pathways." Nucleic Acids Research **34**(21): 6170-6182.

Wang, Z. Q., *et al.* (1995). "Mice lacking ADPRT and poly(ADP-ribosyl)ation develop normally but are susceptible to skin disease." Genes & Development **9**(5): 509-520.
Ward, J. F. (1988). DNA damage produced by ionising radiation in mammalian cells: Identities, mechanisms of formation, and reparability. Progress In Nucleic Acid Research and Molecular Biology. J. N. Davidson, Cohn, W. E., Academic Press. **35**.
Watts, D. J. and J. M. Ashworth (1970). "Growth of myxameobae of the cellular slime mould *Dictyostelium discoideum* in axenic culture." The Biochemical Journal **119**(2): 171-174.
Weijer, C. J., *et al.* (1984). "A revision of the *Dictyostelium discoideum* cell cycle." Journal of Cell Science **70**: 111-131.
Welker, D. L. and R. A. Deering (1976). "Genetic analysis of radiation-sensitive mutations in the slime mould *Dictyostelium discoideum*." Journal of General Microbiology **97**(1): 1-10.
Welker, D. L. and R. A. Deering (1978). "Genetics of Radiation Sensitivity in the Slime Mould *Dictyostelium discoideum*." Journal of General Microbiology **109**: 11-23.
Welker, D. L. and R. A. Deering (1979). "Interactions between radiation-sensitive mutations in double-mutant haploids of *Dictyostelium discoideum*." Molecular & General Genetics **167**(3): 265-270.
Weterings, E., *et al.* (2003). "The role of DNA dependent protein kinase in synapsis of DNA ends." Nucleic Acids Research **31**(24): 7238-7246.
Whitehouse, C. J., *et al.* (2001). "XRCC1 stimulates human polynucleotide kinase activity at damaged DNA termini and accelerates DNA single-strand break repair." Cell **104**(1): 107-117.
Wiederhold, L., *et al.* (2004). "AP endonuclease-independent DNA base excision repair in human cells." Molecular Cell **15**(2): 209-220.
Willers, H., *et al.* (2004). "Repair of radiation damage to DNA." British Journal of Cancer **90**(7): 1297-1301.
Wilson, T. E., *et al.* (1997). "Yeast DNA ligase IV mediates non-homologous DNA end joining." Nature **388**(6641): 495-498.
Woodhouse, B. C., *et al.* (2008). "Poly(ADP-ribose) polymerase-1 modulates DNA repair capacity and prevents formation of DNA double strand breaks." DNA Repair (Amst) **7**(6): 932-940.
Wu, L. and I. D. Hickson (2003). "The Bloom's syndrome helicase suppresses crossing over during homologous recombination." Nature **426**(6968): 870-874.
Wu, W., *et al.* (2002). "Solution structure of the hydroperoxide of Co(III) phleomycin complexed with d(CCAGGCCTGG)2: evidence for binding by partial intercalation." Nucleic Acids Research **30**(22): 4881-4891.
Wu, W., *et al.* (2008). "Repair of radiation induced DNA double strand breaks by backup NHEJ is enhanced in G2." DNA Repair **7**(2): 329-338.
Wu, Y., *et al.* (2006). "DNA annealing mediated by Rad52 and Rad59 proteins." The Journal of Biological Chemistry **281**(22): 15441-15449.
Xie, A., *et al.* (2009). "Role of mammalian Mre11 in classical and alternative nonhomologous end joining." Nature Structural & Molecular Biology **16**(8): 814-818.
Xu, Q., *et al.* (2004). "Transcriptional transitions during *Dictyostelium* spore germination." Eukaryotic Cell **3**(5): 1101-1110.

Yamaguchi-Iwai, Y., *et al.* (1998). "Homologous recombination, but not DNA repair, is reduced in vertebrate cells deficient in RAD52." Molecular and Cellular Biology **18**(11): 6430-6435.

Yaneva, M., *et al.* (1997). "Interaction of DNA-dependent protein kinase with DNA and with Ku: biochemical and atomic-force microscopy studies." The EMBO Journal **16**(16): 5098-5112.

Yanez, R. J. and A. C. Porter (1999). "Gene targeting is enhanced in human cells overexpressing hRAD51." Gene Therapy **6**(7): 1282-1290.

Yang, Y. G., *et al.* (2004). "Ablation of PARP-1 does not interfere with the repair of DNA double-strand breaks, but compromises the reactivation of stalled replication forks." Oncogene **23**(21): 3872-3882.

Yannone, S. M., *et al.* (2008). "Coordinate 5' and 3' endonucleolytic trimming of terminally blocked blunt DNA double-strand break ends by Artemis nuclease and DNA-dependent protein kinase." Nucleic Acids Research **36**(10): 3354-3365.

Yano, K. and D. J. Chen (2008). "Live cell imaging of XLF and XRCC4 reveals a novel view of protein assembly in the non-homologous end-joining pathway." Cell cycle **7**(10): 1321-1325.

Yano, K., *et al.* (2011). "Functional significance of the interaction with Ku in DNA double-strand break recognition of XLF." FEBS letters **585**(6): 841-846.

Yano, K., *et al.* (2008). "Ku recruits XLF to DNA double-strand breaks." EMBO Reports **9**(1): 91-96.

Yu, S. L., *et al.* (1998). "Rapid changes of nucleotide excision repair gene expression following UV-irradiation and cisplatin treatment of *Dictyostelium discoideum*." Nucleic Acids Research **26**(14): 3397-3403.

Yu, X. and J. Chen (2004). "DNA damage-induced cell cycle checkpoint control requires CtIP, a phosphorylation-dependent binding partner of BRCA1 C-terminal domains." Molecular and Cellular Biology **24**(21): 9478-9486.

Yun, M. H. and K. Hiom (2009). "CtIP-BRCA1 modulates the choice of DNA double-strand-break repair pathway throughout the cell cycle." Nature **459**(7245): 460-463.

Zahradka, P. and K. Ebisuzaki (1982). "A shuttle mechanism for DNA-protein interactions. The regulation of poly(ADP-ribose) polymerase." European journal of biochemistry / FEBS **127**(3): 579-585.

Zhang, X. Y., *et al.* (2009). "Xpf and not the Fanconi anaemia proteins or Rev3 accounts for the extreme resistance to cisplatin in *Dictyostelium discoideum*." PLoS genetics **5**(9): e1000645.

Zhang, Y., *et al.* (2007). "Role of Dnl4-Lif1 in nonhomologous end-joining repair complex assembly and suppression of homologous recombination." Nature Structural & Molecular Biology **14**(7): 639-646.

Zhang, Y. and M. Jasin (2011). "An essential role for CtIP in chromosomal translocation formation through an alternative end-joining pathway." Nature Structural & Molecular Biology **18**(1): 80-84.

Zhou, B. B. and S. J. Elledge (2000). "The DNA damage response: putting checkpoints in perspective." Nature **408**(6811): 433-439.

Zhu, Z., *et al.* (2008). "Sgs1 helicase and two nucleases Dna2 and Exo1 resect DNA double-strand break ends." Cell **134**(6): 981-994.

9: Appendix

Appendix A: Primer sequences

Regions of the primer sequence which are underlined indicate epitope tags and those regions which are in italics indicate restriction enzyme sites.

Knockout construct

Adprt1a *Kpn*I

5'-GG*GGTACC*GTTCAATCTCATGGTGGTGAAG-3'

Adprt1a *Not*I

5'-GG*AAGCTT*CTTGAGAGGTTGAAGTTGTTGTTG-3'

Adprt1a *Bam*HI

5'-GG*GGATCC*GTGCTCCATTTCCTCTAGCC-3'

Adprt1a *Not*I

5'-GG*GCGGCCGC*CCCAAAGGAGGACCCAGAGC-3'

Adprt2 *Kpn*I

5'-GG*GGTACC*CAATACAAGTGAAGCTGAAACC-3'

Adprt2 *HindIII*

5'-GG*AAGCTT*TGGTAGCGATTTCGATATCGG-3'

Adprt2 *Bam*HI

5'-GG*GGATCC*GTCTACTTGATTCAGTTTCTTCGG-3

Adprt2 *Not*I

5'-GG*GCGGCCGC*TGAAGTTCATCCAGAGAACCC-3'

Ku70 *Kpn*I

5'-GG*GGTACC*CAGATGGTGTTACAGGCTGGG-3'

Ku70'*Hind*III

5'-GG*AAGCTT*CAAGTATTGGTTCCACTCAT-3'

Ku70*Pst*I

5'-GG*CTGCAG*CAACAAATGGTGGTGATGACGATGAT-3'

Ku70 *Bam*HI

5'-GG*GGATCC*GTTGTTTATTTGTACGATAGCA-3

Screening primers

BSR CHK1

5'-GGATGGATCAATTTAACATTTCTC-3'

BSR REV2

5'-GTAGTTTTGACTAACTTGCC-3'

BSR 5' ARM

5'-GAGAAATGTTAAATTGATCCATT-3'

BSR 3' ARM

5'-GGCAAGTTAGTCAAAACTAC-3'

CDK8 5' SCREEN

5'-CGCTCTCTCATAAACATACA-3'

Adprt1a 5' SCREEN

5'-TTATTAGGGATGTATCATGGCATCATT-3'

Adprt2 5' SCREEN

5'-GAAGGTTGTGGCGCATCAACCTCAAAAACATGC-3'

Adprt2 3' SCREEN

5'-CATCATAGATTCTGAAATTGTTGAACAAAT-3'

RasC 5' SCREEN

5’-GTGTTTGATCAATAGCATC-3’

Exo1 5’ SCREEN

5’-ATTGGAGAATTGGAAGTCGC-3’

Expression plasmids

Ku70-N-Myc

5’-

GCAAGGTACCGAACAAAATTATTTCAGAAGAAGATTTAATGAGTGGAACC

AATAGTTGG-3’

Ku70C

5’-AAGCTCTAGATTATTGATGTCTATATTCATCAAG-3’

Ku70-WT-BSERI

5’-GCAACAATGAATAAAAAAGCTCCTCCAAA-3’

Ku70-C-PBZ DELETION

5’-AAGCTCTAGATTACAAACATACCATTATTGACAAAGTTG-3’

Ku70 PBZ MUTATION

5’-

AAGCTCTACATTATTGATGTCTATATTCATCAAGATGTTGTTTTATTTGTAC

GATAGGCGTTTTTACCATATTTGGCTAATT-3’

RT-PCR

Ku70 RT-PCR 332bp

5’-CAAGTGATAGTGATTTAATTGGTGT-3’

Ku70 RT-PCR 1707bp

5’-GGTATTATTATTTGATTGTTGAGATG-3’

Sequencing primers

Ku70 260bp Rev

5’-GGTTCAAACATTGCTTTTGATGCATCTATT-3’

Ku70 332bp Rev

5’-ACACCAAATTAAATCACTATCACTTG-3’

Ku70 332bp FWD

5’-CAAGTGATAGTGATTTAATTGGTGT-3’

Ku70 732bp FWD

5’-CAATCCGAATGCATACAATGATAG-3’

Ku70 1145bp FWD

5’-ACCAGTTAAACAATTGATAAAGAATG-3’

Ku702507bp REV

5’-CTTTGGAGCTTTTTTATTCATTG-3’

Ku702107bp REV

5’-GTTTTGCAGAAGAGGATGAGGTA-3’

Ku70 1707bp REV

5’-GGTATTATTATTTGATTGTTGAGATG-3’

Appendix B: Publications arising from this work

Couto, C. A., *et al.* (2011). "PARP regulates nonhomologous end joining through retention of Ku at double-strand breaks." The Journal of Cell Biology **194**(3): 367-375.

Hsu, D. W., *et al.* (2011). "DNA double-strand break repair pathway choice in *Dictyostelium*." Journal of Cell Science **124**(Pt 10): 1655-1663.

DNA glycosylase	Damage recognised	Mono/bifunctional (Nth/Nei)
UNG	Uracil	Monofunctional
SMUG1	Uracil	Monofunctional
TDG	U and T in U(T):G mispairs	Monofunctional
MPG	3-methyladenine; hypoxanthine	Monofunctional
MYH	A in 8-oxo-G:A mispairs	Monofunctional
NTH1	Thymine glycol	Bifunctional (Nth)
OGG1	8-oxoG	Bifunctional (Nth)
NEIL1	Thymine glycol; 5-hydroxyuracil	Bifunctional (Nei)
NEIL2	5-hydroxyuracil	Bifunctional (Nei)

Table 1.1 Non-exhaustive list of mammalian DNA glycosylases.

Adapted from Hedge *et al*. 2008

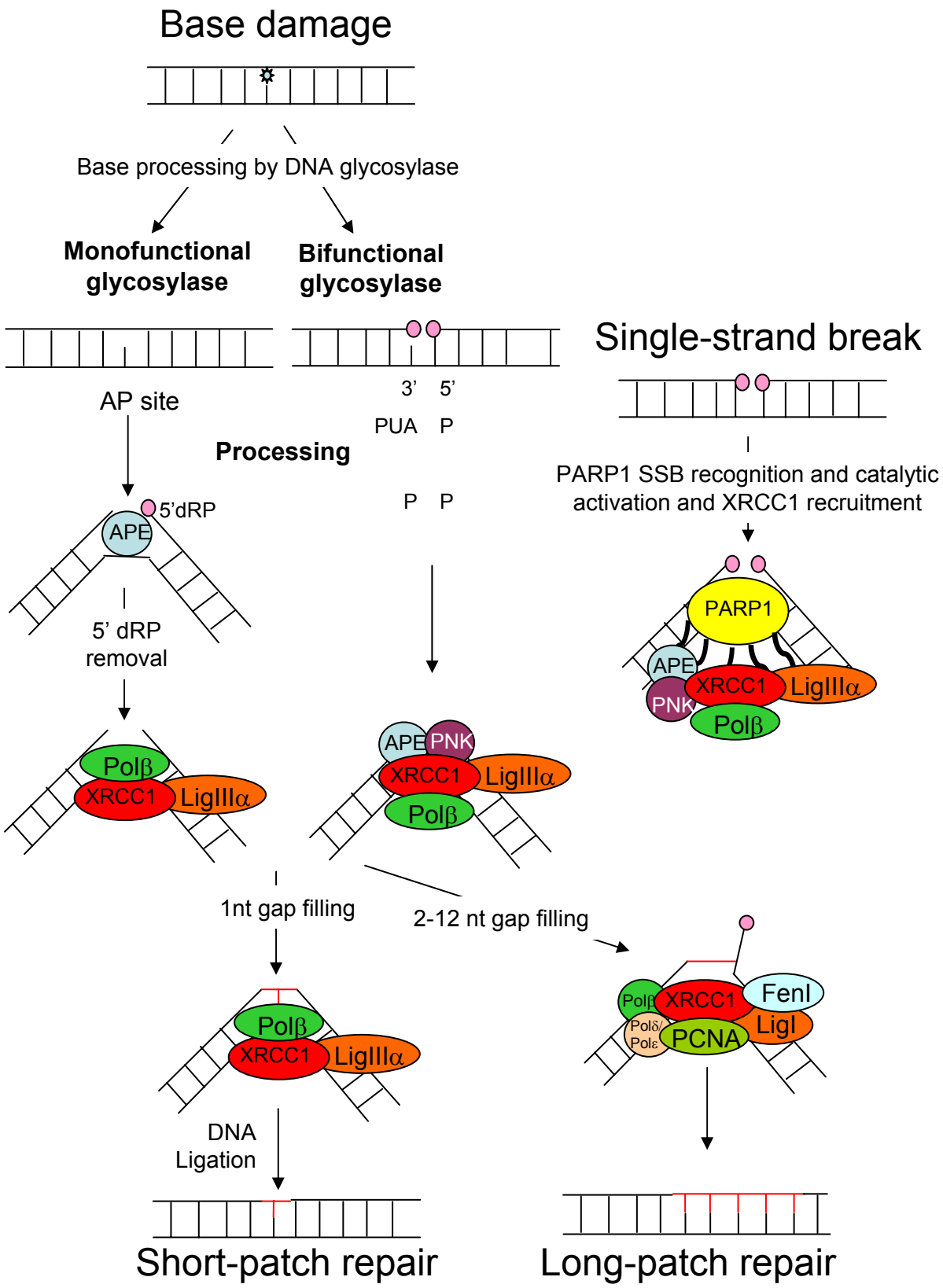

Figure 1.1 Base excision repair and single-strand break repair

Figure 1.1 Mammalian base-excision and single-strand break repair

Base damage is recognised by DNA glycosylases which excise the damaged base. In the case of bifunctional DNA glycosylases, the DNA backbone is additionally cleaved. Monofunctional DNA glycosylases produce an AP site that is a substrate for the AP endonuclease (APE), that incises the DNA backbone. In all cases, the DNA ends created are refractory to ligation (represented by pink circles) and need to be processed by enzymes to recreate the 3' OH and 5' P flanking the ssDNA nick/gap. The SSBs created directly, or as intermediates in BER, can be recognised by PARP1. PARP1 becomes activated and synthesises PAR chains (represented by thick black lines), predominantly on itself. PARylated PARP1 facilitates the recruitment of XRCC1 to promote either short-patch or long-patch repair. Prior to the subsequent steps in SSBR, autoPARylated PARP1 loses its affinity for the DNA SSB and detaches from the lesion, whilst XRCC1 is retained at the breaksite. In short-patch repair, a single nucleotide is inserted by DNA Polymerase β (DNAPolβ), before ligation by XRCC1/DNA Ligase IIIα. When the DNA end 5' to the gap cannot be processed, repair proceeds by long-patch repair via the action of PCNA in association with either Polβ/Polδ/Polε, which inserts between 2-12 nucleotides. The displaced DNA is cleaved by Fen1 and the DNA ends are ligated by Ligase I.

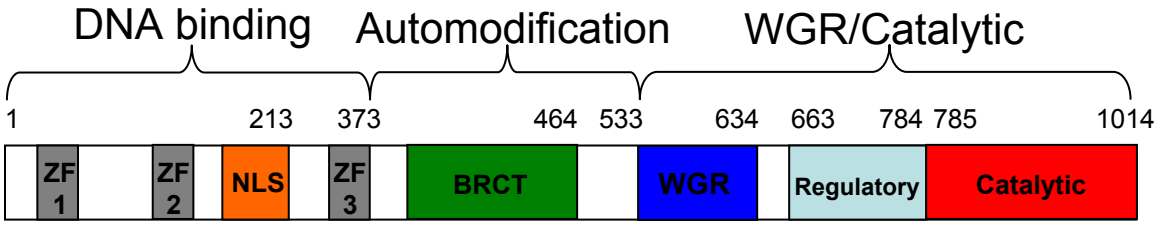

Figure 1.2 Human PARP1 structure

Human PARP1 can be divided into three major sections: the DNA binding domain, the automodification domain and the catalytic domain. In the DBD, ZF1 and ZF2 are implicated in DNA binding, whilst ZF3 transmits the DNA binding signal to the catalytic domain to give rise to catalytic activation. The automodification domain is a main acceptor of PAR chains synthesised by PARP1, and in particular contains 3 lysines that are the major acceptors of PARylation although minor sites outside the automodification domain also exist. The BRCT domain within the automodification domain can enable PARP1 interaction with other proteins. The catalytic domain is responsible for the synthesis of PAR chains, and contains the WGR domain, and the catalytic domain that is further divided into regulatory and catalytic segments. The catalytic site in particular contains the NAD^+ binding site, and is responsible for the initiation, elongation and branching of PAR chains on target proteins. PAR chain formation is initiated by the addition of an ADP-ribose unit on the target protein, which then becomes elongated, and can reach up to 200 units in length.

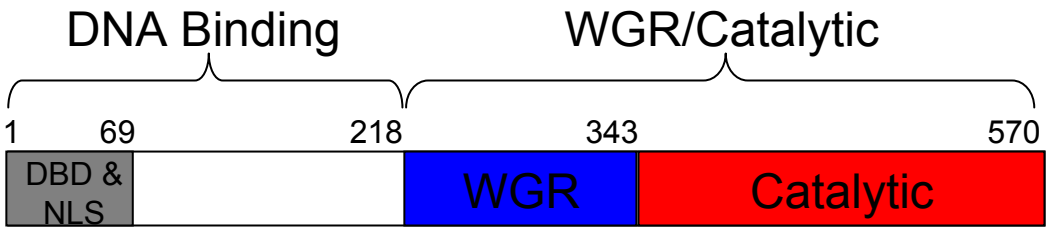

Figure 1.3 Human PARP2 structure

Human PARP2 can be divided into two main sections: The DNA binding domain, of which the residues between amino acids 1-69 represents the site of DNA binding and contains the nuclear localisation signal (NLS). In addition, 2 lysine residues within the DNA binding domain have been identified as sites of automodification *in vitro*. The catalytic domain contains the WGR domain and the catalytic domain. The region between residues 343 and 570 of the catalytic domain can be further divided into the catalytic and regulatory domain, and is the site of PAR chain initiation, elongation and branching, using NAD^+ as a substrate.

Type of damage	Processing enzyme
3’ phosphate	PNKP
3’ phosphoglycolate	APE1
3’ αβ unsaturated aldehyde (PUA)	APE1
3’ covalently linked Topoisomerase I	TDP1
5’ hydroxyl	PNKP
5’ aldehyde	?
5’ dRP	DNA Polβ
5’ AMP	APTX

Table 1.2 Non-exhaustive list of processing enzymes in SSBR

Table modified from Caldecott *et al* (Caldecott *et al*. 2008) showing the processing enzymes that deal with the different DNA ends prior to ligation. Some of the modified DNA ends can arise as intermediates in the BER pathway (3’ Phosphate, 3’ PUA, 5’dRP), whilst others are the product of oxidative damage. The covalent linkage of Topoisomerase I to DNA can be the result of abortive topoisomerase reaction, or alternatively can arise from the action of topoisomerase I inhibitors (e.g. Camptothecin), giving rise to 3’ covalently linked Topoisomerase I and 5’ hydroxyl damage. Abortive ligation reactions can give rise to 5’ AMP, which is repaired by Aprataxin (APTX).

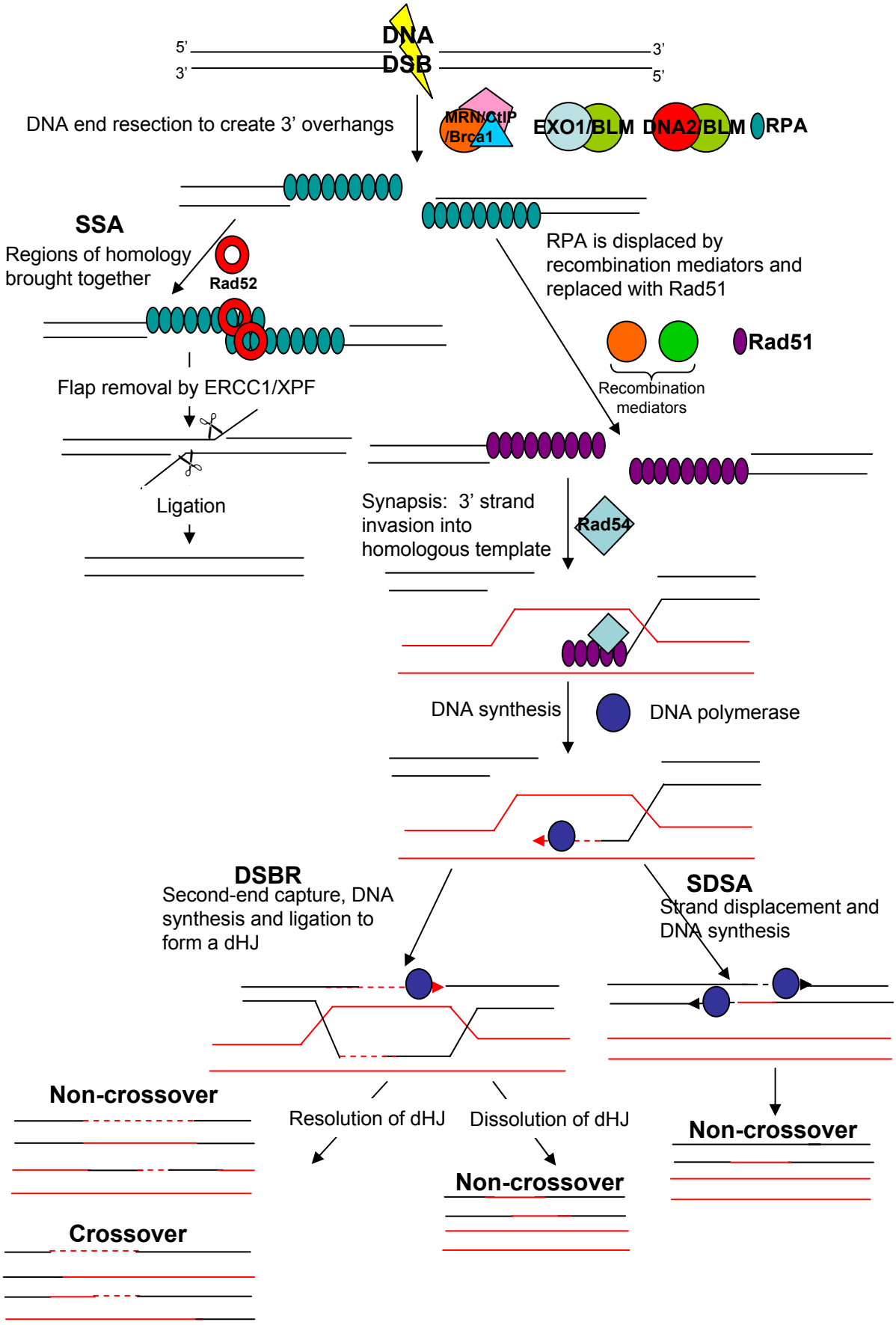

Figure 1.4 Homologous recombination

Figure 1.4 Schematic of mammalian Homologous recombination

Following DSB formation, DNA-ends are resected by nucleases in a 5'-3' direction to generate 3'overhangs. DNA end resection is initiated by the MRN/CtIP/Brca1 complex, which generates a short stretch of ssDNA, precluding Ku heterodimer binding to the DNA DSB. Longer range resection is mediated by two nuclease complexes, EXO1/BLM and DNA2/BLM. Following resection, the 3' ssDNA overhangs become coated in Replication protein A (RPA). Hereafter, HR can proceed in numerous ways. Single-strand annealing (SSA) is a non-conservative subset of repair involving Rad52, and occurs between direct repeats, leading to loss of information. Alternatively, RPA can be displaced by Rad51 to form the presynaptic-filament, facilitated by recombination mediators including Brca2 and other Rad51 paralogues. The Rad51 presynaptic-filament then mediates homology search and strand invasion, followed by Rad51 displacement. Both these processes may involve Rad54, in accordance with its *in vitro* activity. The 3' end of the presynaptic-filament primes DNA synthesis using the homologous chromosome as a template, and DNA synthesis across the break may involve Polη. In synthesis dependent strand annealing (SDSA) the invading 3' strand is then displaced and reanneals with the other end of the DSB, and the ends are ligated. In DSBR, repair proceeds by second-end capture which is catalysed by Rad52. This results in formation of a double Holliday junction (dHJ) which is resolved to give crossover or non-crossover products. An alternative to HJ resolution is HJ dissolution, forming non-crossover products.

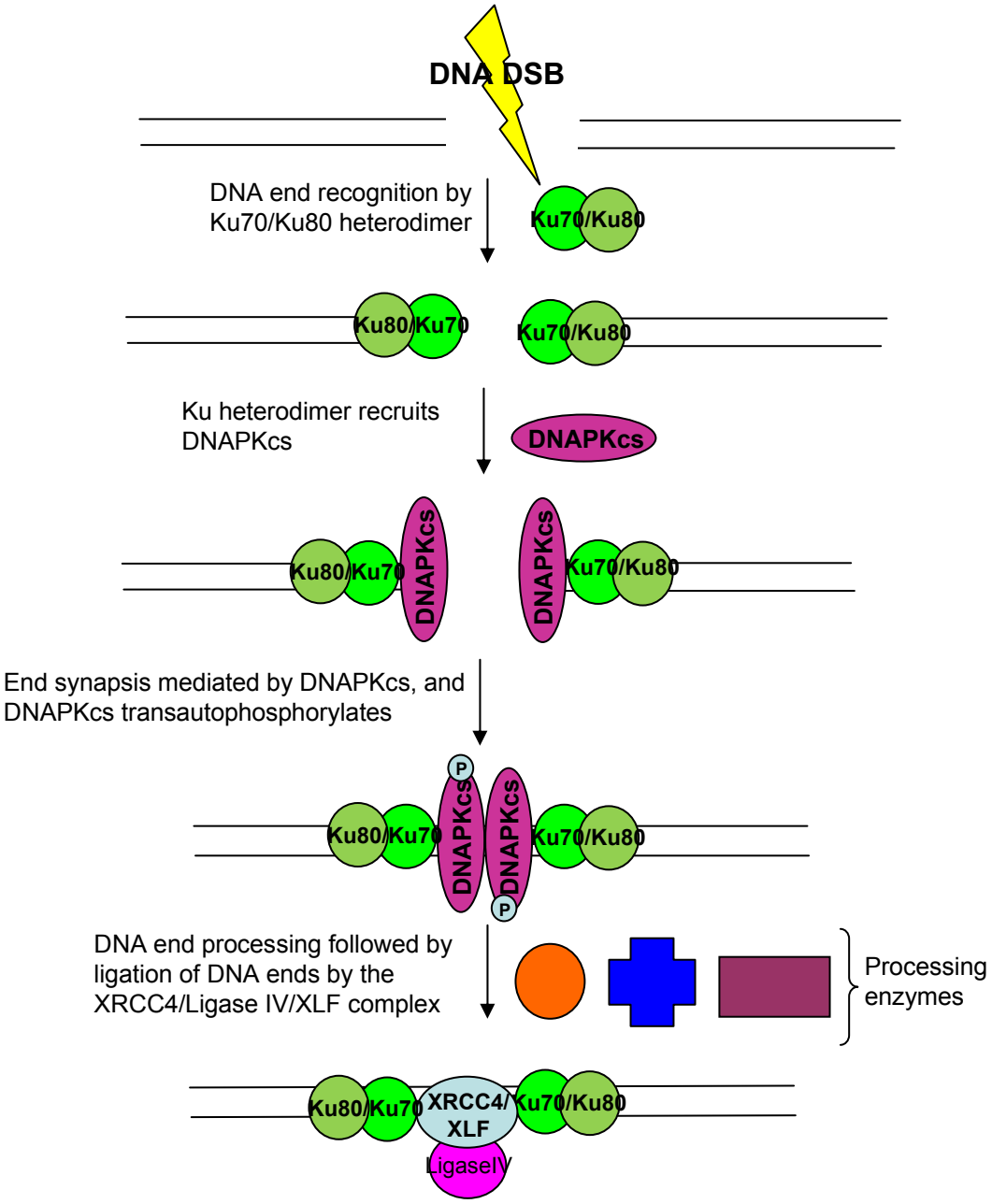

Figure 1.5 NHEJ The first step in NHEJ is recognition and recruitment of the Ku-heterodimer to DNA DSB-ends, which then recruits DNAPKcs, forming the DNAPK-holoenzyme. DNAPKcs mediates DNA-end synapsis and becomes phosphorylated by the combined action of ATM and DNAPKcs. The DNAPK-holoenzyme recruits various factors, which process DNA-ends to make them ligatable. This includes: Artemis; PolX-family polymerases (Polμ,Polλ); PNKP and APLF. Finally, Ligase IV/XRCC4/XLF is recruited which rejoins the DNA-ends.

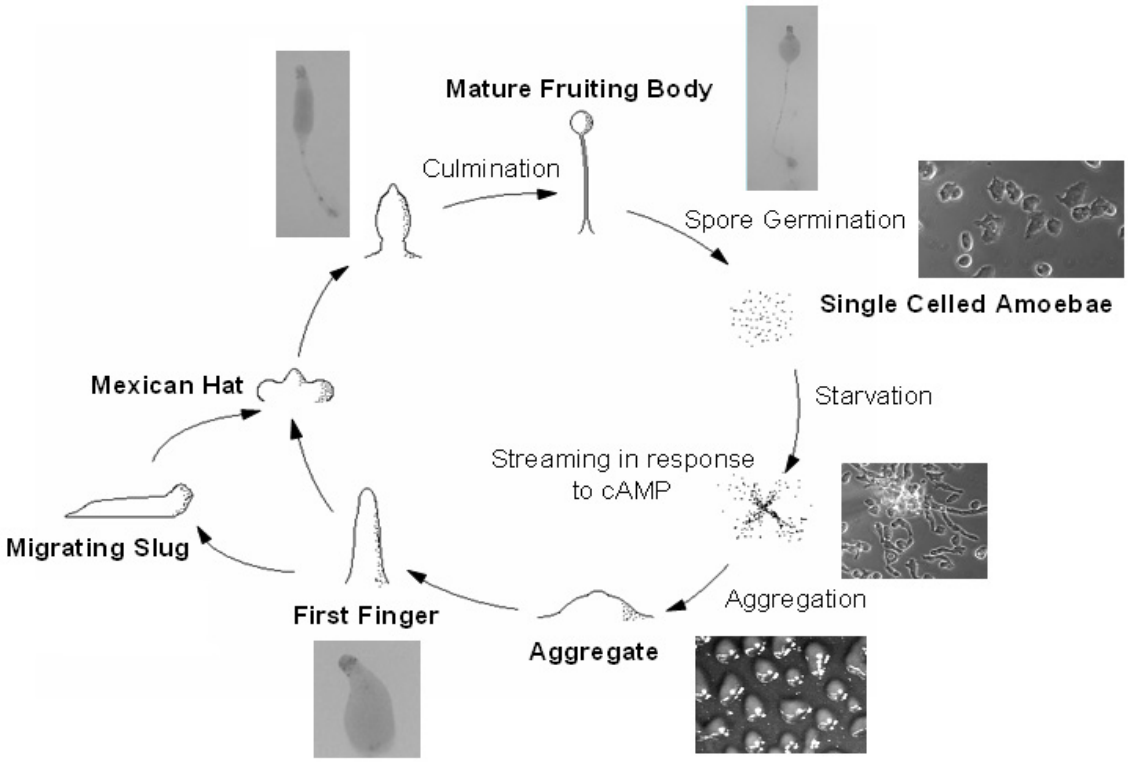

Figure 1.6 *Dictyostelium discoideum* developmental cycle

In the presence of a food source, *Dictyostelium* cells are unicellular amoebae. However, when food becomes scarce, cells synchronously enter a developmental cycle, culminating in multicellular fruiting body formation. This fruiting body consists of two major cell types: a head of spores supported by a stalk of vacuolated cells. The initial developmental stage, aggregation, relies on starvation-induced cyclic-AMP (cAMP) secretion by *Dictyostelium* cells. cAMP binds to membrane-receptors on nearby cells, inducing chemotaxis up the cAMP gradient and cAMP production (cAMP relay) to amplify and relay the signal. The aggregate can then develop further to form a fruiting body. Under favourable conditions, spores within the fruiting body can germinate and return to their unicellular state. Germination can also be induced under laboratory conditions by heat-shock. Figure from Strmecki *et al*. 2005.

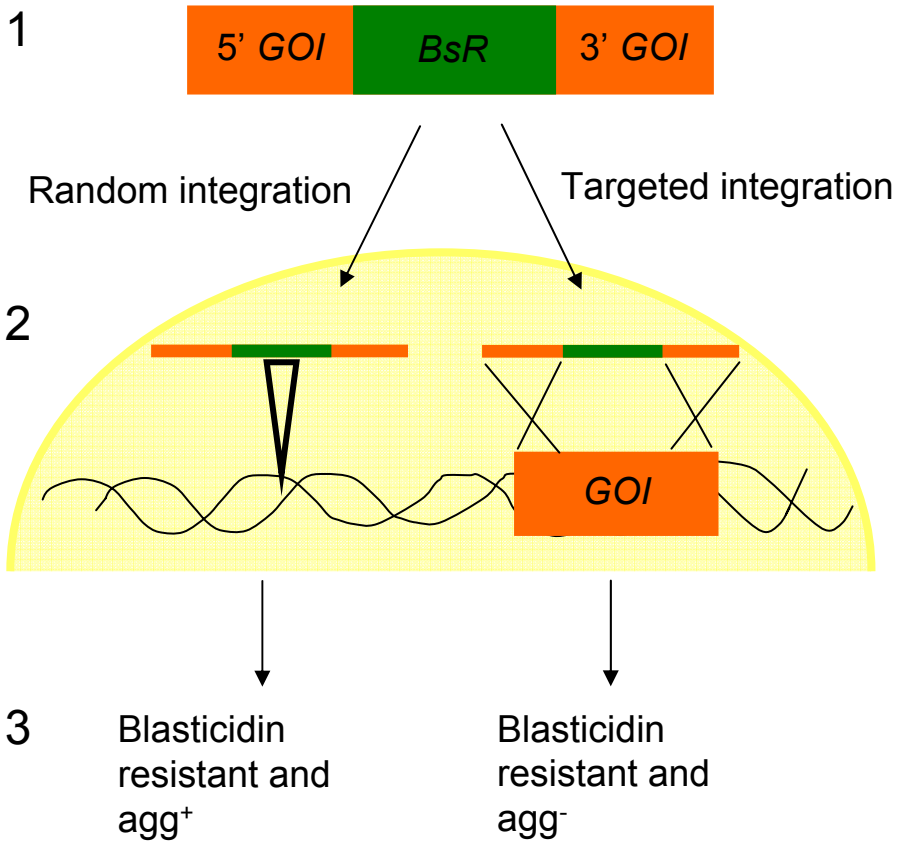

Figure 3.1 – Schematic of HR assay.

1) A disruption construct is transfected into *Dictyostelium*. Each arm of the construct bears homology to the 5' or 3' regions of a gene (GOI) involved in starvation-induced aggregation, separated by *bsr* (blasticidin-resistance gene). **2)** Following transfection, the cassette can integrate into the *Dictyostelium* genome. Integration can occur **randomly** or via **targeted** integration into the GOI. **3)** Cassette integration is determined by blasticidin resistance. The nature of integration can be further dissected into targeted- or random-integration based on the phenotype of colonies (agg^+ or agg^-). Briefly, clonal populations of blasticidin-resistant cells are spotted onto a bacterial lawn, where they form colonies by feeding on bacteria. As colonies expand, cells in the centre starve and would normally form fruiting bodies. However, cells incorporating the cassette via targeted-integration cannot aggregate (agg^-), and can be distinguished from random integrants (agg^+).

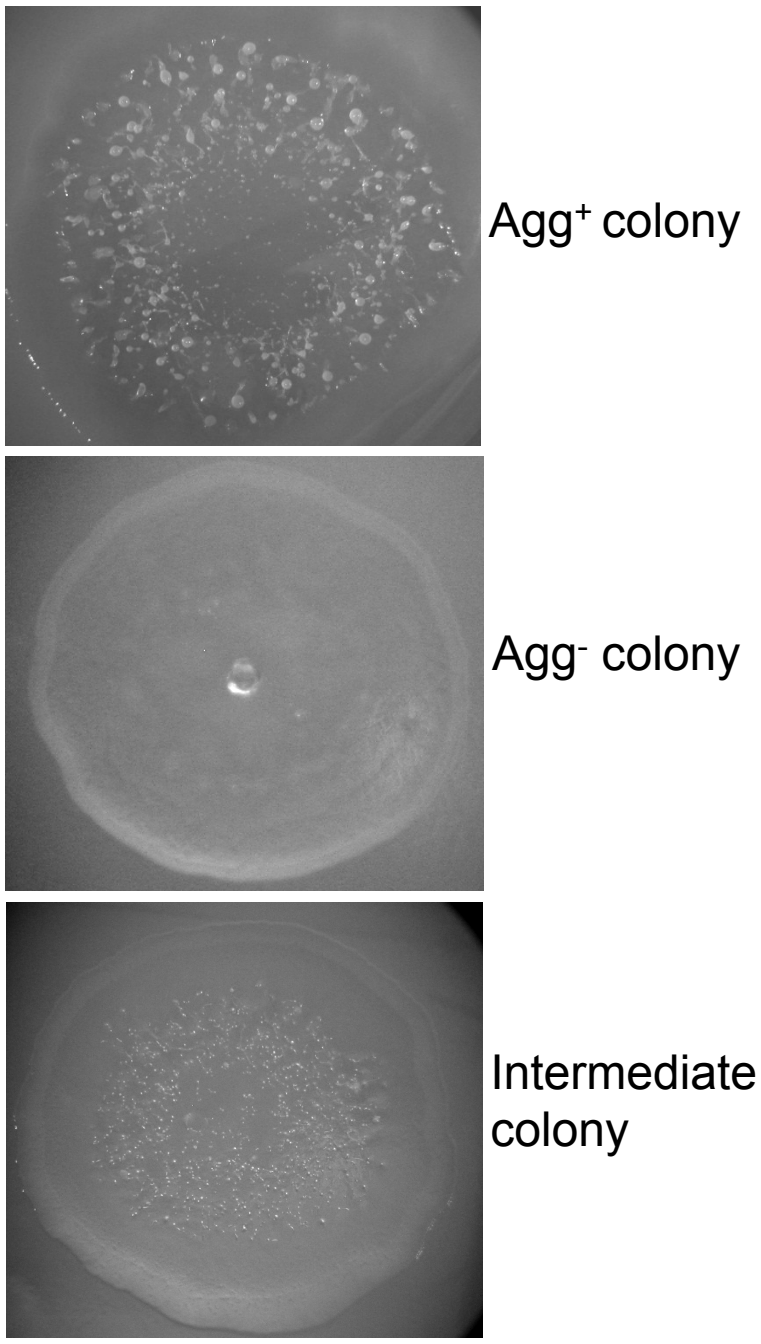

Figure 3.2 – Representative colonies from transfection of Ax2 with *erkB*-BSR construct.

Representative agg$^+$, agg$^-$ and intermediate colonies arising from transfection of Ax2 with the *erkB*-BSR disruption construct. Following selection in blasticidin, Ax2 were assayed as in Figure 3.1. Four days after spotting cells onto bacterial lawns, colonies were large enough to be phenotypically assessed. Both agg$^+$ and agg$^-$ colonies were observed, in addition to colonies with an intermediate phenotype. To identify revertants, colonies were once again assessed following a further 48 hours.

A

cdk8

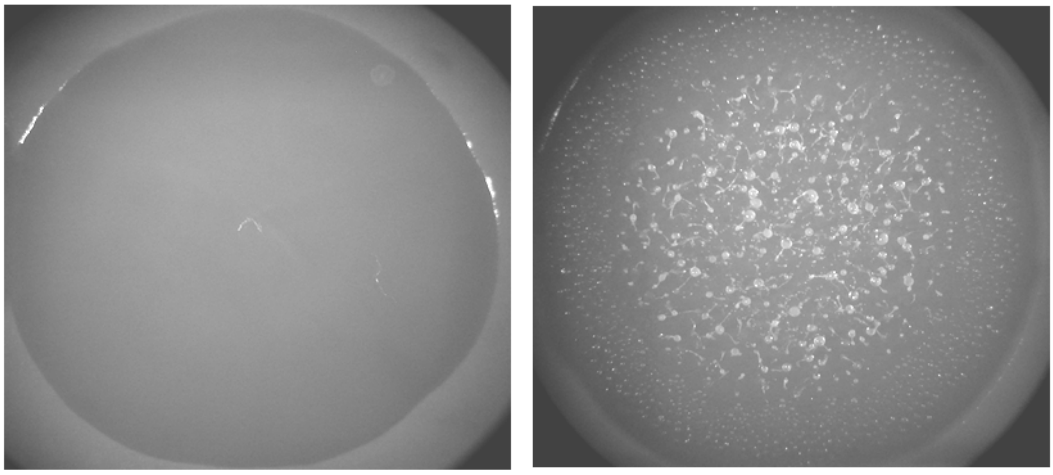

Agg^{-} Agg^{+}

B

rasC

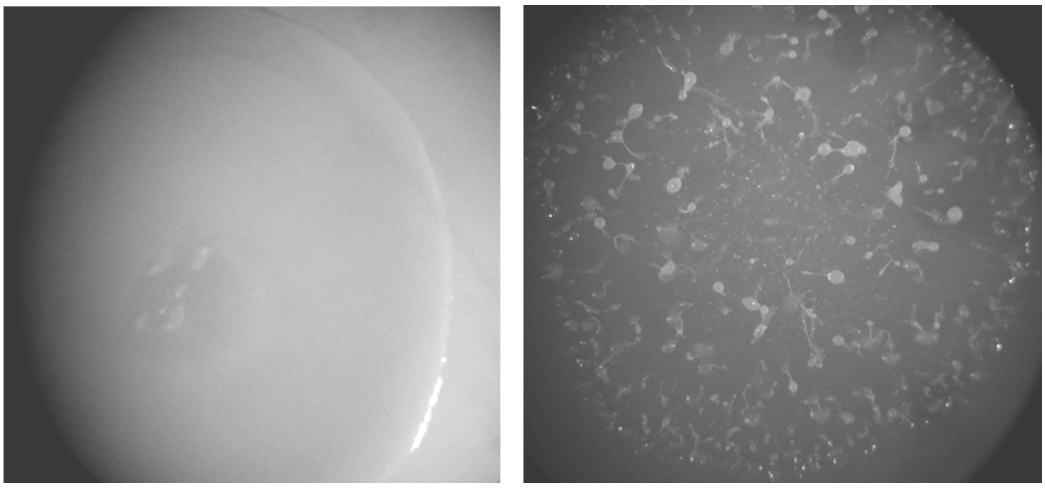

Agg^{-} Agg^{+}

Figure 3.3 – Representative agg^{+} and agg^{-} colonies from transfection of Ax2 with disruption constructs targeting *cdk8* (A) or *rasC* (B)

Figure 3.3 – Representative agg$^+$ and agg$^-$ colonies from transfection of Ax2 with disruption constructs targeting *cdk8* (A) or *rasC* (B)

Ax2 were assayed as in Figure 3.1 using constructs targeting *cdk8* or *rasC.* Representative pictures were taken 6 days after spotting cells onto bacterial lawns. Agg$^+$ and agg$^-$ colonies were observed after 4 days. However, another 48 hours was allowed before final phenotypic assessment to ensure colonies were sufficiently large, and to identify potential revertants. The phenotype between days 4 and 6 remained unchanged. For *rasC* and *cdk8*, agg$^+$ and agg$^-$ colonies were easily distinguishable, and *cdk8* agg$^-$ colonies were indistinguishable from a *cdk8*$^-$ strain (data not shown). This provides evidence of the suitability of assessing the aggregation-defect as a potential readout of targeted integration.

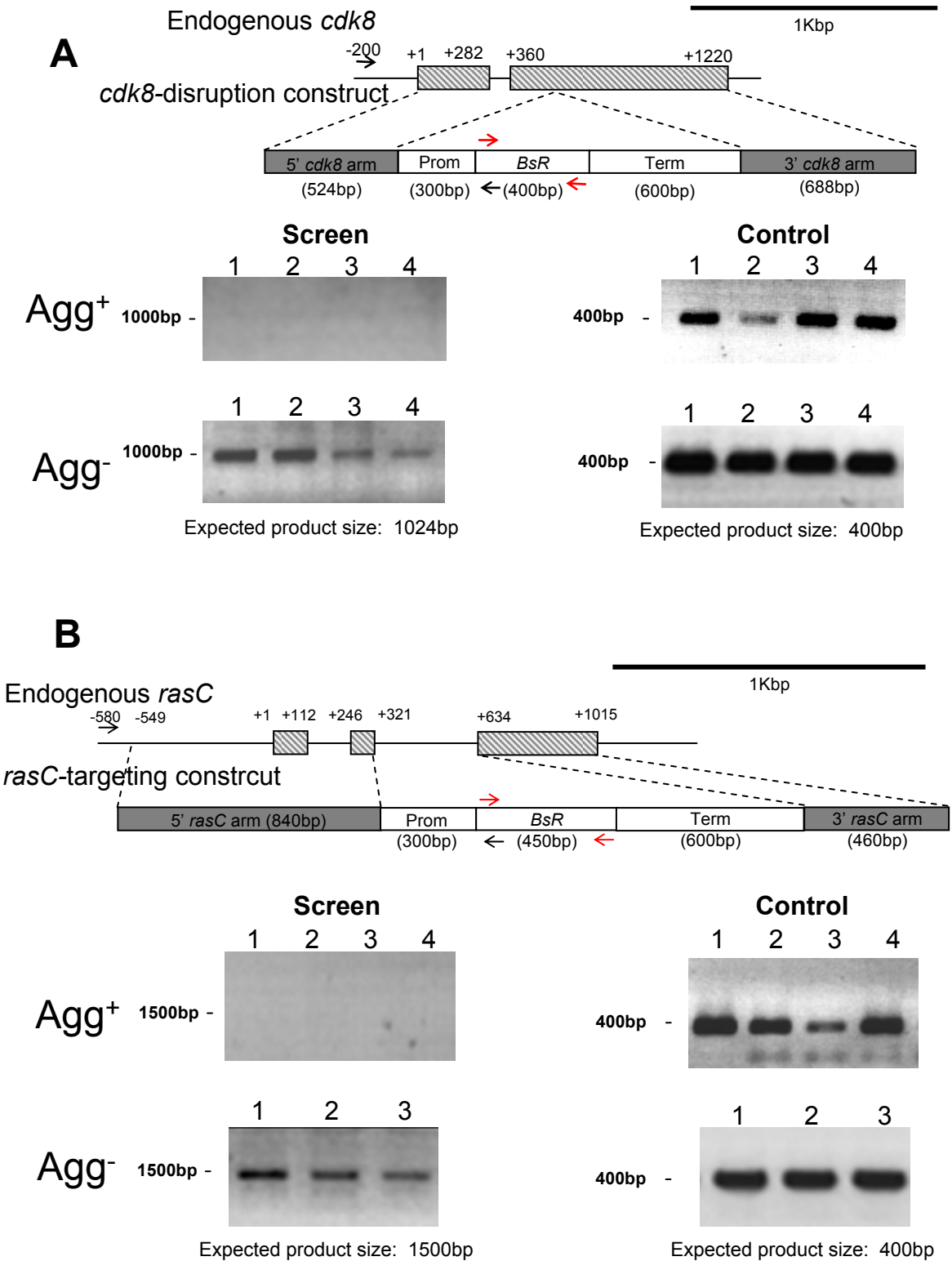

Figure 3.4 – Genotype verification of *cdk8* (A) and *rasC* (B) agg$^+$ and agg$^-$ colonies by PCR. Representative images shown.

Figure 3.4 – Genotype verification of *cdk8* (B) and *rasC* (C) agg$^+$ and agg$^-$ colonies by PCR. Representative images shown.

A) HR assay at the ***cdk8* locus**. Upper panel: schematic representation of the genomic endogenous *cdk8* gene and *cdk8* targeting-construct containing the *BsR* resistance cassette. Exons of the endogenous gene are represented by hashed boxes which are separated by introns. Numbers refer to nucleotide positions with the initiating ATG codon at +1. The arms of the *cdk8* targeting construct are represented by grey boxes with the *BsR* resistance cassette indicated by white boxes, flanked by the promoter (Prom) and Terminator (Term). Arrows represent PCR primer positions, with black arrows representing the screening PCR primer pair and red arrows representing the control PCR primer pair. Targeted integration of the construct would lead to disruption of *cdk8* with *BsR* at position +524. Genomic DNA was isolated from agg$^+$ and agg$^-$ colonies and screened by PCR using the indicated screening and control primers pairs. The screening PCR would generate a 1024bp product for targeted-integrants (agg$^-$) only. The control PCR would generate a product for both agg$^+$ and agg$^-$ colonies of 400bp. PCR products were run on a 1% agarose gel, and representative pictures have been illustrated in the lower panel (labelled 1-4 for the screening PCR and 1-4 for the control for both agg$^+$ and agg$^-$ colonies). Primer sequences can be found in Appendix A. **B)** HR assay at the ***rasC* locus**. Upper panel: schematic representation of the genomic endogenous *rasC* gene and *rasC* targeting-construct containing the *BsR* resistance cassette. Exons of the endogenous gene are represented by hashed boxes which are separated by introns. Numbers refer to nucleotide positions with the initiating ATG codon at +1. The arms of the *rasC* targeting construct are represented grey boxes with the *BsR* resistance cassette indicated by white boxes, flanked by the promoter (Prom) and Terminator (Term). The arrows represent PCR primer positions, with black arrows representing the screening PCR primer pair and red arrows representing the control PCR primer pair. Targeted integration of the construct would lead to disruption of *rasC* with *BsR* at position +291. Genomic DNA was isolated from agg$^+$ and agg$^-$ colonies and screened by PCR using the indicated screening and control primers pairs. The screening PCR would generate a 1.5KBp product for targeted-integrants (agg-) only. The control PCR would generate a product for both agg$^+$ and agg$^-$ colonies of 400bp. PCR products were run on a 1% agarose gel, and representative pictures have been illustrated in the lower panel (labelled 1-4 or 1-3 for the screening and control PCRs for agg$^+$ or agg$^-$ colonies, respectively). Primer sequences can be found in Appendix A.

Locus	Number of blasticidin-resistant colonies assessed	% agg$^-$ colonies
cdk8	788	2.03
rasC	273	1.1

Table 3.1 – Assessment of targeting efficiency in Ax2 at the *cdk8* and *rasC* loci

Ax2 was transfected with disruption constructs targeting either *cdk8* or *rasC* and the aggregation-capacity of blasticidin-resistant colonies assessed on SM-agar containing a lawn of *Ka*. The % Agg$^-$ colonies is expressed as the percentage of agg$^-$ colonies over the total number of colonies assessed. Blasticidin-resistant colonies from at least 2 independent experiments were analysed and data combined and presented in the table above.

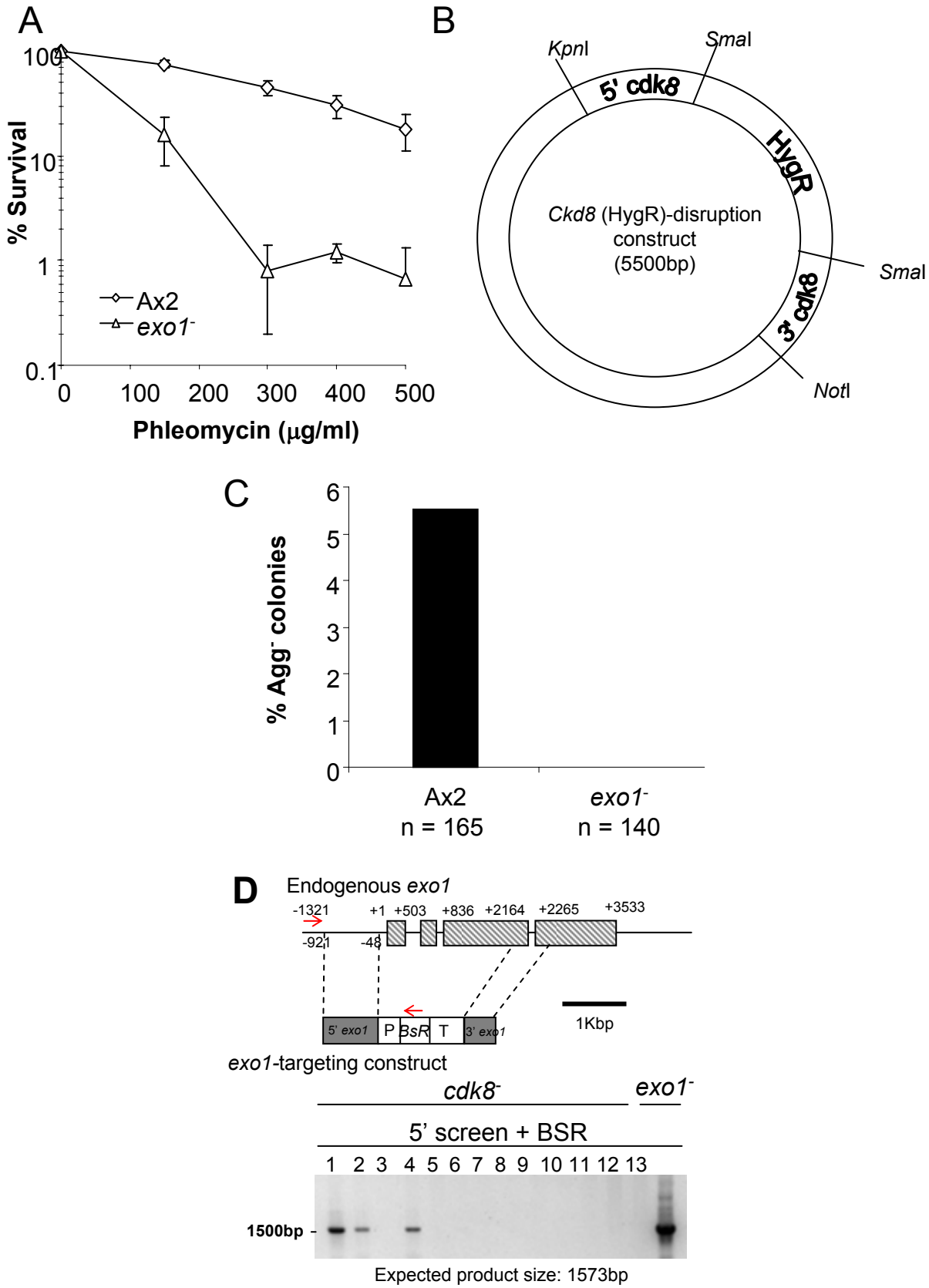

Figure 3.5 – Vegetative Ax2 show enhanced dependence on HR and Exo1

Figure 3.5 – Vegetative Ax2 show enhanced dependence on HR and Exo1

A) Ax2 and *exo1*$^{-}$ cells were exposed to increasing concentrations of phleomycin as indicated and cell survival assessed. Error bars represent the SEM of three independent experiments. **B)** The hygromycin-resistance cassette from pHyg-Tm (Plus) was excised with *Sma*I and ligated into the *cdk8*-disruption construct from which the blasticidin-resistance cassette had been removed by *Sma*I digestion. The cassette from the *cdk8*(Hyg)-disruption construct was acquired by digestion with *Kpn*I/*Not*I as before and transfected into *Dictyostelium*. **C)** Ax2 and *exo1*$^{-}$ were transfected with the *cdk8*(Hyg)-disruption cassette and the phenotype of blasticidin-resistant colonies assessed on SM-agar containing a lawn of *Ka*. % agg^{-} colonies was calculcated as the number of agg^{-} colonies over the total number of colonies analysed. Colonies from three independent experiments were assessed. **D)** Upper panel: endogenous *exo1* gene with exons represented by hatched boxes. Numbers correspond to nucleotide positions with +1 representing the initiating ATG codon. The targeted construct arms are represented by grey boxes flanking the central white *BsR* resistance cassette with P representing the Promoter and T the terminator. Targeted integration of the *exo1*-targeting construct would lead to disruption at -48, upstream of the +1 initiating codon. The PCR screening primers utilised are represented by red arrows. The primer sequences can be found in Appendix A. Lower Panel: The *cdk8*$^{-}$ strain was transfected with the *exo1*-disruption cassette and genomic DNA was isolated from pools of blasticidin-resistant colonies, with each pool containing eight independent blasticidin-resistant clones. The isolated genomic DNA was assessed by PCR, using the screening primers indicated in the upper panel, to identify targeted-integration of the *exo1*-disruption cassette. PCR products were run on a 1% agarose gel, and targeted integrants would be expected to give rise to a 1573bp PCR product. The final lane contains the PCR product generated from PCR of the *exo1*$^{-}$ strain genomic DNA and serves as a control.

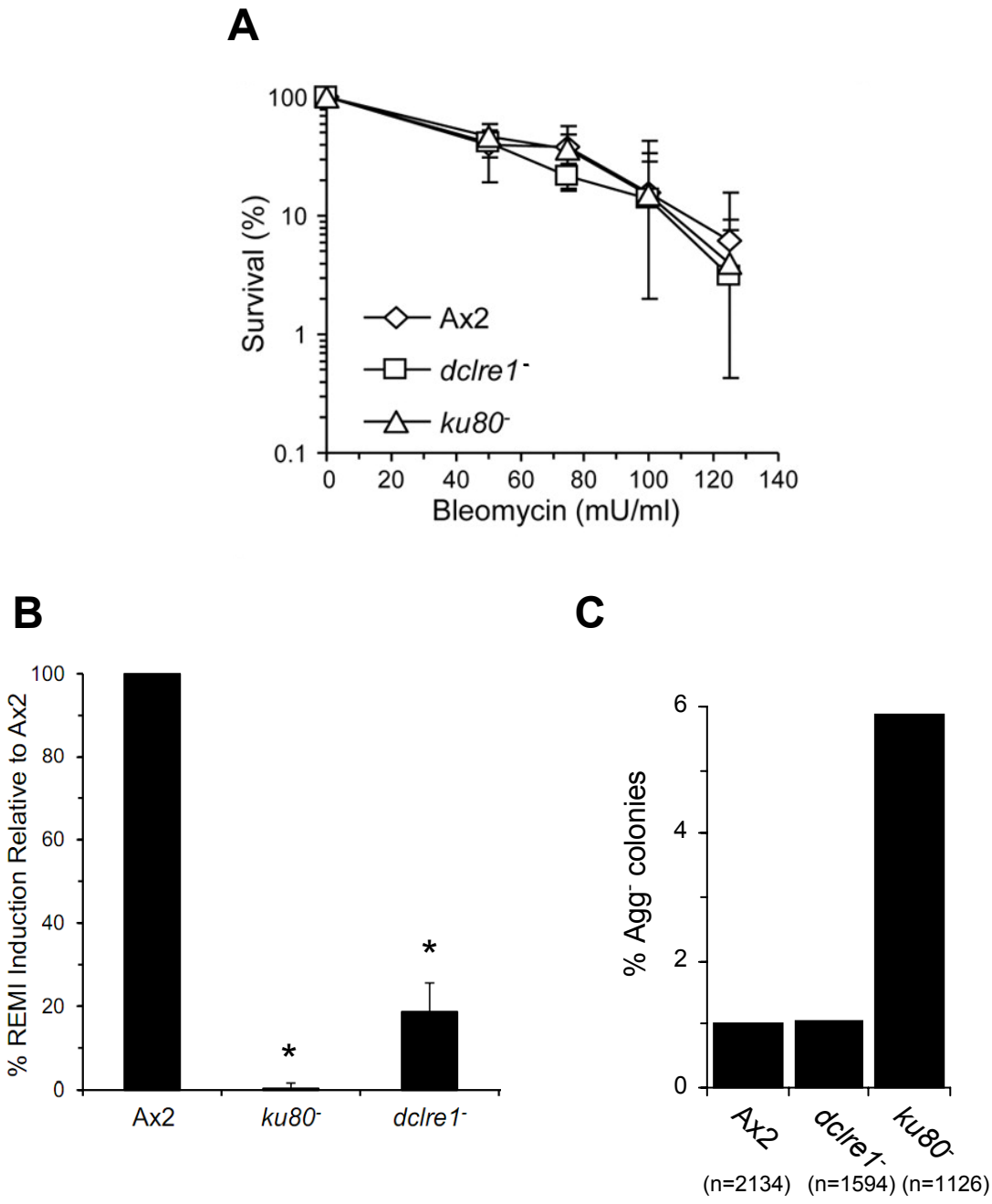

Figure 3.6 – Ku80 and Dclre1 function in NHEJ in vegetative *Dictyostelium*

Figure 3.6 – Ku80 and Dclre1 function in NHEJ in vegetative *Dictyostelium*

A) Ax2, *ku80*$^{-}$ and *dclre1*$^{-}$ cells were treated with increasing concentrations of bleomycin for 1 hour and survival assessed. Error bars represent the SEM from three independent experiments. Work for this figure was carried out by R. Kiely **B)** REMI efficiency of the indicated strains was assessed as described in Materials and Methods. The numbers analysed were such that experimental strains were compared to >200 colonies from the positive control (Ax2 plus restriction enzyme). Data is represented as % REMI induction relative to parental Ax2 controls. Error bars represent the SEM from three independent experiments. * $p<0.05$ compared to the positive control (Ax2). **C)** Homologous recombination was assessed in Ax2, *dclre1*$^{-}$ or *ku80*$^{-}$ cells by measuring targeted integration at the *cdk8* locus. Strains were selected with blasticidin following transfection with the *cdk8*-knockout construct. The aggregation phenotype of blasticidin-resistant colonies was assessed on SM-agar containing a lawn of *Ka*. Data from at least three independent transfections were assessed and data combined to determine % targeting efficiency for each strain

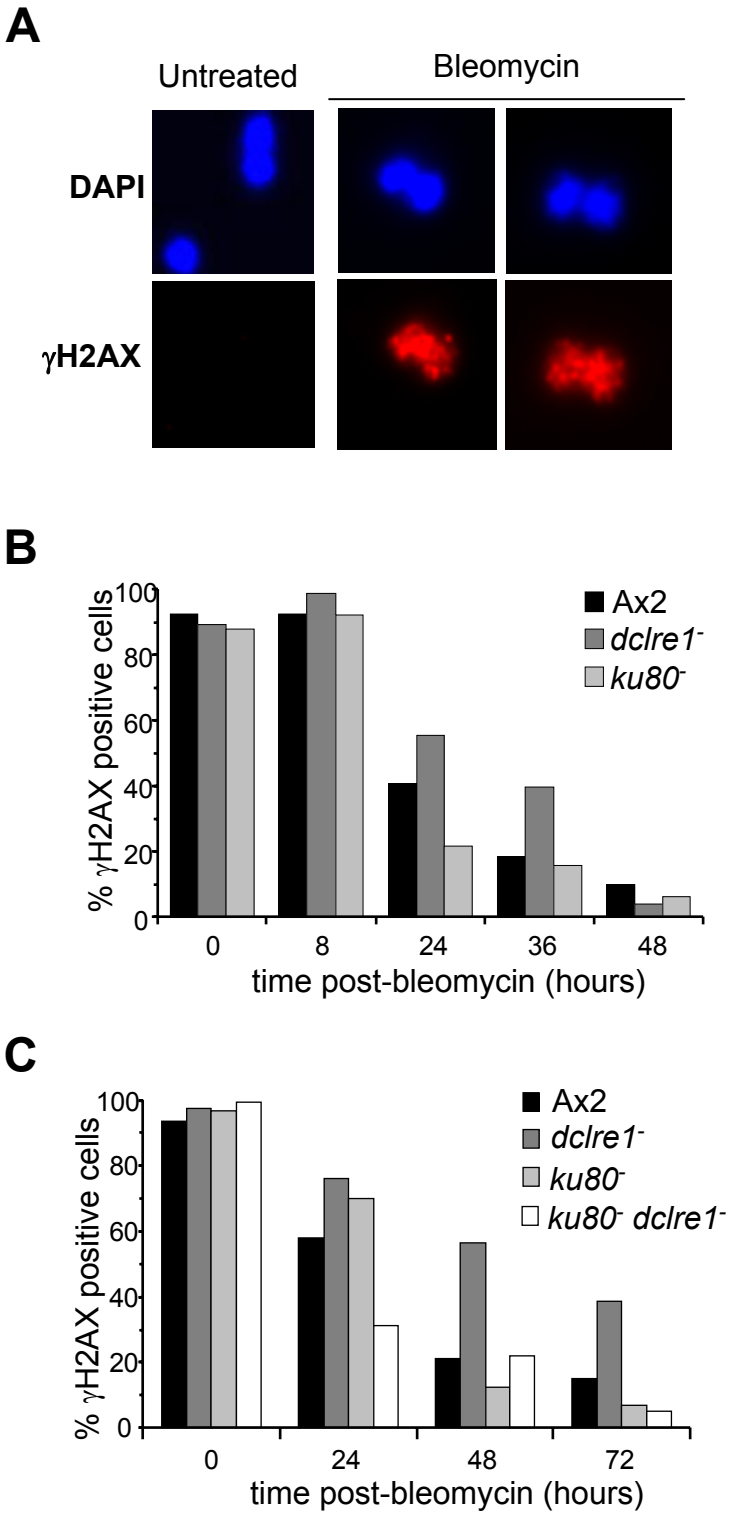

Figure 3.7 – γH2AX decay kinetics are altered in the *dclre1*⁻ strain relative to Ax2

Figure 3.7 – γH2AX decay kinetics are altered in the *dclre1*$^{-}$ strain relative to Ax2

A) Ax2 cells were treated with 100mu/ml bleomycin for 1 hour and processed for immunofluorescence using an antibody against γH2AX. Pictures of representative cells were taken and illustrate the nature of the staining pattern assessed in figures B and C. **B)** Ax2, *dclre1*$^{-}$ and *ku80*$^{-}$ cells were treated with 100mU/ml bleomycin for 1 hour and resuspended to 1x10^{6}cells/ml in HL5 containing no DNA damaging agents. At the indicated time points, cells were processed for immunofluorescence using an antibody against γH2AX and the % γH2AX positive cells scored from a population of >200 cells. The graph illustrates a single representative experiment that was repeated three times. Work for this figure was carried out by R. Kiely **C)** Ax2, *dclre1*$^{-}$, *ku80*$^{-}$ and *ku80*$^{-}$*/dclre1*$^{-}$ cells were treated with 100mU/ml bleomycin for 1 hour and resuspended to 1x10^{6} cells/ml in HL5 containing no DNA damaging agents. At the indicated time points, cells were processed for immunofluorescence using an antibody against γH2AX and the % γH2AX positive cells scored from a population of >200 cells. The graph illustrates a single experiment that was repeated three times. Work for this figure was carried out by R. Kiely.

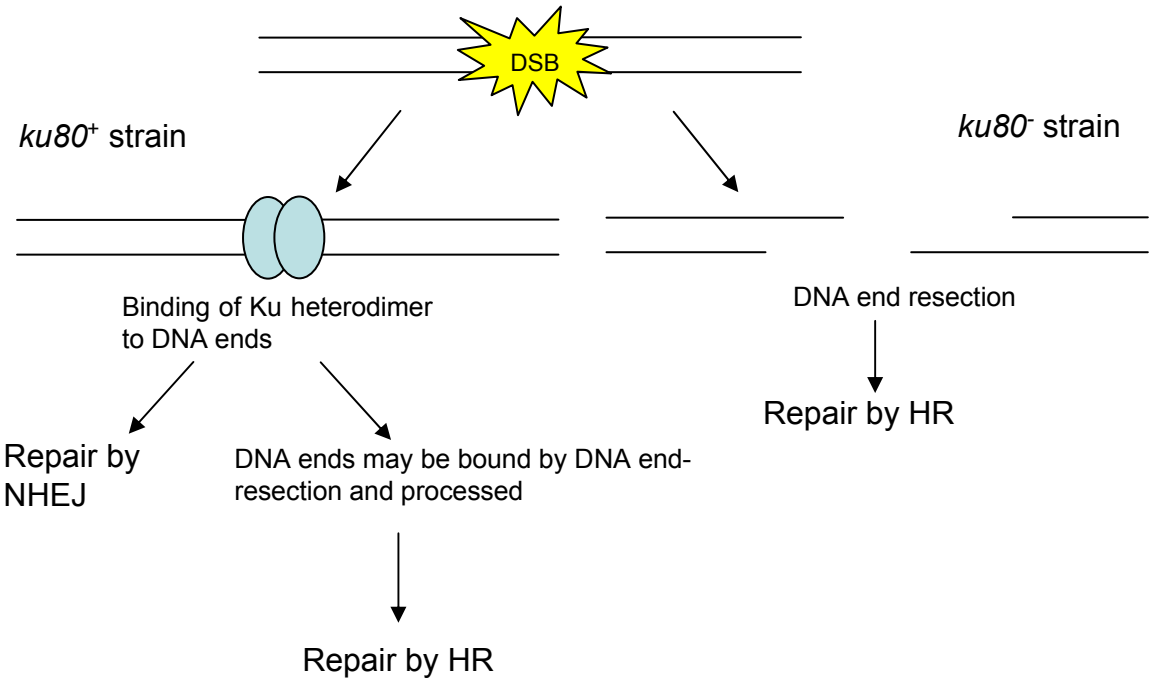

Figure 3.8 – *ku80*$^{-}$ strains show enhanced HR

Model presenting one interpretation of our findings in *Dictyostelium.* In the parental strain, Ku can bind to DNA DSB ends, preventing DNA end resection, and directing repair towards NHEJ. In the absence of Ku (*ku80*$^{-}$ strain), DNA ends are no longer protected, and can be resected to give rise to the 3' overhangs that initiate repair by HR. The ability of Ku-proficient cells to undertake HR at a DSBs may be due to the dynamic association of Ku at DNA ends (possibly representing failed NHEJ attempts), which can then be engaged by other repair components. This may include resection enzymes which process DNA ends to create 3' ssDNA overhangs that are no longer suitable substrates for NHEJ. Alternatively, post-translational modifications or the nature of DNA ends or the chromatin context of damage may influence repair pathway utilisation, by altering affinity of Ku for DNA ends to direct repair pathway choice.

Human	*S. cerevisiae*	*Dictyostelium*	Function in SSBR/BER
APE1 APE2	APN2 APN1	DDB_G0279923 DDB_G0277701	Cleaves 5' to the AP-site generated spontaneously or by a DNA glycosylase to create a DNA nick flanked by a 3'OH and 5'deoxyribose phosphate (5' dRP).
XRCC1	-	DDB_G0275653	Scaffolding protein – interacts with Ligase III
Polβ	Pol4	DDB_G0284713	Short-patch repair polymerase. Inserts a single nucleotide at the AP-site and removes the 5' dRP using its dRP lyase activity.
Polδ PCNA	Pol3 Pol30	DDB_G0285381 DDB_G0287607	Functions in long-patch repair with PCNA to insert 2-12 nucleotides at the AP-site
Fen 1	Rad27	DDB_G0284987	Flap-endonuclease that removes the displaced DNA strand following DNA synthesis by long-patch repair
Ligase III	-	DDB_G0283857	In a complex with XRCC1, ligates DNA ends following DNA synthesis in short-patch repair
Ligase I	Cdc9	DDB_G0274493	Carries out ligation in long-patch repair
PNKP	TPP1	DDB_G0281229	Processing function via its 3' phosphatase and 5' kinase activity. The yeast orthologue only possesses 3' phosphatase activity
APTX	-	DDB_G0293866	Removes the 5' AMP products of abortive ligation reactions
APLF	-	-	Putative endo and exonuclease activity and scaffolding function via interactions with PAR and the Ligase III/XRCC1 complex

Table 4.1 – Non-exhaustive table showing conservation of the core BER proteins in *Dictyostelium*.

The annotated *Dictyostelium* and *S. cerevisiae* protein database were searched for orthologues of proteins comprising the core BER pathway in humans. The functions column refers to the role of the indicated genes in the human SSBR/BER pathway.

Gene ID	Gene name	Alternative protein names
DDB_G0278741	***adprt1A***	**PARP1, pARTa**
DDB_G0279195	***adprt1B***	**PARP3, pARTd**
DDB_G0292820	***adprt2***	**PARP2, pARTc**
DDB_G0291788	***adprt3***	**TNKS, pARTb**
DDB_G0267468	***adprt4***	**PARP4, pARTe**
DDB_G0289141	***pART***	**pART**
DDB_G0286613	***DDB_G0286613***	-
DDB_G0274389	***pARTf***	**TNKS2**
DDB_G0271766	*pARTg*	PARP14
DDB_G0284015	***DDB_G0284015***	**-**
DDB_G0288069	*DDB_G0288069*	-
DDB_G0287911	*DDB_G0287911*	-
DDB_G0276785	***DDB_G0276785***	**-**
DDB_G0278045	*DDB_G0278045*	-
DDB_G0271966	*DDB_G0271966*	-

Table 4.2 – Conservation of PARPs in the *Dictyostelium* genome.

Table 4.2 – Conservation of PARPs in the *Dictyostelium* genome.

A BLASTp search of the *Dictyostelium* genome against the catalytic domain of hPARP1 identified 10 putative PARP orthologues, which are shown in bold. DDB_G0284015 and DDB_G0276785 were identified in the BLASTp search only when the e-value threshold was increased to 1. Further e-value threshold increases revealed no further genes. Additional genes (red font) were identified by searching the annotated database for genes with putative NAD^+-ribosyl transferase activity. DDB_G0278045 was identified as a PARP by Citerelli *et al* 2010. The hPARP1 sequence was acquired from NCBI and the boundaries of the catalytic domain identified from Altmeyer *et al*. Identification of *Dictyostelium* orthologues was performed on dictyBase.org.

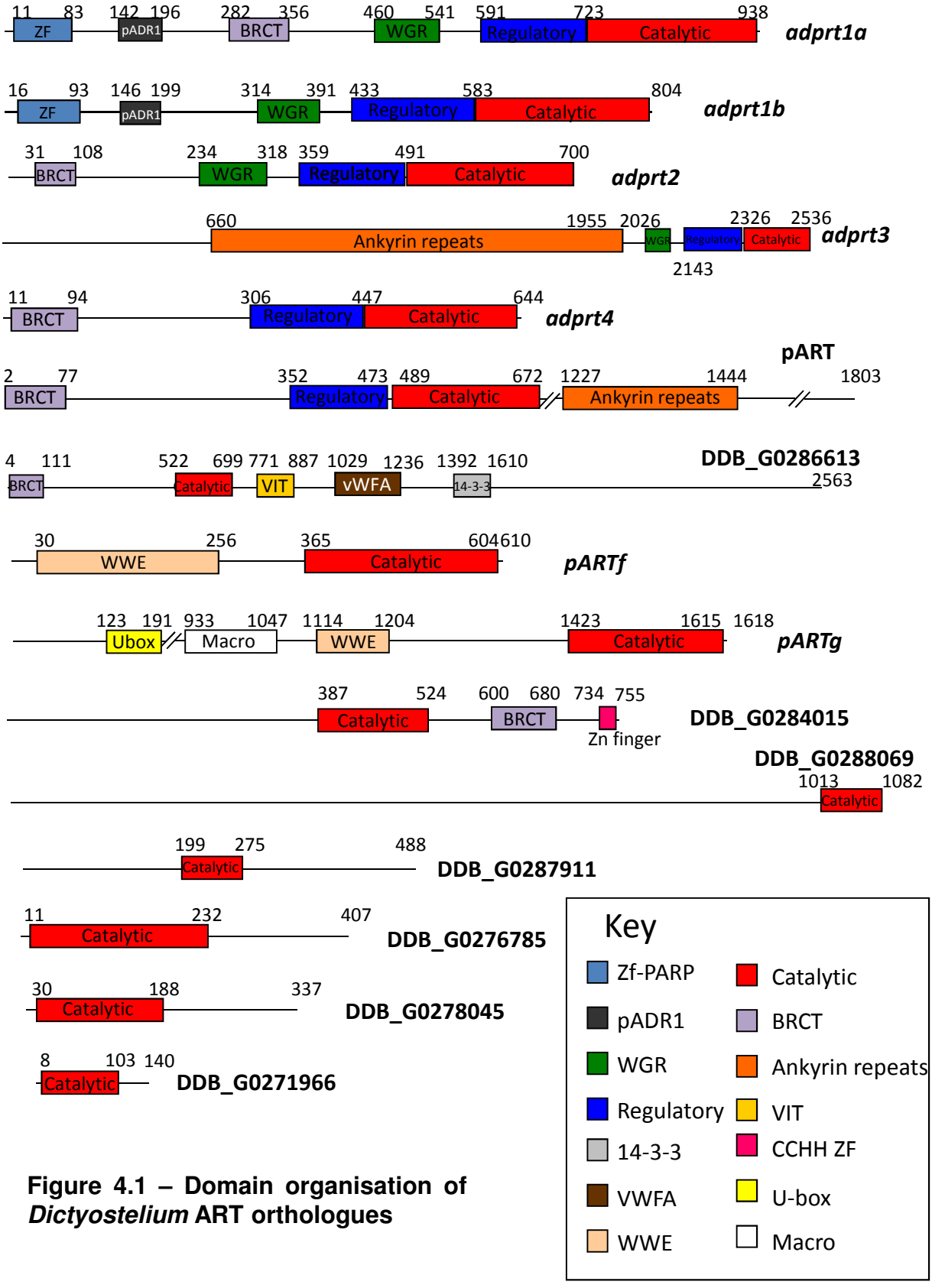

Figure 4.1 – Domain organisation of *Dictyostelium* ART orthologues

Figure 4.1 – Domain organisation of *Dictyostelium* ART orthologues.

Putative protein domains were identified by IntroPro on dictyBase.org and are indicated by the coloured boxes. The Zf domain is identical to the hPARP1 zinc-finger 1 and is proposed to confer DNA binding function. The pADR1 domain has unknown function, but contains the recently identified ZF3 which transmits the DNA binding signal to the catalytic domain to achieve activation. WGR domains are putative nucleic acid binding domains with possible RNA binding capacity. The regulatory domain has been shown to increase the catalytic activity of proteins that contain it, and may be involved in regulating branching activity. The 14-3-3, WWE, vWFA, BRCT (Breast cancer suppressor protein-1 C-terminal), Ankryin repeat and VIT domains are all thought to be involved in mediating protein-protein interactions. U-box domains are salt-bridge and hydrogen-bond stabilised domains found in E3 Ubiquitin ligases that are disctinct from Ring-finger domains. CCHH zinc fingers are putative DNA/RNA binding motifs. The macrodomain is a PAR binding motif. The catalytic domain may confer PARP catalytic activity and contains the highly conserved NAD^+ binding signature.

A) Full-length hPARP1

Gene	Identity (%)	Similarity (%)
adprt1a	30	45
adprt1b	31	50
adprt2	29	41
adprt3	7	12
adprt4	18	33
pART	6	11
DDB_G0286613	1	2
pARTf	4	5
pARTg	4	6
DDB_G0276785	5	11

B) Catalytic domain

Gene	Identity (%)	Similarity (%)
adprt1a	43	62
adprt1b	37	57
adprt2	44	61

C) NAD^+ catalytic triad

Gene	Identity (%)	Similarity (%)
adprt1a	78	84
adprt1b	50	66
adprt2	80	90

Table 4.3 – Degree of homology between hPARP1 and *Dictyostelium* PARP orthologues.

A) A BLASTp search using full-length hPARP1 was performed against the *Dictyostelium* protein database on dictyBase.org. **B and C)** Using BLASTp, the degree of sequence identity and similarity of the three putative *Dictyostelium* DNA damage response ARTs, *adprt1a, adprt1b* and *adprt2* were calculated against the hPARP1 **B)** catalytic domain (amino acids 663-1014) and **C)** amino acids incorporating the NAD^+ catalytic triad (amino acids 862-988). The hPARP1 sequence was acquired from NCBI.

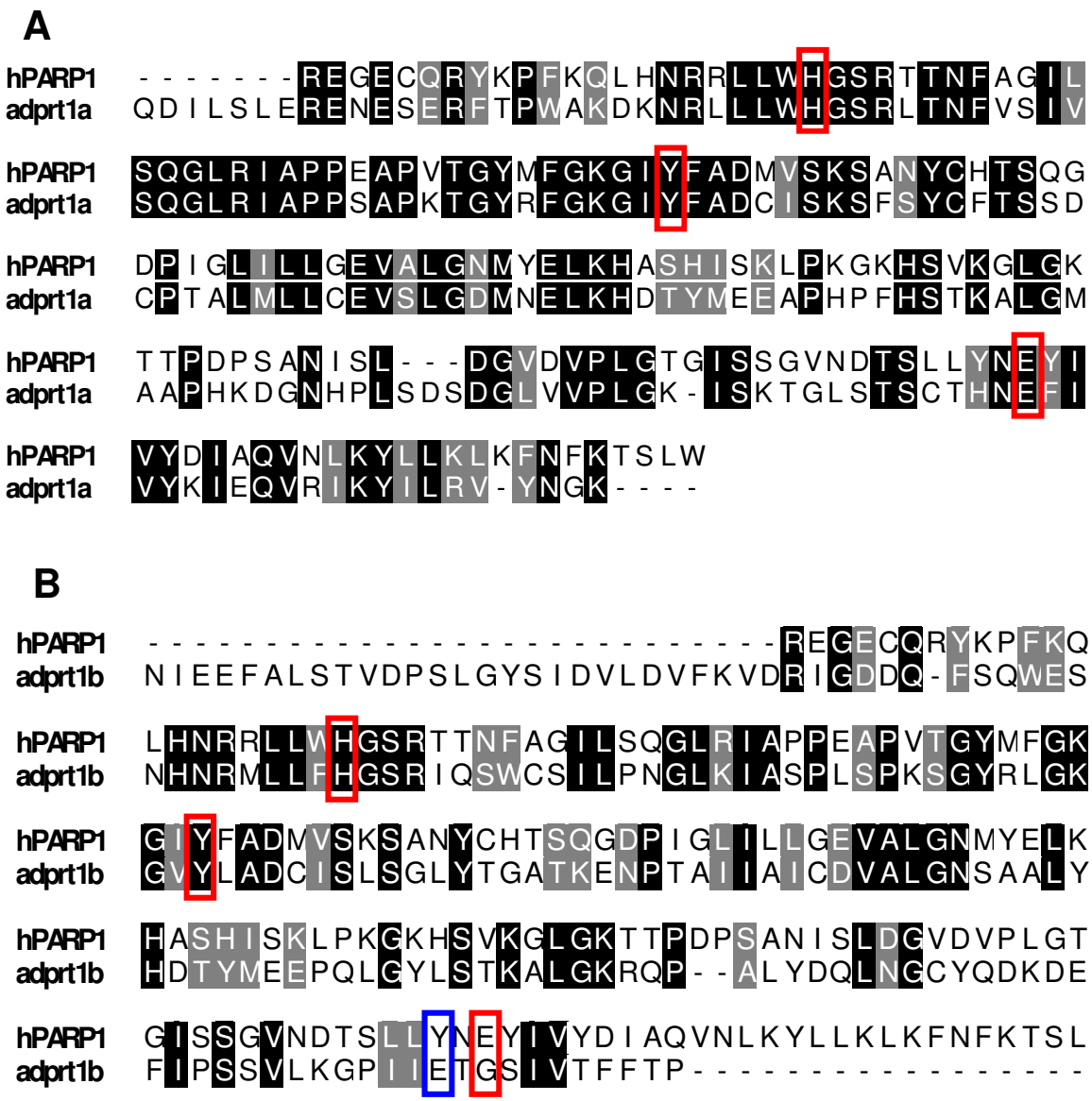

Figure 4.2 – The degree of conservation of the HYE catalytic triad in putative *Dictyostelium* DNA damage response PARPs

The hPARP1 sequence incorporating the amino acids of the catalytic triad (amino acids 859-988) was aligned with full-length *Dictyostelium* **A)** *adprt1a* and **B)** *adprt1B* using ClustalW and presented with Bioedit. Conserved amino acids are shaded in black, and similar amino acids are shaded in grey. Those residues outlined in red represent the human HYE catalytic triad, and the corresponding amino acids in *Dictyostelium*. For *adprt1b* **(B)**, the residue highlighted in blue may function as the catalytic glutamate.

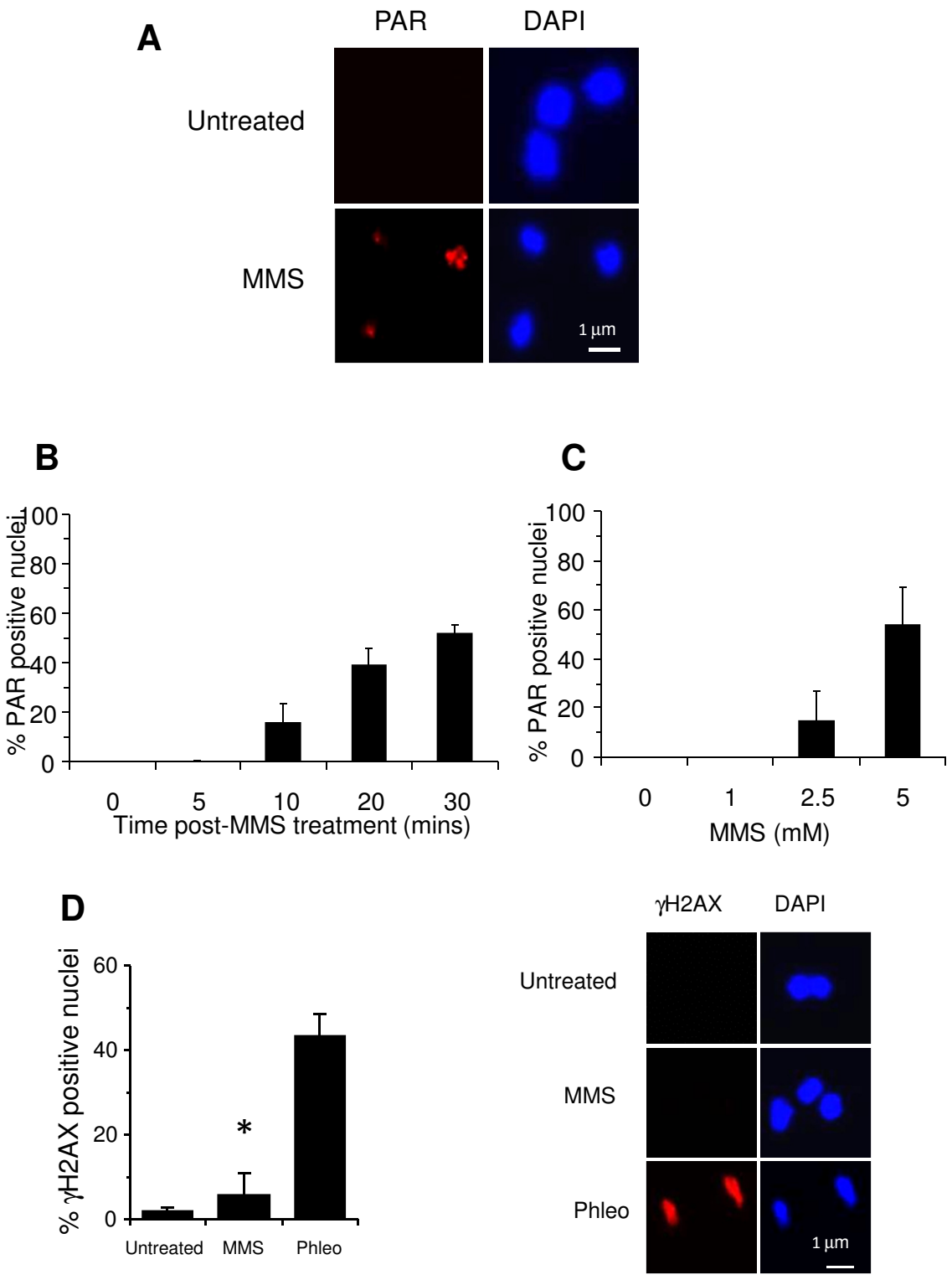

Figure 4.3 – PARylation is induced in *Dictyostelium* following MMS treatment in a time- and concentration-dependent manner

Figure 4.3 – PARylation is induced in *Dictyostelium* following MMS treatment in a time- and concentration-dependent manner.
A) Exponentially growing Ax2 cells were untreated or treated with 5mM MMS for 30 mins on coverslips. Coverslips were processed for immunofluorescence and stained with PAR antibodies. **B)** Ax2 cells were left untreated or treated with 5mM MMS for the indicated times. Coverslips were processed for immunofluorescence using PAR-specific antibodies and the % PAR positive nuclei scored from a population of >200 nuclei. Error bars represent the SEM from 3 independent experiments. **C)** Ax2 cells were left untreated or treated with the indicated concentrations of MMS for 30 minutes. Coverslips were processed for immunofluorescence using PAR-specific antibodies and the % PAR positive nuclei scored from a population of >200 cells. Error bars represent the SEM from 3 independent experiments **D)** Ax2 cells were left untreated or treated with MMS (5mM) or phleomycin (Phleo; 100 μg/ml) for 30 min and processed for immunofluorescence using γ-H2AX specific antibodies. Representative images are illustrated in the right panel. The % γ-H2AX positive cells were scored from a population of >200 cells (Left panel). Error bars represent the SEM from 3 independent experiments. * $P<0.05$ compared to the phleomycin treated control. No significant difference in γH2AX foci between the MMS treated and untreated control was calculated.

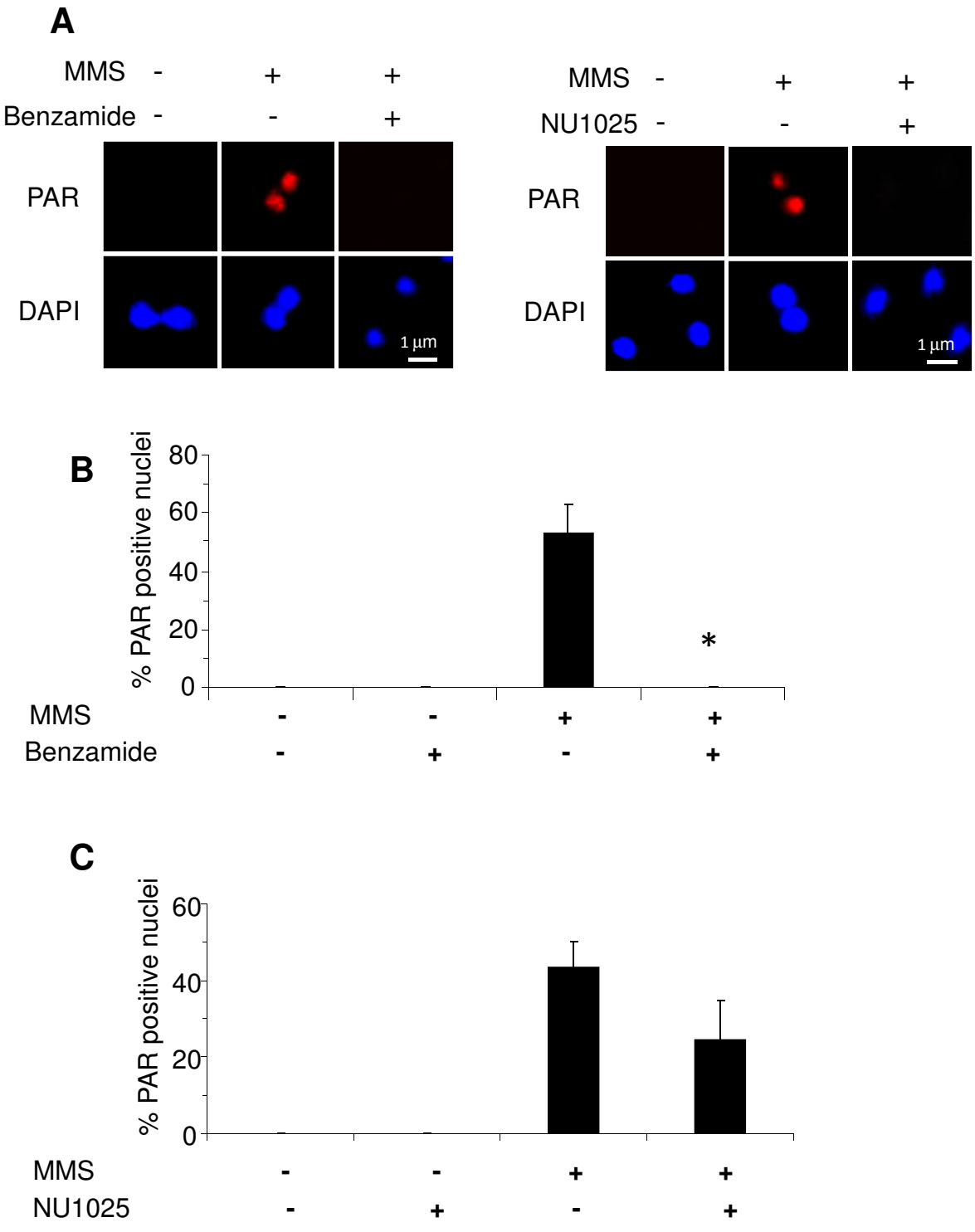

Figure 4.4 – MMS induced PARylation can be inhibited by the PARP inhibitors Benzamide and NU1025

Figure 4.4 – MMS induced PARylation can be inhibited by the PARP inhibitors Benzamide and NU1025

A) Ax2 cells were pretreated with 5mM benzamide or carrier (ethanol) (left panel) or 1mM NU1025 or carrier (DMSO) (right panel) and then exposed to 5mM MMS for 30 mins. Coverslips were processed for immunofluorescence using PAR antibodies. **B and C)** Quantification of immunofluoresence carried out above for either **B)** Benzamide or **C)** NU1025. The % PAR positive nuclei were scored from a population of >200 nuclei. Error bars represent the SEM from three independent experiments. * $p<0.05$ compared to MMS treated carrier control.

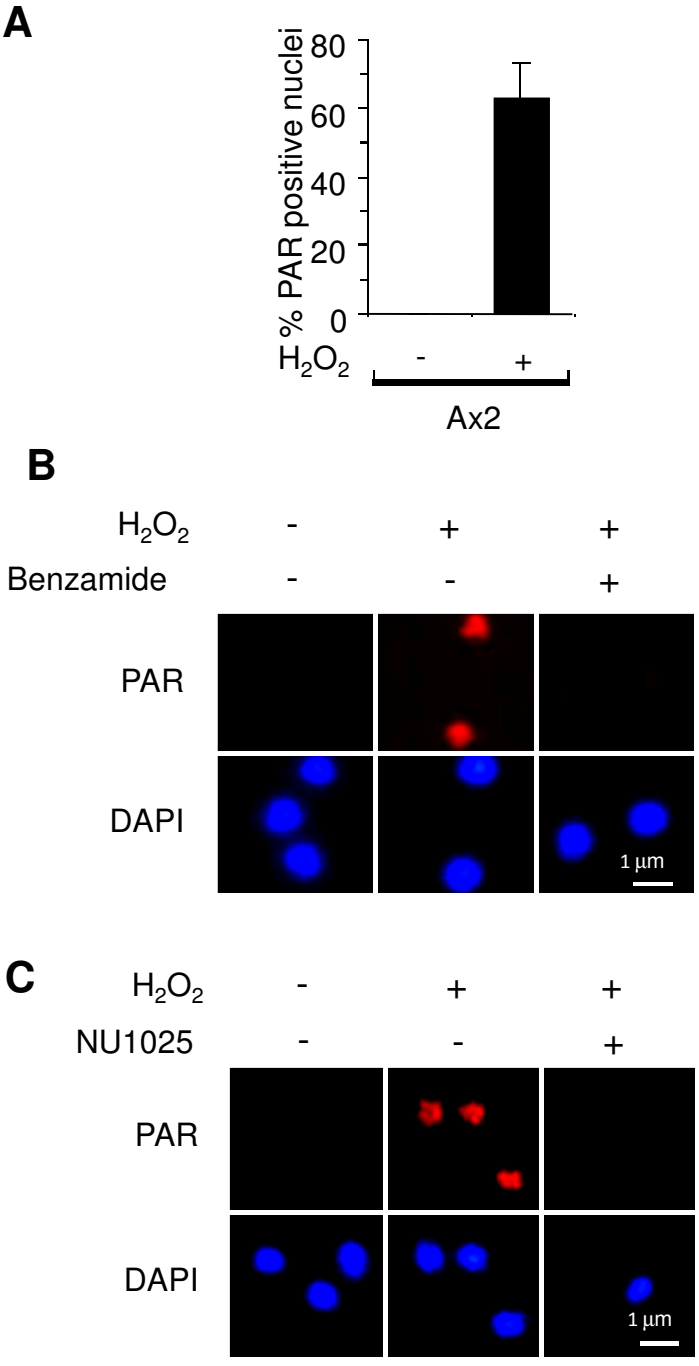

Figure 4.5 – H_2O_2 induced PARylation can be inhibited by the PARP inhibitors Benzamide and NU1025

Figure 4.5 – H_2O_2 induced PARylation can be inhibited by the PARP inhibitors Benzamide and NU1025

A) Ax2 cells were treated with 0.5mM H_2O_2 for 10 mins. Coverslips were processed for immunofluorescence using an antibody against PAR. % PAR positive nuclei were scored from a population of >200 nuclei. Error bars represent the SEM from three independent experiments. **B and C)** Ax2 cells were pretreated with 5mM benzamide or carrier (ethanol) (B) or 1mM NU1025 or carrier (DMSO) (C) and then exposed to 0.5mM H_2O_2 for 10 mins. Coverslips were processed for immunofluorescence using an antibody against PAR.

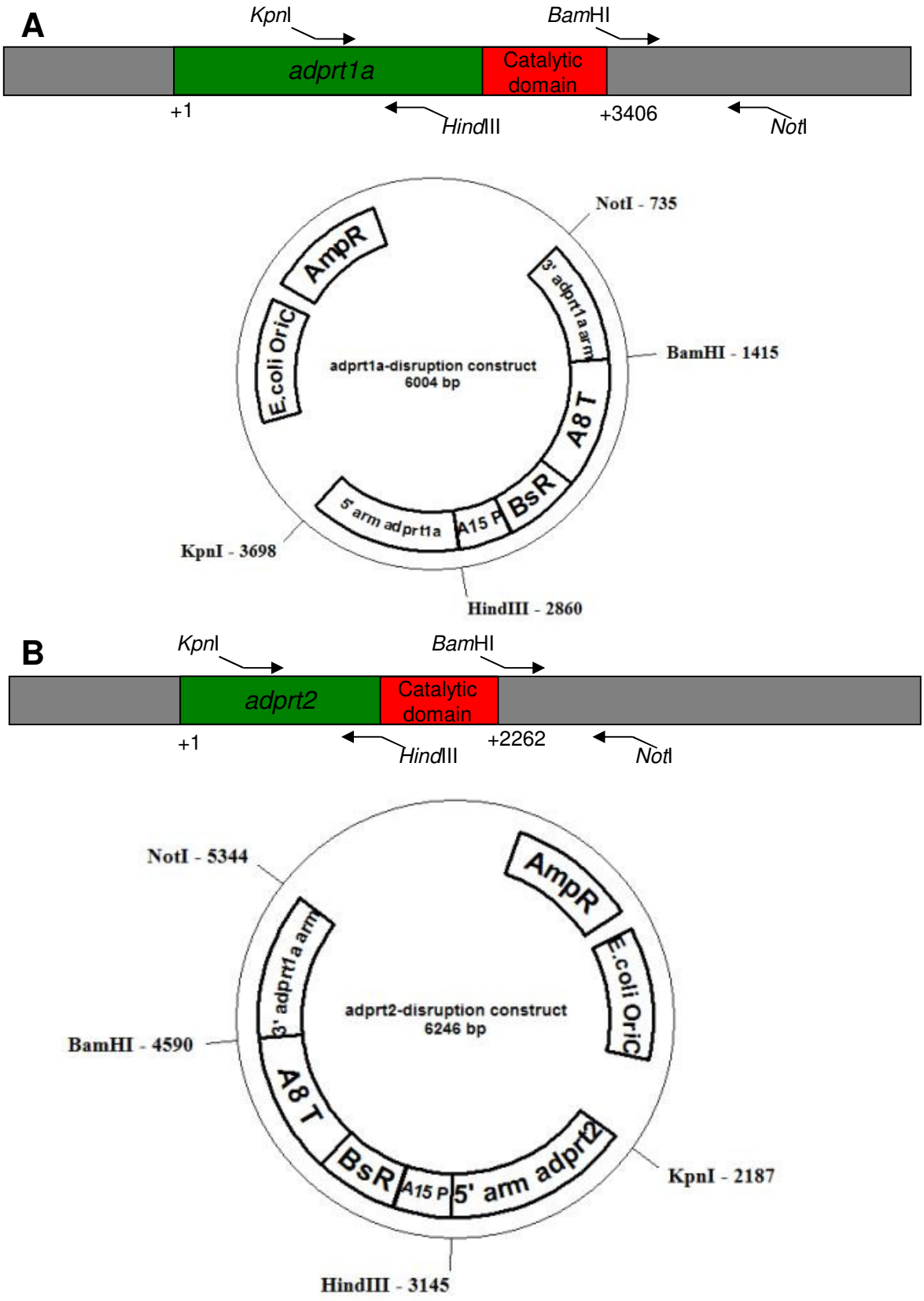

Figure 4.6 – Generation of the *adprt1a*- and *adprt2*-disruption constructs

Figure 4.6 – Schematic diagram to represent the generation of the *adprt1a* and *adprt2* disruption constructs.

A) The region shaded in green represents the *adprt1a* gene in the context of *Dictyostelium* genomic DNA (grey), with the *adprt1a* catalytic domain highlighted in red. Genomic DNA upstream (+1070 to +1907) and downstream (+3643 to +4375) of the *adprt1a* catalytic domain was amplified by PCR using primers that were designed with the indicated restriction enzyme sites incorporated into the sequence. +1 represents the A of the initiating ATG codon and positively numbered basepairs refer to sequences downstream of the initiating ATG codon. The position +3406 represents the final nucleotide of the STOP codon. **B)** The region shaded in green represents the *adprt2* gene in the context of *Dictyostelium* genomic DNA (grey), with the *adprt2* catalytic domain highlighted in red. Genomic DNA upstream (+543 to +1500) and downstream (+2482 to +3236) of the *adprt2* catalytic domain was amplified by PCR using primers that were designed with the indicated restriction enzyme sites incorporated into the sequence. +1 represents the A of the initiating ATG codon and positively numbered basepairs refer to sequences downstream of the initiating ATG codon. The position +2262 represents the final nucleotide of the STOP codon. For generation of disruption constructs for **A) *adprt1a*** and **B) *adprt2,*** the primer pairs used for the 5' (upstream) and 3' (downstream) fragments were *Kpn*I+*Hind*III and *Bam*HI+*Not*I, respectively (primer sequences are listed in Appendix A, and these fragments were digested with the relevant restriction enzymes. The 5' arm was cloned into *Kpn*I/*Hind*III digested pLPBLP, before digesting the resulting vector with *Bam*HI/*Not*I to clone in the 3' arm. The success of the cloning strategy was verified by restriction enzyme digests and sequencing (data not shown). In both cases, prior to transfection into Ax2, the disruption constructs were digested with *Kpn*I and *Not*I and cleaned up as outlined in the materials and methods. Plasmid maps were drawn using pDRAW32 and sequences were acquired from dictyBase.org.

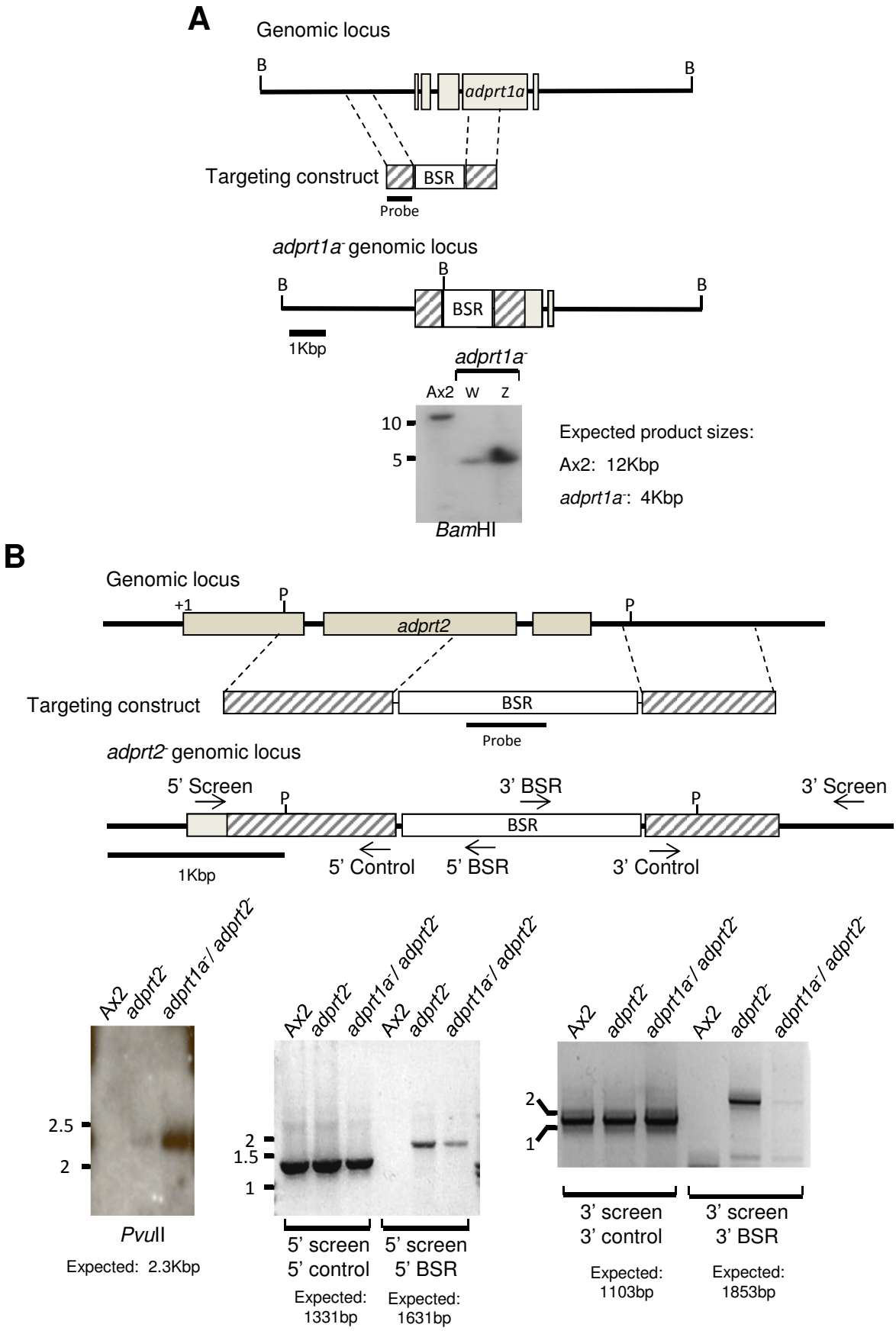

Figure 4.7 – Verification of the *adprt1a*⁻, *adprt2*⁻ and *adprt1a*⁻/*adprt2*⁻ strains by Southern blotting

Figure 4.7 – Verification of the *adprt1a*$^-$, *adprt2* and *adprt1a*$^-$/*adprt2*$^-$ strains by Southern blotting

A) Map of *adprt1a* locus in the parental and disruption strains are illustrated (upper and lower panels respectively). Hatched boxes represent the regions of homology used in the disruption construct. Grey boxes in genomic locus indicate exons of the *adprt1a* gene, and the +1 indicates the A of the initiating ATG codon. The disruption strategy leads to replacement of the entire *adprt1a* catalytic domain with the BSR cassette. Integrants were screened by PCR (data not shown) and two clones that exhibited disruption of the *adprt1a* gene selected. These clones were further verified by Southern blotting using the indicated probe, against *Bam*HI (B)-digested genomic DNA. In Ax2, Southern hybridisation gives rise to a band of 12kbp which is reduced to 4kbp in the *adprt1a*$^-$ strain. An additional Southern blot was performed with a BSR probe to confirm a single integration event (data not shown). **B)** Map of the *adprt2* locus in the parental and disruption strain are illustrated (upper and lower panels respectively) with *Pvu*II restriction sites (P) marked. Hatched boxes represent the regions of homology used in the disruption construct. Grey boxes in genomic locus indicate exons of the *adprt1a* gene, and the +1 indicates the A of the initiating ATG codon. The disruption strategy leads to replacement of the *adprt2* region that encodes the catalytic domain with the BSR cassette. Ax2 and *adprt1a*$^-$ cells were transfected with the disruption construct to generate *adprt2*$^-$ and *adprt1a*$^-$/*adprt2*$^-$ strains, respectively. Preliminary verification was by PCR with the indicated screening primers giving rise to products in successful integrants only. Further verification to confirm a single integration event was by Southern hybridisation using a probe against the BSR cassette on *Pvu*II (P)-digested genomic DNA (Left hand panel), which gives rise to a 2.3kbp band in the disruptants. The screening of the *adprt2*$^-$ and *adprt1a*$^-$/*adprt2*$^-$ disruptants was carried out by J. Green and H. Wang.

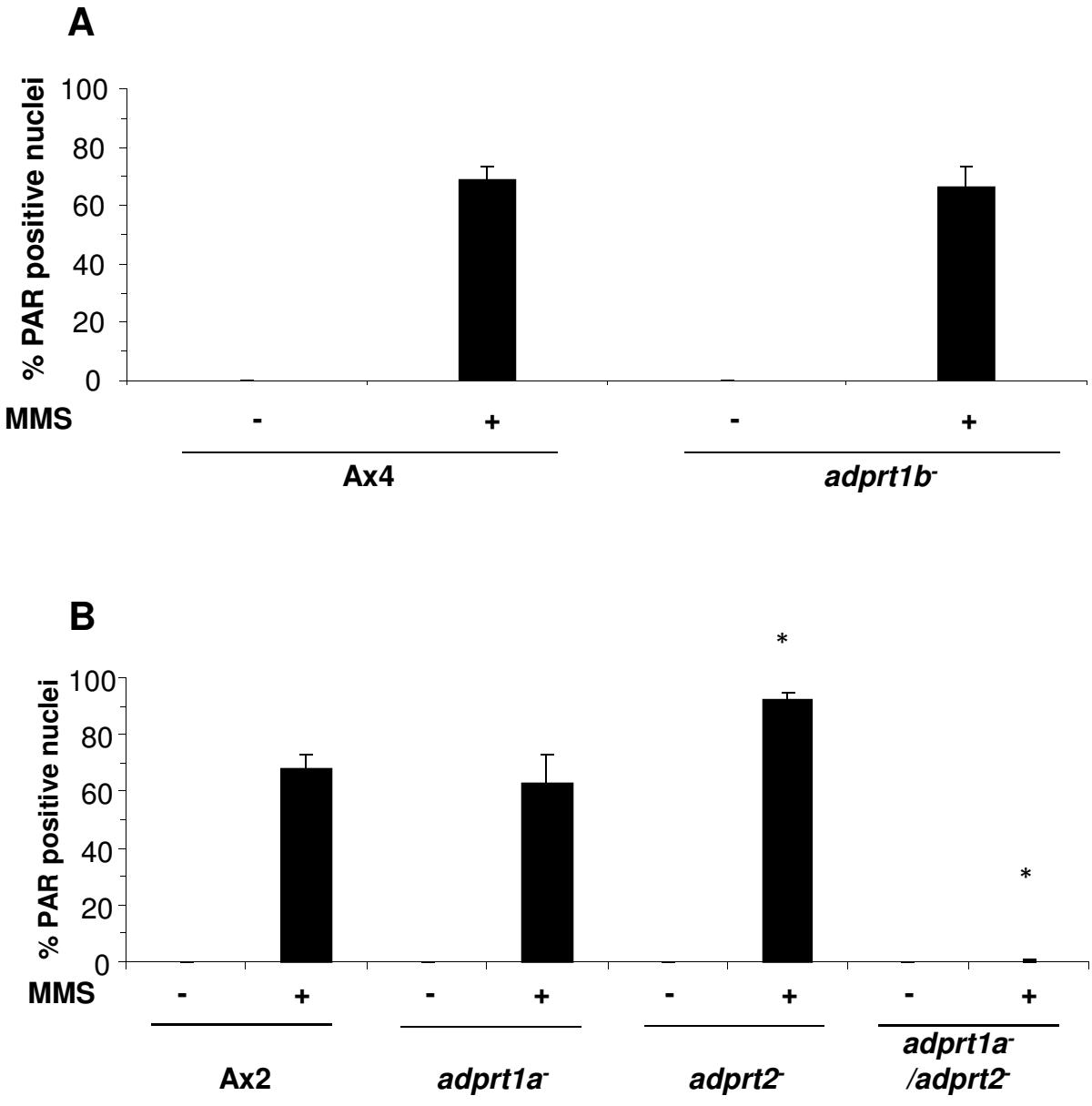

Figure 4.8 – Analysis of MMS induced PARylation in the *adprt1a*$^-$, *adprt2*, *adprt1a*$^-$/*adprt2*$^-$ and *adprt1b*$^-$ strains relative to their parental controls

A) Exponentially growing Ax4 and *adprt1b*$^-$ strains were treated with 5mM MMS for 30 mins and coverslips processed for immunofluorescence using an antibody against PAR. %PAR positive nuclei were scored from a population of >200 nuclei. Error bars represent the SEM from three independent experiments **B)** Exponentially growing Ax2, *adprt1a*$^-$, *adprt2*$^-$ and *adprt1a*$^-$/*adprt2*$^-$ strains were treated with 5mM MMS for 30 mins and coverslips processed for immunofluorescence using an antibody against PAR. %PAR positive nuclei were scored from a population of >200 nuclei. Error bars represent the SEM from three independent experiments. *$p<0.05$ relative to MMS treated Ax2.

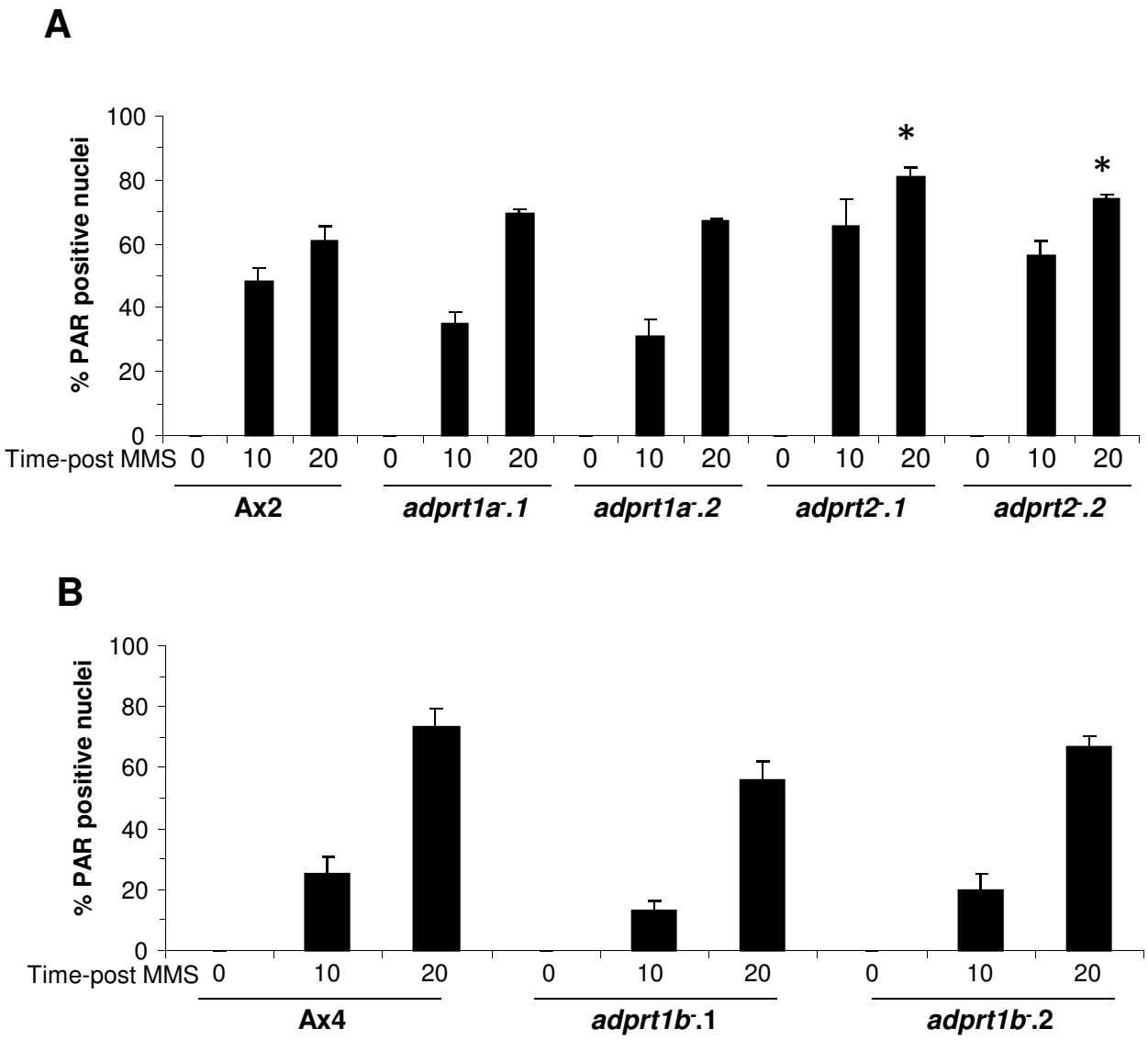

Figure 4.9 – PARylation time-course following 5mM MMS treatment
A) Exponentially growing Ax2, and both clones of *adprt1a*$^-$ and *adprt2*$^-$, were treated with 5mM MMS, and coverslips processed for immunofluorescence at the indicating times using an antibody against PAR. %PAR positive nuclei were scored from a population of >200 nuclei. Error bars represent the SEM from three independent experiments. *$p<0.05$ relative to MMS treated Ax2 at the equivalent time point. **B)** Exponentially growing Ax4 cells and both *adprt1b*$^-$ clones were treated with 5mM MMS, and coverslips processed for immunofluorescence at the indicating times using an antibody against PAR. %PAR positive nuclei were scored from a population of >200 nuclei. Error bars represent the SEM from three independent experiments.

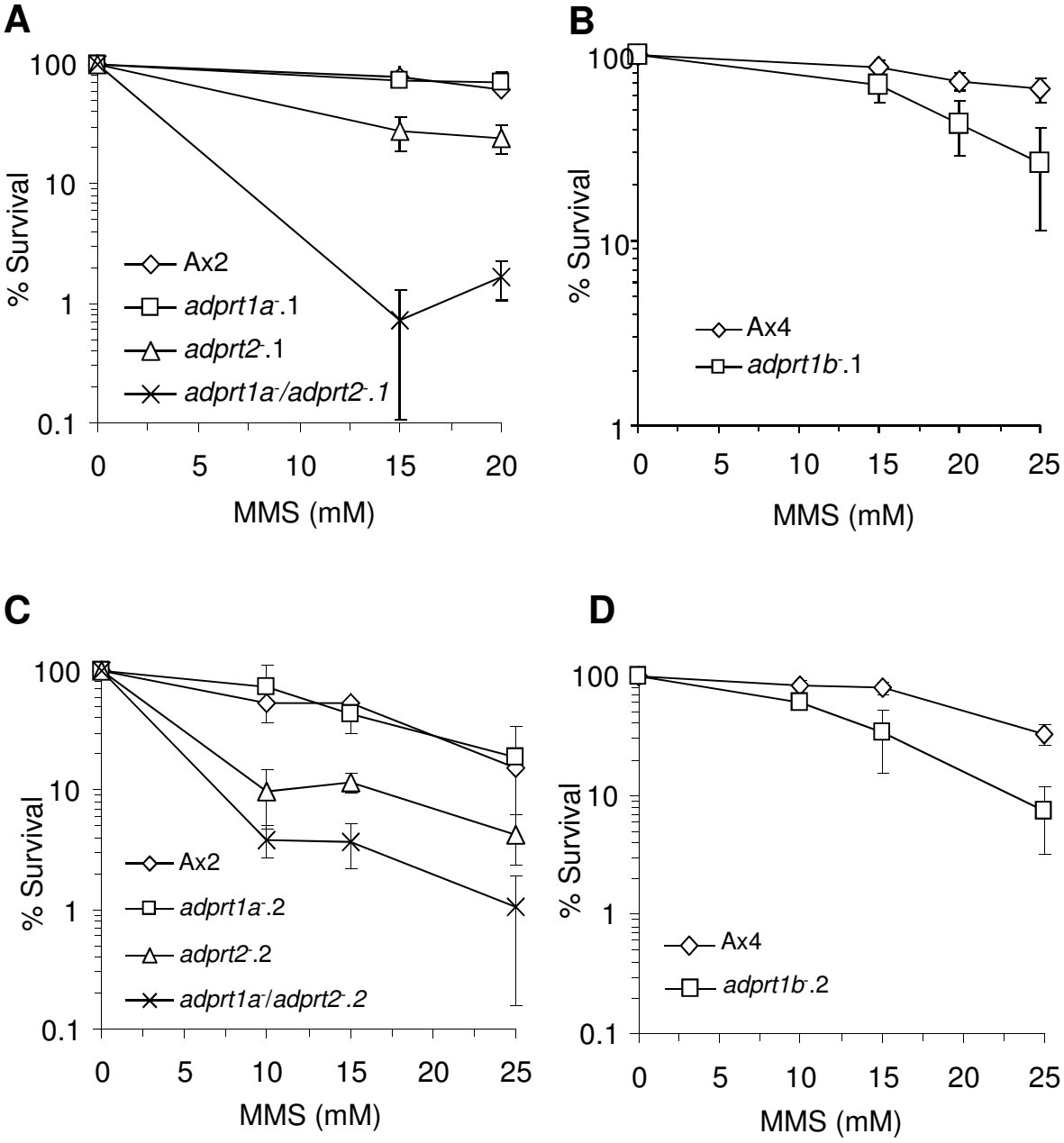

Figure 4.10 – Survival of *adprt1a*$^-$, *adprt2*$^-$, *adprt1a*$^-$/*adprt2*$^-$ and *adprt1b*$^-$ to increasing concentrations of MMS

Figure 4.10 – Survival of *adprt1a*$^-$, *adprt2*$^-$, *adprt1a*$^-$*/adprt2*$^-$ and *adprt1b*$^-$ to increasing concentrations of MMS

A) Ax2, *adprt1a*$^-$.1, *adprt2*$^-$.1 and *adprt1a*$^-$*/adprt2*$^-$.1 were exposed to increasing concentrations of MMS for 1 hour, and survival assessed. Error bars represent the SEM from three independent experiments. **B)** Ax4 and *adprt1b*$^-$.1 were exposed to increasing concentrations of MMS for 1 hour, and survival assessed. Error bars represent the SEM from three independent experiments. **C)** Ax2, *adprt1a*$^-$.2, *adprt2*$^-$.2 and *adprt1a-/adprt2*$^-$.2 were exposed to increasing concentrations of MMS for 1 hour, and survival assessed. Error bars represent the SEM from three independent experiments. **D)** Ax4 and *adprt1b*-.2 were exposed to increasing concentrations of MMS for 1 hour, and survival assessed. Error bars represent the SEM from three independent experiments.

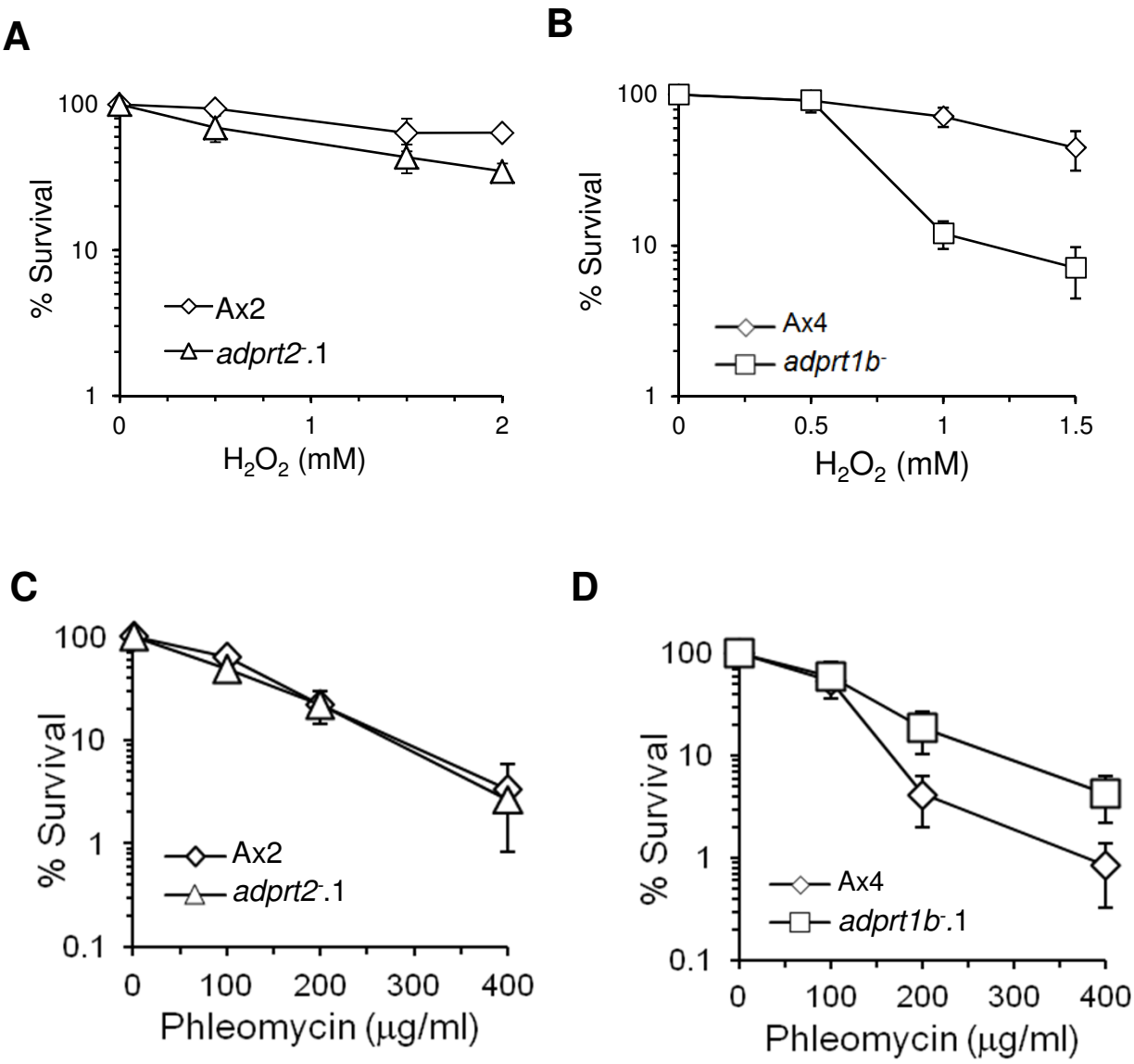

Figure 4.11 – Survival of *adprt1a*$^-$, *adprt2*$^-$, *adprt1a*$^-$/*adprt2*$^-$ and *adprt1b*$^-$ to increasing concentrations of MMS

A) Ax2 and *adprt2*$^-$.1 were exposed to increasing concentrations of H_2O_2 for 1 hour, and survival assessed. Error bars represent the SEM from three independent experiments. **B)** Ax4 and *adprt1b*$^-$.1 were exposed to increasing concentrations of H_2O_2 for 1 hour, and survival assessed. Error bars represent the SEM from three independent experiments. **C)** Ax2, and *adprt2*$^-$.1 were exposed to increasing concentrations of phleomycin for 1 hour, and survival assessed. Error bars represent the SEM from three independent experiments. **D)** Ax4 and *adprt1b*-.1 were exposed to increasing concentrations of phleomcyin for 1 hour, and survival assessed. Error bars represent the SEM from three independent experiments.

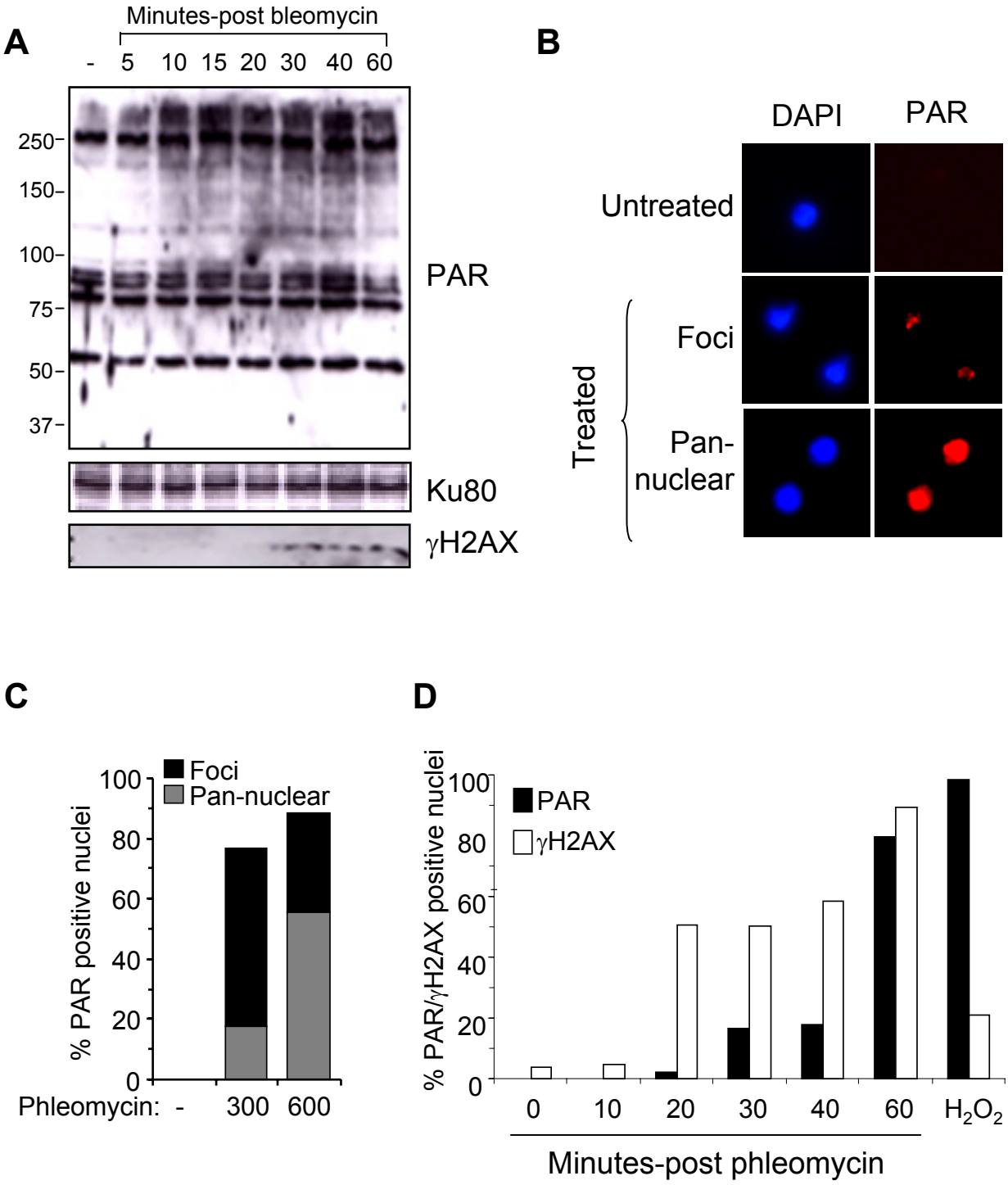

Figure 5.1 - PARylation is induced in *Dictyostelium* following treatment with both phleomycin and bleomycin

Figure 5.1 - PARylation is induced in *Dictyostelium* following treatment with both phleomycin and bleomycin

A) Ax2 were left untreated or treated with 100mU/ml bleomycin. At the indicated timepoints, whole-cell lysates were prepared and analysed by Western blot using a polyclonal antibody against PAR. Samples were also probed with Ku80 as a loading control and γH2AX as a marker for the induction of DNA DSBs. **B)** Ax2 were treated with 300μg/ml or 600μg/ml phleomycin for 30 mins, and processed for immunofluorescence using an antibody against PAR. **C)** Quantitative analysis of B). % PAR positive nuclei were scored from a population of >200 nuclei and catagorised according to the extent of PARylation (focal or pan-nuclear). The graph represents data from a single experiment that was repeated three times. **D)** Exponentially growing Ax2 were treated with either 100μg/ml phleomycin for the indicated time points, or 0.5mM H_2O_2 for 10 mins. Coverslips were processed for immunofluorescence using an antibody against PAR or γH2AX, and % PAR or % γH2AX nuclei were scored from a population of >200 nuclei. The graph represents data from a single experiment that was repeated two times.

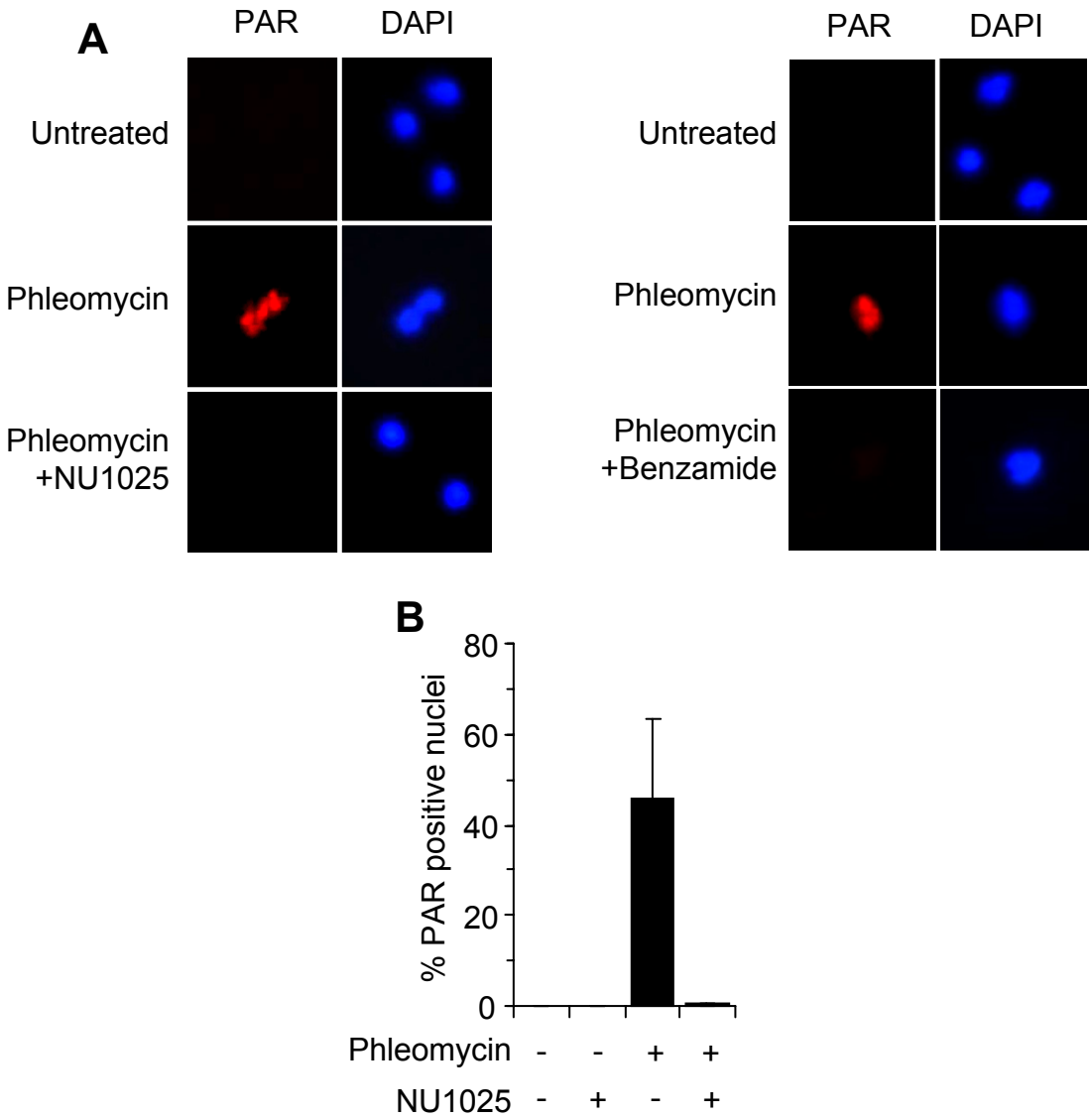

Figure 5.2 - DSB-induced PARylation can be inhibited by PARP inhibitors Benzamide and NU1025

A) Exponentially growing Ax2 were pretreated for 1 hour with 1mM NU1025 or DMSO (left panel) or 5mM Benzamide or ethanol (right panel) before being exposed to 100μg/ml phleomycin for 30 mins. Coverslips were processed for immunofluorescence using an antibody against PAR. **B)** Quantification of inhibition of phleomycin-induced PARylation by NU1025. Cells were processed as in B) and the % PAR positive nuclei scored from a population of >200 nuclei. Error bars represent the SEM from three independent experiments.

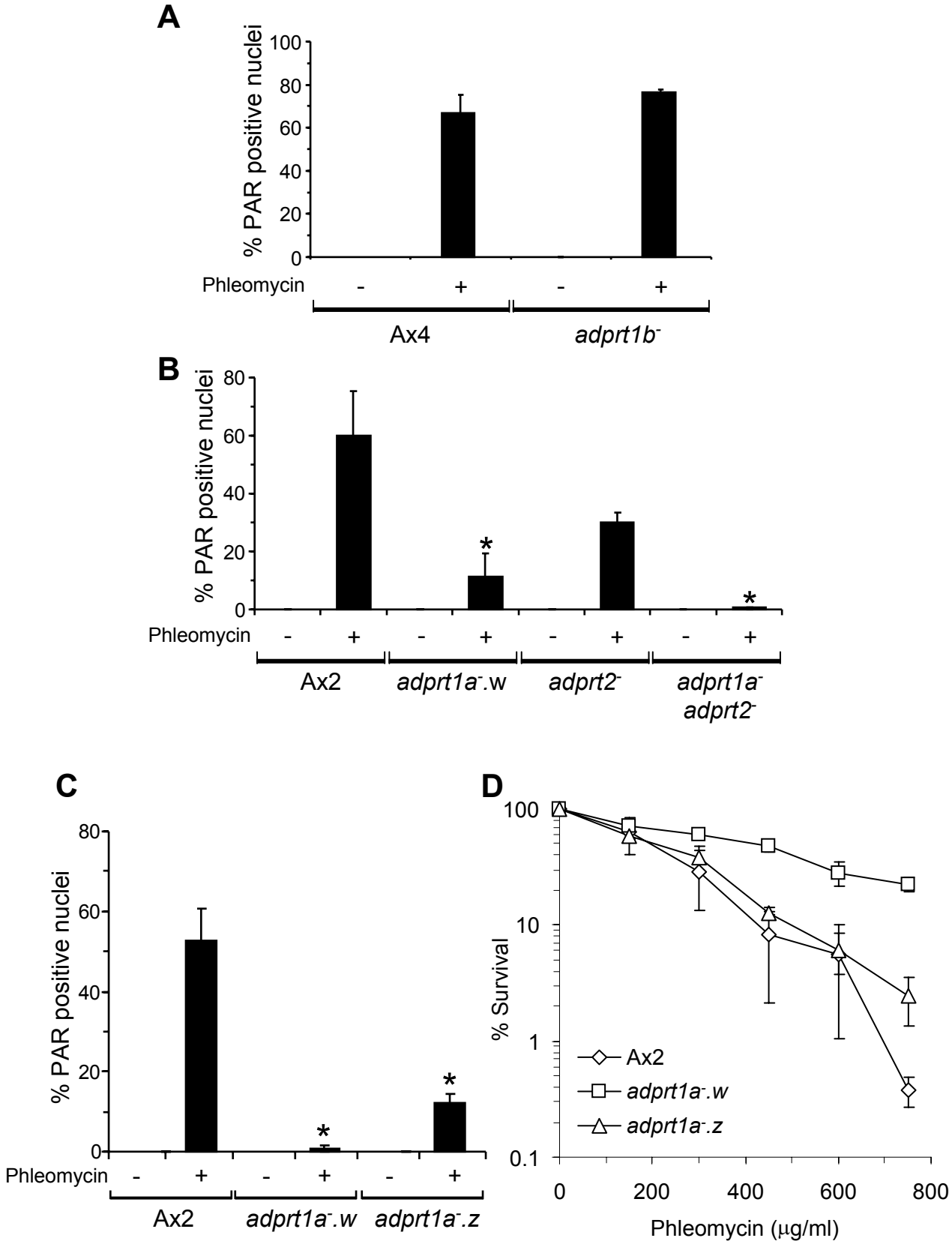

Figure 5.3 - Analysis of phleomycin induced PARylation in the *adprt1a*$^-$, *adprt2*$^-$, *adprt1a*$^-$/*adprt2*$^-$ and *adprt1b*$^-$ strains relative to their parental controls

Figure 5.3 - Analysis of phleomycin induced PARylation in the *adprt1a*-, *adprt2*$^-$, *adprt1a*$^-$/*adprt2*$^-$ and *adprt1b*$^-$ strains relative to their parental controls.

A) Exponentially growing Ax4 or *adprt1b*$^-$ were treated with 100μg/ml phleomycin for 30mins, and coverslips processed for immunofluorescence using an antibody against PAR. % PAR positive nuclei were scored from a population of >200 nuclei. Error bars represent the SEM from three independent experiments. **B)** Exponentially growing Ax2, *adprt1a*$^-$, *adprt2*$^-$, *adprt1a*$^-$/*adprt2*$^-$ were treated with 100μg/ml phleomycin for 30mins, and coverslips processed for immunofluorescence using an antibody against PAR. % PAR positive nuclei were scored from a population of >200 nuclei. Error bars represent the SEM from three independent experiments. * $p<0.05$ relative to phleomycin treated Ax2. **C)** Exponentially growing Ax2 and two *adprt1a*$^-$ clones were treated with 100μg/ml phleomycin for 30mins, and coverslips processed for immunofluorescence using an antibody against PAR. % PAR positive nuclei were scored from a population of >200 nuclei. Error bars represent the SEM from three independent experiments. *$p<0.05$ relative to phleomycin treated Ax2. **D)** Ax2 and two *adprt1a*$^-$ clones were treated with increasing concentrations of phleomycin for 1 hour and survival assessed. Error bars represent the SEM from three independent experiments.

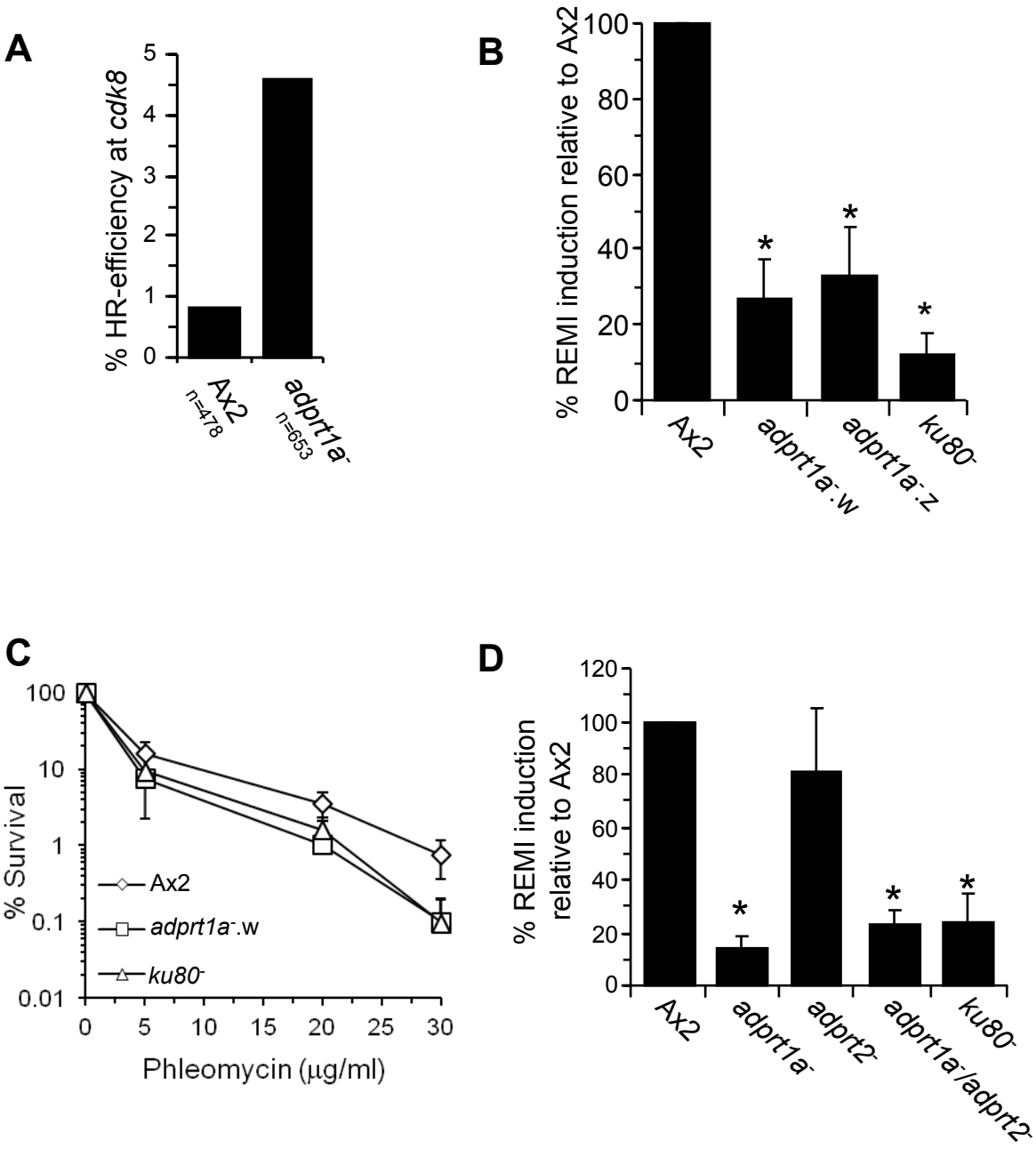

Figure 5.4 - Analysis of DSB repair in the *adprt1a*$^{-}$, *adprt2*$^{-}$ and *adprt1a*$^{-}$/*adprt2*$^{-}$ strain

Figure 5.4 - Analysis of DSB repair in the *adprt1a*$^{-}$, *adprt2*$^{-}$ and *adprt1a*$^{-}$/*adprt2*$^{-}$ strain

A) Ax2 and *adprt1a*$^{-}$ cells were assessed for HR efficiency by measuring targeted integration of the blasticidin resistance cassette at the *cdk8* locus. The % HR is the proportion of aggregation-deficient colonies against the total number of blasticidin resistant colonies. The *n* number represents to total of blasticidin resistant colonies analysed from multiple independent transfections. **B and D)** REMI efficiency of the indicated strains was assessed as described in Materials and Methods. The numbers analysed were such that experimental strains were compared to >200 colonies from the positive control (Ax2 plus restriction enzyme). Data is represented as % REMI induction relative to parental Ax2 controls. Error bars represent the SEM from three independent experiments. * $p<0.05$ compared to the positive control (Ax2). **C)** Ax2, *adprt1a*$^{-}$ and *ku80*$^{-}$ spores were germinated prior to exposure to increasing concentrations of phleomycin and cell survival established as described in Materials and Methods. Error bars represent the SEM from three independent experiments.

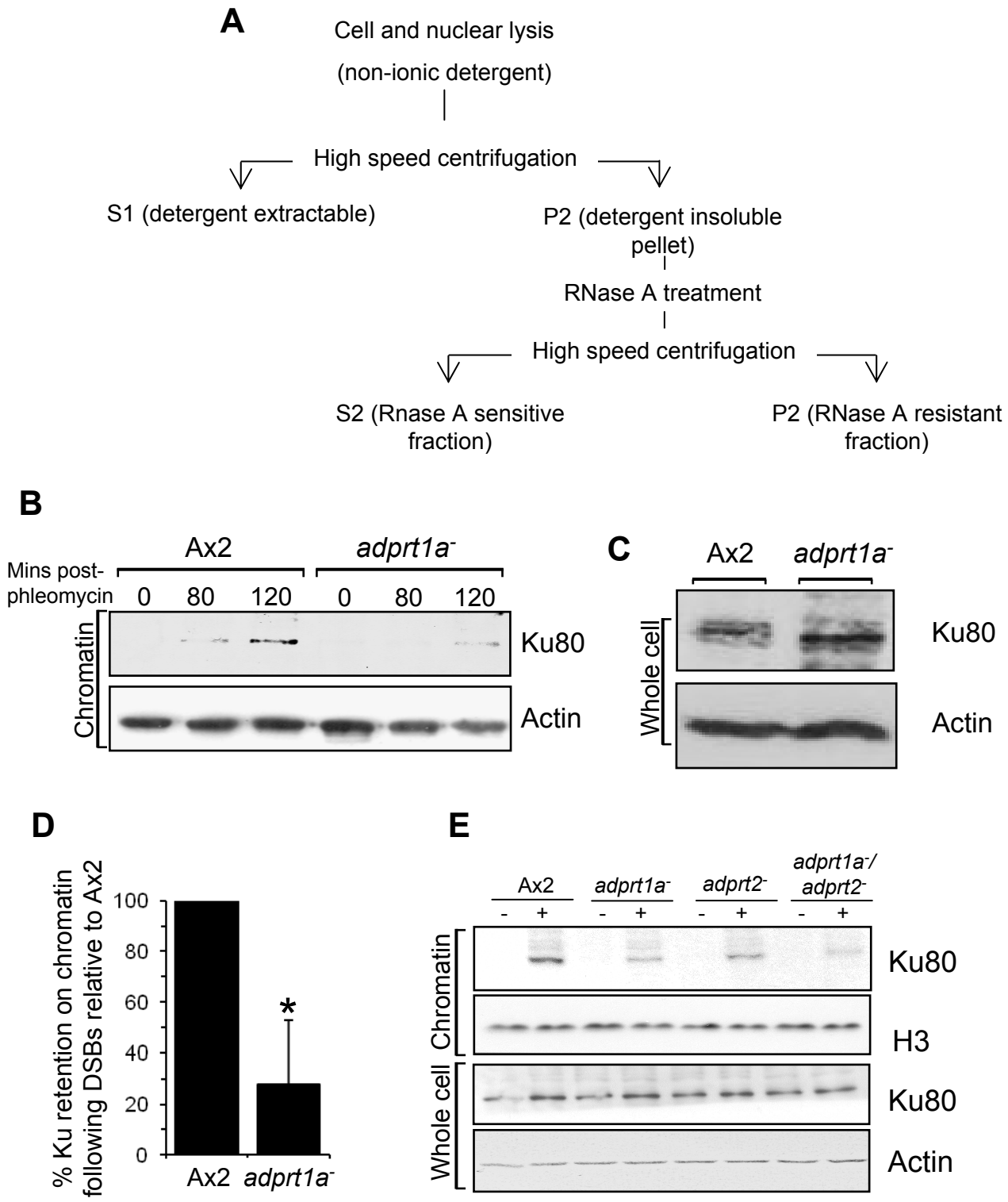

Figure 6.1 – The *adprt1a*$^-$, *adprt2*$^-$ and *adprt1a*$^-$/*adprt2*$^-$ strains shows reduced Ku80 chromatin recruitment following DNA DSBs.

Figure 6.1 – The *adprt1a*$^-$, *adprt2*$^-$ and *adprt1a*$^-$/*adprt2*$^-$ strains shows reduced Ku80 chromatin recruitment following DNA DSBs

A) Schematic of the chromatin isolation protocol. Fraction P2, which corresponds to the detergent insoluble, RNase A resistant fraction is presumed to contain chromatin and its associated proteins, including those proteins that mobilise to chromatin post-DNA damage. This fraction was therefore assessed by Western blot. **B)** Exponentially growing cells were treated with 100μg/ml phleomycin and at the indicated times, sub-cellular fractionation was performed as outlined in materials and methods. The detergent resistant fraction was analysed by Western blot and probed with antibodies against Ku80 or the loading control actin. **C)** A representative Western blot of whole-cell extracts from untreated Ax2 or *adprt1a*$^-$ cells. Blots were probed with antibodies against Ku80 or the loading control actin. **D)** Exponentially growing Ax2 and *adprt1a*- cells were left untreated or exposed to 100μg/ml phleomycin for 80 mins. Chromatin fractions were prepared and analysed by Western blot using antibodies against Ku80 or the H3. Following development with ECL, signals were detected using the Gel DocTM XR+ System (Bio-Rad), and their intensities quantified with image Lab software (Bio-Rad). Data was normalised to H3, and the fold induction of Ku80 signal in chromatin fractions determined relative to untreated controls. Data is represented as the % induction of Ku80 retention on chromatin induced on phleomycin treatment relative to Ax2. Error bars represent the SEM from three independent experiments. * $p<0.05$ compared to Ax2. Experiments for this figure were performed by H. Wang **E)** Top panel: Ku80 chromatin enrichment at 0 and 80 mins post-phleomycin treatment was determined for Ax2, *adprt1a*$^-$, *adprt2*$^-$ and *adprt1a*$^-$*/adprt2*$^-$ as in A). Samples were analysed by Western blot using antibodies against Ku80 and H3. Bottom panel: Whole cell extracts were prepared from the indicated strains at 0 and 80 mins post-phleomycin treatment. Samples were analysed by Western blot and probed with an antibody against Ku80 or Actin. Experiments for this figure were performed by H. Wang

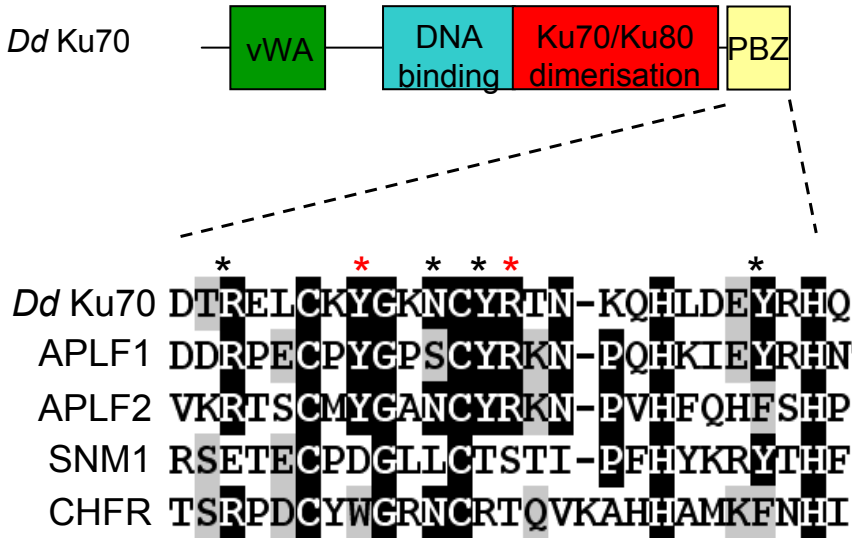

Figure 6.2 – The PBZ domain of Ku70 shows a high degree of sequence conservation to the PBZ domains of vertebrate proteins

Alignment of the PBZ domains present in *Dictyostelium* Ku70 and vertebrate APLF (APLF1 and APLF2), SNM1 and CHFR using ClustalW. Using the Bioedit programme, conserved amino acids were highlighted in black and similar amino acids highlighted in grey. Starred residues play key roles in interacting with PAR, with red starred residues making particularly important interactions.

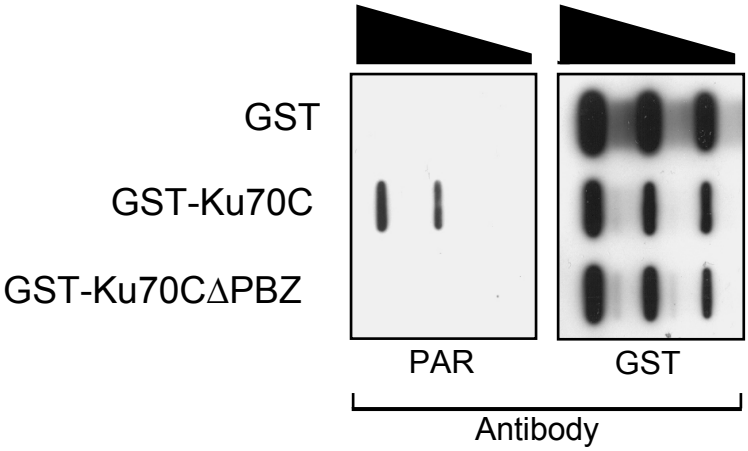

Figure 6.3 – The PBZ domain of Ku70 possesses PAR binding ability *in vitro*

A GST-tagged C-terminal 74 amino acid (GST-Ku70C) fragment, or the same fragment lacking the final 25 amino acids (GST-Ku70ΔPBZ) of *Dictyostelium* Ku70 were expressed in *E. coli* and purified via the GST tag. Proteins were slot-blotted onto a nitrocellulose membrane and incubated with commercially synthesised PAR. The membrane was probed with an antibody against PAR, and PAR binding visualised with ECL. Protein loading was verified with an antibody against GST. Experiments for this figure were performed by H. Wang

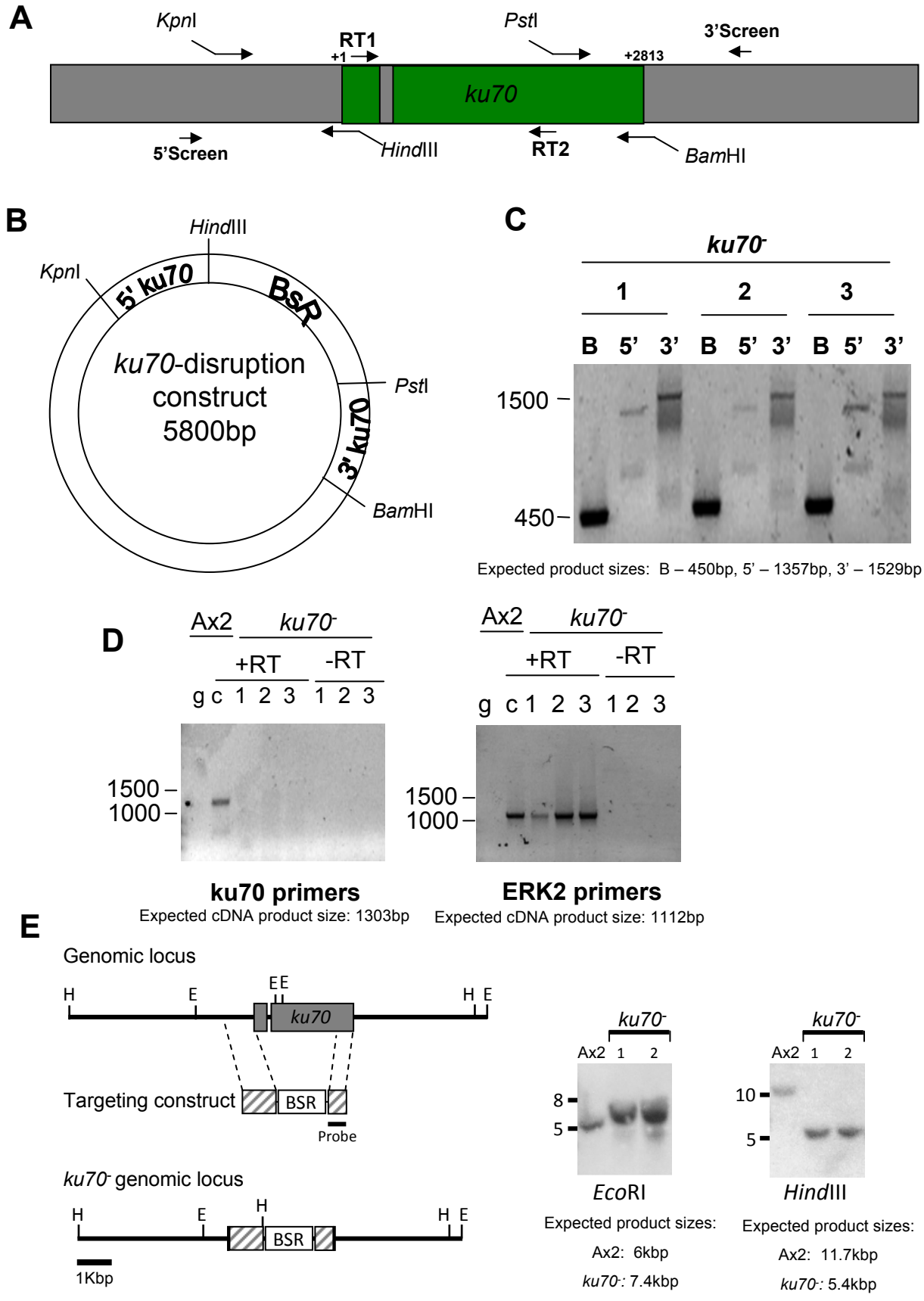

Figure 6.4 - Verification of *ku70*⁻ strain

Figure 6.4 - Verification of *ku70*$^{-}$ strain

A) Schematic diagram showing the *ku70* gene, represented by the green boxes. The gene is separated into two exons by an intron between positions +372bp to +456bp relative to the ATG (+1bp). Primers are represented by arrows and include: knockout construct cloning primers (*Kpn*I/*Hind*III and *Pst*I/*Bam*HI), RT-PCR primers (RT1/RT2) and screening primers (5' screen and 3' screen). The screening primers were used in combination with a BSR specific primer, and thus would only give rise to a product in targeted integration events. **B)** Schematic of the *ku70*-disruption construct. Genomic DNA upstream (-880 to +27) and downstream (+2357 to +2786) of the *ku70* gene (+1 to +2813) were amplified by PCR using *KpnI/HindIII* and *Pst*I/*Bam*HI primers illustrated in A) with the indicated restriction enzyme sites incorporated into the sequence. The PCR fragments were cloned into pLPBLP using the indicated restriction enzymes, and the success of cloning was verified by restriction enzyme digests and sequencing. Prior to transfection into Ax2, the *ku70*-disruption construct was digested with *Kpn*I and *Bam*HI, and cleaned up as outlined in the materials and methods section. Primer sequences are listed in Appendix A. **C)** PCR screening gel of putative *ku70*$^{-}$ clones 1, 2 and 3. The 5' and 3' screening primers indicated in A) were used in combination with primers specific to the *BsR* cassette (not shown), and would give rise to a product only when integration was targeted at the *ku70* locus. The control PCR amplifies the *BsR* cassette and would give rise to a PCR product for random and targeted integration events. PCR products were run on a 1% TAE-agarose gel and visualised with ethidium bromide. The labelling on the gel is as follows: B, BSR control; 5': 5' screen; 3': 3' screen **D)** The expression of Ku70 was judged by RT-PCR. The reverse transcription reaction to generate cDNA is outlined in the materials and methods and was carried out on both Ax2 and the *ku70*$^{-}$ RNA. Where indicated, no reverse transcriptase (-RT) was added to the RT reaction to serve as a control against contaminating gDNA. Primers utilised in the RT-PCR reaction are RT1 and RT2 (see schematic in A) against the *ku70* gene (left panel) and primers specific to ERK2 (right panel, primers not shown) were run as a control. PCR products were run on a 1% TAE-agarose gel and DNA visualised with ethidium bromide. The labelling on the gel is as follows: g: gDNA; c: Ax2 cDNA control; 1,2,3: putative *ku70*$^{-}$ clones **E)** Map of the *ku70*- locus in the parental and disruption strains are illustrated (left panel). Hatched boxes represent the regions of homology used in the disruption construct. The disruption strategy leads to replacement of *ku70* exons (grey) with the *BsR* cassette. The Southern hybridisation probe is targeted to the 3' arm of the *ku70*-disruption cassette, as indicated. Genomic DNA was isolated from Ax2 or the *ku70*$^{-}$ clones and digested with *Eco*RI (E) or *Hind*III (H) before being processed for Southern blotting. In Ax2 and *ku70*-, respectively, genomic DNA digestion with *Eco*RI would be expected to give rise to 6kbp and 7.4kbp bands and *Hind*III digestion would give rise to bands of 11.7kbp and 5.4kbp (right panel). An additional Southern blot was performed with a probe against BSR to confirm that only a single integration event had occurred in the disruption strains (data not shown). Data is only shown for clones 1 and 2 of *ku70*$^{-}$ strains, as clone 3 had an extra integration event as evidenced by the *BsR* probe (data not shown).

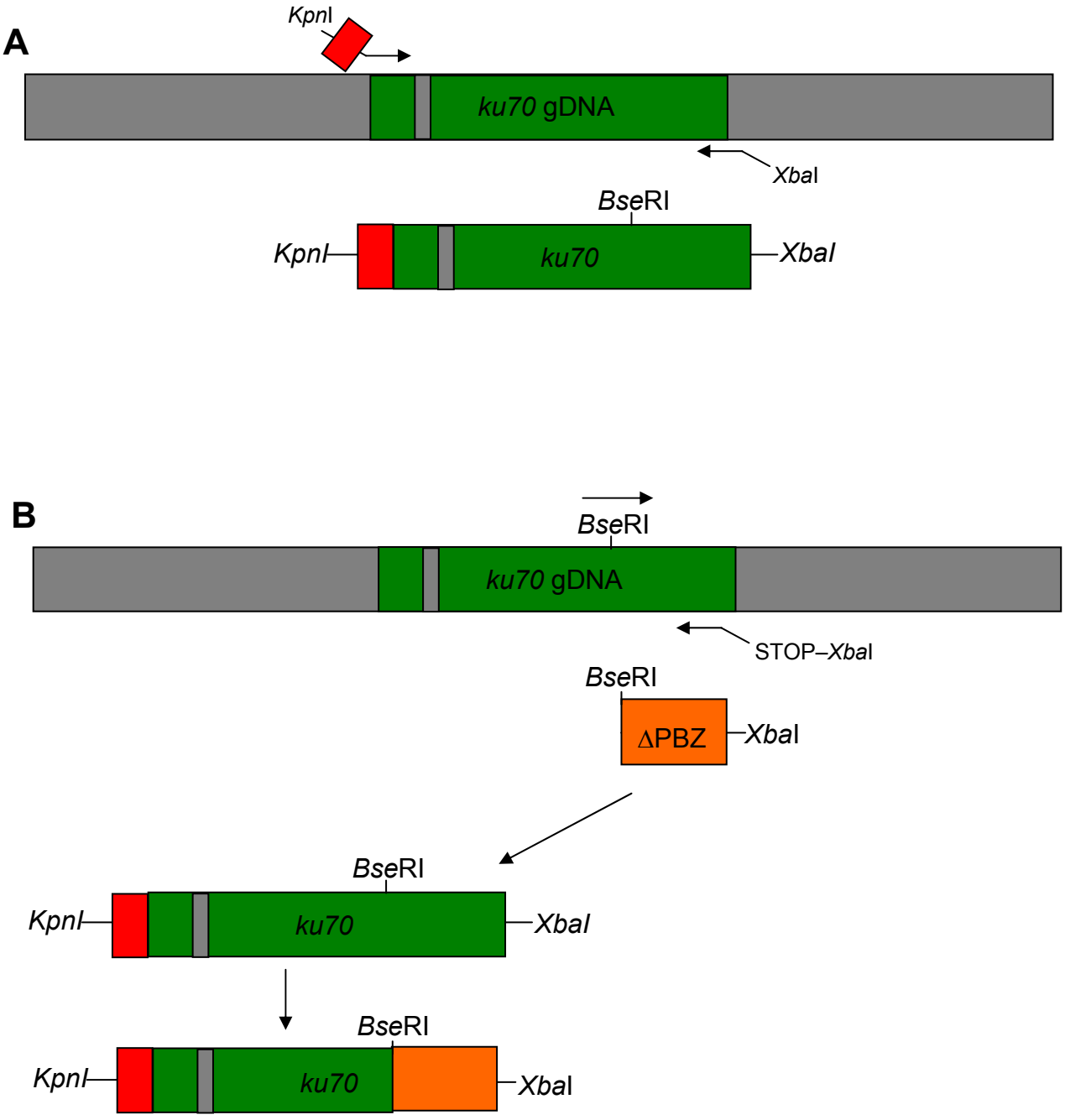

Figure 6.5 - Schematic diagram representing the generation of plasmids encoding pDXA-MYC-Ku70 and pDXA-MYC-Ku70ΔPBZ

Figure 6.5 - Schematic diagram representing the generation of plasmids encoding pDXA-MYC-Ku70 and pDXA-MYC-Ku70ΔPBZ

A) To generate the PCR fragment containing the full-length Ku70 gene required for the construction of pDXA-MYC-Ku70, the entire Ku70 gene (+1 to +2813) was amplified by PCR using an N-terminal primer containing a MYC-tag (represented by a red box) downstream of a *Kpn*I site and a C-terminal primer containing an *Xba*I site. The MYC-tag was cloned downstream and in-frame of the ATG start codon, whilst the *Xba*I site was downstream of the endogenous stop codon. Primer sequences are listed in Appendix A. The resultant PCR product was digested with *Kpn*I and *Xba*I and cloned into the multiple cloning site of pDXA. Diagnostic restriction enzyme digests and sequencing confirmed the nature of the insertion and the lack of mutations. **B)** To generate the the pDXA-MYC-Ku70ΔPBZ, the Ku70 gene was amplified from the internal *Bse*RI site to a site 25 amino acids upstream of the Ku70 STOP codon. This gave rise to a PCR product lacking the PBZ domain. The N-terminal primer spanned the sequence incorporating the *Bse*RI site and the C-terminal primer contained a STOP codon and an *Xba*I site. Primer sequences are listed in Appendix A. To generate the pDXA-MYC-Ku70ΔPBZ plasmid, pDXA-MYC-Ku70 was digested with *Bse*RI and *Xba*I to liberate the C-terminal fragment, and this was replaced by the ΔPBZ PCR product which had been previously digested with *Bse*RI and *Xba*I. The success of integration was determined by restriction enzyme digests, and the lack of mutations and the PBZ domain was confirmed by sequencing. The pDXA plasmid into which MYC-Ku70 and MYC-Ku70ΔPBZ were inserted contains the Neomycin resistance gene (Tn5 Neo) for antibiotic selection in *Dictyostelium*, and drives constitutive expression of proteins cloned into the multiple cloning site through an actin 15 promoter (PAct15).

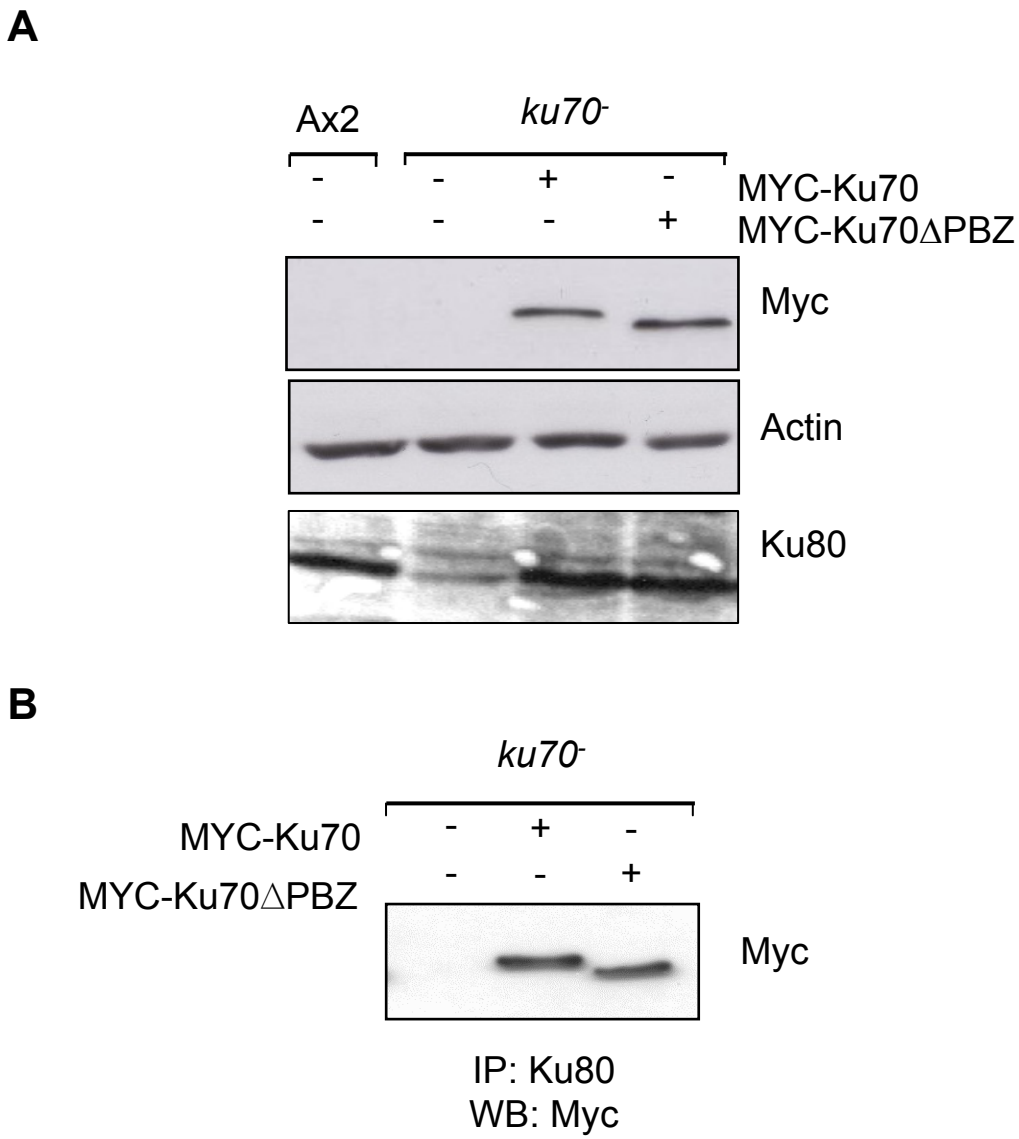

Figure 6.6 - The exogenously expressed MYC-Ku70 and MYC-Ku70ΔPBZ can interact with endogenous Ku80 to form a heterodimer

A) The indicated cells were transformed with pDXA, pDXA-MYC-Ku70 or pDXA-MYC-Ku70ΔPBZ and selected with G418. Following selection, whole-cell extracts were analysed by Western blot using antibodies against MYC, Ku80 and the loading control Actin. **B)** The indicated exponentially growing cells were exposed to 100μg/ml phleomycin for 30 mins and Ku80 immunoprecipated. Immunoprecipitated samples were analysed by Western blot and the co-immunoprecipitation of Ku70 and Ku70ΔPBZ confirmed using the MYC antibody.

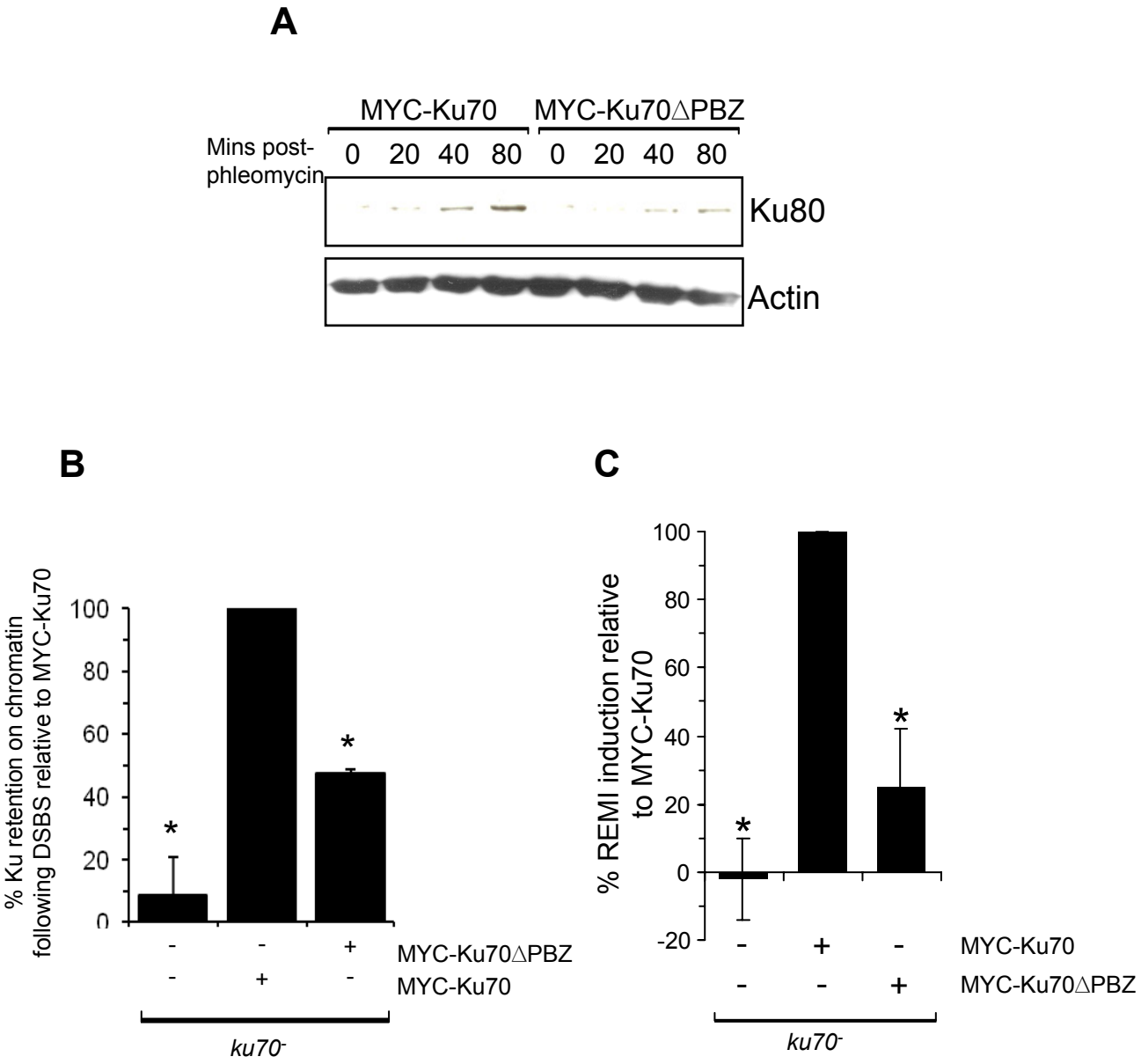

Figure 6.7 - The Ku70 PBZ domain is required for NHEJ in *Dictyostelium*

Figure 6.7 - The Ku70 PBZ domain is required for NHEJ in *Dictyostelium*

A) Exponentially growing cells were treated with 100μg/ml phleomycin and at the indicated times, sub-cellular fractionation was performed as outlined in materials and methods. The detergent resistant fraction was analysed by Western blot and probed with antibodies against Ku80 or the loading control actin. **B)** Exponentially growing cells were left untreated or exposed to 100μg/ml phleomycin for 80 mins. Chromatin fractions were prepared and analysed by Western blot using antibodies against Ku80 or the loading control H3. Following development with ECL, signals were detected using the Gel DocTM XR+ System (Bio-Rad), and their intensities quantified with image Lab software (Bio-Rad). Data was normalised to H3, and the fold induction of Ku80 signal in chromatin fractions determined relative to untreated controls. Data is represented as the % induction of Ku80 retention on chromatin induced on phleomycin treatment relative to MYC-Ku70. Error bars represent the SEM from three independent experiments. * $p<0.05$ compared to Ax2. Experiments for this figure were performed by H. Wang **C)** REMI efficiency of the indicated strains was assessed as described in Materials and Methods. The numbers analysed were such that experimental strains were compared to >200 colonies from the positive control (MYC-Ku70 plus restriction enzyme). Data is represented as % REMI induction relative to MYC-Ku70. Error bars represent the SEM from three independent experiments. * $p<0.05$ compared to the positive control (Ax2).